NASA CR-135051
CASD-NAS-76-018

(NASA-CR-135051) THERMAL PERFORMANCE OF A CUSTOMIZED MULTILAYER INSULATION (MLI) Final Report (General Dynamics Corp.) 274 p HC $9.00 CSCL 20D

N76-31449

Unclas
G3/34 02423

National Aeronautics and
Space Administration

THERMAL PERFORMANCE OF A CUSTOMIZED MULTILAYER INSULATION (MLI)

FINAL REPORT

GENERAL DYNAMICS
Convair Division

1. Report No.	2. Government Accession No.	3. Recipient's Catalog No.
NASA CR-135051		

4. Title and Subtitle	5. Report Date / 6. Performing Organization Code
Thermal Performance of a Customized Multilayer Insulation (MLI)	April 1976

7. Author(s)	8. Performing Organization Report No.
Karl E. Leonhard	CASD-NAS76-018

9. Performing Organization Name and Address	10. Work Unit No. / 11. Contract or Grant No.
General Dynamics Convair Division P.O. Box 80847 San Diego, CA 92138	NAS3-17756

12. Sponsoring Agency Name and Address	13. Type of Report and Period Covered / 14. Sponsoring Agency Code
National Aeronautics and Space Administration Lewis Research Center, Cleveland, Ohio	Contractor Report

15. Supplementary Notes

Project Manager, J. R. Barber, Fluid System Section of Chemical Energy Division of the Space Technology and Material Directorate, NASA Lewis Research Center, Cleveland, Ohio 44135

16. Abstract

The study was conducted to experimentally investigate the thermal performance of a LH_2 tank on a shroudless vehicle. The 1.52 m (60 in) tank was insulated with 2 MLI blankets consisting of 18 double aluminized Mylar radiation shields and 19 silk net spacers. The temperature of outer space was simulated by using a cryoshroud which was maintained at near liquid hydrogen temperature. The heating effects of a payload were simulated by utilizing a thermal payload simulator (TPS) viewing the tank. The tank and cryoshroud were provided by NASA/LeRC and modified by General Dynamics. The test program consisted of three major test categories: 1) null testing, 2) thermal performance testing of the tank installed MLI system, and 3) thermal testing of a customized MLI configuration. The TPS was not insulated during test category 1 and 2. Null tests were conducted utilizing zero, 0.2, 0.4 watts power input to an internal tank heater. TPS surface temperatures during the null test were maintained at near hydrogen temperature and during test categories 2 and 3 at 289K (520R). The heat flow rate through the "tank installed MLI" at a tank/TPS spacing of 0.457 m was 1.204 watts with no MLI on the TPS and 0.659 watts through the customized MLI with three blankets on the TPS. Reducing the tank/TPS spacing from 0.457 m to 0.152 m the heat flow through the customized MLI increased by 10 percent.

17. Key Words (Suggested by Author(s))	18. Distribution Statement
Customized MLI thermal performance, shroudless vehicle, payload effect	Unclassified - Unlimited

19. Security Classif. (of this report)	20. Security Classif. (of this page)	21. No. of Pages	22. Price*
Unclassified	Unclassified		

* For sale by the National Technical Information Service, Springfield, Virginia 22151

NASA-C-168 (Rev. 6-71)

Page
Intentionally
Left Blank

ABSTRACT

The study was conducted to experimentally investigate the thermal performance of a liquid hydrogen tank on a shroudless vehicle. The 1.52 m (60 in.) tank was insulated with two MLI blankets consisting of 18 double aluminized Mylar radiation shields and 19 silk net spacers. The temperature of outer space was simulated by using a cryoshroud which was maintained at near liquid hydrogen temperature. The heating effects of a payload were simulated by utilizing a thermal payload simulator (TPS) viewing the tank. The tank and cryoshroud were provided by NASA/LeRC and modified by General Dynamics Convair Division.

The test program consisted of three major test categories, 1) null testing, 2) thermal performance testing of the tank installed MLI system and 3) thermal testing of a customized MLI configuration. The TPS was not insulated during test category 1 and 2. Null tests were conducted utilizing zero, 0.2, 0.4 watts power input to an internal tank heater. TPS surface temperatures during the null test were maintained at near hydrogen temperature and during test categories 2 and 3 at 289K (520R).

The heat flow rate through the "tank installed MLI" at a tank/TPS spacing of 0.457 m was 1.204 watts with no MLI on the TPS and 0.059 watts through the customized MLI with three blankets on the TPS.

Reducing the tank/TPS spacing from 0.457 m to 0.152 m the heat flow through the customized MLI increased by 10 percent.

PRECEDING PAGE BLANK NOT FILMED

Page Intentionally Left Blank

FOREWORD

This report was prepared by General Dynamics Convair Division under Contract NAS3-17756, "Thermal Performance of a Customized Multilayer Insulation." The work was administered under the technical direction of Mr. J. R. Barber, Fluid System Section of Chemical Energy Division of the Space Technology and Material Directorate and Mr. W. R. Johnson, Thermal Technology Section, Propulsion Technology Branch, Chemical Propulsion Division, NASA/Lewis Research Center.

In addition to the project leader, K. E. Leonhard, the following Convair personnel were major contributors to the study:

Thermodynamics	M. D. Walter G. B. Yates
Predesign	J. P. Hancock R. S. Ringwald
Structural Analysis	J. E. Dyer
Manufacturing Research	H. E. Kobrich E. Catton N. L. Frederick V. V. Sowinski E. L. Christian C. J. Langford G. T. Lundquist
Reliability Laboratory	G. Gross W. L. Colahan
Test Laboratory	B. A. Ganoe H. G. Brittain

Approved by: ______________

R. E. Tatro
Chief of Thermodynamics
667-2

PRECEDING PAGE BLANK NOT FILMED

Page Intentionally Left Blank

PRECEDING PAGE BLANK NOT FILMED

TABLE OF CONTENTS

TABLE OF CONTENTS, Contd

TABLE OF CONTENTS, Contd

TABLE OF CONTENTS, Contd

LIST OF FIGURES

LIST OF FIGURES, Contd

LIST OF FIGURES, Contd

LIST OF FIGURES, Contd

LIST OF FIGURES, Contd

LIST OF FIGURES, Contd

LIST OF TABLES

LIST OF TABLES, Contd

NOMENCLATURE

A, a	area, m^2 (in^2)
c	weld distance, m (in)
C_r	constant = 5.39×10^{-8} for $\bar{N}$ in layers/m (T in °K, and q in W/m^2)
C_r	constant = 1.10×10^{-11} for $\bar{N}$ in layers/in (T in °R, and q in Btu/hr ft^2)
Cs	constant = 8.95×10^{-6} for $\bar{N}$ in layers/m (T in °K, and q in W/m^2)
C_s	constant = 8.06×10^{-10} for $\bar{N}$ in layers/in (T in °R, and q in Btu/hr ft^2)
E	modulus of elasticity, kN/m^2 (psi)
F_{su}	ultimate shear, kN/m^2 (psi)
F_{tw}	ultimate strength, kN/m^2 (psi)
F_{ty}	yield strength, kN/m^2 (psi)
F_{bru}	ultimate bearing stress, kN/m^2 (psi)
I	moment of inertia, (section area), m^4 (in^4)
M	moment, m-kN/m (in-lb/in)
m	reciprocal of Poisson's ratio, dimensionless
M. S.	margin of safety, dimensionless
N_s	number of radiation shield layers
$\bar{N}$	number of layers/m or layers/in
N_x	shear load, kN/m (lb/in)
P	pressure, kN/m^2 (psi)
P	vertical load, kN (lb)
q	heat flux, W/m^2 (BTU/hr ft^2)
Q_c	corrected flow rate, kg/hr (lb/hr)
Q_M	measured flow rate, kg/hr (lb/hr)
R	radius, m (in)
T	temperature, K (R)
t	thickness, m (in)
t	time, s, hr

W	total applied load, kN (lb)
w	unit applied load, kN/m^2 (lb/in^2)
ϵ	emissivity, dimensionless
υ	Poisson's ration, dimensionless
σ_ϕ	total stress, kN/m^2 (psi)

Subscripts

c	center; cold
h	hot
m	mean
s	shear
t	tension
tot	total
u	ultimate
w	weld
x	location
y	yield

SUMMARY

This program report covers the work performed under NASA contract NAS3-17756, "Thermal Performance of a Customized Multilayer Insulation (MLI)." The major objective of the total program was to design, fabricate, and experimentally evaluate the thermal performance of a selected, customized MLI system. NASA/LeRC provided the basic design of the MLI configuration to be tested, the 1.52 m (60 in) test tank to be insulated, and the 2.44 m (96 in) cryoshroud for simulating a deep space environment.

The total program objectives accomplished were:

- Design and Fabrication of Test Tank Modifications
- Design and Fabrication of Test Tank Support System
- Design and Fabrication of the Thermal Payload Simulator
- Modification of the Cryoshroud Assembly
- Design and Fabrication of the Thermal Payload Simulator Multilayer Insulation
- Design and Fabrication of the Tank Mounted Multilayer Insulation
- Design and Fabrication of Test Equipment, Test Facilities and Instrumentation
- Thermal Performance Testing and Evaluation of the "Tank Installed" and "Customized" Multilayer Insulation System

DESIGN OF TEST TANK MODIFICATIONS AND TANK SUPPORT SYSTEM

Modification drawings were established for

1. Replacement of the existing tank manhole access door/neck with a flush door design.
2. Removal of the outlet flange and replacing it with a contoured, outlet cap design.
3. Removal of the existing conical support ring assembly at its mechanical joint.

The new access door, 0.566 m (22.3 in) in diameter, is a 0.038 m (1.5 in) thick circular, flat plate of 6061-T6 aluminum alloy material. The design provides openings through the door for a fill and drain line/vent line and electrical pass throughs. Double Conoseals were used to further reduce anticipated leakage. An outlet cap 0.215 m (8.43 in) diameter was formed to a spherical radius of 0.762 m (30.0 in) from a 0.008 m (0.32 in) thick 6061 aluminum alloy plate. The existing conical support ring at the tank equator was removed.

The new tank support system is a three point system, designed to suspend the tank inside the cryoshroud. It consists of three lugs at the tank door ring, three adjustable turnbuckles and three attachment fittings located at the LH_2 guard tank.

A structural analysis was performed to verify the capability of the basic test tank and the modifications performed by GD/C to support the required test loads. The investigation included a combined membrane and discontinuity stress analysis of the tank wall near the door and the tank support. Conservative methods used showed a positive margin of safety.

FABRICATION OF TEST TANK MODIFICATIONS AND TANK SUPPORT SYSTEM

The tank modifications included:

1. Preparation of the tank for welding the new large manhole access door ring and tank outlet cap.
2. Machining of the door, door ring, tank outlet cap and tank support lugs.
3. Welding of the tank outlet cap.
4. Welding of the manhole access door ring.
5. Welding of the tank support lugs onto the tank.
6. Removal of the existing conical support.

The inspection methods included dye penetrant and radiography. Unforeseen severe distortions were encountered in cutting out the original manhole access door ring. The distortion problems were directly attributed to the initial fabrication of the 1.52 m (60 in) tank by its original manufacturer. The original welding resulted in excessive defects causing resident distortions in the tank. A combination of mechanical and machining techniques was used to reduce mismatch and distortion to a satisfactory level. In an effort to define conditions in the original weld zones, x-rays were taken in various areas untouched by the modification of the tank. The x-rays showed the presence of tungsten inclusions, porosities, weld folds, foreign material and cracks. Repair work was considered outside the scope of the program.

The test tank was proof pressure tested at 276.0 kN/m^2 (40 psig). A final leak test was conducted utilizing helium gas and a Veeco leak detector, Model MS17. The leakage measured at a pressure differential of 138.0 kN/m^2 (20 psid), was 2.8 × 10^{-7} scc/sec. This amount of gas leakage was less than the allowable leakage of 1 × 10^{-6} scc/sec.

THERMAL PAYLOAD SIMULATOR (TPS)

The thermal payload simulator was designed and fabricated to provide a constant temperature surface in the range of 20.5 to 417K (37 to 750R) for the insulated tank to view. It consists of a 1.83 m (72 in) diameter 0.0095 m (0.375 in) thick, highly polished aluminum disc. An emissivity of 0.03 was measured utilizing the Lion emissometer Model 25 B-7. The thermal payload simulator is cooled by liquid hydrogen flowing through circumferential, aluminum coils. The TPS heaters were designed for an operating range of 0.01 to 55 watts. Due to the radially nonuniform heat load on the TPS, individual heaters were mounted in the inner, mid and outer zone.

CRYOSHROUD ASSEMBLY MODIFICATION

The NASA/LeRC furnished cryoshroud, 2.44 m (96.0 in) in diameter, was modified to establish a low temperature black body cavity while limiting liquid hydrogen usage to a minimum feasible rate. The modification of the cryoshroud was performed in these steps:

1. Cryoshroud shell modifications
2. Cryoshroud thermal analysis
3. Cryoshroud baffle design and fabrication
4. Thermal payload simulator and baffle positioning mechanism design and fabrication
5. Guard tank design and fabrication
6. Assembly of the cryoshroud components

The cryoshroud shell modification consisted of reworking the top cover to accommodate the guard tank, removal of the existing baffles and preparing the bottom cover for the baffle positioning mechanism. An analysis was performed to determine the number and location of the liquid hydrogen cooled baffles required to intercept the thermal radiation within the cryoshroud. The analysis revealed that three baffles are required, one fixed baffle located at the test tank equator, one baffle in the same plane as the thermal payload simulator and one baffle between the thermal payload simulator and fixed baffle. The baffle structure is a sandwich consisting of a flat plate with cooling coils welded to its upper surface as the main structural element and honeycomb bonded to one or both of the surfaces. The lower two baffles and the thermal payload simulator are designed to move together. The bottom baffle remains in the same plane with the payload simulator as it is positioned by the jack screw mechanism.

All lines going to the test tank pass through the 0.610 m (24 in) diameter liquid hydrogen guard tank as shown in Figure S-1 in order to prevent entry of extraneous heat to the test tank. All instrumentation lines into the test tank are passed through the vent line.

Before installing the test tank all interior surfaces including cryoshroud, baffles, and attachment hardware in view of the test package were painted with 3M "Nextel" Black Velvet paint to achieve the highest emissivity possible. Where welding was not possible for tubing joints, single Conoseals were utilized for stainless steel joints while double Conoseals were applied for bi-metal joints.

DESIGN AND FABRICATION OF THE THERMAL PAYLOAD SIMULATOR (TPS) MULTILAYER INSULATION

The goal of this task was to design and fabricate the multilayer insulation (MLI) for the thermal payload simulator. The application of this insulation is shown in figure S-1. The multilayer insulation system is composed of three blankets each consisting of 18 double aluminized Mylar radiation shields (DAM) and 19 double silk net spacers. Both sides of each blanket are protected by a cover shield which is a laminate of Mylar and aluminum foil, bonded together. The aluminum provides high lateral conductivity. The radiation shields and spacers of each blanket are interconnected by nylon button pin studs to control the blanket thickness to 0.008 m (0.312 in). Velcro hook and pile type fasteners are used to attach adjacent blankets together as well as attaching the initial blanket to the TPS surface. An annulus zone on the blanket facing the test tank is painted with a low gloss, low outgassing, black velvet paint to increase the emissivity of thi area. The manufacturing aids required for fabricating the thermal payload simulator blankets consisted of a wooden frame to stretch-form the silk net spacer material and a MLI manufacturing aid to lay up the cover shields, the radiation shields and spacers.

DESIGN AND FABRICATION OF THE TANK MOUNTED MULTILAYER INSULATION

The tank mounted MLI consists of an inner and outer blanket lay up. The material, number of layers, and construction of these blankets was similar to the design of the TPS blankets. The primary differences from the TPS system are the requirements for forming all components to fit the spherical tank. The inner blanket layup consists of six 1.047 rad (60 deg) gore sections and one 0.406 m (16 in) diameter circular blanket, located at the tank pole, viewing the TPS (Figure S-1). The gore sections are assemblies running continuously from the access tank door to the circular blanket. Butt joints are used between the gore and circular sections. The outer blanket lay up is the same as that outlined for the inner blanket except for the addition of cover shield strips applied over the butt joints between the gore sections and between the gore sections and the circular blankets. The butt joints are staggered relative to the inner blanket sections. The girth area of the outer blanket

Note: All fill and vent lines are insulated with 10 layers of MLI.

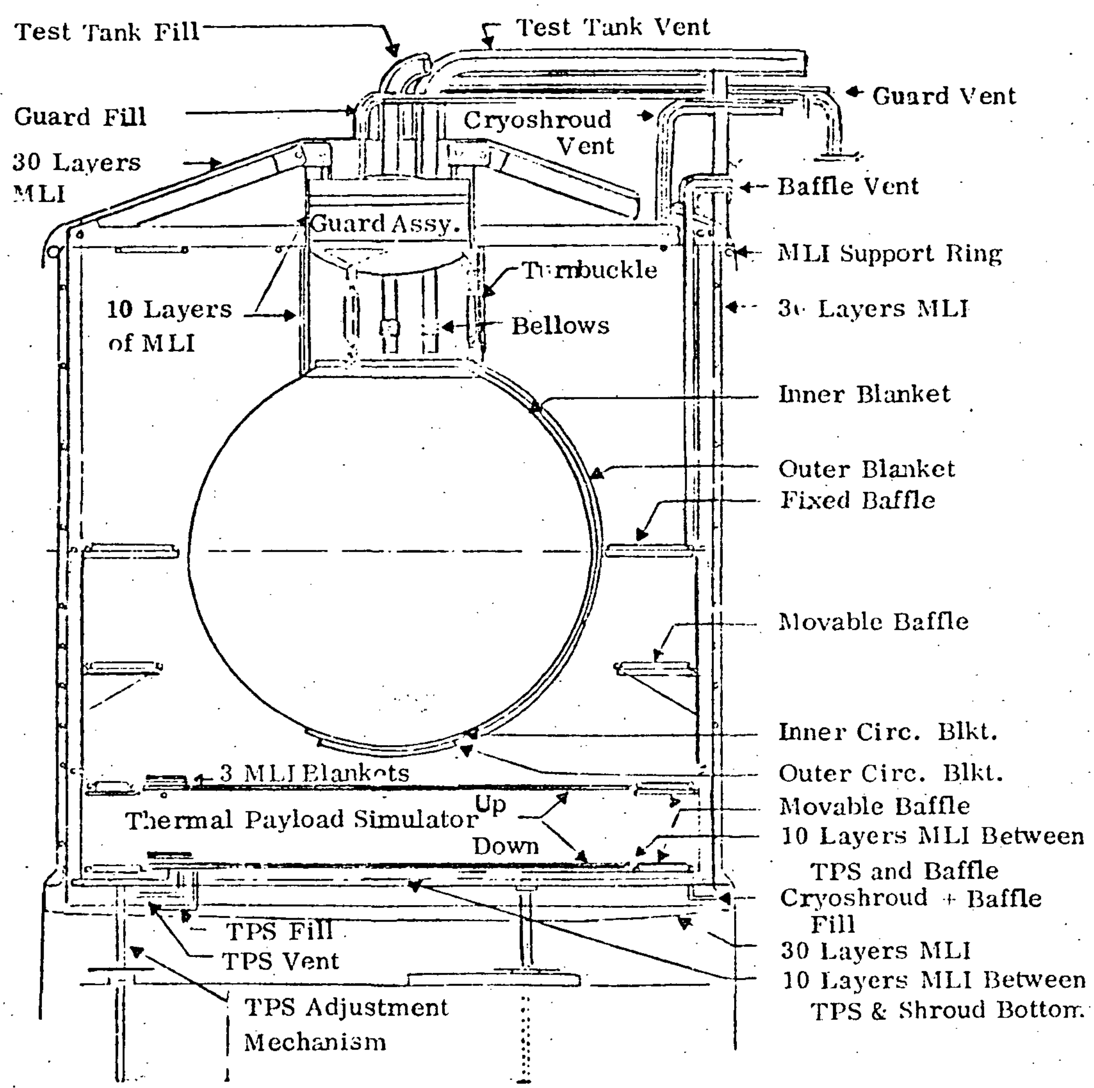

Figure S-1. Schematic of Test Article and Cryoshroud Assembly is coated with Black Velvet paint. The outer and inner blankets are attached to each other and to the tank by Velcro fasteners. The fabrication of the MLI system for the tank mounted insulation required the manufacturing of a fiberglass inner and outer blanket layup aid for the gore and circular sections. The cover shields for the gore sections were manufactured utilizing a vacuum forming tooling aid. The silk net spacer material for each blanket was stretch-formed using the appropriate layup aid.

The blanket lay up and assembly operation consisted of joining the prefabricated components into the required multilayer lay up of cover shields, radiation shields and silk net spacers. A female cover plate of the lay up manufacturing aid was used as both a hole template and in combination with the male base plate as a guide for trimming the blanket periphery. The button pin assemblies were then installed. All blankets were outgassed in a vacuum chamber at a temperature of 339K (610R) before installation to the tank.

TEST FACILITIES

All systems tests were conducted at the Convair Liquid Hydrogen Test Center Site "B" thermal vacuum facility. The major components of the test facility are the test chamber, the test tank pressure control system, the guard tank pressure control system, the fluid system and the test tank heater. The test chamber was a 3.66 m (144 in) water jacketed vacuum chamber and was serviced by a 0.813 m (32 in) oil diffusion pump, a LN_2 cold trap, and backed by two 14.2 m^3/min (500 ft^3/min) Kinney mechanical vaccum pumps. Controls for these pumps, along with all fluid system controls and the data acquisition equipment, were located in a blockhouse.

A MKS Baratron pressure control system was used during testing to control the ullage pressure in the liquid hydrogen test tank. The system maintained the test tank pressure within ± 1.38 N/m^2 (0.0002 psi) of the set point.

A NBS Barostat device was utilized to control the pressure of the guard tank during the null test. The guard tank boiloff was found to vary from a high of greater than 0.0047 m^3/sec (10 scfm) immediately after filling to a low of less than 0.00024 m^3/sec (0.5 scfm) after the temperature had stabilized (approx. 12 hours). This resulted in the need for constant adjustments of the Barostat control weights to maintain the required narrow guard tank pressure band. Before the start of the customized MLI tests, the Barostat was replaced with a pressure transducer/closed loop controller/flow control valve system.

The fluid system was designed to achieve minimum hydrogen usage. The system connected the test tank, guard tank, cryoshroud and baffles. Welding and silver brazing were used as the principal means of joining parts of the system. All the aluminum to stainless steel transitions were made using double seal Conoseal flanges with the interseal cavity vacuum pumped to less than 1.0×10^{-5} m (10 μ). A 5.7 m^3 (1500 gal) LH_2 supply tank was maintained at an approximate pressure of 41.4 kN/m^2

(6 psig) all the time by a pneumatic pressure controller and vent valve. When empty, the supply tank was filled with liquid hydrogen through the LH_2 make-up valve from the 49.2 m^3 (13,000 gal) site LH_2 storage tank or from the 3.78 m^3 (1000 gal) catch tank through the LH_2 recovery valve. The catch tank was vented to the atmosphere while acting as a liquid vapor separator for the cryoshroud, baffles and TPS vents. When full, it was isolated from the cryoshroud, baffles and TPS vents, pressurized to approximately 172.5 kN/m^2 (25 psig), and drained into the supply tank. In normal operation the system was able to run for a minimum of 15 hours before the supply tank needed to be filled or for 5 hours before the catch tank needed to be emptied. Transfer from the catch to supply tank took less than 15 minutes. Flow through the cryoshroud, baffle, and the TPS (when required) was continuous and was "recovered" about 95% of the time.

An electric heater installed in the test tank was used to supply a known heat input to the test tank during the null test. The heater was designed to provide a maximum heat flow of one watt into the tank.

TEST INSTRUMENTATION

Instrumentation selection for the full scale test specimen was based upon measurement of the independent and dependent variables required for demonstrations of system overall thermal performance, system efficiency, and system component operation. Independent variables included hydrogen liquid level, chamber pressure and ullage pressure. Dependent variables included temperature distribution, MLI thermal gradients and LH_2 boiloff rate. The instrumentation tree platinum resistors within the tank permitted LH_2 level measurement. Chromel/Constantan thermocouples were used for all other temperature measurement. Chamber and shroud pressure measurements were made with hot filament ion gages (Bayard-Alpert) in their respective ranges. Liquid hydrogen boiloff flow rates were measured with TSI hot-film anemometers and a water displacement apparatus. Pressures other than the test tank pressure were measured with Statham strain gage transducers.

TESTING

The test program included three major test categories, 1) null testing, 2) thermal testing of the tank installed MLI system and 3), thermal testing of the customized MLI configuration. The objective of the null testing was to verify satisfactory operation of all components and to determine extraneous heat flows into the test tank. The thermal payload simulator surface temperature was maintained below 27.8K (50R). The objective of the tank installed MLI test was to determine the thermal performance of the tank insulation at a TPS temperature of 289K (520R). The thermal payload simulator was uninsulated during the preliminary null testing and the tank installed MLI testing. The objective of the customized MLI test was to determine the thermal performance of the tank insulation at a TPS temperature of 289K (520R), with distances between test tank and thermal payload simulator of 0.457 m (18 in), 0.305 m (12 in) and 0.152 m (6 in). During this test the thermal payload simulator was insulated. During all testing the cryoshroud including baffles were maintained below 27.8K (50 R) to simulate outer space at a vacuum pressure of less than 1.333×10^{-4} N/m^2 (1×10^{-6} torr). The criteria for thermal equilibrium was the achievement of a LH_2 boiloff rate which changes not more than 0.5% per hour and a temperature variation of three selected test tank MLI thermocouple readings of not more than ± 0.56K (1R) in 10 hours. The test article was designed for a maximum extraneous heat flow of 0.0293 watt (0.1 Btu/hr) into the test tank when the internal heater element was turned off.

A summary of the test results is shown in table S-1.

Table S-1. Summary of Test Results

Test No.	Heat Flow Experimental Watts(Btu/hr)	Heat Flow Predicted Watts (Btu/hr)
Null Test No 1	0.068 (0.2321)	0.0293 (0.1000)
Null Test No 2	0.187 (0.6387)	0.2293 (0.7826)
Null Test No 3	0.367 (1.2524)	0.4293 (1.4652)
Null Test No 4	0.239 (0.8170)	0.2293 (0.7826)
Tank Installed MLI*	1.204 (4.1100)	0.3519 (1.201)
Customized MLI		
Initial Null Test	0.350 (1.1950)	0.2293 (0.7826)
Thermal Test No 1*	0.059 (0.2013)	0.0114 (0.0390)
Thermal Test No 2*	0.063 (0.2167)	-
Thermal Test No 3*	0.065 (0.2224)	-
Final Null Test	0.409 (1.3944)	0.2293 (0.7826)

* Heat Flow Through MLI

NULL TESTING

Four null tests were conducted utilizing zero, 0.2 watts (0.683 BTU/hr), 0.4 watts (1.3652 BTU/hr) and 0.2 watts 0.683 BTU/hr) power input to the internal tank heater. The table S-1 indicates that the measured heat flow rate of the zero power input test was 2.3 times higher than the estimated heat flow rate. It is anticipated that the MLI outgassing was not completed and that the presence of thermal acoustic oscillations within fill and vent line produced additional heat leakage into the test tank. The boiloff rates of null test No. 2 and No. 3 were below the predicted rates. This indicates that a portion of the energy created by the internal test tank heater was stored within the bulk of the LH_2 fluid. Null Test No. 4, which was a repetition of Null Test No. 2 resulted in a heat flow rate which was only 4% over the predicted rate.

TANK INSTALLED MLI

This test was conducted immediately after the null test program without increasing the vacuum chamber pressure or refilling of the test tank with LH_2. The thermal payload heater was turned on at 220 hours after 0-time (beginning of first null test). The required TPS temperature of 289K (520R) was achieved after 18 hours. The test continued for 134 hours at which time the LH_2 boiloff rate was dropping at the rate of 0.15% per hour. The decision was made to terminate the test due to the projection that several days or weeks would be required to achieve a true thermal equilibrium condition. It was concluded that the insulation was still outgassing. The final 28 hours of testing resulted in an average heat flow rate through the MLI of 1.204 watts (4.110 BTU/hr), not including the extraneous heat flow of 0.0293 watts (0.1 BTU/hr) and power input to the internal heater of 0.2 watts (0.683 BTU/hr).

The heat flow rate was estimated to be 0.3519 watts (1.201 BTU/hr) not including the extraneous heat flow, heat leakage through insulation attachments and heat leaks caused by thermal acoustic oscillations and MLI outgassing.

CUSTOMIZED MLI THERMAL PERFORMANCE TEST

Prior to this test three prefabricated MLI blankets were added to the TPS. The test included two null tests, one at the beginning and one at the end of the test operation and three customized MLI thermal performance tests. The power input to the internal test tank heater was maintained at a level of 0.2 watts (0.683 BTU/hr). The total test time was 715 hours. During the initial and final null test the TPS surface temperature was maintained below 27.8 K (50R). The initial null test was conducted for 91 hours. At this time the boiloff rate was dropping at the rate of 0.2% per hour, mainly due to the MLI outgassing. The decision was made to terminate the test before a true thermal equilibrium condition was achieved. The total average heat flow rate achieved within the equilibrium criteria including power input and extraneous heat flow during the final 16 hours was 0. 50 watts (1.1950 BTU/hr). The predicted heat flow (table S-1) was 0.2293 watts (0.7826 BTU/hr).

During the final null test the test conditions were the same as those of the initial null test except that the spacing between the test tank and thermal payload simulator was changed from 0.457 m (18 in) to 0.152 m (6 in). The average heat flow rate including power input and extraneous heat flow was 0.409 watts (1.3944 BTU/hr). This test was conducted for a total period of 116 hours. The deviation of the initial and and final null test from the estimated heat flow rates is mainly due to the incomplete thermal equilibrium condition, incomplete outgassing of the MLI and the presence of thermal acoustic oscillations through the fill and vent line. These effects are significant for a cryogenic tank operating in an extremely low temperature environment, resulting in very low boiloff rates.

The results of the thermal performance of the insulation not including heater power input and extraneous heat flow for the customized MLI test No. 1, 2 and 3 with TPS-test tank spacings of 0.457 m (18 in), 0.305 m (12 in) and 0.152 m (6 in) are shown in table S-1. The increase in heat transfer through the MLI, resulting from the TPS position change from the 0.457 m (18 in) position to the 0.152 m (6 in) position was approximately 10%. The experimental heat flow through the insulation during the customized MLI test No. 1 was approximately five times the estimated heat flow. However, no consideration was given to incomplete equilibrium conditions or heat leaks through MLI attachments and heat leaks caused by MLI outgassing or thermal acoustic oscillations of the hydrogen gas within the fill and vent line. It is also noted that the experimental heat flow through the tank installed MLI at the 0.457 m (18 in) TPS-test tank spacing with no MLI blankets on the thermal payload simulator was approximately 20 times higher than the heat flow rate obtained for the customized MLI during test No. 1.

During the total test operation of 1091 hours the facility performed exceptionally well. No leakage was experienced within the chamber in spite of the existence of 140 m (460 ft) of LH_2 tubing including 9 m (30 ft) of welds, 100 welded butt joints and 11 conoseals.

1

INTRODUCTION

The effective storage of liquid hydrogen in space can be accomplished by using high performance multilayer insulation. Heat-transfer characteristics of these insulations protected by a shroud and operating between ambient and liquid hydrogen temperatures have been investigated in numerous experiments by NASA and independent contractors. The results of a study conducted by NASA/LeRC (Ref. 1-1) assuming a hypothetical vehicle with a completely unshrouded liquid hydrogen tank showed that the thermal performance of a conventional constant thickness MLI can be significantly improved by

1. Using a variable MLI thickness over the surface of the tank
2. Using several high lateral thermal conductivity shields
3. Increasing the MLI surface emissivity in certain areas

The hypothetical vehicle assumed by NASA was sun-oriented, thus ensuring the liquid hydrogen tank to always be in the shadow of the vehicle payload. The payload exchanges heat with the cryogenic tank. In a shroudless vehicle a portion of the energy can be rejected directly into space. The number of radiation shields for such a cryogenic tank would be determined by 1) ground hold and ascent thermal protection requirements, 2) estimated time of near-planetary operation (albedo effects), 3) estimated time during mid-course corrections when the vehicle is not sun-oriented and 4) prevention of localized propellant freezing.

The purpose of this contract was to experimentally investigate the thermal performance of a liquid hydrogen tank of a shroudless vehicle. The tank was insulated with a constant thickness multilayer insulation system. The temperature of outer space was simulated by using a cryoshroud which was maintained at near liquid hydrogen temperature. The heating effects of a payload were simulated by utilizing a highly polished, flat disc (payload simulator) viewing the cryogenic tank. The tank and cryoshroud were provided by NASA/LeRC. A variation of the tank insulation thickness, however, was not a requirement of this contract.

2

DESIGN OF TEST TANK MODIFICATIONS AND TANK SUPPORT SYSTEM

The task consisted of the evaluation and the design of the 1.52 m (60 in) diameter thin walled aluminum tank which was furnished by NASA-LeRC as the tank to be insulated under this program. The existing versus the modified tank configuration is shown in Figure 2-1. Tank geometry and weights are presented in Table 2-1.

Table 2-1. Tank Geometry and Weights

Nominally Spherical 1.52 m (60 in)		
Bulkhead Centers Offset by 0.0485 m (1.906 in)		
Diameter	1.520 m	(60 in)
Volume	1.900 m^3	(67 ft^3)
Surface Area	6.875 m^2	(74 ft^2)
Maximum Thickness (at welds)	0.0079 m	(0.31 in)
Minimum Thickness (shell)	0.0025 m	(0.10 in)
Total Weight (Approximate)	108.454 kg	(238.6 lbs)
Basic Shell	82.109 kg	(180.64 lbs)
Bottom Half	34.100 kg	(75.02 lbs)
Top Half	43.009 kg	(105.62 lbs)
Door	23.982 kg	(52.76 lbs)
Lugs	0.241 kg	(0.53 lbs)
Bolts, Misc.	2.127 kg	(4.68 lbs)

2.1 TEST TANK MODIFICATION

As shown in Figure 2-1, the following tank modifications were required:

1. Removal of the large manhole access door ring, machining of the flange as required and replacement of the previous tank neck/door section with a flush door design.

2. Removal of the outlet flange and welding in a contoured plate (tank outlet cap) to obtain a smooth exterior contour. This area of the tank will be viewing the thermal payload simulator.

3. Removal of the conical support ring assembly at its mechanical joint and machining off the outstanding support ring flange.

The design and material requirements are shown in Table 2-2.

Table 2-2. Tank Design Requirements

Design Pressure:	241.5 kN/m^2 (35.0 psig) Working		
	362.2 kN/m^2 (52.5 psig) Proof		
	483.0 kN/m^2 (70.0 psig) Burst		
Materials	Shell	6061T6	Al Aly
	Door	6061T651	Al Aly
	Ring	6061T651	Al Aly
	Cap	6061T651	Al Aly
	Lugs	6061T651	Al Aly
	Struts	304	CRES

2.1.1 LARGE MANHOLE ACCESS DOOR. The large manhole access door was placed in a plane close to the intercepted contour of the tank surface by incorporating a flush door design. The design of the door is shown in Figure 2-2. The access door is a 0.038 m (1.5 in) thick circular flat plate, machined from 6061-T6 aluminum alloy plate stock. The diameter of the door is 0.566 m

8 | 7

H | G | F | E | D | C | B | A

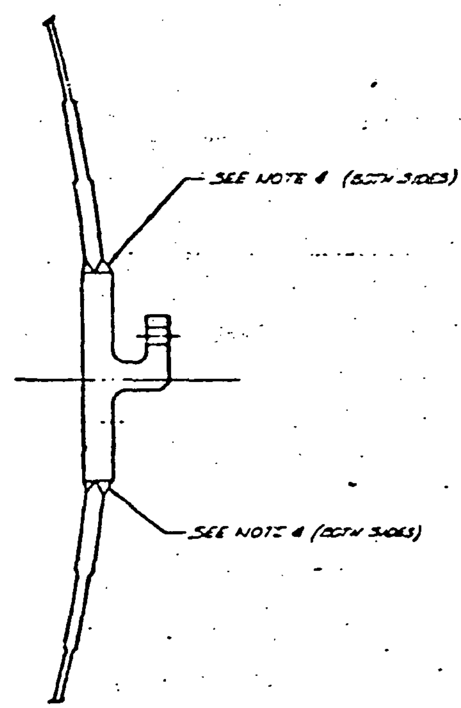

DETAIL C 4/5
SCALE 1/1

FOLDOUT FRAME /

ORIGINAL PAGE IS
OF POOR QUALITY

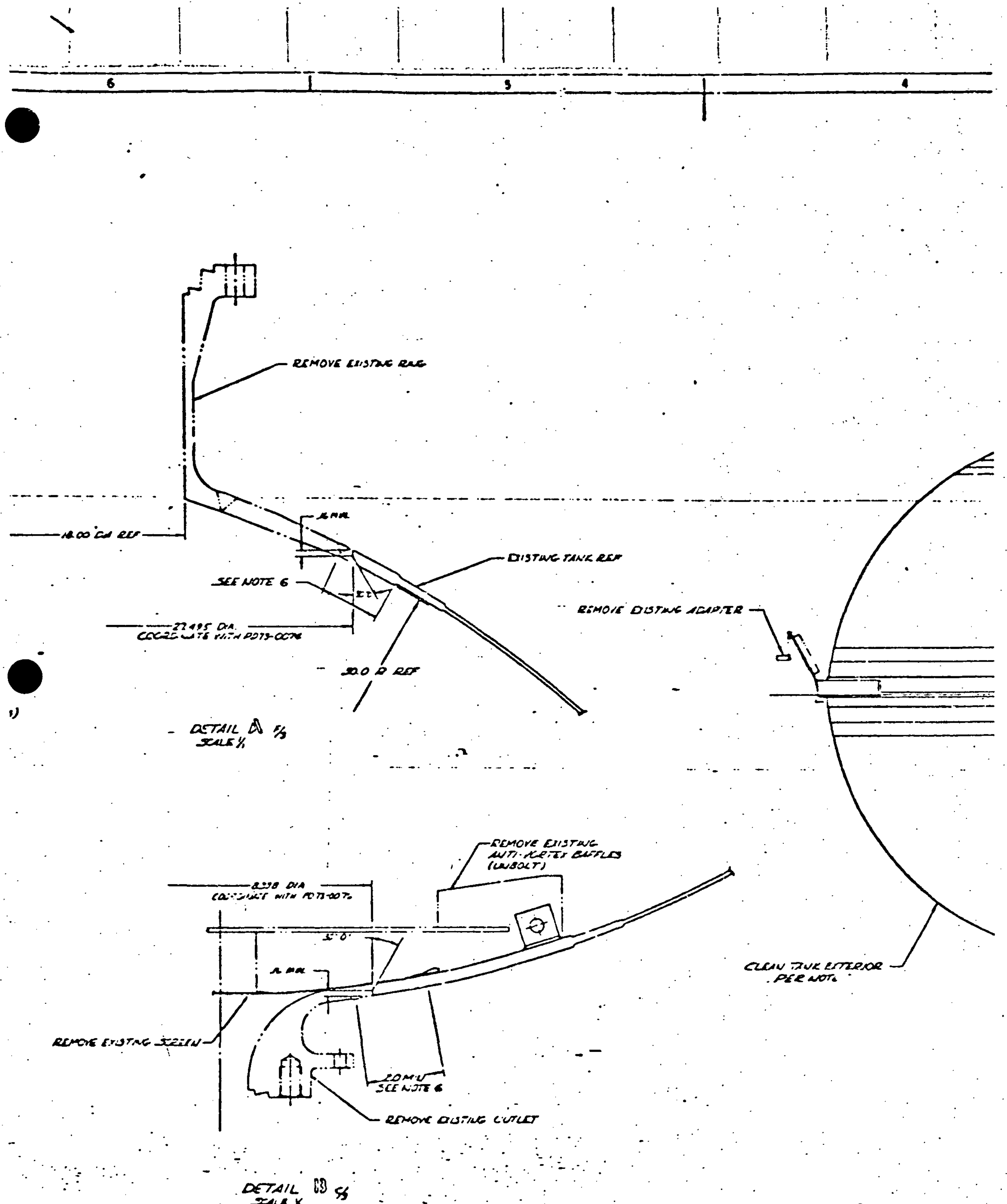
6
5
4
REMOVE EXISTING
18.00 DIA REF
EXISTING TANK REF
SEE NOTE 6
22.495 DIA.
REMOVE EXISTING ADAPTER
30.0 R REF
DETAIL A
REMOVE EXISTING
ANTI-VORTEX BAFFLES
(UNBOLT)
CLEAN TANK EXTERIOR
PER NOTE
REMOVE EXISTING SCREEN
SEE NOTE 6
REMOVE EXISTING OUTLET
DETAIL B

NOTES-

1. IMPRESSION MARKING OF PARTS NOT PERMITTED.
2. IDENTIFY PER [illegible]. LOCATE APPROX AS SHOWN
3. CLEAN OUTSIDE OF TANK TO MEET THE REQUIREMEN
4. PENETRANT INSPECT INDICATED WELDS AND OTHER NOTED
5. ACCEPT PENETRANT PER [illegible].
6. RADIOGRAPH INSPECT AREAS SHOWN PER MIL-STD-453
7. RADIOGRAPH ACCEPT PER [illegible]. ADJUST TEN

Dimensions: All dimensions are in inch

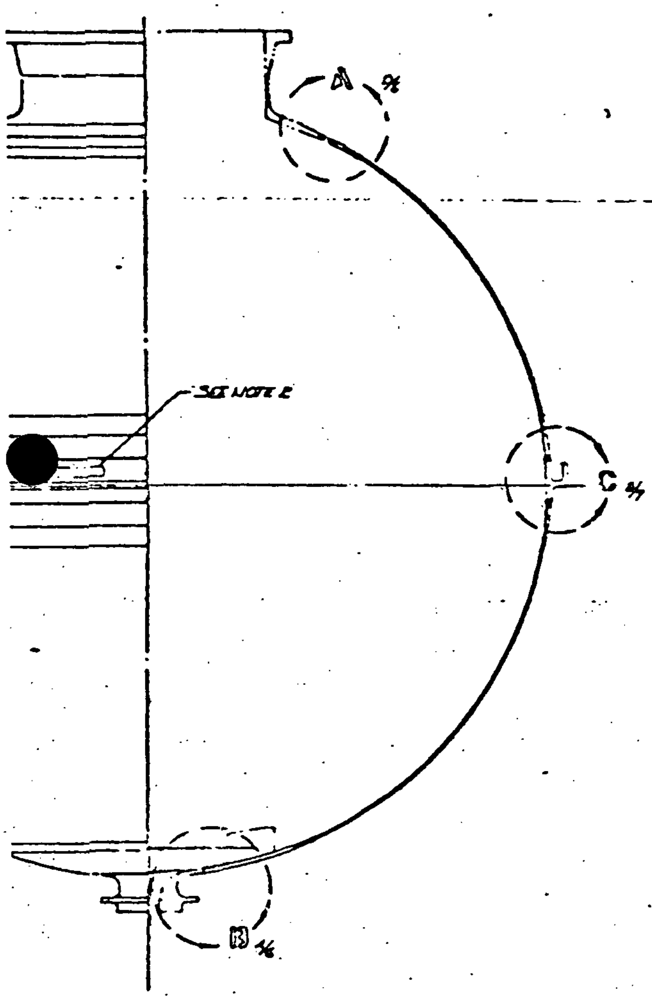

-1 TANK

UT FRAME 2

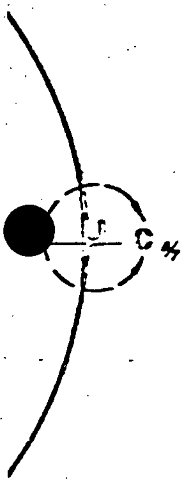

NOTES -

1. IMPRESSION MARKING OF PARTS NOT PERMITTED.
2. IDENTIFY PER 0-70048-83, LOCATE APPROX AS SHOWN.
3. CLEAN OUTSIDE OF TANK TO MEET THE REQUIREMENTS OF 0-73194-3.
4. PENETRANT INSPECT INDICATED WELDS AND OTHER NOTED AREAS PER 0-73176-4.
5. ACCEPT PENETRANT PER 0-770-0-2.
6. RADIOGRAPH INSPECT AREAS SHOWN PER MIL-STD-453.
7. RADIOGRAPH ACCEPT PER WELDING SPEC. ADJUST TRIM DIA AS REQUIRED.

Dimensions: All dimensions are in inches

FOLDOUT FRAME 4

TANK PRESSURIZATION - BASIC

J 14170 073-0072

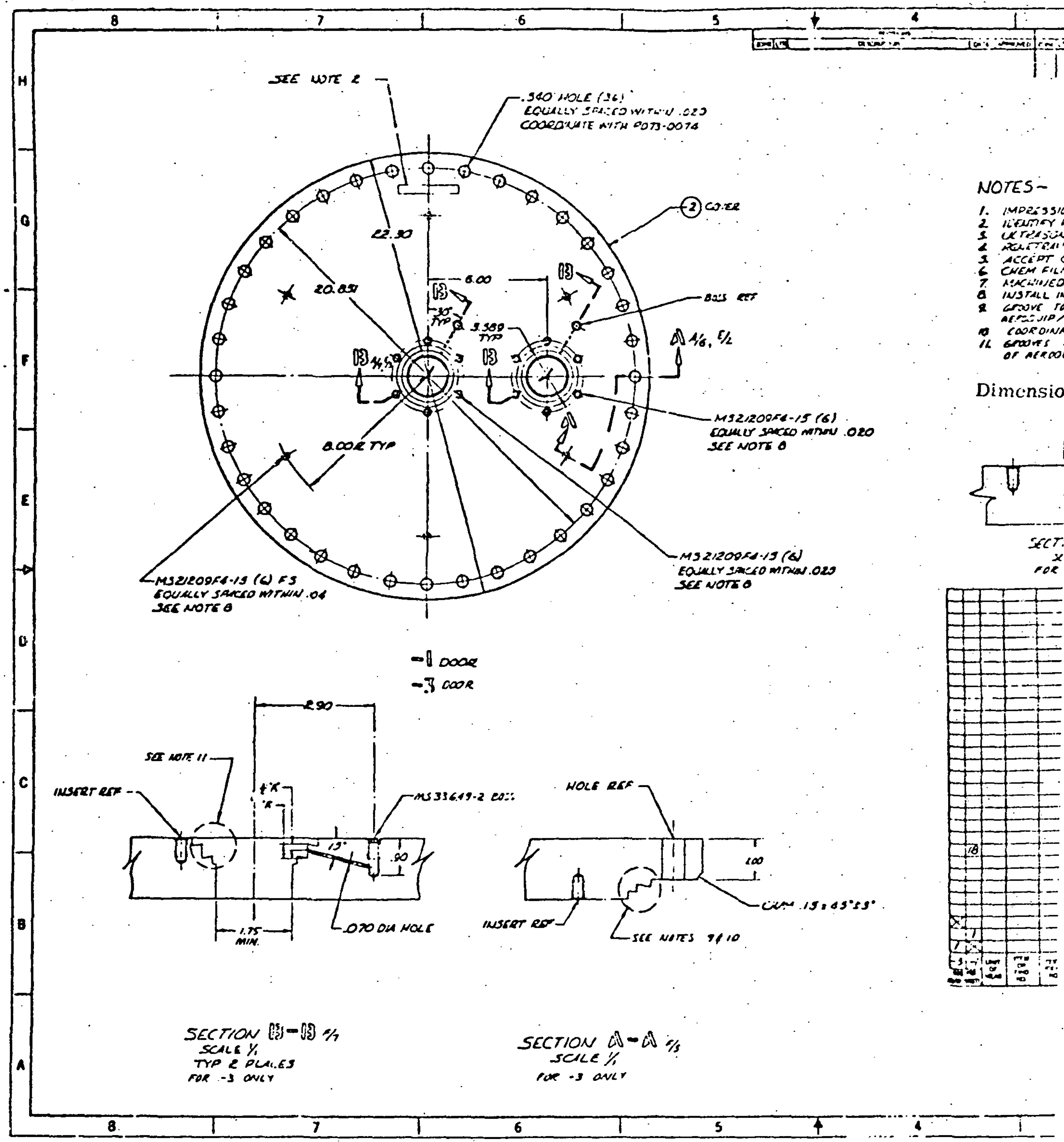

PRECEDING PAGE BLANK NOT FILMED

ORIGINAL PAGE IS
OF POOR QUALITY

FOLDOUT FRAME

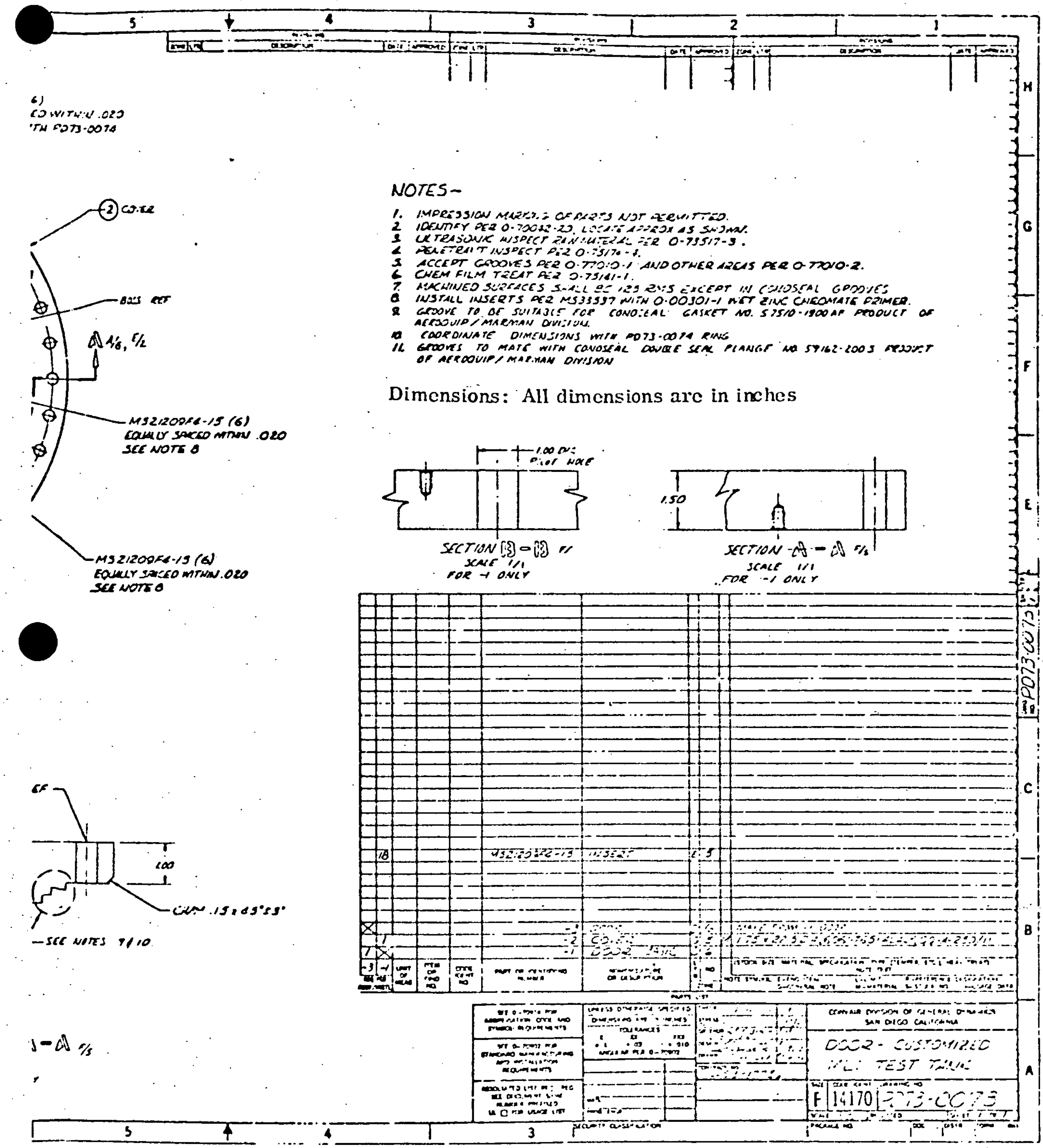

Figure 2-2. Door - Customized MLI Test Tank

(22.30 in). Openings are provided through the door for a fill and drain line, vent line, and electrical pass throughs. The door design uses double Aeroquip/Marman Division Conoseals. The grooves are suitable for Conoseal gaskets No. 57510-1900 AF, also a product of Aeroquip/Marman Division. The dimensions are patented by Aeroquip and are not indicated on the drawing. The grooves are designed for the Conoseal, double seal flange No. 59162-200S, a product of Aeroquip/Marman Division. Thirty-six bolt holts, 0.0137 m (0.540 in) in diameter are equally spaced at a diameter of 0.529 m (20.851 in) to bolt the door to the door ring. The door is designed for an operating pressure of 241.5 kN/m^2 (35 psig) with a leakage rate of less than 1×10^{-6} standard cubic centimeters of helium per second. Due to a bi-metal (al and CRES) condition at the tank to door seal, where dissimilar metal flanges are connected, double conoseals are used to reduce the magnitude of anticipated leaks. The bleed ports, shown in Figure 2-2, Section B-B, F/7 are intended to reduce leakage during transient temperature conditions. These ports are evacuated with an auxiliary vacuum system. The evacuation lines, leading to the outside of the vacuum chamber can be easily isolated and checked for leakage. The purpose of the six inserts shown in Section A-A of Figure 2-2 is to support internal tank equipment or instrumentation such as liquid level sensors and internal heater elements.

The large manhole access door ring is designed to match the contour of the 1.52 m (60 in) tank. The design is shown in Figure 2-3. All dimensions are coordinated with Figure 2-2. The ring has an outside diameter of 0.699 m (27.525 in) and an inside diameter of 0.47 m (18.5 m). The thickness is 0.041 m (1.62 in).

2.1.2 TANK OUTLET CAP. The existing outlet flange was replaced by the tank outlet cap design shown in Figure 2-4. The cap is formed from a 0.00811 m (0.32 in) thick, 6061 aluminum alloy plate to a spherical radius of 0.762 m (30.0 in). The diameter of the plate is 0.214 m (8.432 in).

2.1.3 REMOVAL OF THE TANK SUPPORT RING ASSEMBLY. The existing support ring assembly to be removed from the tank is shown in Figure 2-1. The specific details are given in NASA LeRC drawing CF 620559 (not shown in this document). The ring, 0.046 m (1.81 in) high, 0.01905 m (0.75 in) thick is located at the tank equator at a diameter of approximately 1.60 m (63 in). The modification required a removal of the ring material to approximately 0.00076 m (0.030 in) to the tank equator. This task is shown in Figure 2-5.

2.2 TANK SUPPORT SYSTEM DESIGN

2.2.1 THREE POINT SUPPORT SYSTEM. The tank support system is a three point system designed to suspend the tank inside the cryoshroud. The system consists of three lugs welded to the test tank door ring, three adjustable 304 steel

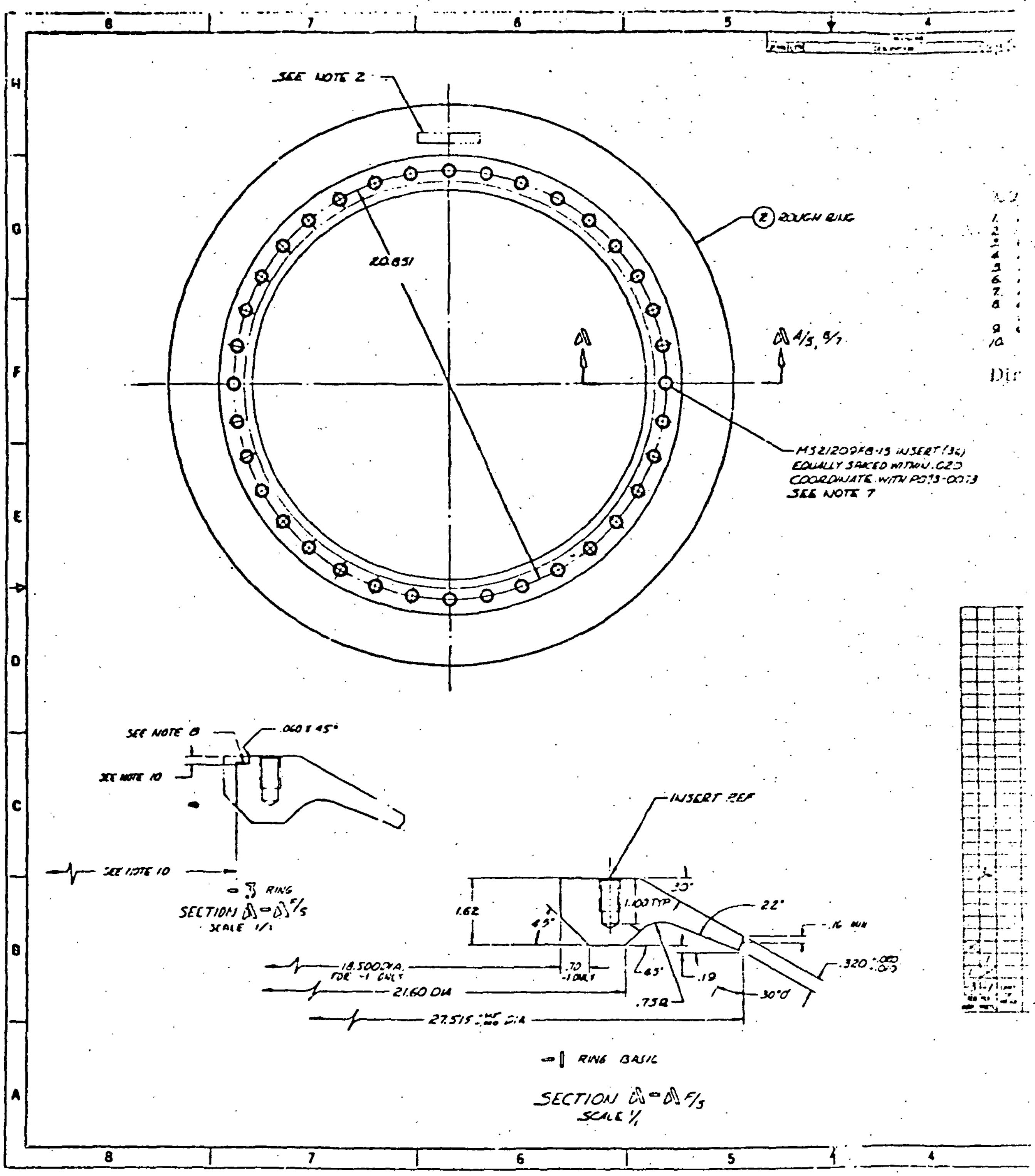

ORIGINAL PAGE IS
OF POOR QUALITY

Figure 2-3. Ring

FOLDOUT FRAME /

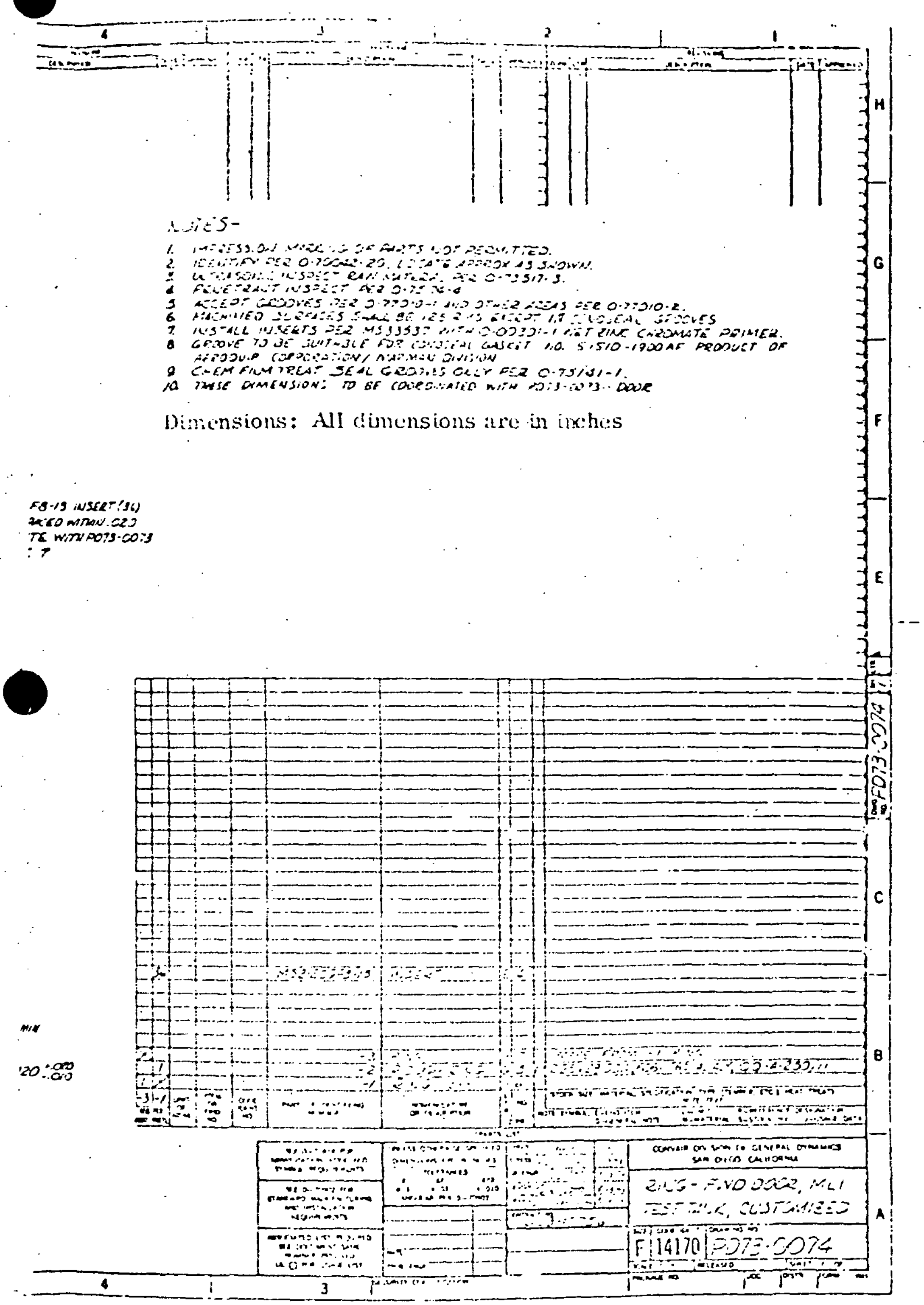

Figure 2-3. Ring - Forward Door, MLI Test Tank

FOLDOUT FRAME 2

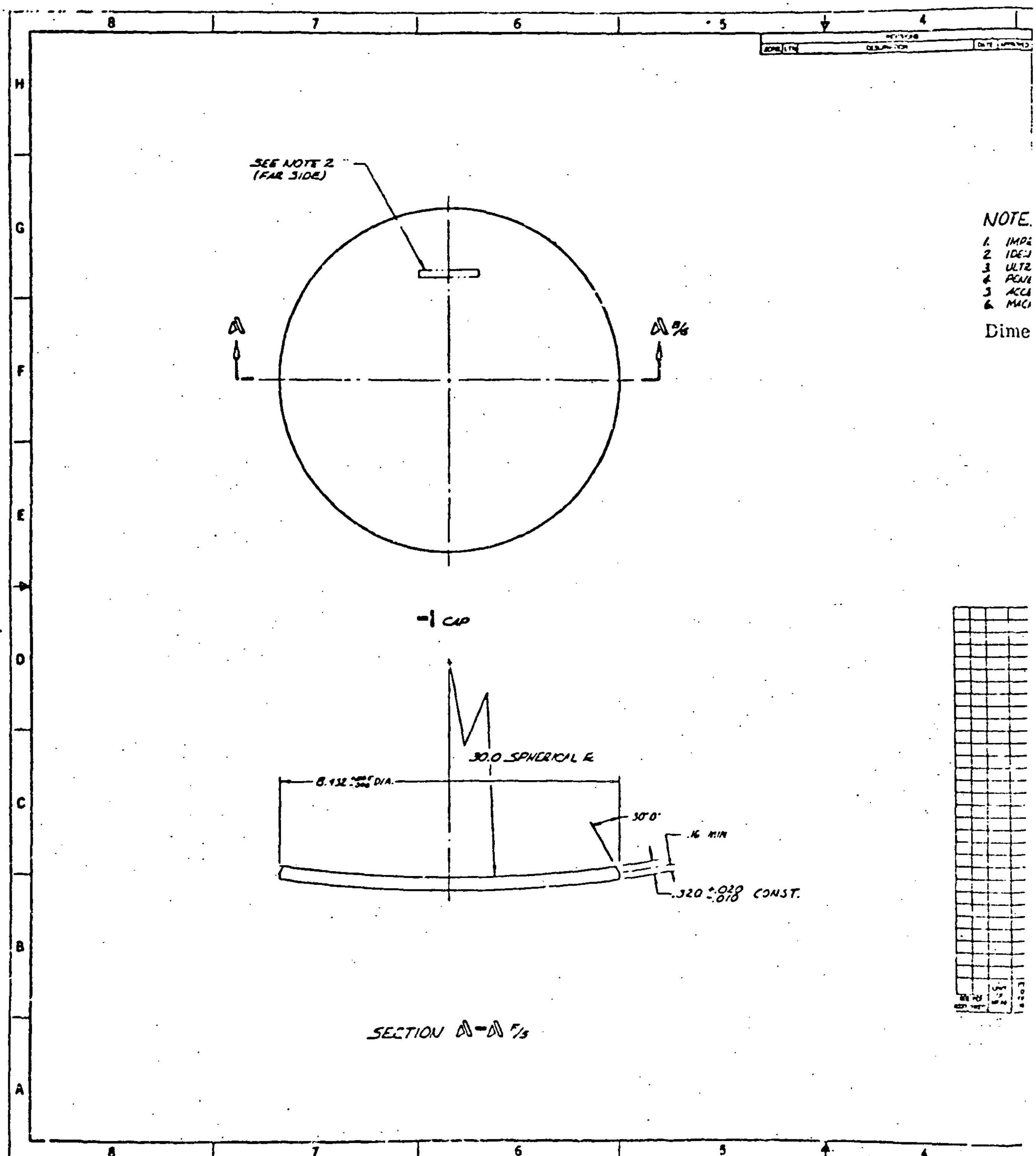

FOLDOUT FRAME /

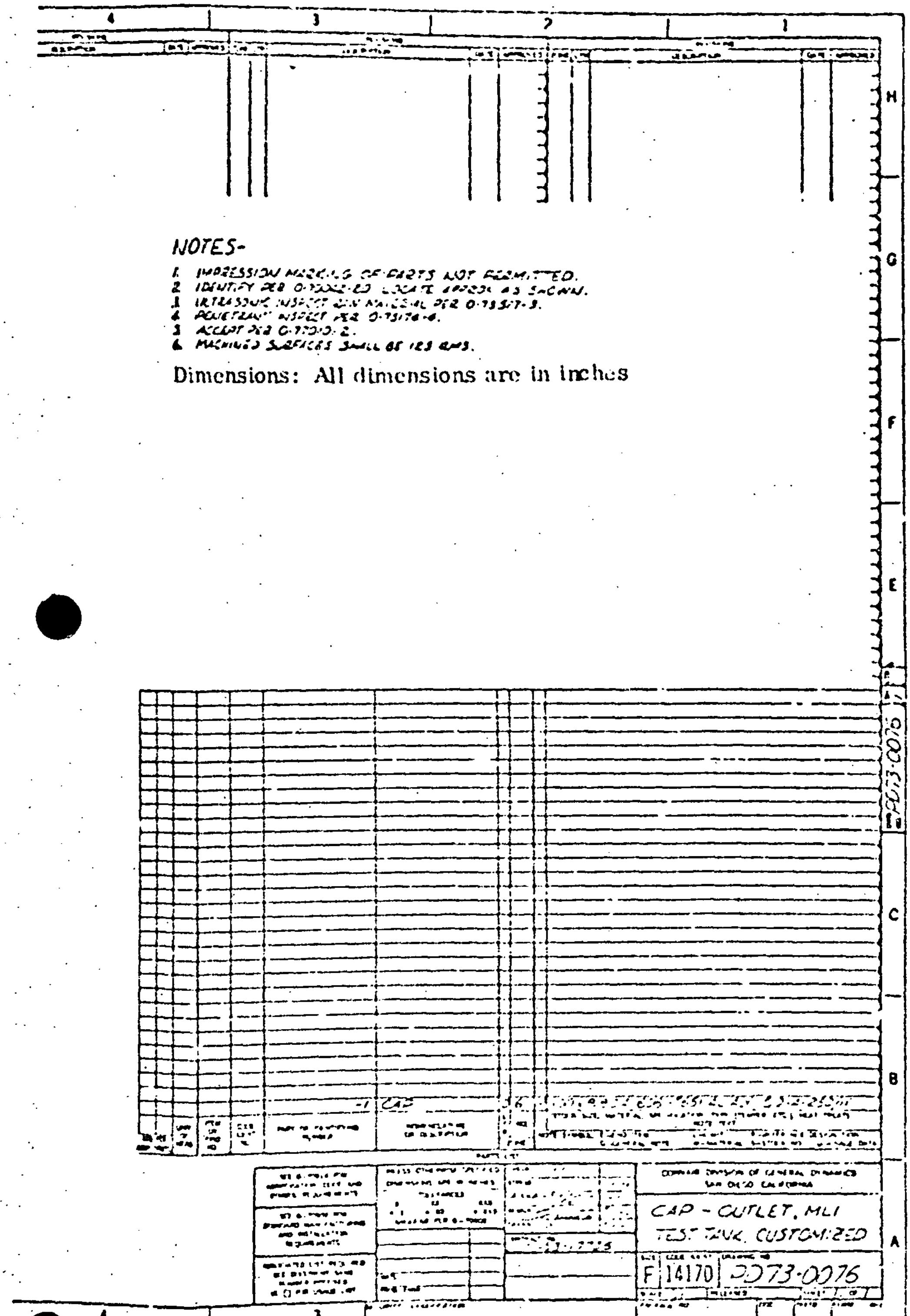

Figure 2-4. ... Outlet MLI Test Tank, Customized

FOLDOUT FRAME 2

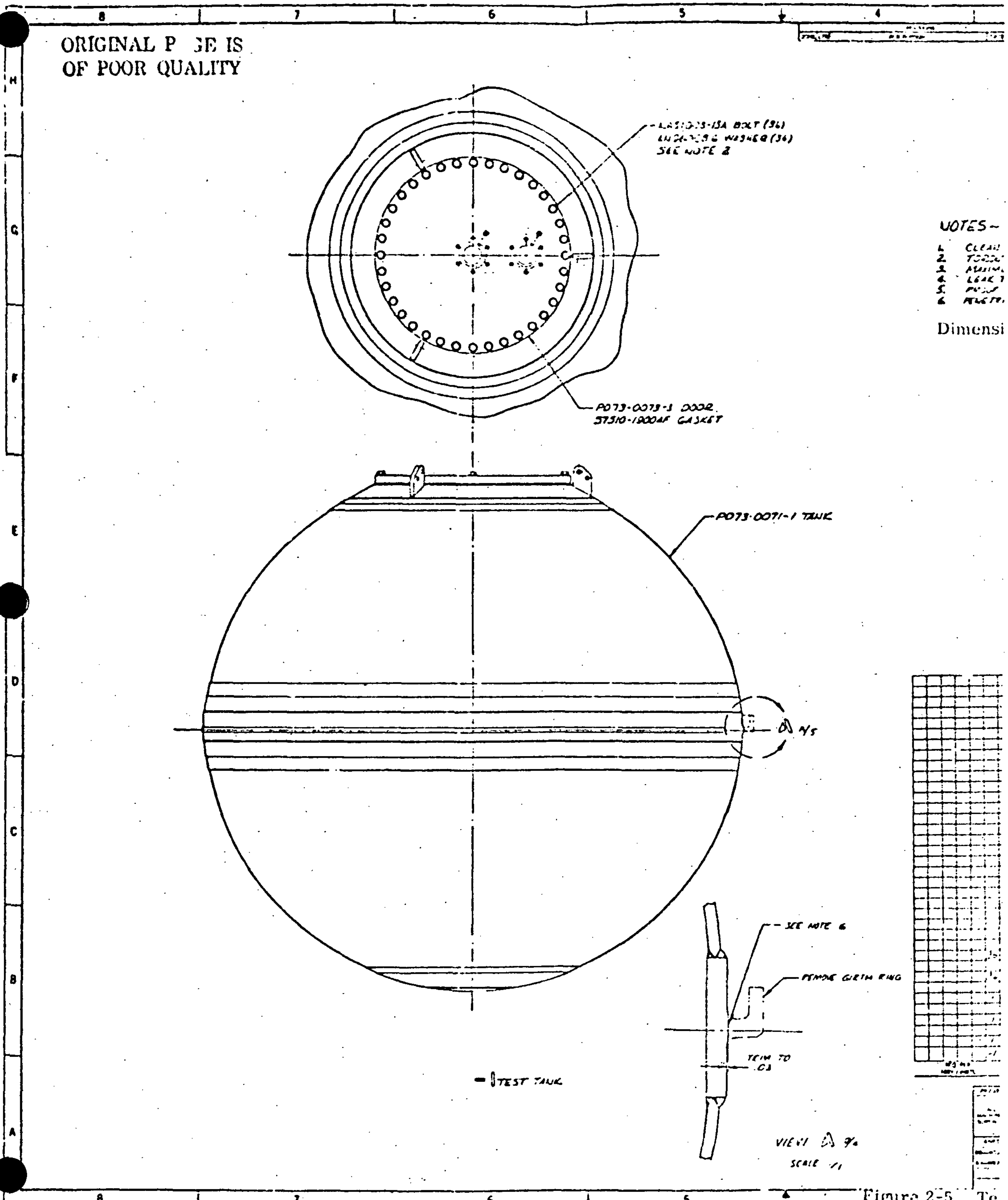
SEE NOTE 2
P073-0073-1 DOOR
P073-0071-1 TANK
NOTES –
Dimensi
SEE NOTE 6
TEST TANK
VIEW A
SCALE

Figure 2-5. Te

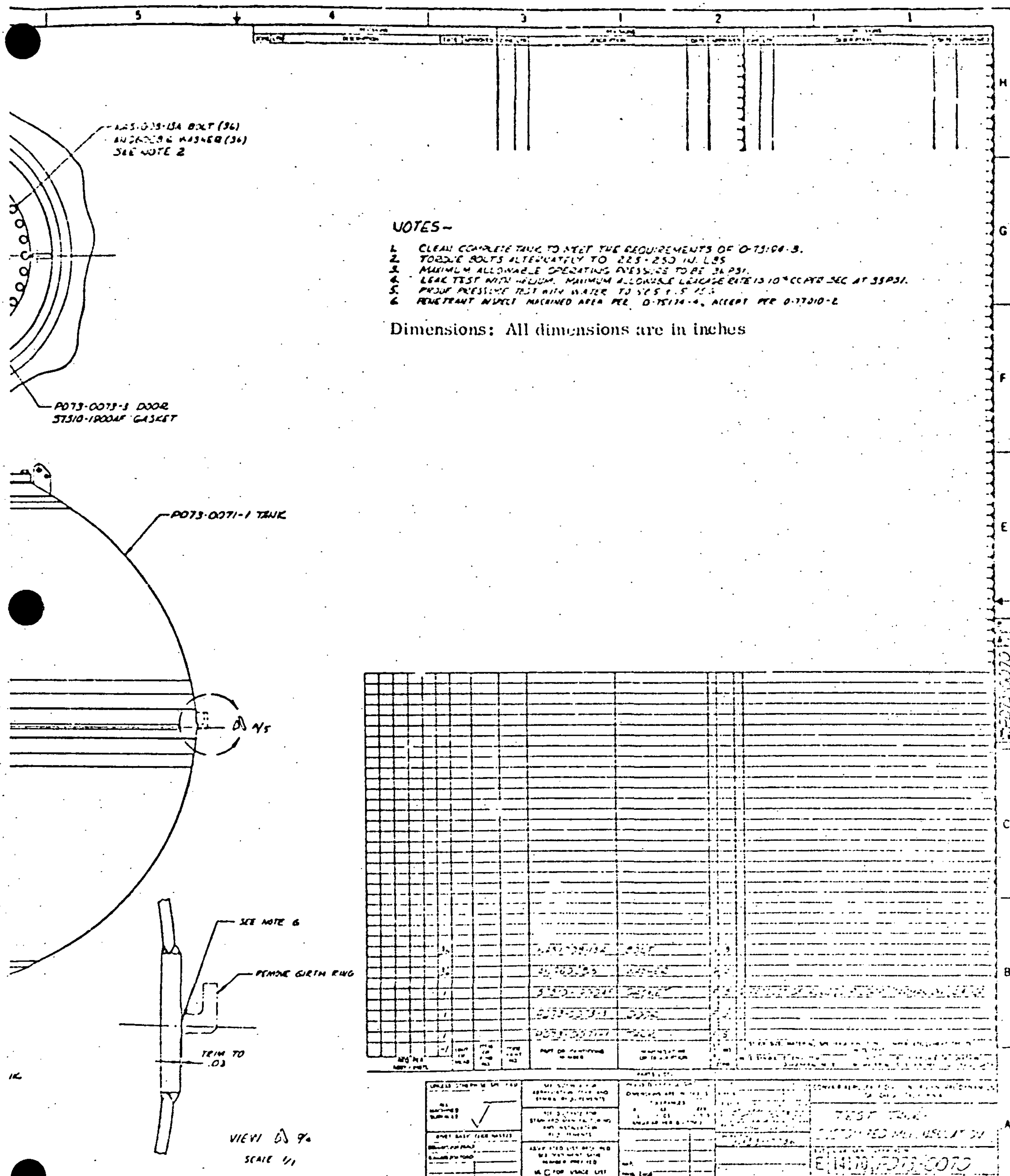

Figure 2-5. Test Tank - Customized MLI

struts, and three attachment fittings welded to the main body of the LH_2 guard tank. This system has a minimum effect on the MLI blanket design and offers practically no interference during the MLI installation.

The support lug is shown in Figure 2-6. These lugs are welded to the door ring after the ring is welded to the tank. The MLI blankets can be easily slit and fitted around each lug. The width of the lug is 0.056 m (2.2 in) and its thickness is 0.013 m (0.5 in).

During the layout phase, it was noted that an auxiliary support was necessary in the tank support lugs to be used in the ground handling. This became apparant when it was noted that the access door would be installed before the cold guard tank was brought into place. Thus the door ring holes could not be used in support handling and a second hole was added. Both holes are equal in size. Figure 2-7 shows the tank with the welded door ring and lugs. In Figure 2-5, the door is mounted to the modified tank.

The basic strut is a threaded steel rod with clevises and lock nuts on both ends. These struts are in effect turnbuckles that can be adjusted during tank installation. The struts used in the design are Merrill Brothers, N. Y., M-16ST 0.013 m × 0.152 cm (0.5 in × 6 in) turnbuckles. The tank is supported from the door itself during insulation installation. During preparation of the tank for installation into the cryoshroud, the cryoshroud lid is positioned above the support beam and the support struts attached. The support struts are attached directly to the LH_2 guard tank structure, which guards the tank fill and drain, vent and electrical lines (Figure 2-8). Thus, the single tank will act as a guard tank for all the test tank penetrations and supports.

2.2.2 "A" FRAME HANDLING AID. During the modification of the tank, the existing tank support is used until the large manhole access door and outlet flange modifications are accomplished. When the large manhole access door ring has been installed, the support of the tank is transferred to the "A" frame handling aid design presented in Figure 2-9. The design consists of a welded steel tube construction except for the aluminum cross channels which support the tank. The usable height of the aid is 1.87 m (73.5 in). The overall height and width is 2.045 m (80.5 in) and 2.29 m (90 in), respectively. The aluminum channels are designed to be removable to permit the transfer of the tank to the top cover and guard tank of the cryoshroud as shown in Figure 2-9.

2.3 STRUCTURAL ANALYSIS OF THE MODIFIED TANK

The purpose of the structural analysis was to verify the capability of the basic test tank and the modification performed by Convair to support the required test loads. The primary concern in the analysis of the modified tank was the combined membrane

ORIGINAL PAGE IS
OF POOR QUALITY

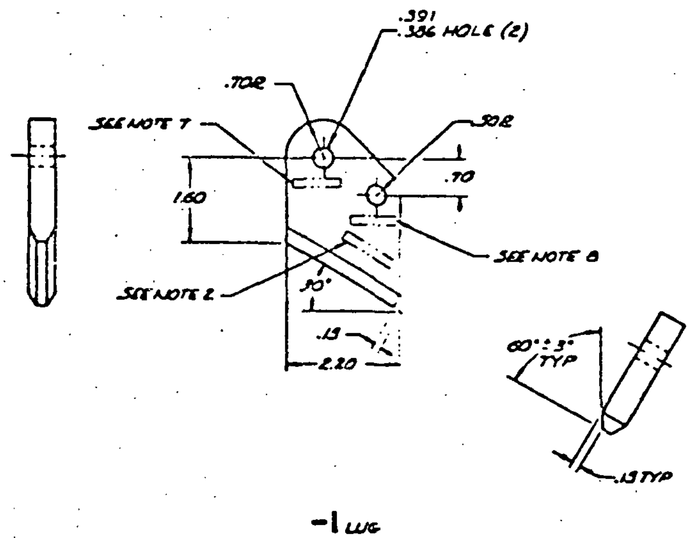

NOTES–

1. IMPRESSION MARK
2. IDENTIFY PER O-7.
3. ULTRASONIC INSP
4. PENETRANT INSP
5. ACCEPT PENETR.
6. MACHINED SURFA
7. STENCIL PER NO.
8. STENCIL PER NO.

Dimensions:

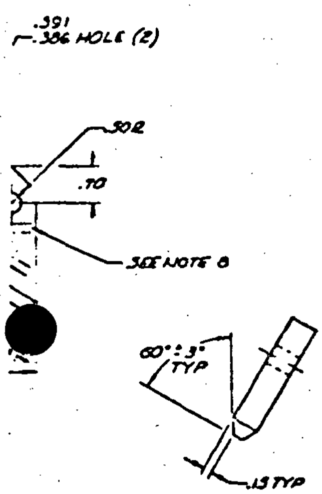

NOTES–

1. IMPRESSION MARKING OF PARTS NOT PERMITTED.
2. IDENTIFY PER 0-73342-20, LOCATE APPROX AS SHOWN.
3. ULTRASONIC INSPECT RAW MATERIAL PER 0-73517-3.
4. PENETRANT INSPECT PER 0-75174-4.
5. ACCEPT PENETRANT PER 0-77010-2.
6. MACHINED SURFACES SHALL BE 125 RMS.
7. STENCIL PER NOTE 2 BOTH SIDES WITH EXACT WORDING–"TEST SUPPORT".
8. STENCIL PER NOTE 2 BOTH SIDES WITH EXACT WORDING–"GROUND SUPPORT".

Dimensions: All dimensions are in inches

-1 LUG

CONVAIR DIVISION OF GENERAL DYNAMICS
SAN DIEGO CALIFORNIA

LUG – TANK SUPPORT,
CUSTOMIZED MLI TEST

F 14170 2073-0075

Figure 2-6. Lug - Tank Support Customized MLI

FOLDOUT FRAME

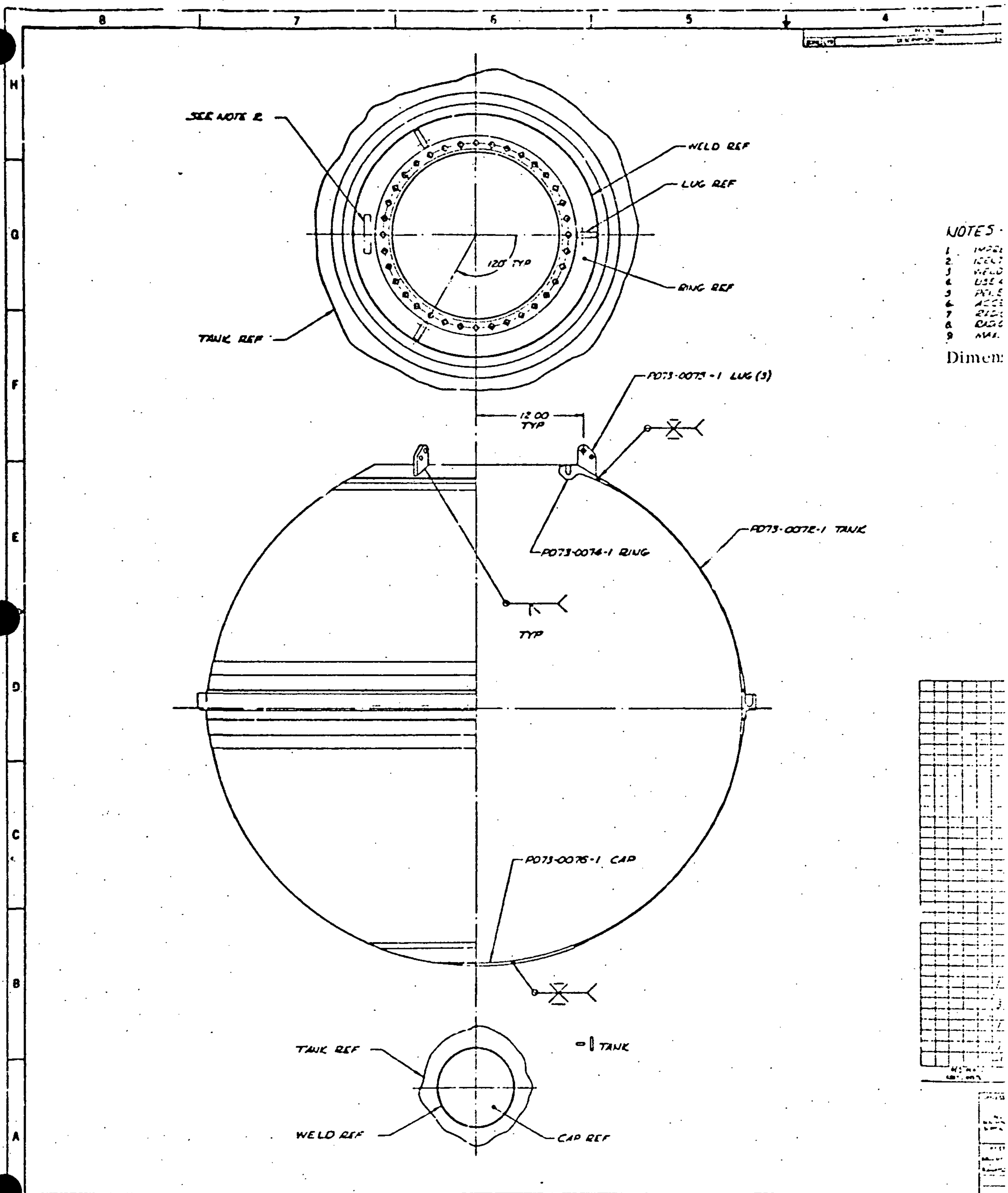

Figure 2-7. Welded Tan

NOTES -

1. IMPRESSION MARKS ON PARTS NOT PERMITTED
2. IDENTIFY PER 0-75532-23, LOCATE APPROX AS SHOWN.
3. WELD PER MIL-W-8604.
4. USE 4043 FILLER ROD.
5. PENETRANT INSPECT ALL WELDS PER 0-75174-4.
6. ACCEPT PENETRANT PER 0-77010-1
7. RADIOGRAPH INSPECT ALL WELDS EXCEPT LUG WELDS PER MIL-STD-453.
8. RADIOGRAPH ACCEPT PER 0-77008-3.
9. MAX. MISMATCH AFTER WELDING SHALL BE .060.

Dimensions: All dimensions are in inches

WELDED TANK - CUSTOMIZED MLI TEST

E14170 PD73-0071

2-. Welded Tank Customized MLI Test

ORIGINAL PAGE IS OF POOR QUALITY

FOLDOUT FRAME 2

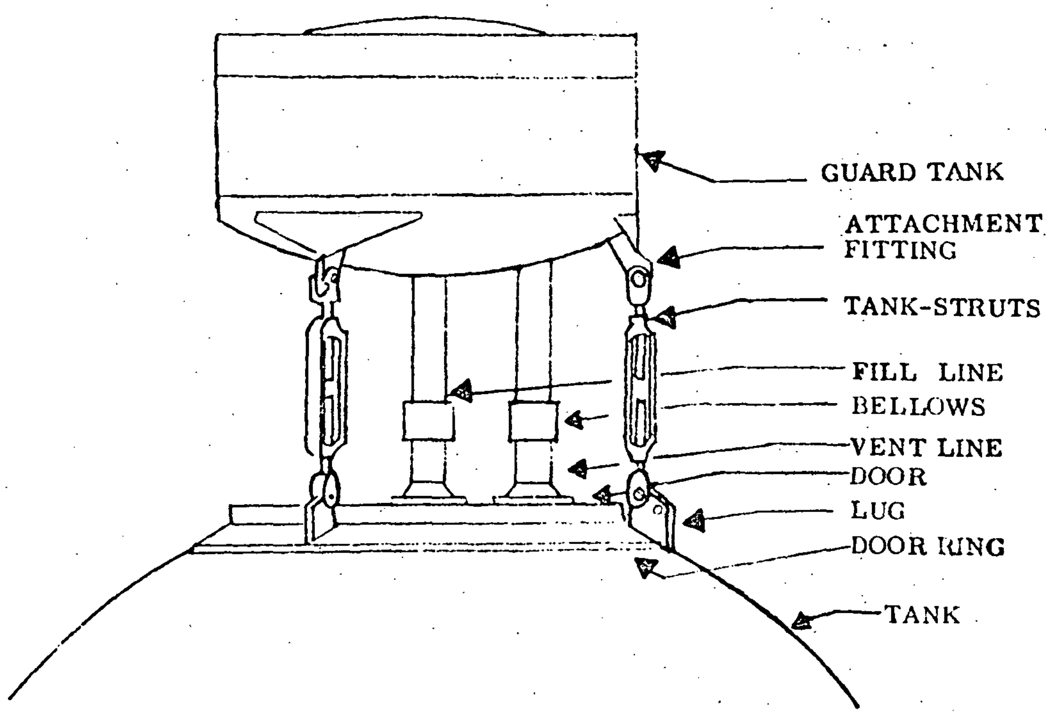

Figure 2-3. Tank Support System Schematic

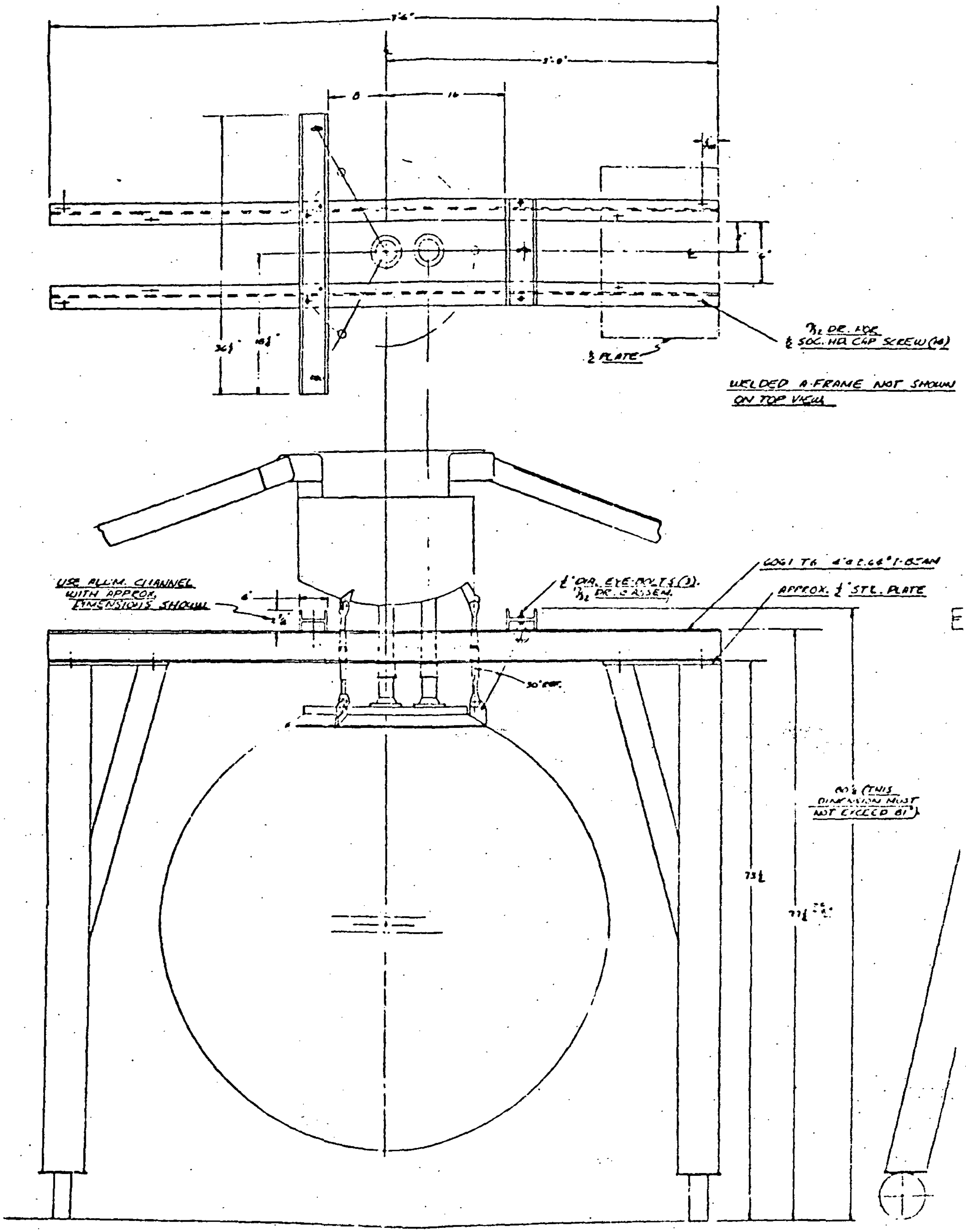

Figure 2-9. "A" Frame Handing Aid

Dimensions: All dimensions are in inches

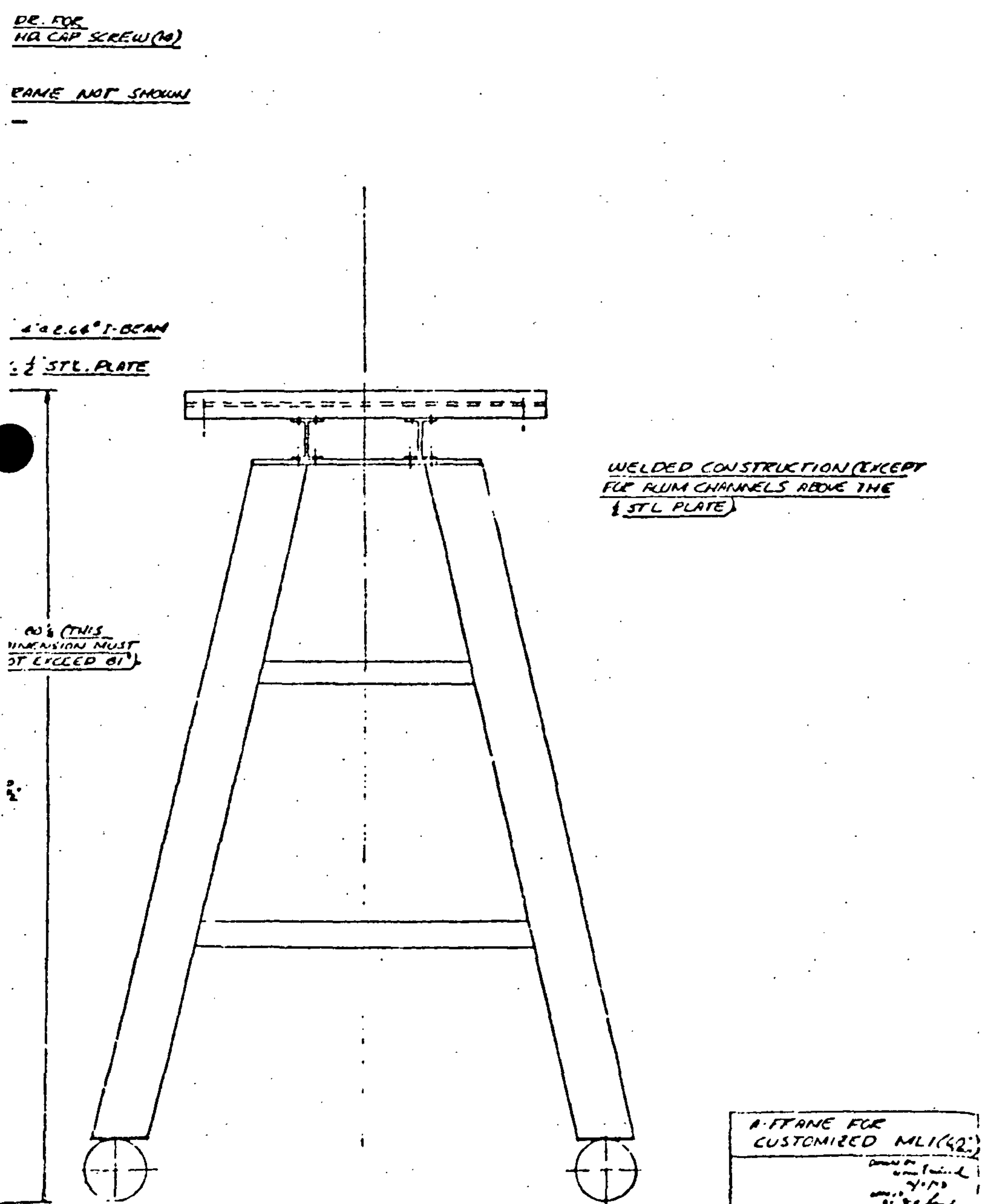

ding Aid

ORIGINAL PAGE IS OF POOR QUALITY

FOLDOUT FRAME 2

and discontinuity stresses in the tank wall near the door. Figure 2-10 shows the new tank components which were analyzed.

2.3.1 DESIGN LOADS. The test tank was originally designed for an operating pressure of 1138.5 kN/m^2 (165 psi) and a proof pressure of 1725 kN/m^2 (250 psi) per NASA Dwg. CF620559.

The modified test tank will be filled with LH_2 at a maximum operating pressure of 241.5 kN/m^2 (35 psig). The analysis was based on the following loads :

1. Internal Pressure

Operating	=	241.5 kN/m^2 (35.0 psig)
Proof	=	363.6 kN/m^2 (52.5 psig)
Burst	=	483.0 kN/m^2 (70.0 psig)

2. Inertia Loads

   2.0g longitudinal combined with ±.5 g lateral acceleration acting on the tank filled with LH_2.

3. Design Weights (Table 2-1)

LH_2	134 kg (295 lb)
Tank Weight	109 kg (238.6 lb)
Actual Weight	251 kg (533.6 lb)
Weight Assumed for Analysis	273 kg (600 lb)

2.3.2 ANALYSIS METHODS. The analysis was an investigation of the combined membrane and discontinuity stresses in the tank wall near the door. To accurately establish stresses in this region, a detailed computerized analysis was required. The actual analysis performed on the 1.52 m (60 in) test tank was limited due to the following considerations:

1. The tank was originally sized for an operating pressure of 1138.5 kN/m^2 (165 psig). The maximum test pressure is 241.5 kN/m^2 (35 psig). This pressure is less than 1/4 of the original pressure. Therefore, extremely conservative methods can be used to estimate discontinuity stresses and still show a positive margin of safety.

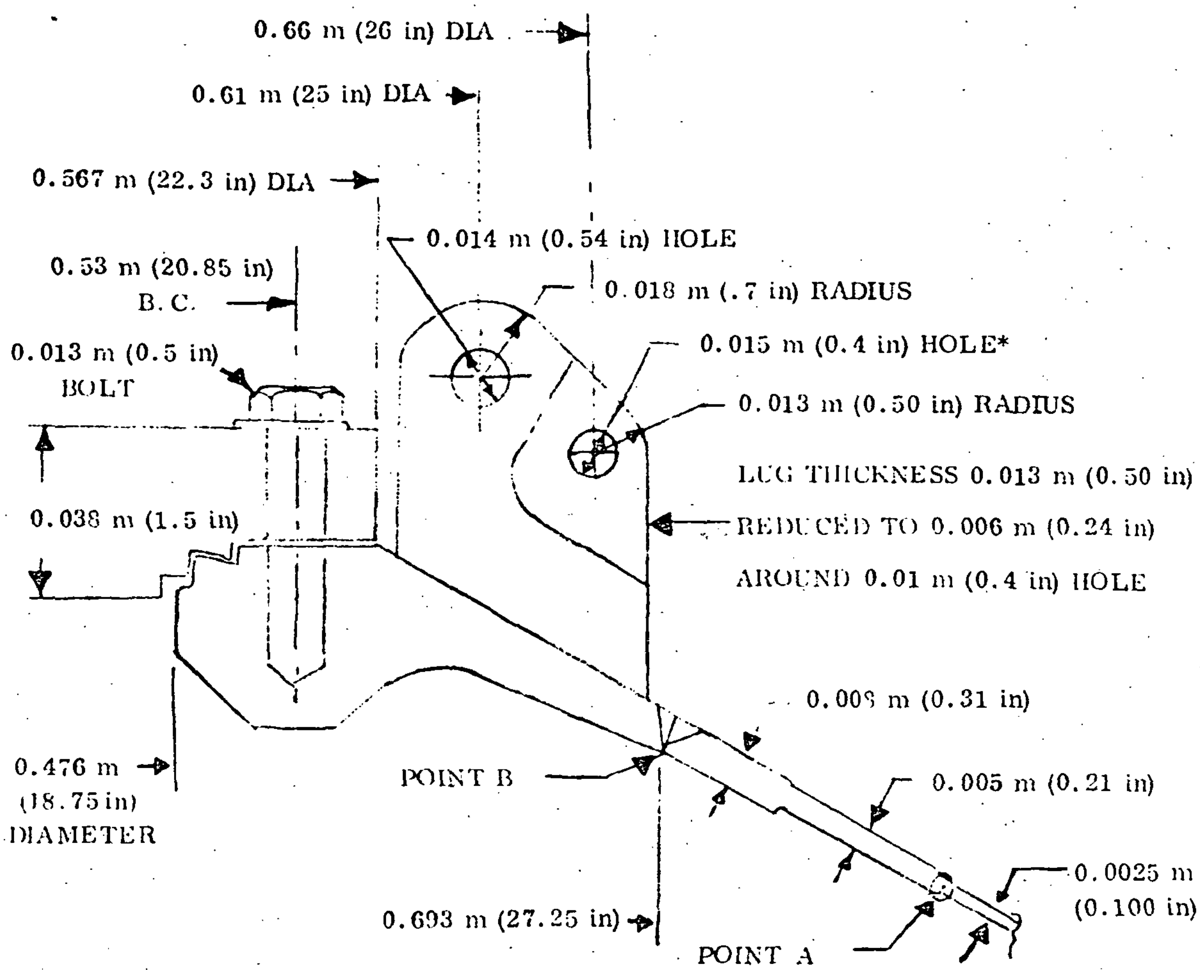

Figure 2-10. Large Manhole Access Door Ring and Lug of 1.52 m (60 in) Tank

*During fabrication of the lug the hole diameter was increased to 0.013 m (0.50 in)

2. A tank of similar geometry, the 1.38 m (54.5 in) diameter methane tank was analyzed in detail under a NASA Contract NAS3-14105 in 1970, Reference 2-1. Results of that analysis were used to predict stresses in the 1.52 m (60 in) diameter test tank.

The test tank analysis includes:

a. Door Ring Discontinuity Analysis

b. Door & Door Attachment Analysis

c. Tank Support Analysis

2.3.3 MATERIAL ALLOWABLES. The entire tank is fabricated from 6061-T6 Aluminum. The room temperature design mechanical properties for this material are:

Parent Material ("A" values, MIL-HDBK-5A, Reference 2-2)

Ultimate Strength F_{tu} = 289.8×10^3 kN/m^2 (42×10^3 psi)

Yield Strength F_{ty} = 241.5×10^3 kN/m^2 (35×10^3 psi)

ULT Shear F_{su} = 248.4×10^3 kN/m^2 (36×10^3 psi)

Modulus of Elasticity E = 69×10^6 kN/m^2 (10×10^6 psi)

Welded Joint (Reference 2-3)

F_{tu} (0.57) $(289.8 \times 10^3) = 165.2 \times 10^3$ kN/m^2 (24×10^3 psi)

F_{ty} = (0.38) $(289.8 \times 10^3) = 110.2 \times 10^3$ kN/m^2 (16×10^3 psi)

F_{su} = (0.34) $(289.8 \times 10^3) = 98.5 \times 10^3$ kN/m^2 (14×10^3 psi)

E = 69×10^6 kN/m^2 (10.0×10^6 psi)

2.3.4 DOOR RING DISCONTINUITY ANALYSIS. The large manhole access door ring discontinuity analysis was based on membrane point "A", Figure 2-10. The corresponding point for the methane tank is point 55 from the methane tank analysis (Reference 2-1, Page 18 and 40). The meridianal membrane stress calculated for point

55, Ref. 2-1, page 18, was 253.6×10^3 kN/m^2 (36,752 psi). The meridianal membrane stress for the 1.52 m (60 in) tank becomes

$$\sigma_{\phi} = 0.75\ (253.6 \times 10^3 = 190.2 \times 10^3 \text{ kN/m}^2 \text{ (27564 psi)}$$

where 0.75 is the r/t ratio for the two tanks and the total stress $\sigma_{\phi} = 197.9 \times 10^3$ kN/m^2 (28656 psi) from reference 2-1, page 40, including discontinuity stress. The total stress ratio is given by

$$\text{Ratio} = 197.9/190.2 = 1.04$$

The discontinuity stress is therefore 4% of the membrane stress for the methane tank. Conservatively, this stress was doubled. For the 1.52 m (60 in) test tank

$$\sigma_{\phi \text{ proof pressure}} = 1.08\ PR/2t$$

$$\sigma_{\phi \text{ proof pressure}} = \frac{(1.08)\ (363.6)\ (0.76)}{(2)\ (2.29 \times 10^{-3})} = 65.2 \times 10^3 \text{ kN/m}^2 \text{ (9450 psi)}$$

and

$$\sigma_{\phi \text{ burst}} = \frac{(1.08)(483.0)(0.76)}{(2)\ (2.29 \times 10^{-3})} = 86.6 \times 10^3 \text{ kN/m}^2 \text{ (12600 psi)}$$

where

P = pressure, kN/m^2 (psi)

R = radius, m (in)

t = thickness, m (in)

The margin of safety is then

$$\text{M.S. (Proof)} = \frac{F_{ty}}{\sigma_{\phi} \text{ Proof}} - 1 = \frac{241.5 \times 10^3}{65.2 \times 10^3} - 1 = +2.70$$

and

$$\text{M.S. (Burst)} \frac{F_{tu}}{\sigma_{\phi} \text{ Burst}} - 1 = \frac{289.8 \times 10^3}{86.6 \times 10^3} - 1 = +2.35$$

These margins of safety are adequate.

2.3.5 <u>DOOR RING TO TANK WELD ANALYSIS.</u> Figure 2-10, Point "B", was used for this analysis. The corresponding point for the methane tank is Point 24 (Reference 2-1). The meridianal membrane stress was calculated using the methane tank analysis presented in Reference 2-1. The membrane stress for the 1.52 m (60 in) tank becomes:

$$\sigma_{\phi} = 44.2 \times 10^3 \text{ kN/m}^2 \text{ (6416 psi)}$$

and the total stress $\sigma_{\phi} = 95.2 \times 10^3 \text{ kN/m}^2$ (13788 psi)

the resulting stress ratio becomes:

$$\text{Ratio} = 95.2/44.2 = 2.15$$

The discontinuity stress is therefore 115% of the membrane stress for the methane tank. Conservatively this stress was doubled for the 1.52 m (60 in) tank. The total stress is therefore

$$\sigma_{\phi} = (1)\ PR/2t + 2(1.15)\ PR/2t = 3.3\ PR/2t$$

For the proof pressure:

$$\sigma_{\phi}\text{ Proof} = \frac{(3.30)(363.6)(0.76)}{(2)\ (7.62 \times 10^{-3})} - 60.0 \times 10^3 \text{ kN/m}^2 \text{ (8670 psi)}$$

and for the burst pressure

$$\sigma_{\phi} = \frac{(3.30)(483.0)(0.76)}{(2)\ (7.62 \times 10^{-3})} - 79.4 \times 10^3 \text{ kN/m}^2 \text{ (11550 psi)}$$

the margin of safety is then:

$$\text{M.S. (Proof)} = \frac{110.2 \times 10^3}{60.0 \times 10^3} - 1 = +0.84$$

$$\text{M.S. (Burst)} = \frac{165.2 \times 10^3}{79.4 \times 10^3} - 1 = +1.08$$

The safety margins are adequate.

2.3.6 DOOR ANALYSIS. The large manhole access door is conservatively analyzed by using a simply supported circular plate (Figure 2-11).

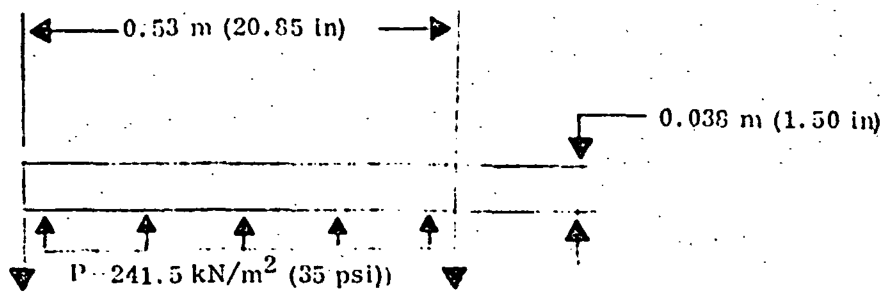

Figure 2-11. Simply Supported Circular Plate

The total applied load W, from Reference 2-4, page 2-16 is given by the equation

$$W = w \pi a^2 = 241.5 \pi (0.265)^2 = 53.3 \text{ kN (12000 lb)}$$

where

w = unit applied load kN/m^2 (lb/in^2)

a = area, m^2 (in^2)

The maximum unit stress at the center of the plate is then from Reference 2-4, page 2-16:

$$\sigma_{max} = \frac{3W}{8 \pi m t^2} (3m + 1) = 14.6 \times 10^3 \text{ kN/m}^2 \text{ (2120 psi) (operating pressure)}$$

where

m = reciprocal of ν Poisson's ratio = 3; ν = 1/3

t = thickness of plate, 0.035 m (1.5 in)

The margin of safety for the operating pressure becomes:

$$M.S._{\text{Operating}} = \frac{241.5 \times 10^3}{14.6 \times 10^3} - 1 = 15.54$$

and the margin of safety for the proof pressure:

$$M.S._{Proof} = \frac{241.5 \times 10^3}{(1.5)(14.6 \times 10^3)} - 1 = 11.03$$

The margin of safety factors are large for both the operating and proof pressures.

2.3.7 DOOR ATTACHMENT BOLT. The large manhole access door is attached to the tank with (36) 0.013 m (0.5 in) diameter bolts. The bolt attachment is shown in Figure 2-12.

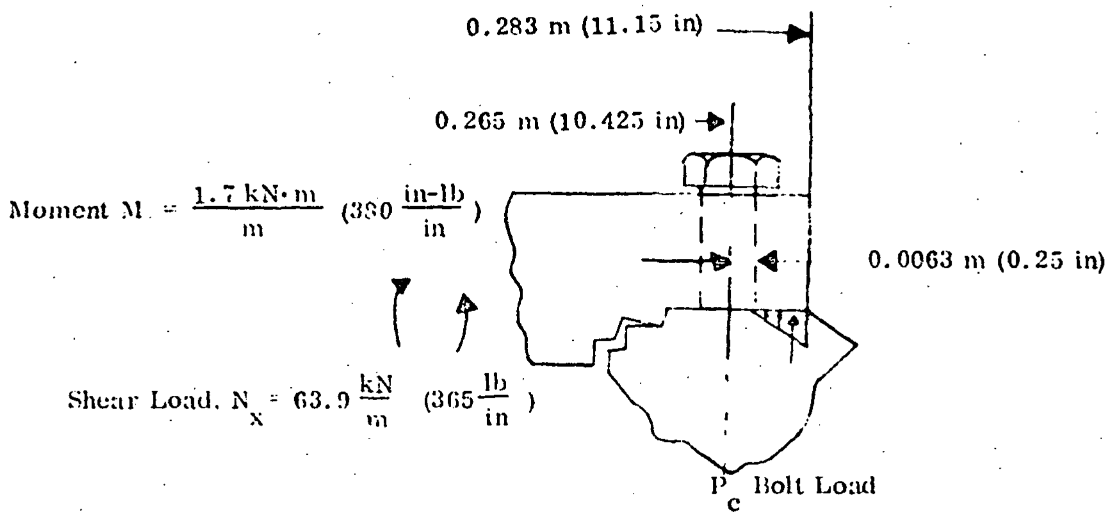

Figure 2-12. Bolt Attachment

Based on the methane tank analysis (Reference 2-1, Pg. 53), the fully-fixed edge moment is 1.65 m · kN/m (371 in-lb/in). Actual edge moment is 0.66 m · kN/m in-lb/in). The moment ratio is then 0.66/1.65 = 0.40.

To analyze the 1.52 m (60 in) test tank door attachment, it was assumed that the actual door edge fixing moment is 0.40 times the fully fixed moment.

$$\text{Fully fixed moment} = \frac{PR^2}{8} = \frac{(241.5)(0.265)^2}{8} = \frac{2.13 \text{ kN}\cdot\text{m}}{\text{m}}$$

(475 in-lb/in) (operating p)

and actual edge moment for the operating pressure = $\frac{0.848 \text{ kN}\cdot\text{m}}{\text{m}}$ $(190 \frac{\text{in-lb}}{\text{in}})$

and for the burst pressure = $\frac{1.69 \text{ kN}\cdot\text{m}}{\text{m}}$ $(380 \frac{\text{in-lb}}{\text{in}})$

The shear loading N_x for the operating pressure can be calculated from the expression

$$N_{x,\text{Operating}} = \frac{PR}{2} = 31.9 \text{ kN/m } (182.5 \text{ lb/in})$$

and the shear loading for the burst pressure becomes

$$N_{x,\text{Burst}} = 63.9 \text{ kN/m } (365 \text{ lb/in})$$

The load P_c at the center of the bolt is evaluated as follows:

$$P_c = 117. \text{ kN/m } (670 \text{ lb/in})$$

The bolt spacing = 0.046 m (1.82 in)

and the ultimate bolt load = 8.38 kN (1880 lb)

The allowable load from Reference 2-2 is 107.8 kN (24190 lb)

The resulting margin of safety

$$M.S. = \frac{107.8}{8.38} - 1 = +11.9$$

The value of 11.9 represents a large margin of safety.

2.3.8 TANK SUPPORT ANALYSIS. During hoisting and handling of the tank 0.010 m (0.400 in) diameter holes in the three lugs will be used (Figure 2-6. Design limit load factors for handling are 2.0g longitudinal and 0.5 g lateral. The empty handling weight of the tank is approximately 1.34 kN (300 lb). The vertical load/lug = 0.89 kN (200 lb) (limit).

It is assumed that the entire side load acts on one lug.

Therefore the side load/lug = 0.67 kN (150 lb) (limit)

The loads acting on the lug are shown in Figure 2-13

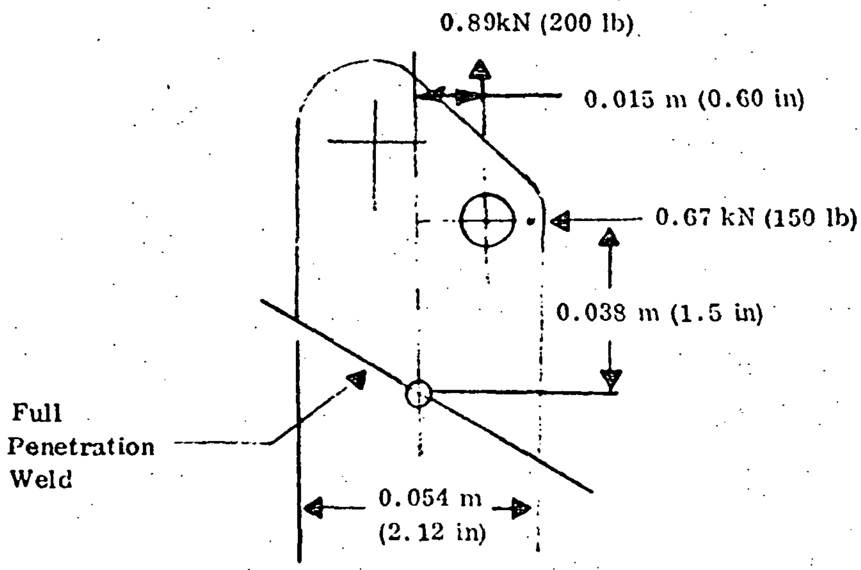

Figure 2-13. Loads Acting on Lug

Lug Bearing

The total lug bearing load becomes:

$$P_{TOT} = \sqrt{(.89)^2 + (.67)^2} = 1.1 \text{ kN } (250 \text{ lb})$$

and the ultimate bearing stress is therefore

$$F_{bru} = \frac{(3.0)\ (1.1)}{61.9 \times 10^{-6}} = 53.3 \times 10^3 \text{ kN/m}^2 \ (7820 \text{ psi})$$

A handling safety factor of 3 was used in this equation.

The bearing area was calculated to be 61.9×10^{-6} m^2 (0.096 in^2). The bearing stress of 53.3×10^3 kN/m^2 (7820 psi) is not critical.

Lug Tear Out

The shear area was conservatively calculated to be 9.3×10^{-5} m^2 (0.144 in^2). The applied shear strength becomes

$$F_{applied} = \frac{(3.0\ (1.1)}{9.3 \times 10^{-5}} = 35.5 \times 10^3 \text{ kN/m}^2 \text{ (5200 psi)}$$

The ultimate shear allowable for 6061-T6 material is

$$F_{su} = 241.5 \times 10^3 \text{ kN/m}^2 \text{ (35000 psi)}$$

Therefore the margin of safety is

$$M.S. = \frac{241.5 \times 10^3}{35.5 \times 10^3} - 1 = +5.80$$

The margin of safety is large.

Lug Welding

The moments around the center of the lug welding base are calculated as follows:

$$M = (0.89)(0.015) + (0.67)(0.038) = 0.039 \text{ kN} \cdot \text{m (345 in-lb)}$$

The maximum stress $F_{t_{max}}$ is given by

$$F_{t_{max}} = \frac{P}{A} + \frac{Mc}{I} = 7.6 \times 10^3 \text{ kN/m}^2 \text{ (1109 psi)}$$

where

P = vertical load, kN (lb)

A = weld area, m^2 (in^2)

M = moment, N$\cdot$m (in-lb)

c = weld distance, m (in)

I = moment of inertia, m^4 (in^4)

Assuming $F_{tw} = 165.6 \times 10^3$ kN/m^2 (24×10^3 psi) for 6061-T6 as welded, the margin of safety:

$$M.S. = \frac{165.6 \times 10^3}{3\ (7.6 \times 10^3)} - 1 = 6.26$$

The margin of safety for the lug to tank weld is also large.

3

FABRICATION OF TEST TANK MODIFICATION AND TANK SUPPORT SYSTEM

3.1 TEST TANK MODIFICATION

The modification of the test tank was initiated by establishing a manufacturing sequence as shown in Table 3-1. The individual tasks consisted of:

1. Preparing the tank for welding of the large manhole access door ring and tank outlet cap.

2. Machining of the manhole access door, door ring, tank outlet cap and tank support lugs.

3. Welding of the tank outlet cap inside and outside of the tank.

4. Welding of the manhole access door ring inside and outside of the tank.

5. Welding of the support lugs onto the tank.

6. Removal of the existing conical support (girth flange) assembly.

The inspection methods included dye penetrant and radiography. It was employed selectively as judged necessary. A new handling "A" frame was fabricated to support the modified tank.

3.1.1 <u>PREPARATION OF TANK.</u> The existing anti-vortex baffles, screen assembly and temperature patch harnessing were removed before the tank was externally cleaned. The removal of the COSMOLENE created a cleaning problem. Convair was not in possession of a tank large enough to chemically degrease the tank. Consequently the tank was cleaned by hand.

Preliminary x-rays were taken at the manhole access door ring and the outlet cap areas. The door ring area, adjacent to the weld appeared clean. The tank outlet area, adjacent to the weld contained tungsten and foreign material throughout. The tank was placed into the "King Boring Mill" to cut the openings for the door ring and tank outlet cap.

Table 3-1. 1.52 m (60 inch) Tank Modification Sequence

Operation

1 Preparation of Tank for Welding

- Removal of interior hardware (antivortex baffles, screen and temperature patch harnessing)
- Cleaning of tank
- Inspection
- Retain tank in NASA support, removal of casters
- Transportation of tank to King Boring Mill
- Large manhole access door boring operation
- Tank outlet cap boring operation
- Inspection
- Transportation of tank to weld lab

2 Fabrication of Large Manhole Access Door and Door-Ring

- Ultrasonic inspection of material
- Machining of door and door ring and Conoseal grooves
- Inspection

3 Fabrication of Tank Outlet Cap

- Ultrasonic inspection of material
- Sawing of material
- Machining of tank outlet cap
- Inspection

Table 3-1. 1.52 m (60 inch) Tank Modification Sequence (Cont'd)

Operation

4 Fabrication of Tank Lugs

- Layout/sawing of material
- Milling/drilling
- Inspection

5 Welding of Tank Outlet Cap – Inside

- Positioning of tank on side for easy entry of welder
- Setting up for inside welding
- Fabrication of LN_2 immersion cryogenic fixture tank
- Welding of closure root
- X-raying and repairing if necessary

6 Welding of Tank Cap Outlet – Outside

- Tank in same position as Operation 5
- Setting up for external weld
- Completion of weld
- Dye inspection, x-raying, and repairing if necessary

Table 3-1. 1.52 m (60 inch) Tank Modification Sequence (Cont'd)

Operation

7 Welding of Manhole Access Door Ring - Inside

- Rebolting of original manhole access door fitting, inversion of tank
- Setting up for inside welding
- Welding of new manhole access door ring root
- X-raying and repairing if necessary

8 Welding of Manhole Access Door Ring - Outside

- Tank in upright position
- Setting up for external welding

9 Welding of Lugs Onto Tank

- Setting up and welding
- Inspection

10 Removal of Existing Conical Support Assembly

- Modifying of an existing machining fixture
- Removal of conical support
- Grinding of surface
- Mounting of tank to new "A" frame support

The existing large manhole access door ring was removed by making a cut of approximately 0.018 m (0.7 in) beyond the previous ring weld. Unforeseen severe distortions due to the previous (original) weld were encountered in cutting out the original door ring. The total dial indicated vertical runout of the tank wall material at the cutout was 0.0114 m (0.450 in). This greatly exceeded the 0.0015 m (0.064 in) permissible runout according to the military specification for welding the 0.008 m (0.320 in) thick joint. The underside of the upper cutout showed a variation of the original weld thickness, weld repair areas and heavy weldments nearby an internal probe (Figure 3-1). These were contributing factors to the tank distortion.

A combination of mechanical and machining techniques were used to reduce the runout and related mismatch to satisfactory levels. For distortion correction the tank was moved from the King Boring Mill to the Bullard Mill. Reliable measurements of the cutout dimensions could not be achieved until vibration of the tank during cutting was eliminated. This required the fabrication of a spool-like internal support and addition of 12 steel blocks between the tank and the holding fixture at the location of the conical tank support. Both of these internal and external supports had to be augmented by extensive use of Tooling Stone (casting plaster for rigidizing a part during machining). The runout thickness variation after the improvement is shown in Table 3-2.

A shallow 0.0005 m (0.020 in) cut was made by taper technique on the outside shoulder of the tank next to the cutout. A total of 0.0009 m (0.035 in) material was finally removed to reduce the wall thickness to the required 0.00812 m (0.34 in) max./0.0079 (0.310 in) minimum dimension. The diameter of the cutout was increased to the final dimensions of 0.648 m (27.294 in). This dimension which was used to fabricate the door ring was checked by the Convair Quality Control department.

The tank outlet cap bore was accomplished using the same Bullard machine tool. Only minor distortions were experienced and no straightening of the tank was required.

Figure 3-2 shows the cutout of the manhole access door ring. Figure 3-3 indicates the cutout area distortion. Note the difference in thickness at various locations of the cutout. A closeup of the distortion measurements by the dial indicator at the door ring cut is presented in Figure 3-4. Figure 3-5 shows the setup of the tank on the Bullard Boring machine to correct the distortions of the manhole access door area and to complete the cutout for the new door ring.

The majority of the problems encountered during the preparation of the tank welding can be directly attributed to the initial fabrication of the 1.52 m (60 in) tank by its original manufacturer. It was noted that there was an excessive amount of trapped welding stresses and distortions which were relieved when the door rings were removed. In addition, there was a large variation in parent metal thickness adjacent to the location where the new components were needed. The problems were magnified by the variations in wall thickness in the existing conical tank support weld area resulting from mismatching the tank halves, as shown in Figure 3-6. The mismatch was corrected by the original

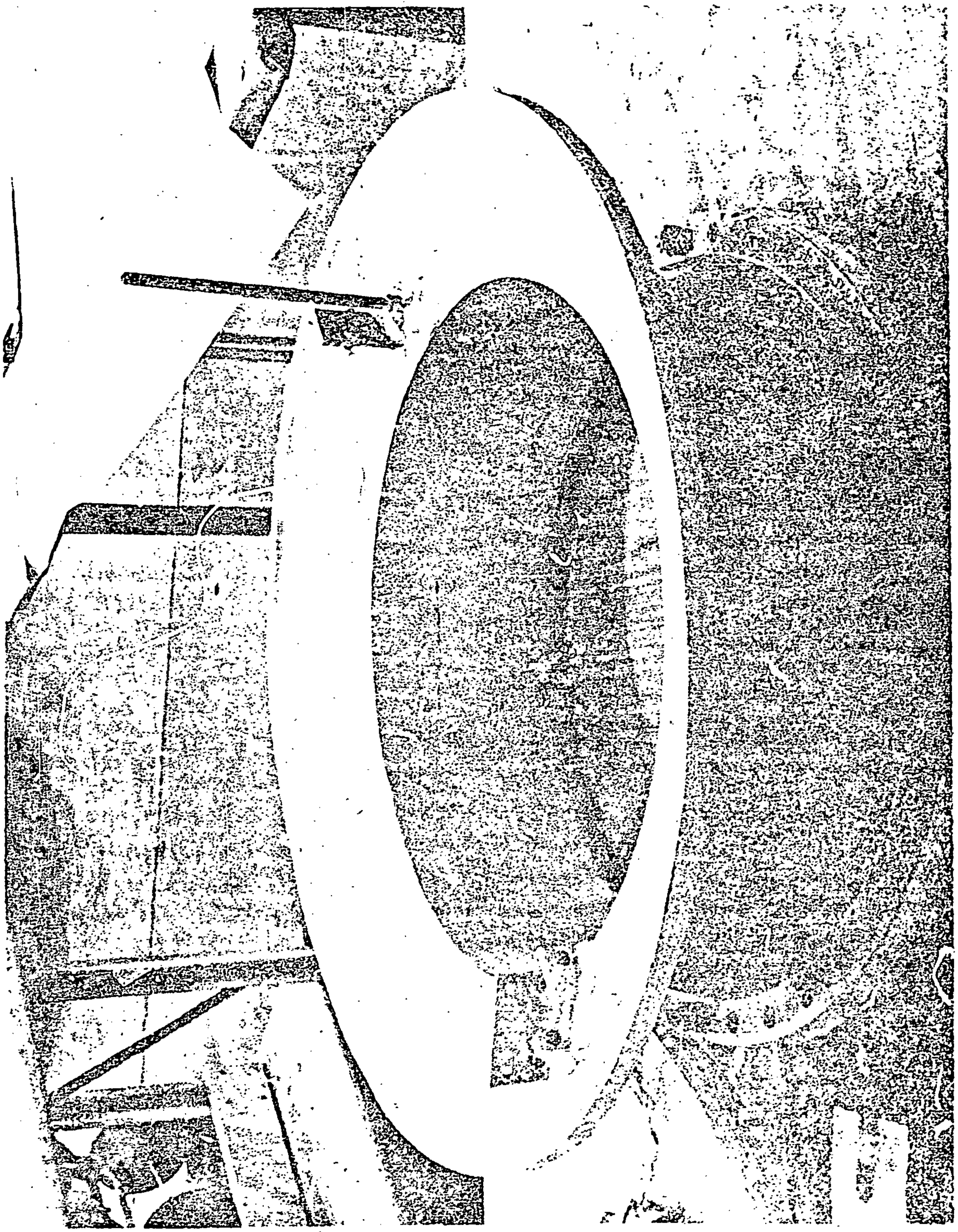

Figure 3-1. Large Manhole Access Door/Neck After Cutout

Table 3-2. Tank Thickness Variations at the Large Manhole Access Door Area Cutout

Location	Runout m (in)	Wall Thickness m (in)
0	0.00000 (.000)	0.00979 (.385)
1	+0.00056 (+.022)	0.00975 (.383)
2	-0.000254 (-.010)	0.00950 (.374)
3	-0.000762 (-.030)	0.00956 (.376)
4	+0.000381 (+.015)	0.00943 (.371)
5	+0.00094 (+.037)	0.00928 (.365)
6	+0.000203 (+.008)	0.00943 (.371)
7	+0.00056 (+.022)	0.00964 (.379)
8	+0.00056 (+.022)	0.00960 (.378)
9	+0.00122 (+.048)	0.00956 (.376)
10	+0.000305 (+.012)	0.00956 (.376)
11	+0.000356 (+.014)	0.00960 (.378)
12	+0.00191 (+.075)	0.00910 (.358)
13	+0.00089 (+.035)	0.00945 (.372)

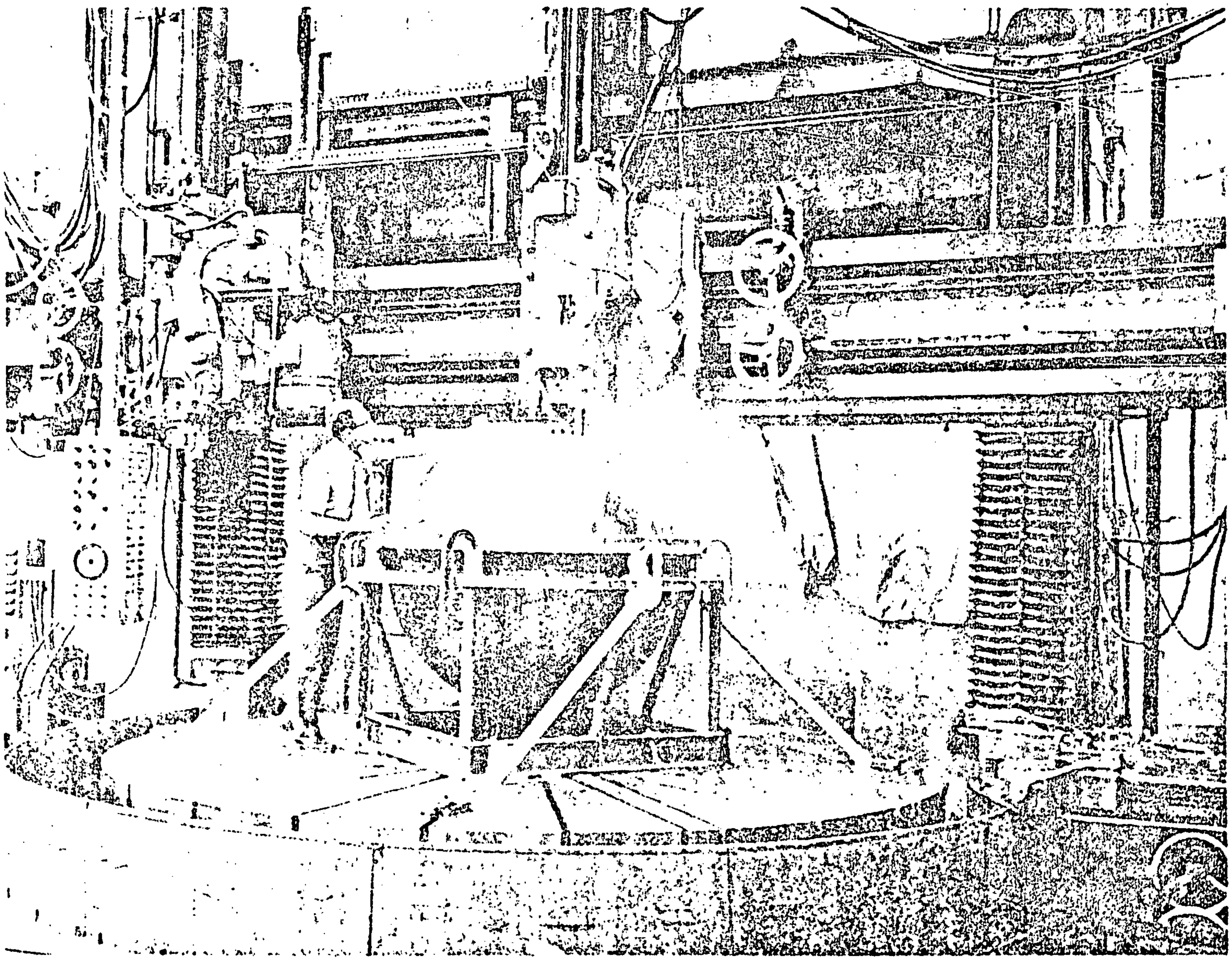

Figure 3-2. 1.52 m (60 in) Tank After Large Manhole Access Door Cutout

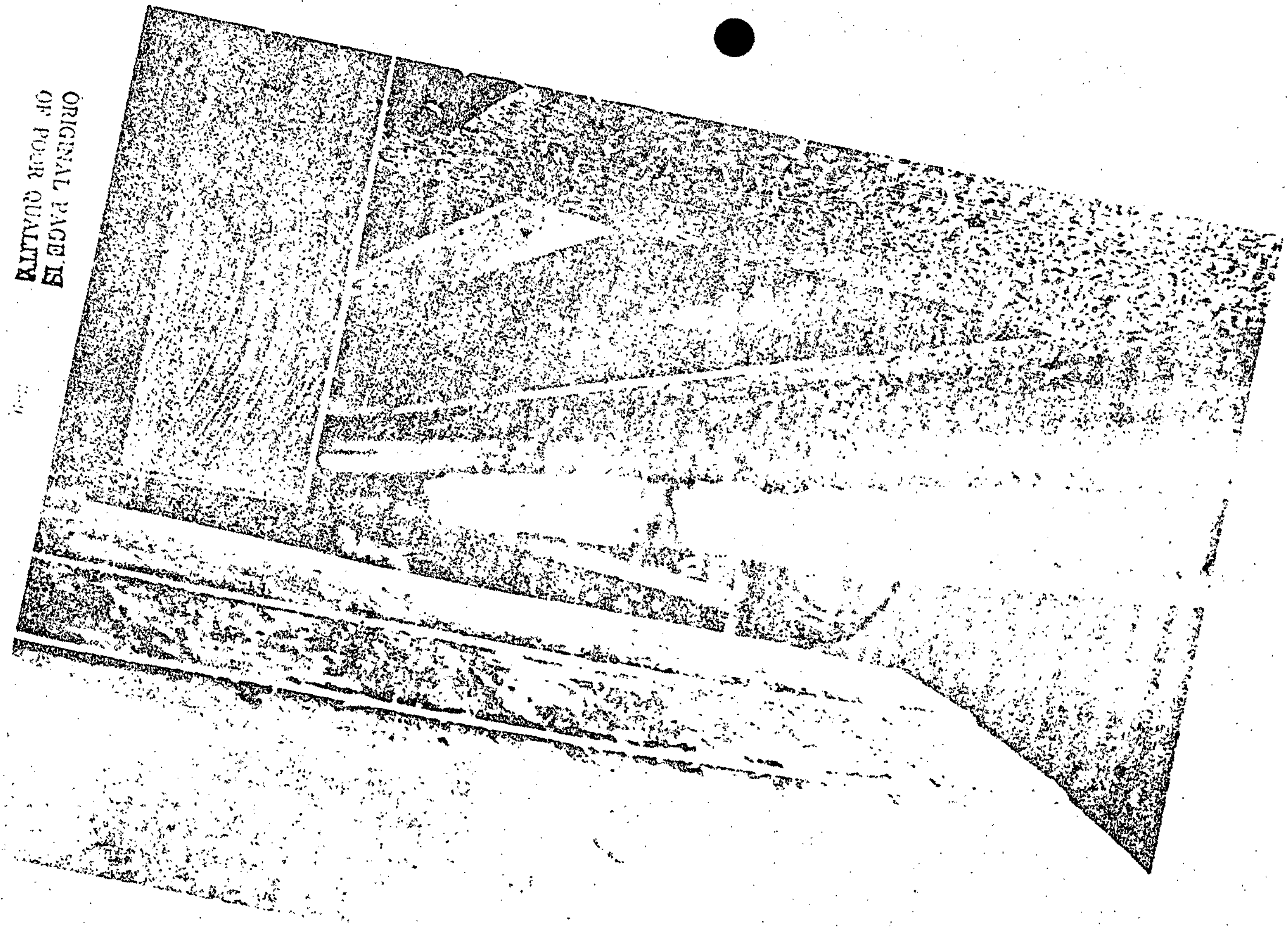

Figure 3-3. Large Manhole Access Door Area Distortion

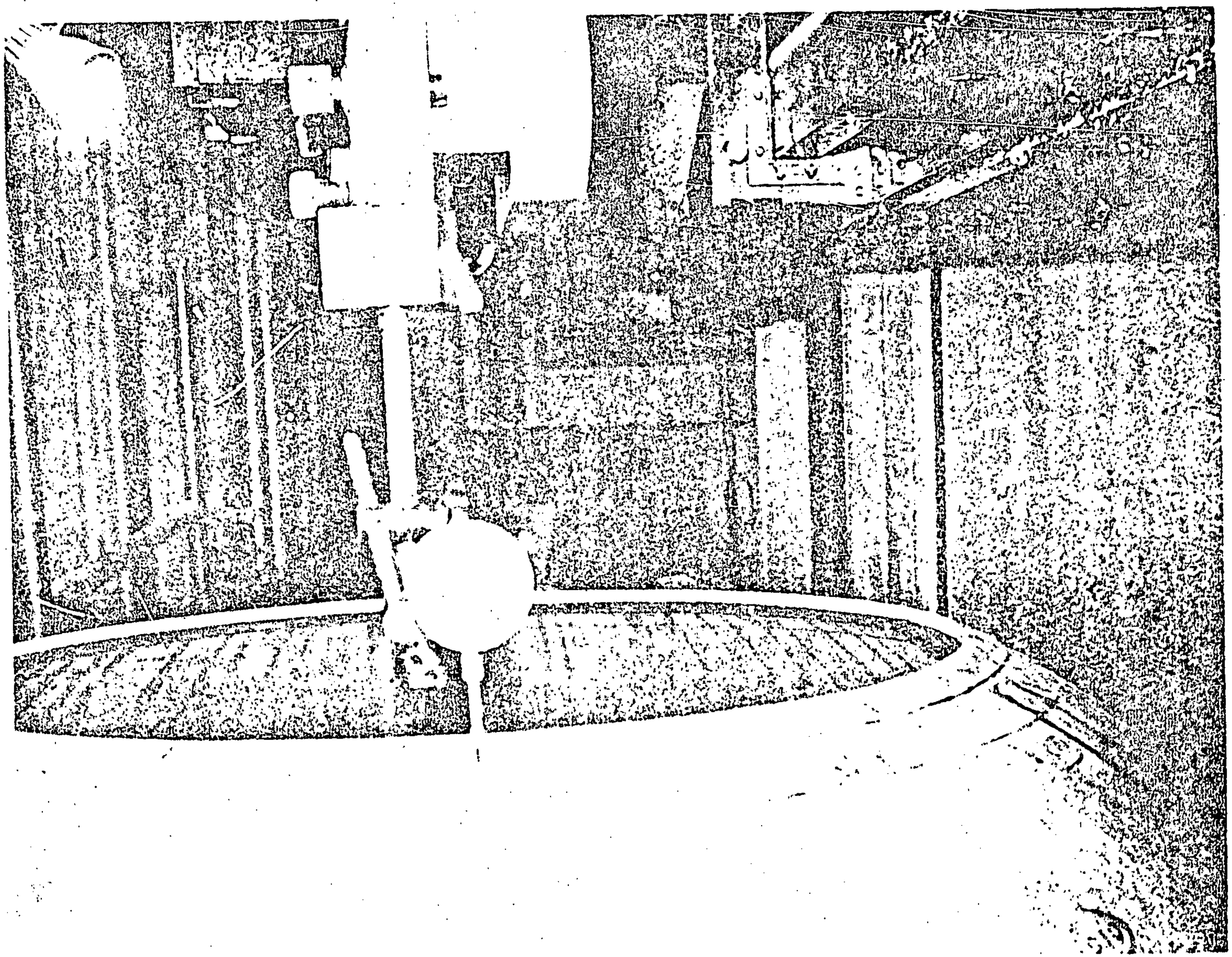

Figure 3-4. Close Up of Distortion Measurements at Large Manhole Access Door Area Cutout

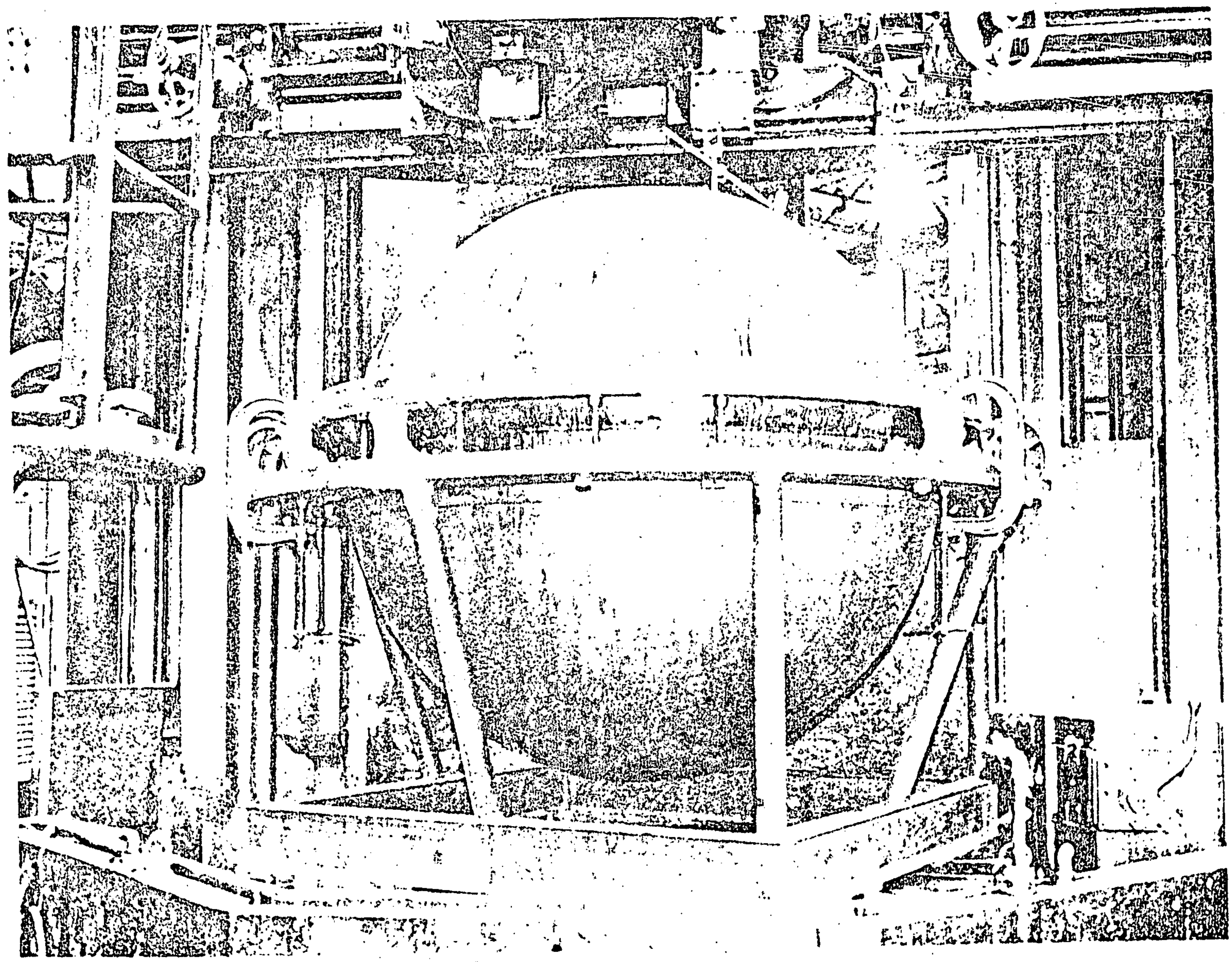

Figure 3-5. Tank Set Up for Distortion Corrections and Final Cutout

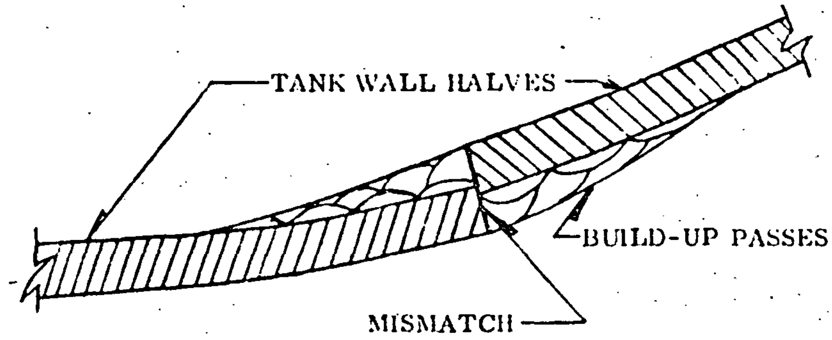

Figure 3-6. Mismatch of Original Tank Halves

manufactured by building up the off set areas with weld passes.

A series of x-rays were taken of the weld zone area that confirmed the presence of porosity, weld folds, inclusions, and cracks. Because of the large area involved, it was concluded that the considerable rework performed had led to the excessive stresses.

The x-ray of the lower tank cap area, Figure 3-7, shows the presence of tungsten inclusions (dark indication), porosities (singular and linear), weld folds, foreign material and cracks (light indication) most of which remained as parent metal problems after the original fitting was removed.

3.1.2 MACHINING AND WELDING OF TANK OUTLET CAP, DOOR ASSEMBLY AND LUGS. The material from which the parts were machined was 6061-T651 aluminum alloy. The material was ultrasonically inspected at Convair Plant 1 facility. The door-ring was machined with the outside diameter 0.0061 m (0.024 in) oversize for shrink fitting it to the tank opening. All conoseal grooves were machined to the patented dimensions supplied by Aeroquip Corporation/Marman Division. Special drawings were made to assure that the grooves were correctly machined to the accuracy necessary for satisfactory seal performance. All machined dimensions were verified by the Quality Control Department.

The manhole access door ring and tank outlet cap were joined to the tank utilizing manual welding procedures. This technique was selected to minimize tooling costs. The use of automatic welding requires backup tooling to locate and support the ring and cap during the welding operation. In addition, tooling for the door ring must be collapsible for assembly and disassembly in the tank.

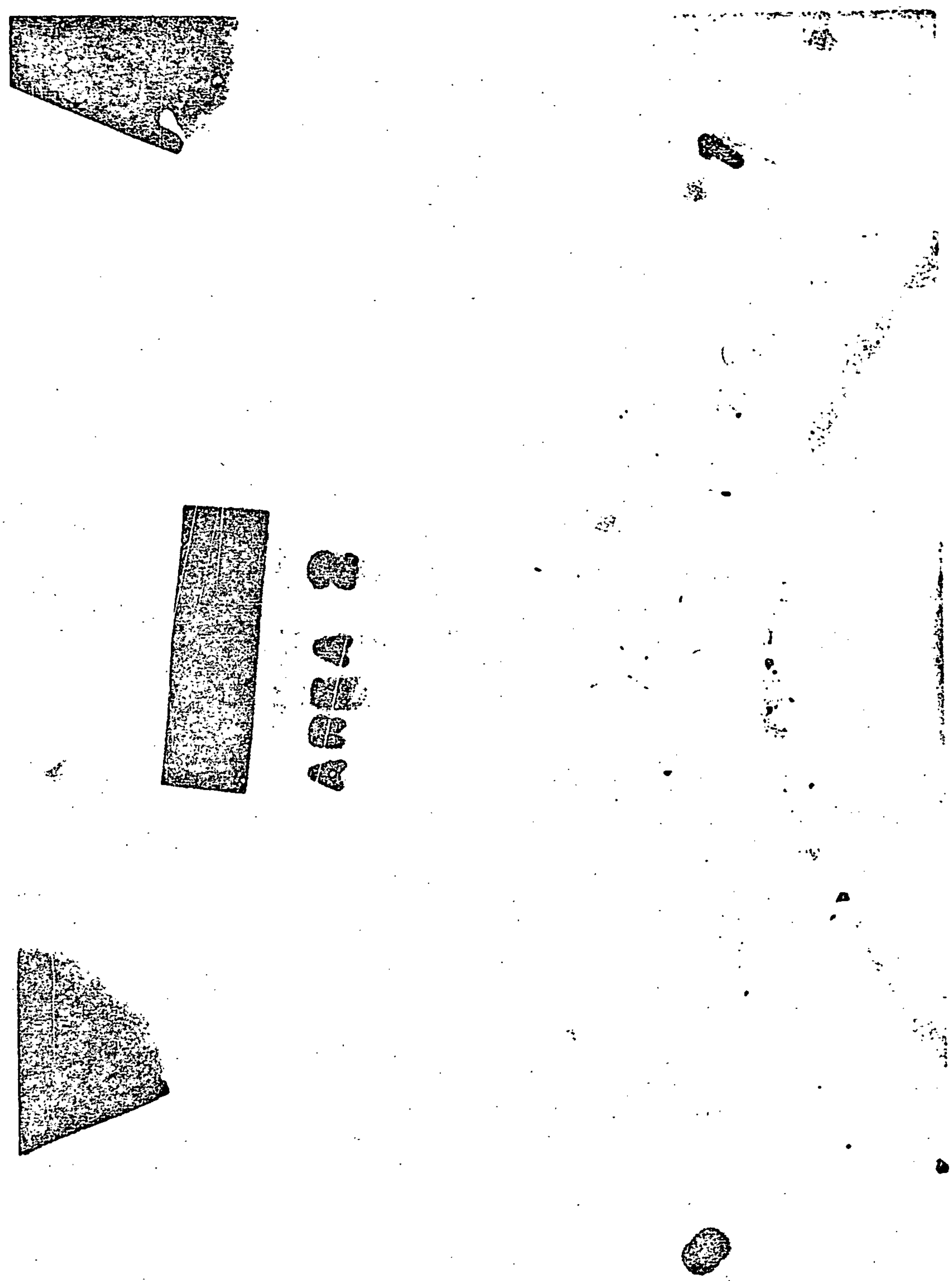

Figure 3-7. X-ray of Original 1.52 m (60 in) Tank Material - Tank Outlet Cap Area

Joining of the manhole access door ring and tank outlet cap was accomplished by welding from both sides of the joint. This technique was selected to minimize distortion. The door ring and cap were submerged in LN_2 then shrink fitted into the tank opening to offset weld shrinkage.

The cap was welded first from the inside with 50% minimum penetration. The opposite side was then prepared for welding from the outside using a routing technique. X-rays were taken after each weld to locate defects for removal before proceeding to subsequent welding. The completed weld was dye penetrant inspected and was x-rayed for final quality assurance acceptance. The x-ray revealed normally unacceptable defects in the tank wall in areas untouched by the modification operation. The defects noted included small internal cracks, porosities and indications of tungsten inclusions as shown in Figure 3-7.

After completion of the tank outlet cap weld, the door ring cutout was approximately 0.00178 m(.070 in) out-of-round. The problem was corrected by fabricating a tooling aid to correct the ring opening. The tooling shown in Figure 3-8 consisted of an aluminum ring, 0.051 m (2 in) thick and 1.22 m (48 in) outside and 0.736 m (29 in) inside diameter, with four aluminum I-beams and threaded rods. The rods were used to apply pressure on the aluminum ring to correct the out-of-round condition. By applying pressure, the 0.00178 m (0.07 in) out-of-round was reduced to 0.000254 m (0.01 in) which was adequate for inserting the ring to be welded. The welding procedure used to weld the door ring to the tank was the same as that for the cap welding. The internal welding of the ring to the tank is shown in Figure 3-9.

3.1.3 <u>REMOVAL OF EXISTING CONICAL SUPPORT RING ASSEMBLY</u>. Removal of the conical support ring as planned in the contractual tank modification revealed the original girth weld. Visual appearance of this weld did not satisfy aerospace standards. The weld condition included an excessive mismatch of the two tank halves. Because of the unsatisfactory appearance of this weld, a section of it was x-ray inspected. Figures 3-10 and 3-11 show sections of the conical support weld, randomly selected, containing weld defects in the parent metal. These defects were created by rework of badly offset areas in the original weldment.

Since all of the noted defects were not in the modified areas, they have not been officially rejected and repaired. Considering the GDCA weld procedures followed during tank modification and the quality assurance used, there was no problem in maintaining the integrity of the modifications through the proof pressure test. There can be no such confidence in the remaining original weld areas without a complete x-ray investigation of the parent material combined with the necessary repair work. This was considered outside the scope of the program and a discussion with the LeRC COR resulted in a decision that no repair work was necessary for the test task under consideration.

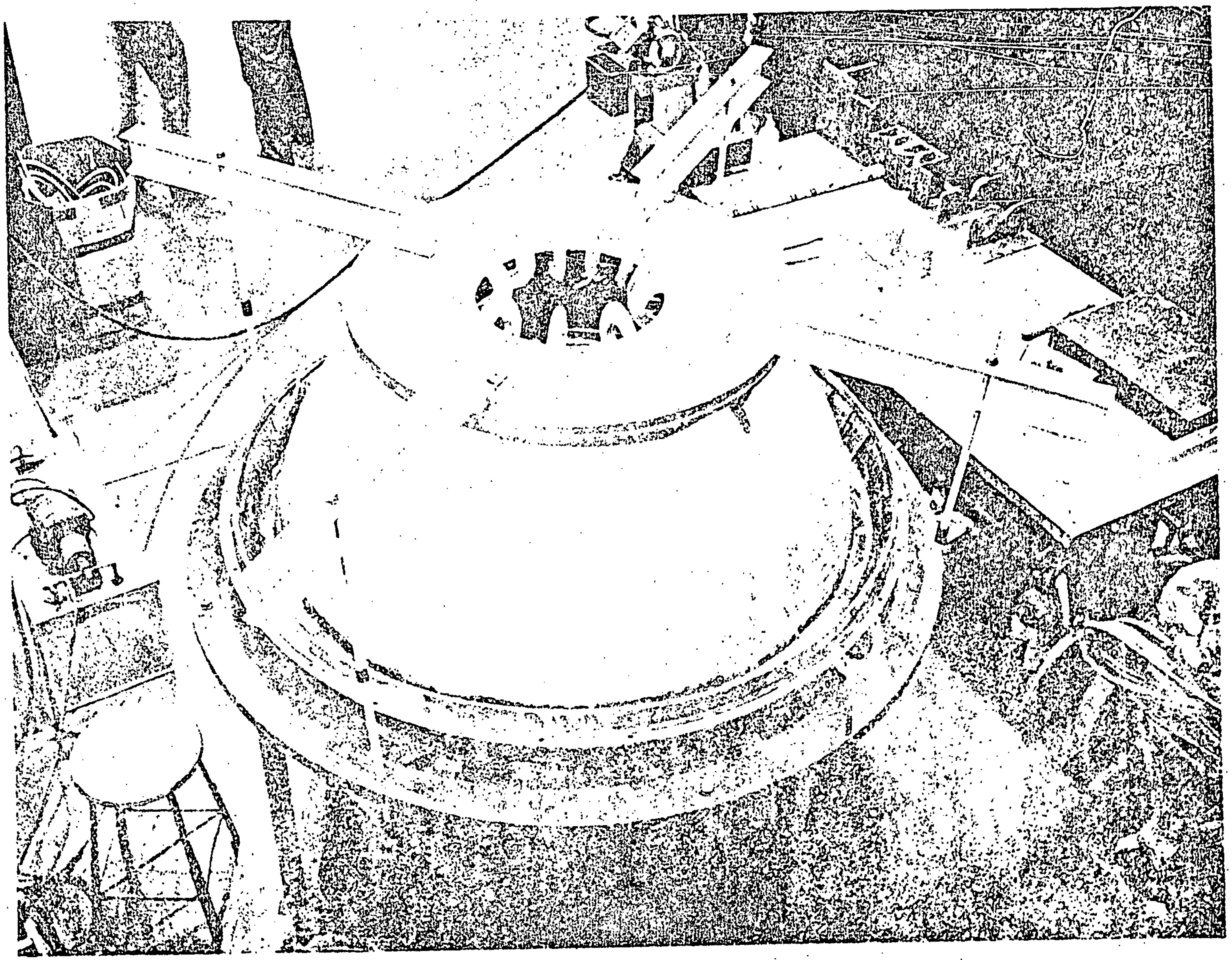

Figure 3-8. Tooling Aid to Correct Large Manhole Access Door Ring Opening

ORIGINAL PAGE IS
OF POOR QUALITY

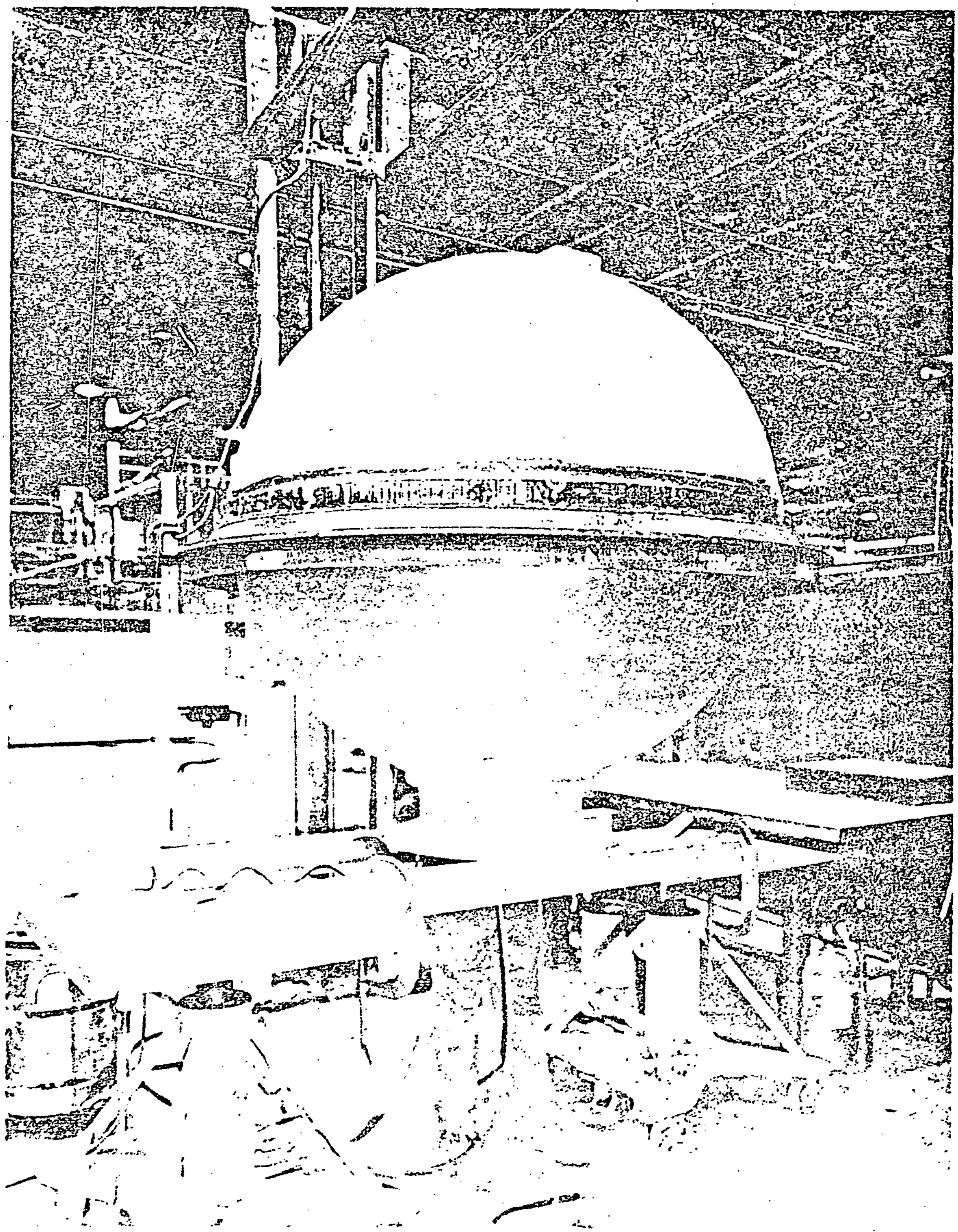

Figure 3-9. Internal Door Ring Welding to Tank

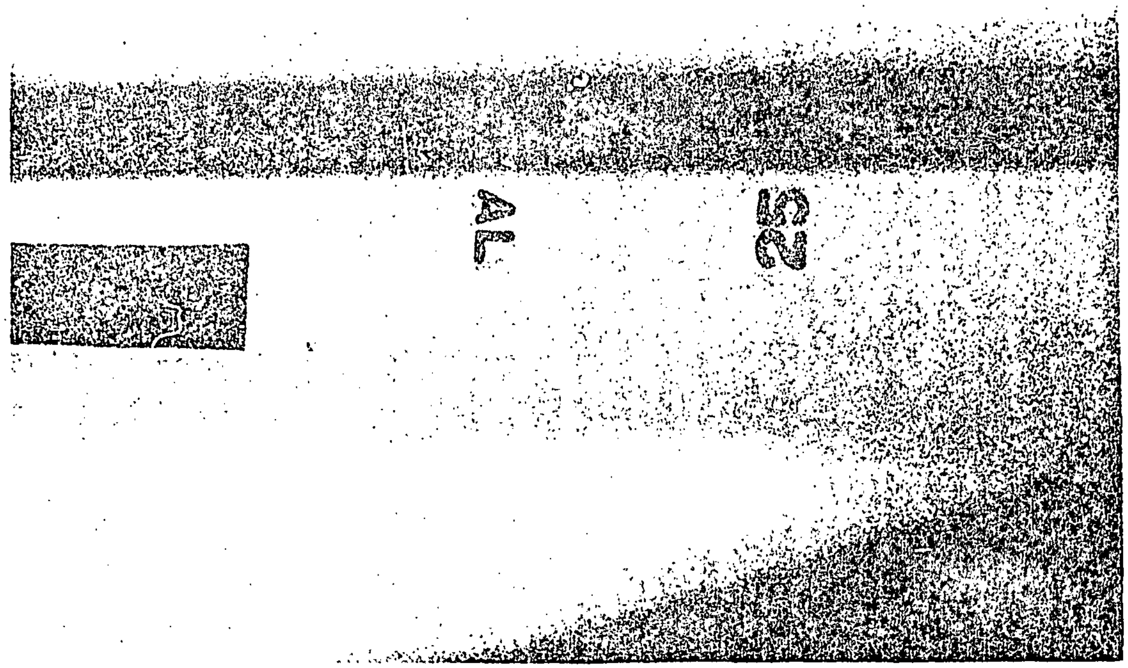

Figure 3-10. X-ray of Original 1.52m (60 in) Tank Material - Conical Support Weld Area

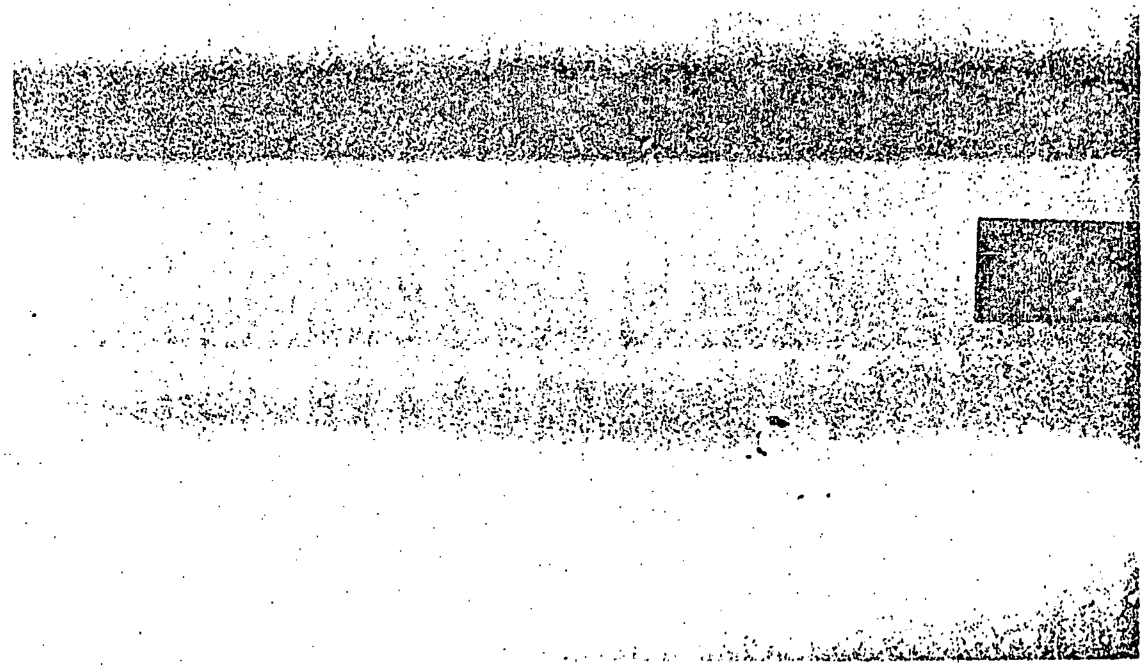

Figure 3-11. X-ray of Original 1.52 m (60 in) Tank Conical Support Weld

3.2 TEST TANK SUPPORT FABRICATION

3.2.1 THREE POINT SUPPORT SYSTEM. The three-point support system consisting of 3 tank lugs (Figure 2-6), three struts and 3 guard tank attachment fittings, was fabricated to support the test tank from the cryoshroud and guard tank structure, as shown in Figure 2-8. The tank lugs and guard tank attachment fittings were welded to the test tank and guard tank as shown in Figures 2-7 and 2-8, respectively. The proper usage of the individual lug holes (Section 2.2), for "Test Support" or "Ground Support" is identified on each lug. Commercially available turnbuckles, M-16ST, 1.77 × 0.152 m (.05 × 6 in) which are used as struts were purchased from MERRILL BROTHERS Company, N.Y. The working load per turnbuckle is 9.604 kN (2150 lbs). The yield and ultimate loads are 19.6 kN (4400 lb), and 47.53 kN (10695 lb), respectively.

3.2.2 "A" FRAME HANDLING AID. A new tank handling aid "A" frame was fabricated. Its function is to support the modified tank from its new door-ring lugs. It is also used for installation of the insulation system and to transfer the tank to the cryoshroud. The modified tank supported by the "A" frame is shown in Figure 3-12.

3.3 PROOF PRESSURE AND LEAKAGE TEST

The test tank modification task was completed after the performance of the tank proof pressure and leakage test. It was decided to proof test the tank at 276.0 kN/m^2 (40 psig). The proof pressure level was changed from 362.2 kN/m^2 (52.5 psig) (Table 2-2) to 276.0 kN/m^2 (40 psig) because of the defects revealed by x-rays in areas untouched by the modification operation (Section 3.1.2). A preliminary leakage test was conducted to check all new tank welds for gas leakage. During this test the tank door was sealed with a 0.00159 m (0.062 in) Teflon gasket and not with the regular Conoseals. The Conoseals were used in the final tank leakage test which was conducted after installation of the internal tank instrumentation. The use of the Teflon seal in the preliminary leakage test saved expensive Conoseals and reduced the possibility of damaging the Conoseal door and ring surfaces. The tank was pressurized to 69 kN/m^2 (10 psig), leak checked with an USON Model 510 leak detector and proof pressure checked at 276.0 kN/m^2 (40 psig) for 5 minutes. The tank was then depressurized to 69 kN/m^2 (10 psig) and leak checked again. There was no evidence of leakage. After fabrication of the internal tank instrumentation tree and attaching it to the tank door, the door and tree assembly was mounted to the tank including the Conoseals. Shortly before closing the door the tank was internally cleaned for LH_2 use. The final leak test was conducted utilizing helium gas and a Veeco leak detector, Model MS17. The leakage measured at a pressure differential of 138 kN/m^2 (20 psig) was 2.8×10^{-7} scc/sec. This amount of gas leakage is less than the allowable leakage rate of 1×10^{-6} scc/sec, shown in Figure 2-5.

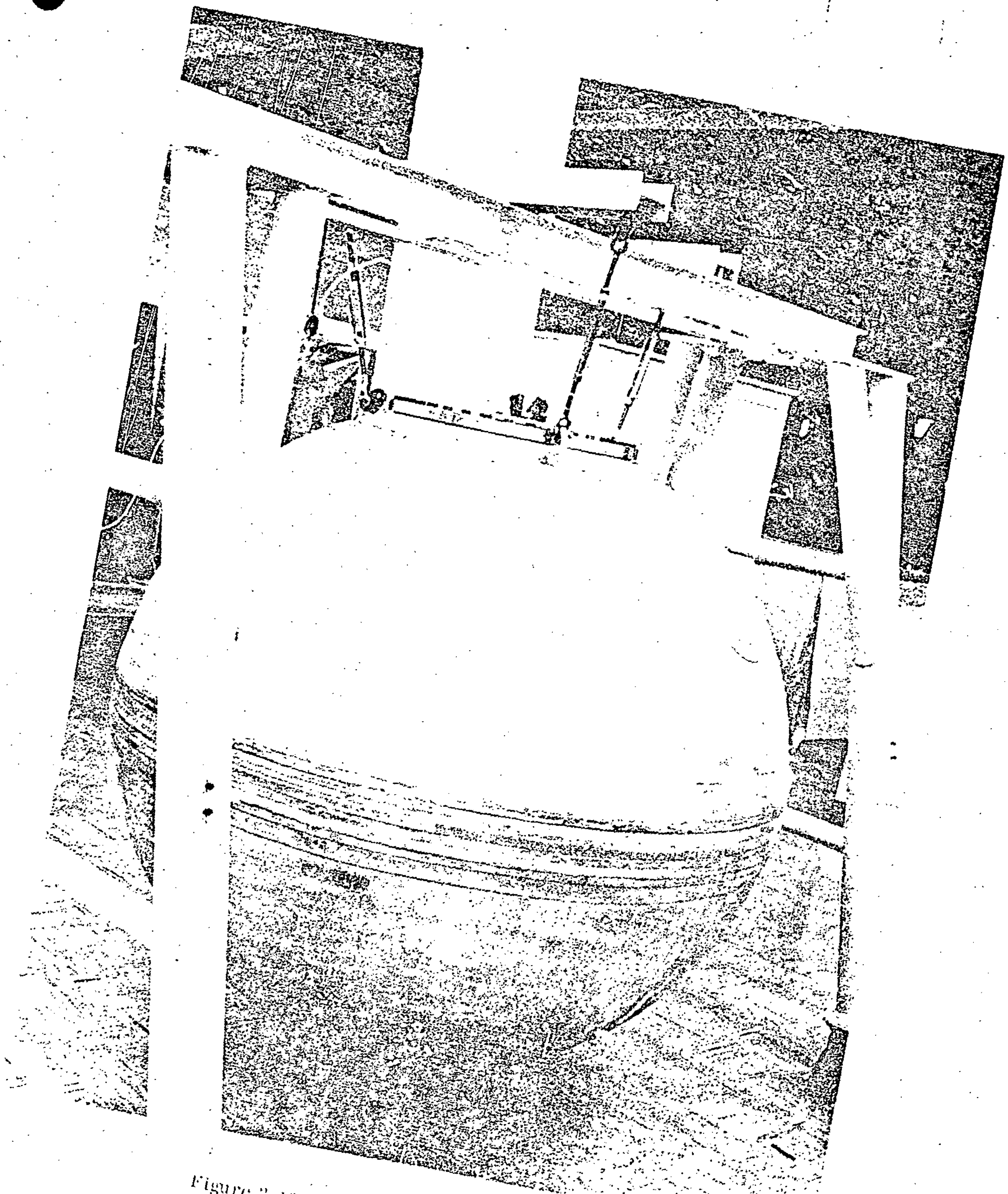

Figure 3-12. The Modified 1.52 m (60 in) Tank

4

THERMAL PAYLOAD SIMULATOR

The purpose of the thermal payload simulator (TPS) was to provide a constant temperature surface for the insulated 1.52m (60 in) tank to view (Figure S-1). The TPS configuration consisted of a 1.83 m (72 in) diameter aluminum plate supported by the cryoshroud assembly. A schematic of the payload simulator is shown in Figure 4-1.

4.1 THERMAL REQUIREMENTS

The following provisions were incorporated in the design of the TPS to meet the thermal conditions during the Null test, the thermal testing of the tank installed system and thermal testing of the customized MLI configuration:

1. Provisions for establishing and maintaining any uniform steady-state temperature in the range of 20.5 to 417K (37 to 750R) over the surface of the payload simulator.

2. Provisions for varying the tank-payload simulator spacing to any value between 0.152 m (6 in) and 0.457 m (18 in).

3. Surface viewing the tank must be flat and free of penetrations.

4. Total hemispherical emittance less than 0.04.

The temperature, ≤27.8K (50R) required during the test operation was achieved by circulating LH_2 through cooling coils welded to the bottom surface of the aluminum plate. Since the TPS was completely surrounded by a LH_2 cold wall, two coils (Figure 4-1) reduced the plate temperature below the required 27.8K (50R) in less than an hour. During the thermal tests electric heaters were used to produce the required surface temperatures. The maximum predicted heat load of approximately 58.6W (200 Btu per hour) was at 289K (520R) during the tank thermal test without the insulation on the plate. Assuming a 103.8 W/mK (60 Btu/hr-ft R) thermal conductivity for the aluminum plate, a heater element spacing of 0.152 m (6 in) produced a temperature variation less than 0.055K (0.1R) at the maximum heat load. There is no circumferential variation in the normal thermal flux. However, there was a radial variation due to the shape of the tank bottom and edge loading by the cryoshroud and baffles. This was corrected by dividing the heater into suitable annular sections, which were independently controlled as shown in Figure 4-1.

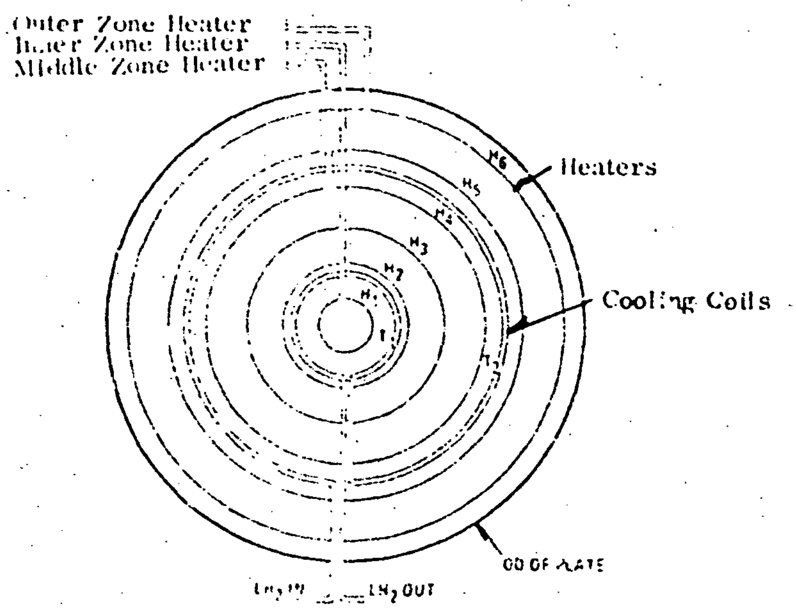

Figure 4-1. Thermal Payload Simulator Schematic

The inner edge of the lower baffle next to the simulator was shielded by ten layers of aluminized Mylar to reduce the thermal load on the outer heater band. Further thermal protection for the simulator was provided by a 10-layer aluminized Mylar insulation blanket placed between the simulator and the bottom of the shroud.

The simulator was positioned along with the lower baffle by moving the TPS adjustment mechanism (Figure 8-1). This baffle was moved by three jackscrews which were controlled from outside the chamber. A linear displacement transducer was used to determine the platform position.

4.2 TPS DESIGN AND FABRICATION

The TPS design configuration is presented in Figure 4-2. The base plate consisted of a disk 0.0095 m (0.375 in) thick and 1.83 m (72 in) in diameter. It was fabricated from a highly polished 6061-T-6 aluminum plate. There were no penetrations on the surface facing the tank. An emissivity of 0.03 was measured by a Lion emissometer Model 25B-7. During installation of the cooling coils and electrical heaters the polished surface was protected with a strippable plastic film, called Spraylab, which was removed after installation of all components.

4.2.1 <u>COOLING COILS</u>. The cooling coils were designed and fabricated utilizing 0.0190 m (0.75 in) O.D. × 0.00152 m (0.060 in) thick, 6061-T6 aluminum tubing. The

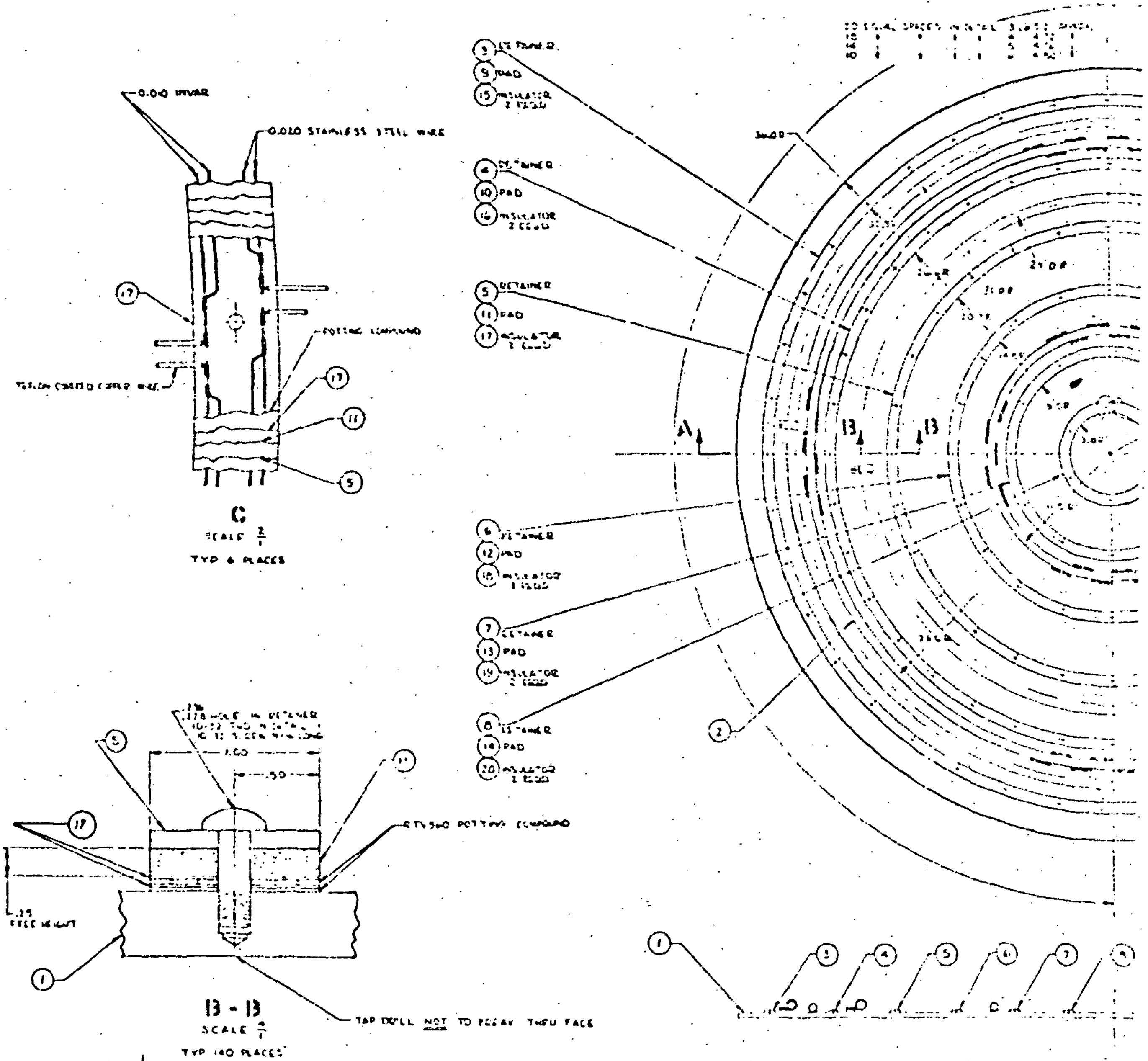

FOLDOUT FRAME 1

14170			

ORIGINAL PAGE IS OF POOR QUALITY

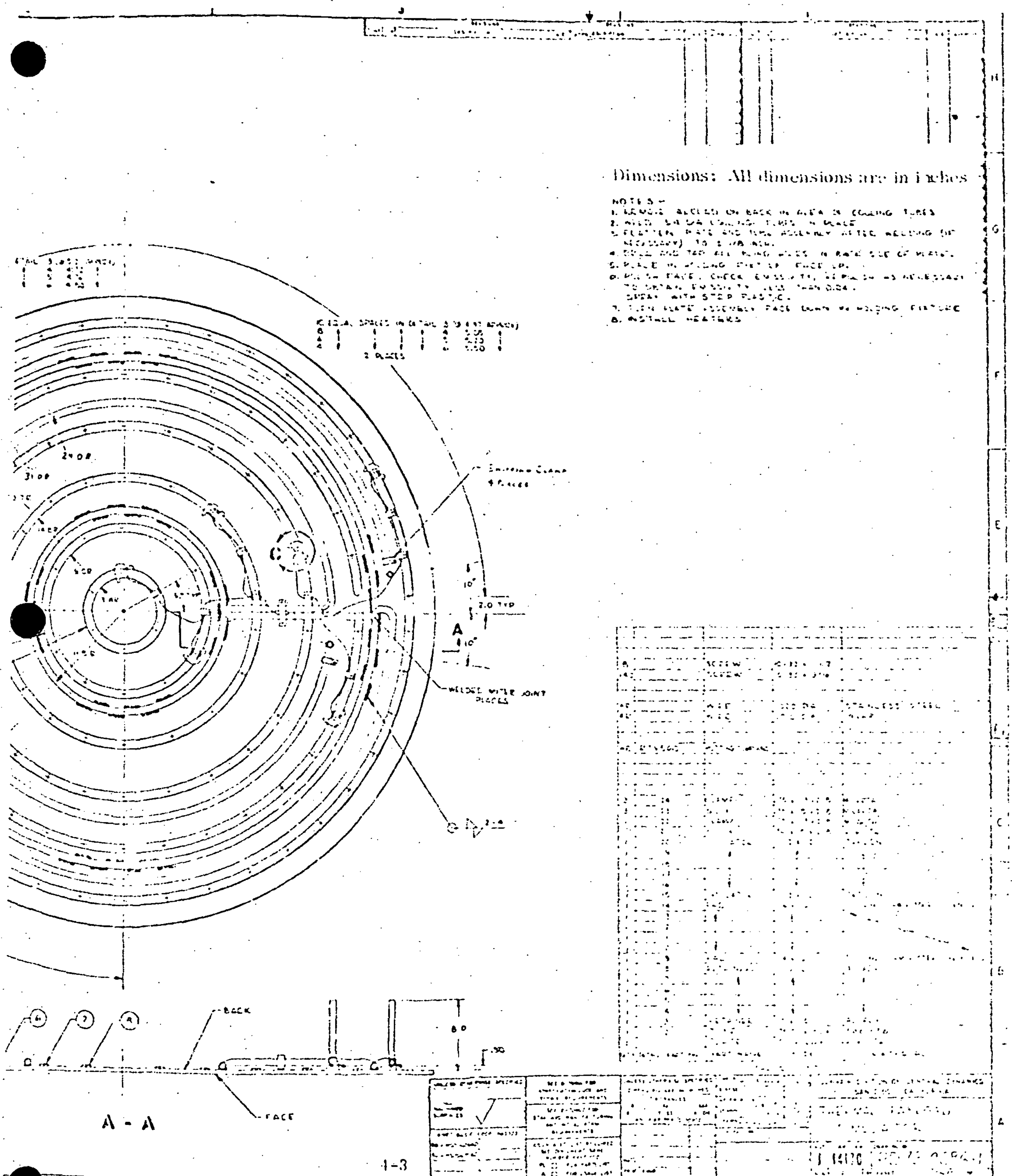

Figure 4-2. Thermal Payload Simulator Design

FOLDOUT FRAME

circumferential coils were welded in place as shown in Figure 4-2. Welds, 0.0254 m (1.0 in) long, spaced at 0.0254 m (1.0 in) were applied on alternate sides of the tubing to ensure good heat conduction between the LH_2 tubing and the TPS plate. Radial feed lines were not fastened to the plate to minimize thermal nonuniformity circumferentially. The tubing loop was leak checked with gaseous helium and a helium mass spectrometer. It was necessary to replace a welded portion of the LH_2 tubing, after a leakage problem could not be resolved. The replacement section was re-checked and found to be free of any leakage.

4.2.2 ELECTRICAL HEATERS. The heat load on the plate at equilibrium temperature was expected to range from 0.01 to 55 watts. To improve the reliability each of the heater rings consists of one high power and one low power heater. Each heater was equipped with two parallel elements.

Due to the radially nonuniform heat load on the TPS, the heaters were divided into three annular zones: 1) an inner zone consisting of three inner rings connected in series; 2) a mid zone consisting of two rings connected in series, and 3) an outer zone consisting of the outer ring. For versatility, each heater element lead wire was extended individually to the outside of the chamber to facilitate regrouping if necessary. The heater design connections are shown in Figure 4-2 and 4-3.

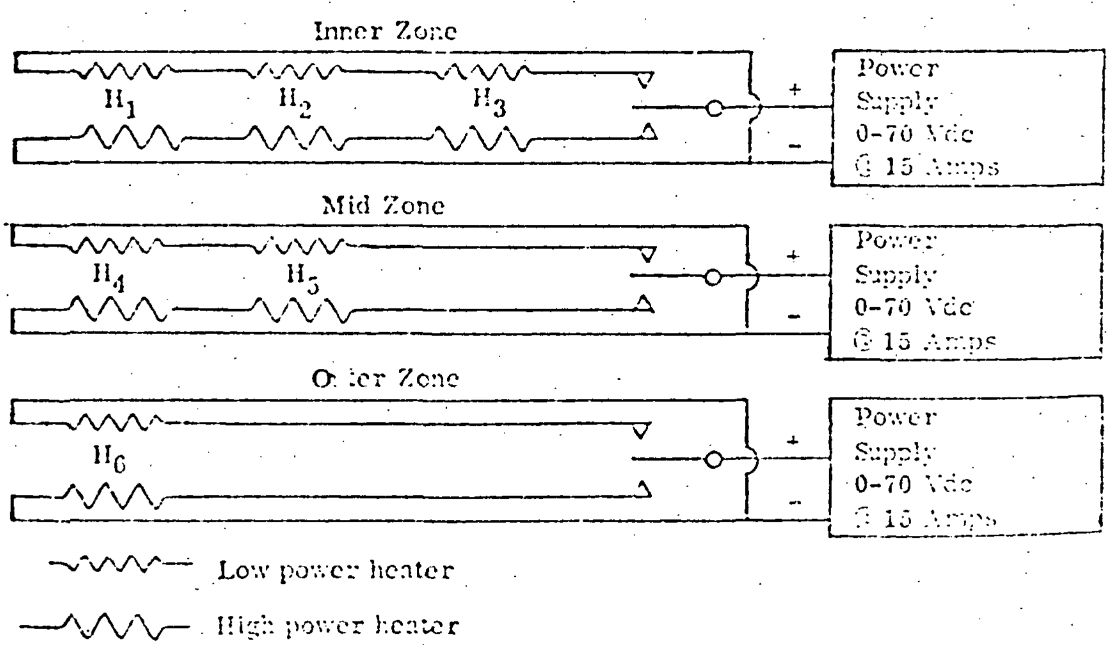

Figure 4-3. Sketch of Electrical Heater Connections

The material selected to construct the electrical heaters was based primarily on the required temperature limits of 20.5K (37R) and 417K (750R) with second consideration being thermal conductivity. The heater was constructed utilizing 0.000254 m (0.010 in) Invar and 0.00058 m(0.020 in) thick stainless steel wires. The Teflon film between the TPS and heater wires was required for electrical insulation. The Teflon film behind the heater wire reduces the area loading on the silicone rubber foam while limiting the force on the wire to prevent its cutting through the insulating Teflon. The silicone foam is a resiliant filler to provide good mechanical contact between the heater and the TPS and some thermal insulation between the heater and the aluminum back-up strip. RTV 560 potting compound is used primarily for thermal conductivity and also as a mechanical bond. A photo of the completed thermal payload simulator in its protective holding fixture is shown in Figure 4-4.

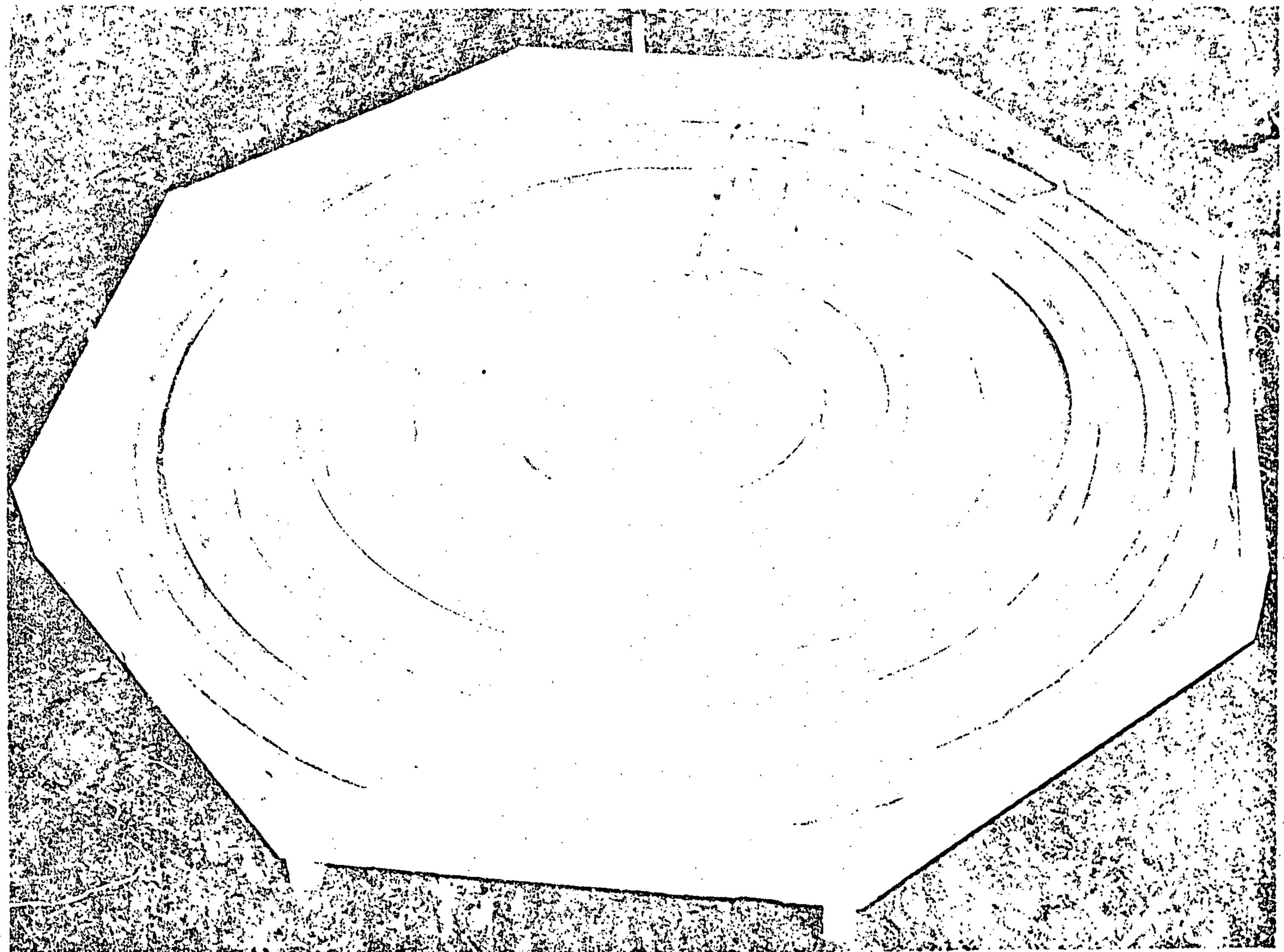

Figure 4-4. Thermal Payload Simulator Assembly

5

CRYOSHROUD ASSEMBLY MODIFICATION

The modification of the cryoshroud was initiated by evaluating the design of the cryoshroud assembly which was furnished by the NASA LeRC to simulate the environment of deep space. The cryoshroud was required to be cooled by liquid hydrogen and to have a high surface emittance on those surfaces viewing the test tank. The objective of the modification was to establish as near a low temperature black body cavity as feasible, and minimize cryoshroud hydrogen usage.

The cryoshroud assembly modification effort was subdivided into five tasks:

1. Cryoshroud modification
2. Cryoshroud baffle thermal analysis
3. Cryoshroud baffle design and fabrication
4. Guard tank design and fabrication
5. Thermal payload simulator and baffle positioning mechanism design and fabrication
6. Assembly of the cryoshroud components

5.1 CRYOSHROUD MODIFICATION

The cryoshroud was a 2.44 m (96 in) diameter by 2.44 m (96 in) high cylindrical shell with top and bottom covers. Cooling coils were welded to all surfaces. A schematic of the cryoshroud is shown in Figure S-1. The material used in the construction of the cryoshroud was principally 6061 aluminum alloy. The basic construction was a framework of 0.076 × 0.076 × 0.0063 m (3 × 3 × 0.25 in) angle and 0.076 × 0.0063 m (3 × 0.25 in) bar stock material with 0.003 m (1/8 in) sheet covering. The top cover had a heavy 0.051 m (2 in) thick mounting ring attached by 0.635 m (25 in) diameter 25.4 cm (10 in) high sleeve. The ring was braced by four radial struts. The cylindrical shell had eight baffle guides which also provided support for the sidewall structure.

The cryoshroud was mounted in the vacuum chamber on pads under the bottom cover rather than supported from the mounting ring in the top. Thus the radial strut load was compression rather than tension. Aluminum angles 0.076 × 0.076 × 0.0063 m (3 × 3 × 0.25 in) were attached to each side of each radial strut (Figure 5-1). The top cover (NASA Drawing CR 62191) was also modified by the addition of a 0.076 (3 in) hole for the baffle vent line to exit the cryoshroud.

The bottom cover (NASA Drawing CF 621922) was modified by the addition of holes for cooling tubes and for the payload simulator lifting jack screws. The new bottom

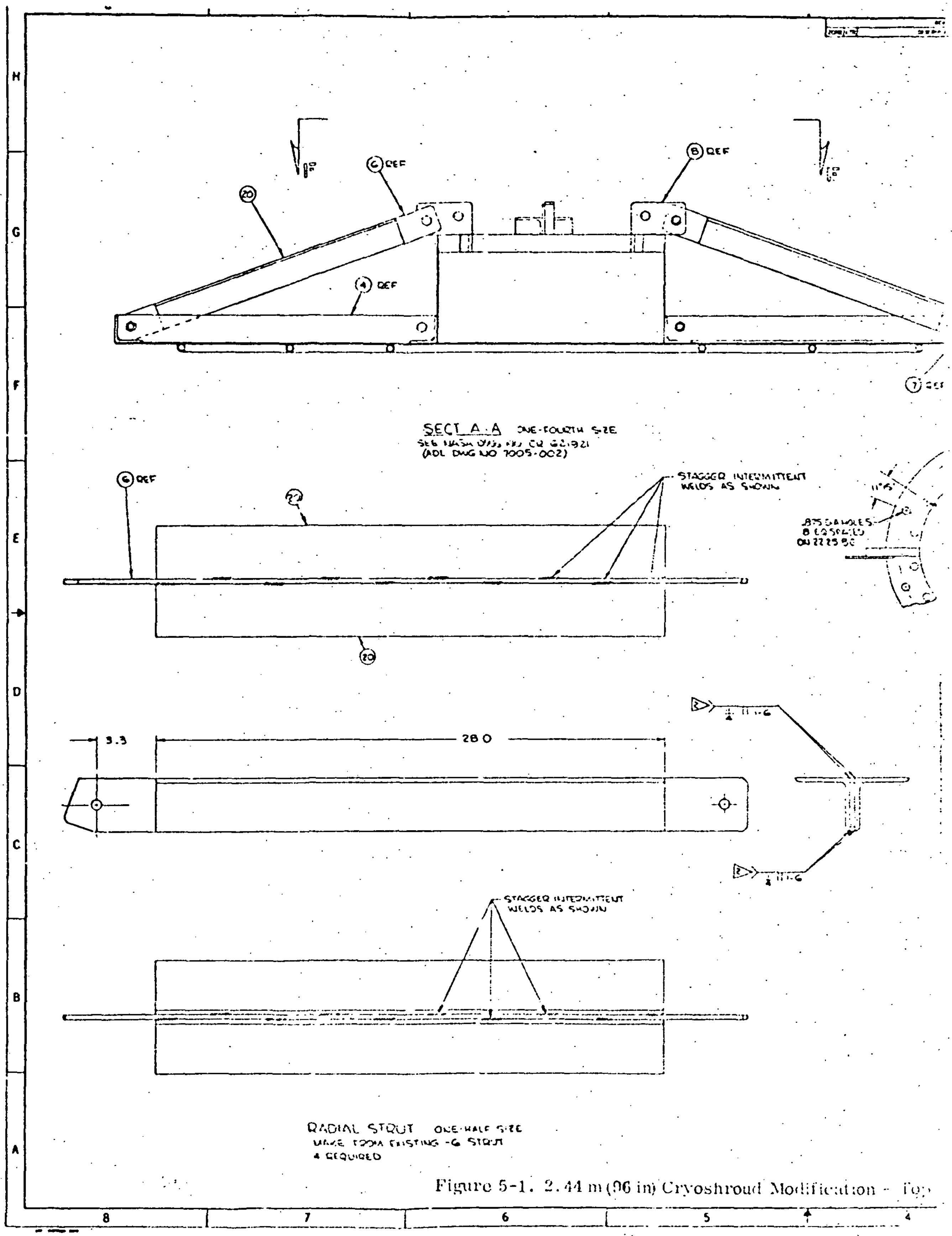

Figure 5-1. 2.44 m (96 in) Cryoshroud Modification - Top

FOLDOUT FRAME 1

Dimensions: All dimensions are in inches

NOTES: UNLESS OTHERWISE SPECIFIED

1. MODIFY THE [illegible] MOUNTING STRUCTURE AND TOP COVER [illegible] BY REWORKING THE FOUR RADIAL STRUTS AS SHOWN
2. WELD PER [illegible]
3. SEE SHEETS 2 & 3 FOR MODIFICATIONS TO BODY SHELL & BOTTOM COVER

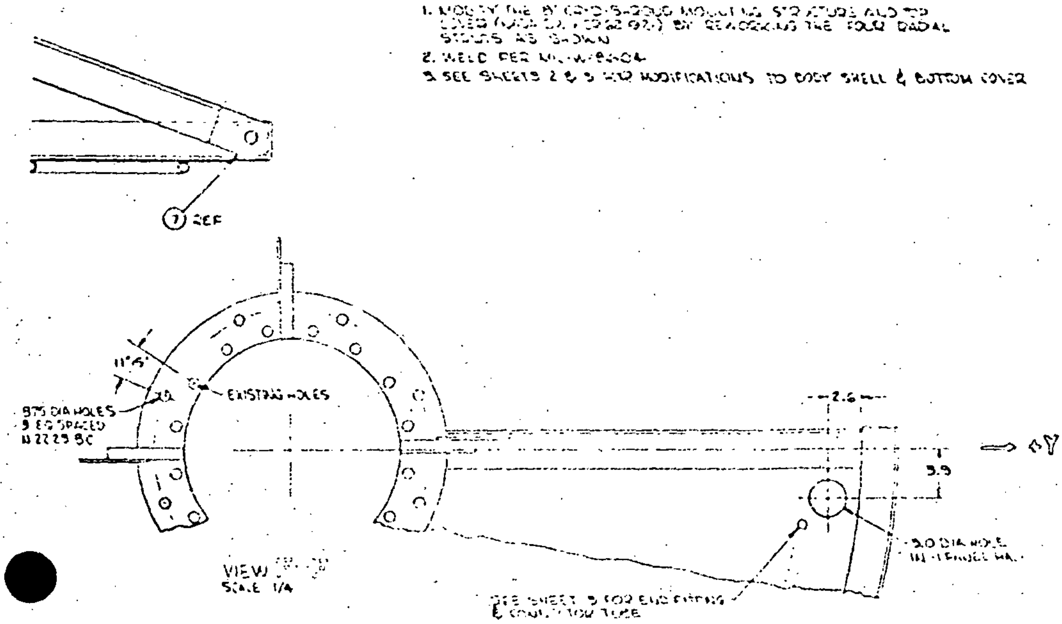

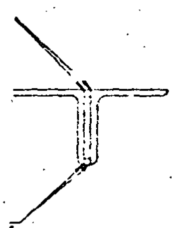

odification - Top Cover

FOLDOUT FRAME 2

cover drawing is presented in Figure 5-2. The only modification to the cylindrical sidewalls was the removal of the existing baffles and replacement of the joints between the upper and lower cooling tubes, Figure 5-3. "Double-Seal" Conoseal fittings were attached to the cryoshroud cooling tube fill and vent lines.

The entire inner surface of the cryoshroud was repainted with low outgassing 3M Nextel Velvet (3M 401-C10) paint to achieve as high an emissivity as possible.

5.2 CRYOSHROUD BAFFLE THERMAL ANALYSIS

The major objective of the cryoshroud thermal analysis was to determine the number and location of the liquid hydrogen cooled baffles required to intercept and absorb both direct and reflected thermal radiation within the cryoshroud. The location of the baffles had to be thermally acceptable for all three "Tank-TPS" spacings (Section 4.1), required during the testing of the customized MLI.

5.2.1 THERMAL ANALYSIS. An analysis was performed on the radiation interchange and heat transfer inside the lower half of the cryoshroud with the thermal payload simulator and insulated cryogenic tank. Two basic radiation interchange models were considered. The reflecting node model is a segment of the axially symmetric installation with boundary nodes having zero emissivity, Figure 5-4. The complete node model, Figure 5-5, includes all the radiative surface areas inside the cryoshroud.

5.2.2 REFLECTING NODE MODEL. The model consists of 19 flat plates and represents a 1/15 segment (24°) of the total installation. Since, in actual practice, the energy exchange will be symmetrical about the vertical tank axis, reflecting nodes (5, 6, 7, 8, 9, 10) with an emissivity, $\epsilon = 10^{-5}$, were placed on the sides of the segment section analyzed. The value, $\epsilon = 10^{-5}$, was used because the computer will not operate with a zero value. Use of reflecting boundaries reduces the number of nodes analyzed from 195 to 19 with a corresponding saving in setup and computer time. The cost of computing view factors and Script F values for radiation increases approximately as the 2.5 power of the number of nodes so that minimizing the number of nodes is significant. It is noted that the node size has been increased from a 1/16 segment to a 1/15 segment in order to reduce the maximum possible number of nodes in the complete model case to less than 200; a computer program limitation.

Four geometrical configurations were evaluated, (1) open-to-space, (2) the cryoshroud only, (3) the cryoshroud and lower baffle, and (4) the cryoshroud and two baffles. The thermal payload simulator in all cases was at its lowest position since this is the location where the greatest amount of reflected energy from the shroud baffle surface will occur. The emissivity of the thermal payload simulator (node 1) was $\epsilon_{TPS} = 0.01$ and the MLI surface on the tank (nodes 2, 3, 4) was $\epsilon_T = 0.03$. The emissivity on the shroud (nodes 13, 14, 15) and baffles (nodes 11, 12 and 16, 17, 18, 19) was varied from 0.85 to 0.96 to simulate different surface coatings.

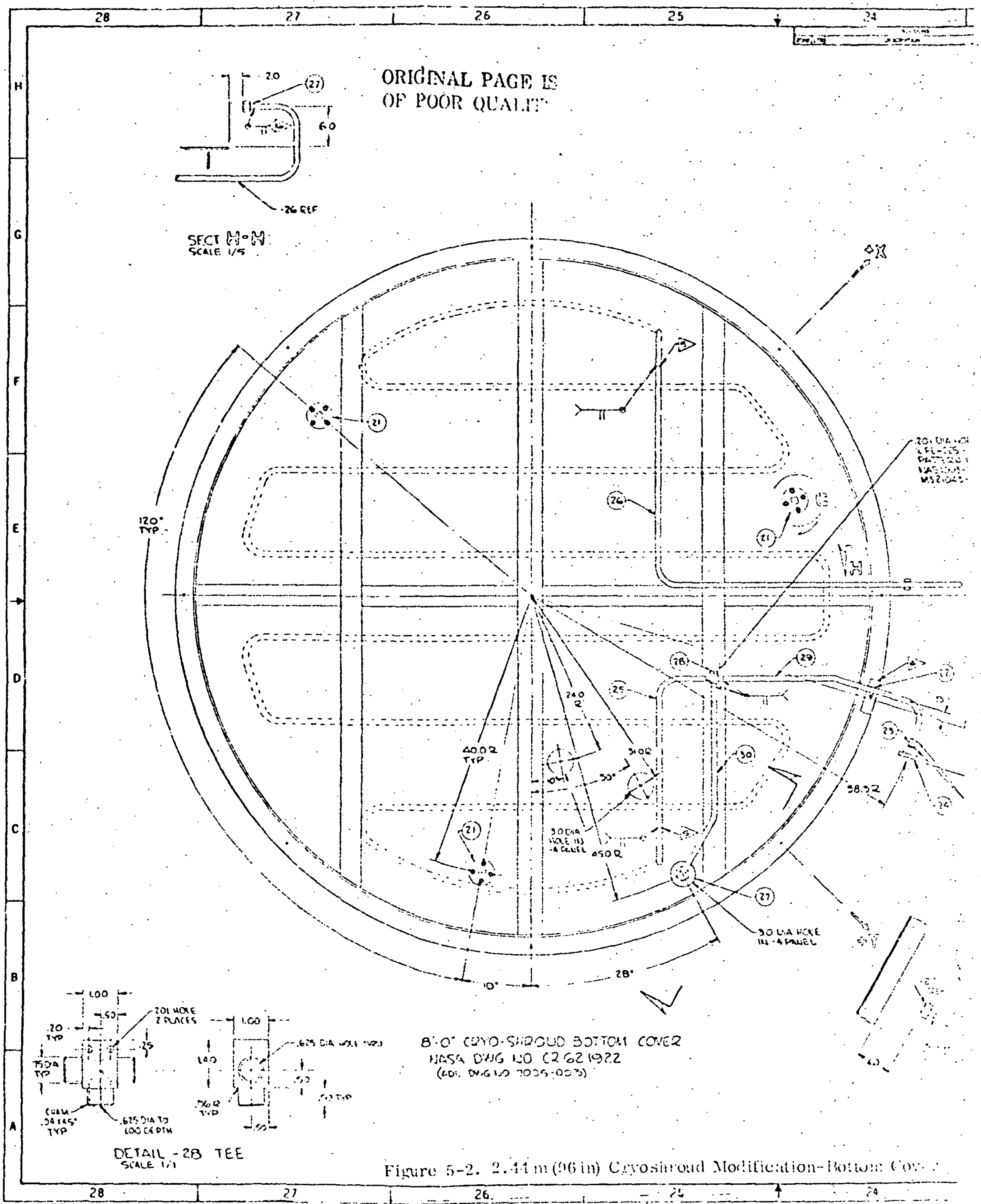

Figure 5-2. 2.44 m (96 in) Cryoshroud Modification-Bottom Cov

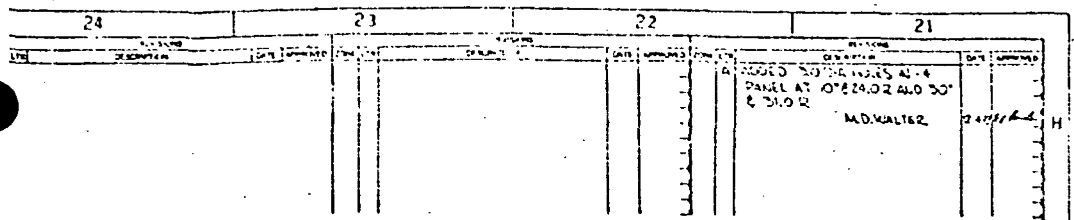

Dimensions: All dimensions are in inches

NOTES: UNLESS OTHERWISE SPECIFIED

1- MODIFY THE 8'0" CRYO-SHROUD BOTTOM COVER (NASA DWG NO CC62-922) AS SHOWN
2- WELD PER MIL-W-8604
3- SEE SHEET 1 FOR LIST OF MATERIALS
4- MOVE EXISTING CHANNELS & CLAMPS TO LOWER SURFACE OF FLANGE. USE EXISTING HOLES & BOLTS
5- REMOVE EXISTING FITTING MOCK UP TUBING APPROXIMATELY AS SHOWN TO MEET REQUIRED END POINTS
6- DO NOT ALLOW FLANGE FACE TEMPERATURE TO EXCEED 275°F DURING WELDING. USE EXTERNAL FLOOD COOL OR CHILL WITH LN2 AS REQUIRED

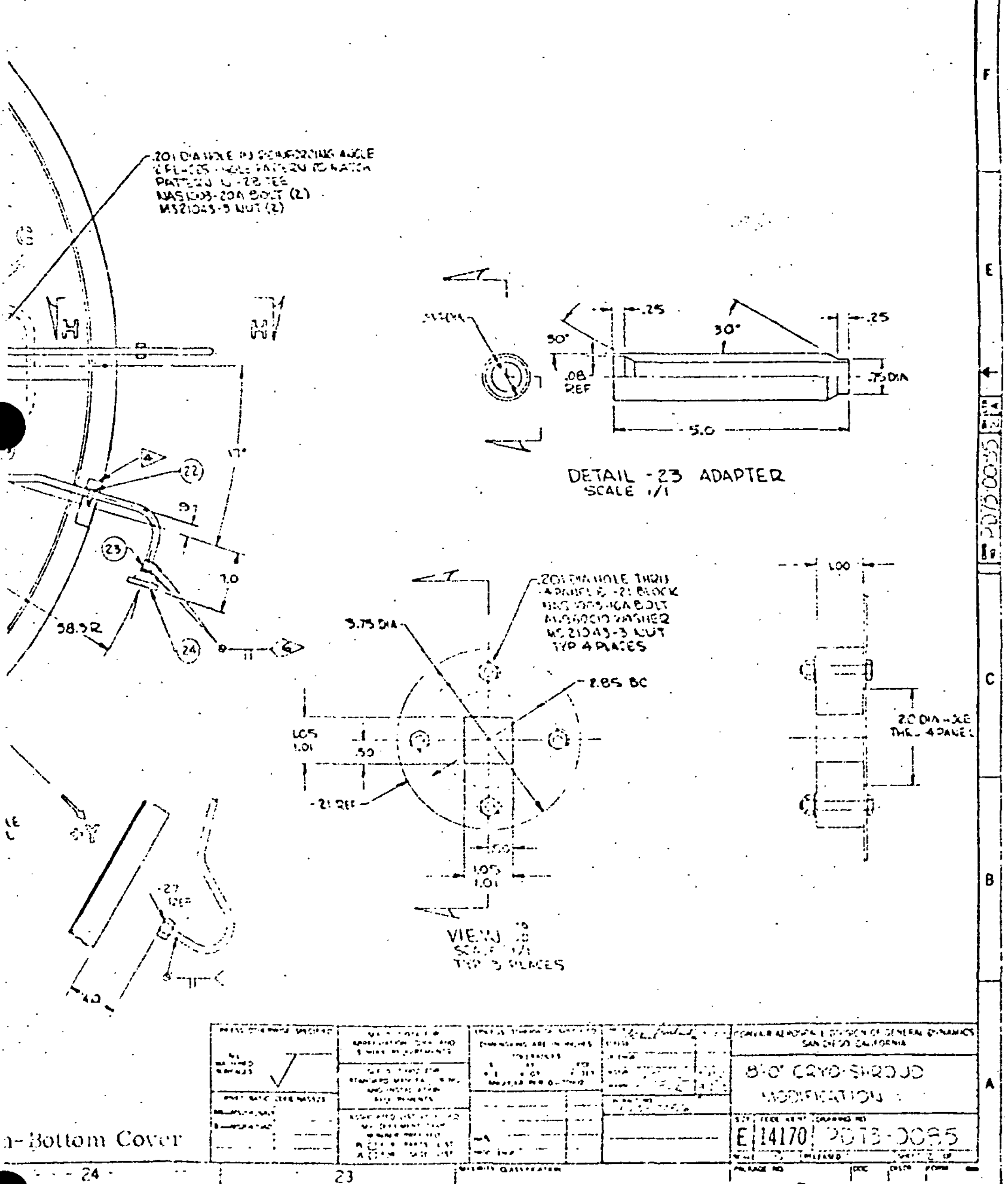

n-Bottom Cover

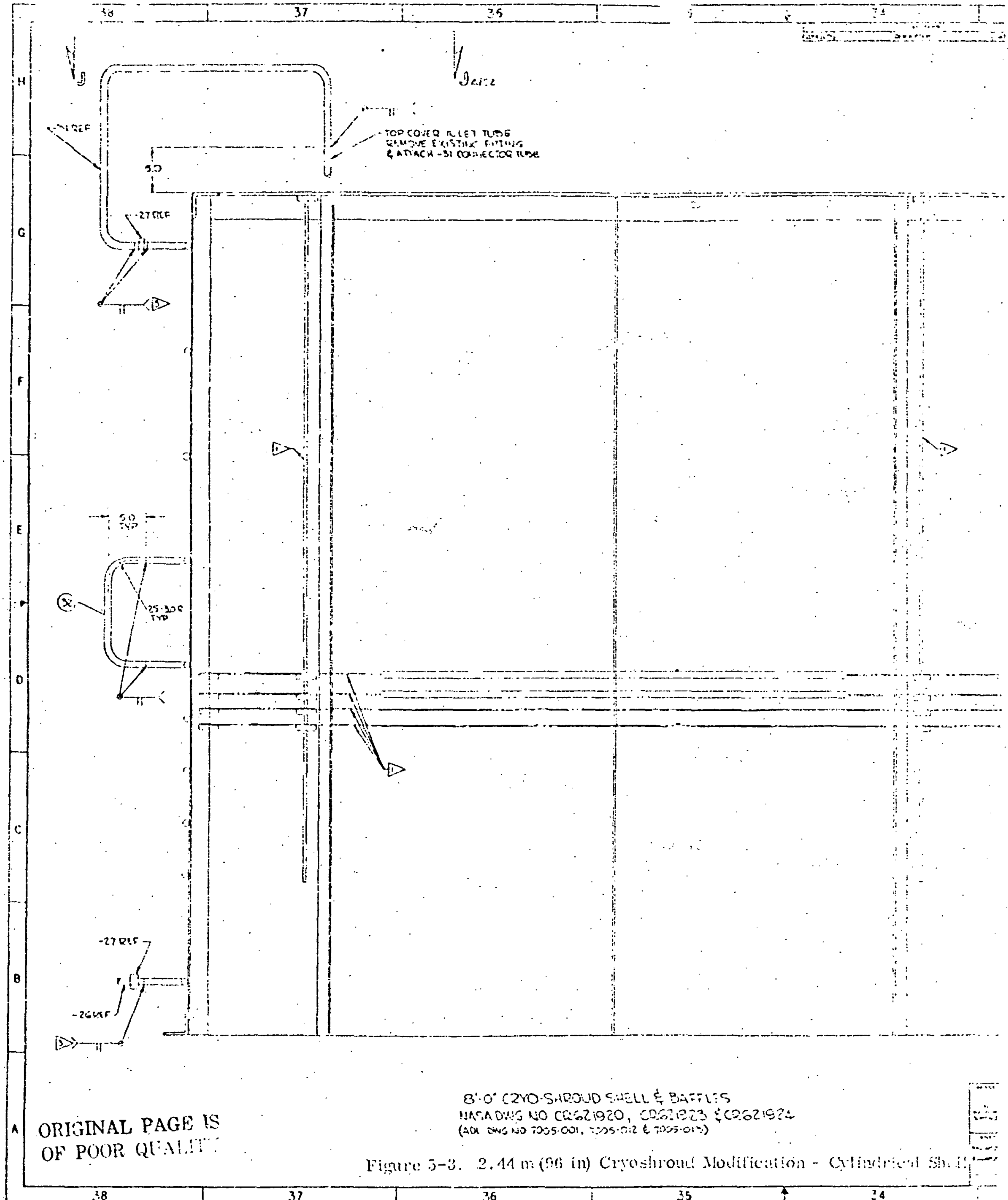

ORIGINAL PAGE IS
OF POOR QUALITY

Figure 5-3. 2.44 m (96 in) Cryoshroud Modification - Cylindrical Shell

FOLDOUT FRAME 1

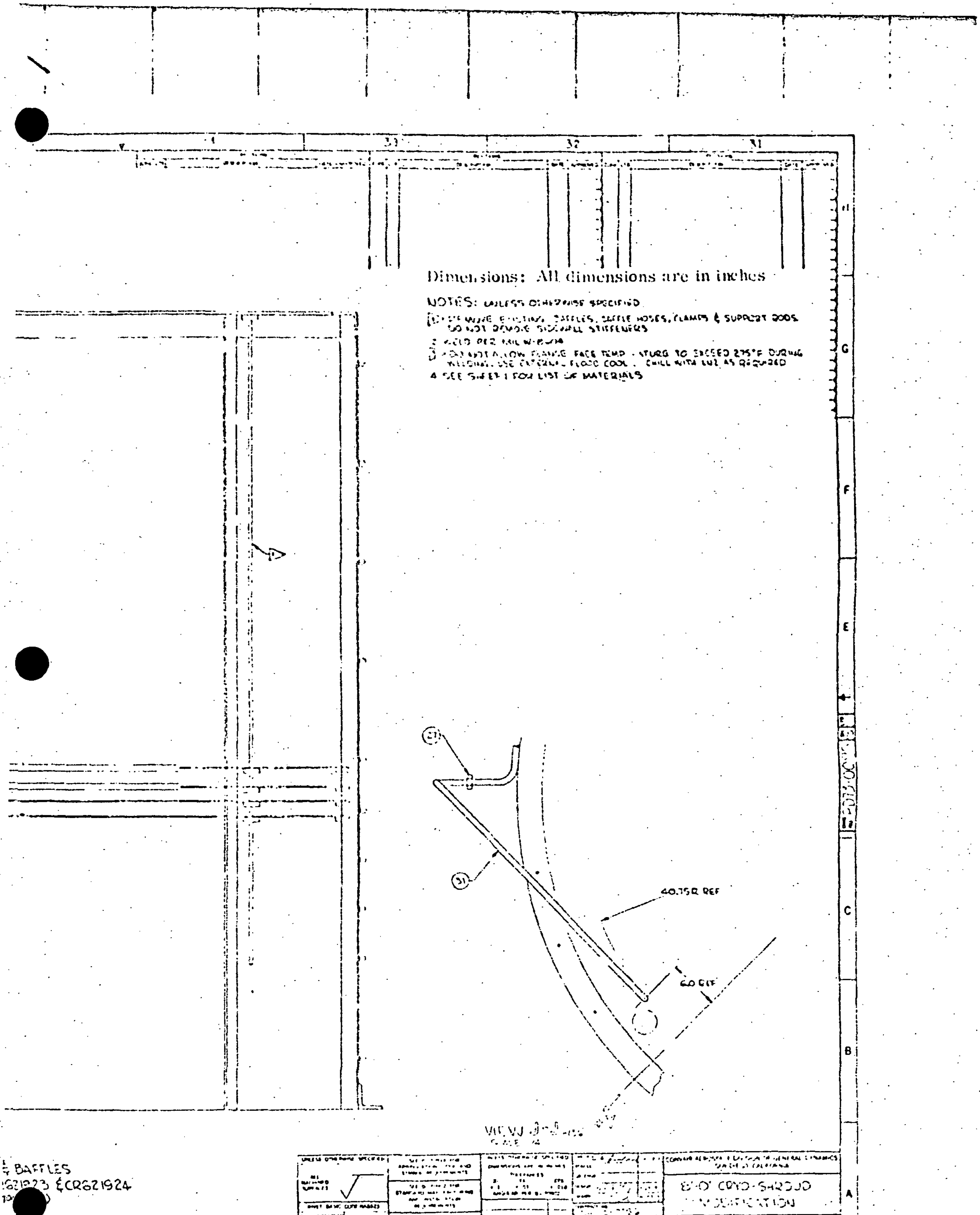

roud Modification - Cylindrical Shell

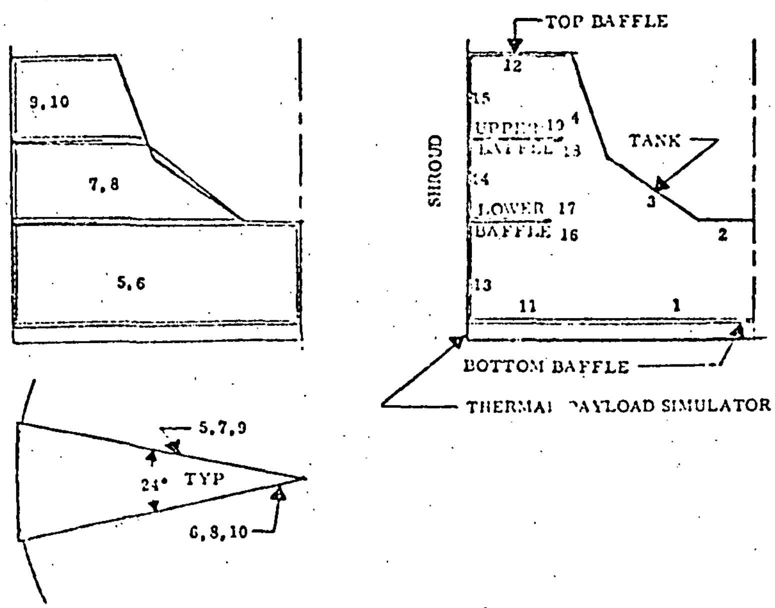

Figure 5-4. Reflecting Node Model of Cryoshroud Illustrating Node Numbers

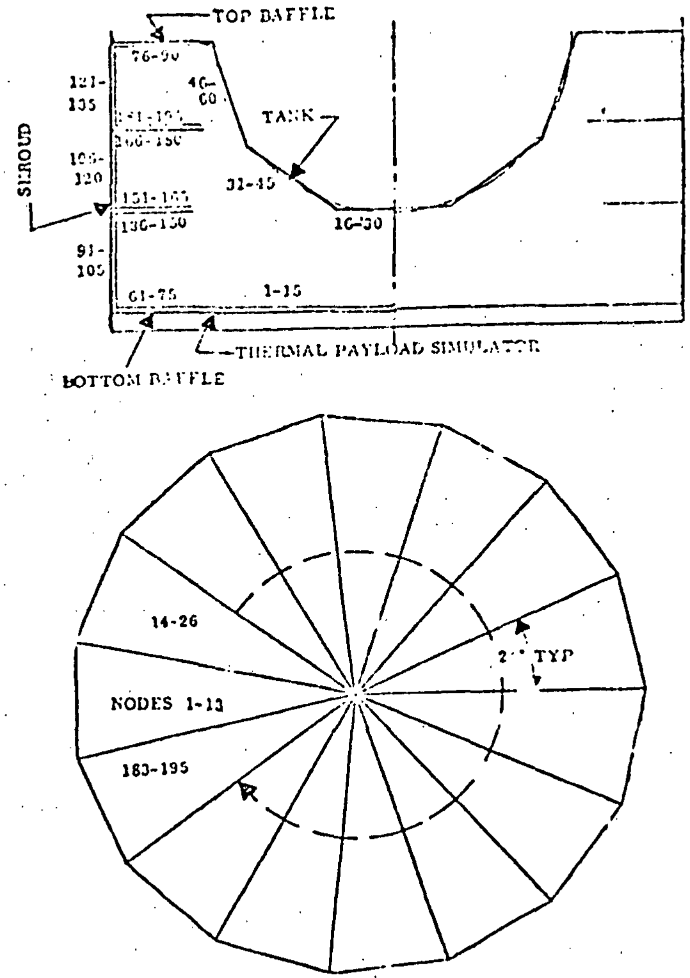

Figure 5-5. Complete Node Model of Cryoshroud Illustrating Node Numbers

ORIGINAL PAGE IS

5.2.3 COMPLETE NODE MODEL. There is some uncertainty in the accuracy of the thermal model using reflecting boundary nodes. The Gebhart technique (Reference 5-1) for determining Script F assumes diffuse reflection from all surfaces according to the Lambert cosine law, whereas specular hemispherical reflection is more representative of the actual case.

The differences are indeterminate except by generating a complete open model with no reflecting nodes. Therefore, for (1) the open-to-space and (2) the cryoshroud with lower baffle configurations, a complete model analysis was made.

The analysis used the same basic node sizes, Figure 5-5, as the reflecting model with each individual segment being 1/15 of the total installation. The directly transmitted and reflected energy from each emitting segment to a 1/15 receiving segment was computed,then the results multiplied by 15 to determine the heat exchange to the entire circumferential surface. This technique reduced the number of nodes actually analyzed in the complete model configuration.

5.2.4 FINITE NUMERICAL APPROXIMATION. The node models consist entirely of flat plates to simulate the curved surfaces. The modeled flat plate surface areas and the actual curved surface areas are listed in Table 5-1. The view factors were determined by breaking each node into smaller finite elements. The node areas and elemental breakdown is listed in Table 5-1. The view factors were computed for the cases of a smaller node to a larger node and the calculated reciprocal used for interchange from large to small nodes. The view factor projection was computed in finite 5° sweep angle increments. All node sizes and finite element breakdowns were identical in the reflecting and complete node cases, therefore view factors within a segment were also identical. View factors from the payload plate to the three tank nodes are given in Table 5-1.

5.2.5 RESULTS. Heat flow values are plotted in Figure 5-6 for the shroud, $\epsilon = 0.85$, and lower baffle, $\epsilon = 0.96$, configuration for both the reflecting node and complete node models. Emissivity of the fixed top and bottom baffles is also 0.96. The complete node model for the case where the emissivities are 1.00, open-to-space, is also plotted in Figure 5-6. Accurate numerical values of the plotted data are listed in Table 5-2. There is a difference of almost 60% between the reflecting and complete node models indicating the reflecting node model is not a suitable representation of the actual installation. It is noted that the heat flow to the shroud and lower baffle configuration is within approximately 6% of the open-to-space case. For example, at a TPS surface temperature of 278K (500R) and a shroud and baffle emissivity of 0.85 and 0.96 respectively, the heat flow from the thermal payload simulator to the cryogenic tank is 0.380 watt (1.295 Btu/hr) utilizing one baffle between the top baffle and the bottom baffle. Using the same temperature for the "Open-to-Space" case, the calculated heat flow is 0.357 watt (1.219 Btu/hr), resulting in a difference of 0.022 watt

Table 5-1. Model Node Description

Node Description	Node Number: Reflecting Model	Node Number: Complete Model	Area Sq Ft: m^2	Area Sq Ft: ft^2	No. * Divisions	No. * Elements
Payload Plate	1	1-15	0.178	1.9130	3	18
Tank Bottom	2	16-30	0.012	0.1335	2	8
Tank Mid	3	31-45	0.090	0.9658	3	18
Tank Upper	4	46-60	0.146	1.5627	3	18
Reflect. Bottom	5	N/A	0.555	5.9774	3	18
Reflect. Bottom	6	N/A	0.555	5.9774	3	18
Reflect. Mid	7	N/A	0.280	3.0153	2	8
Reflect. Mid	8	N/A	0.280	3.0153	2	8
Reflect. Upper	9	N/A	0.189	2.0383	2	8
Reflect. Upper	10	N/A	0.189	2.0383	2	8
Baffle Bottom	11	61-75	0.131	1.4140	3	18
Baffle Top	12	76-90	0.179	1.9293	3	18
Shroud Bottom	13	91-105	0.231	2.4856	3	18
Shroud Mid	14	106-120	0.186	1.9994	3	18
Shroud Upper	15	121-135	0.195	2.1023	3	18
Baffle Lower (lower surface)	16	136-150	0.149	1.6081	3	18
Baffle Lower (upper surface)	17	151-165	0.149	1.6081	3	18
Baffle Upper (lower surface)	18	166-180	0.165	1.7736	3	18
Baffle Upper (upper surface)	19	181-195	0.165	1.7736	3	18

Name	Surface Area: Modeled m^2	Modeled ft^2	Actual m^2	Actual ft^2	Percent Deviation
Payload Plate	2.666	28.695	2.627	28.274	1.5
Tank	3.709	39.930	3.648	39.270	1.7
Shroud	9.179	98.8095	9.145	98.437	0.4
Baffle, Bottom	1.970	21.210	2.043	21.991	3.6
Baffle, Top	2.689	28.940	2.846	30.6305	5.5
Baffle, Lower	2.240	24.1200	2.273	24.464	1.4
Baffle, Upper	2.471	26.604	2.468	26.565	0.2

VIEW FACTORS

Nodes: Reflecting Model	Nodes: Complete Model	VF
1 - 2	1 - 16	0.09128
1 - 3	1 - 31	0.09845
1 - 4	1 - 46	0.01439

* Divisions

N = 1 2 3

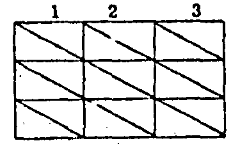

1. Elements - $2N^2$
2. Finite Elements in a Node
3. For computing view factors

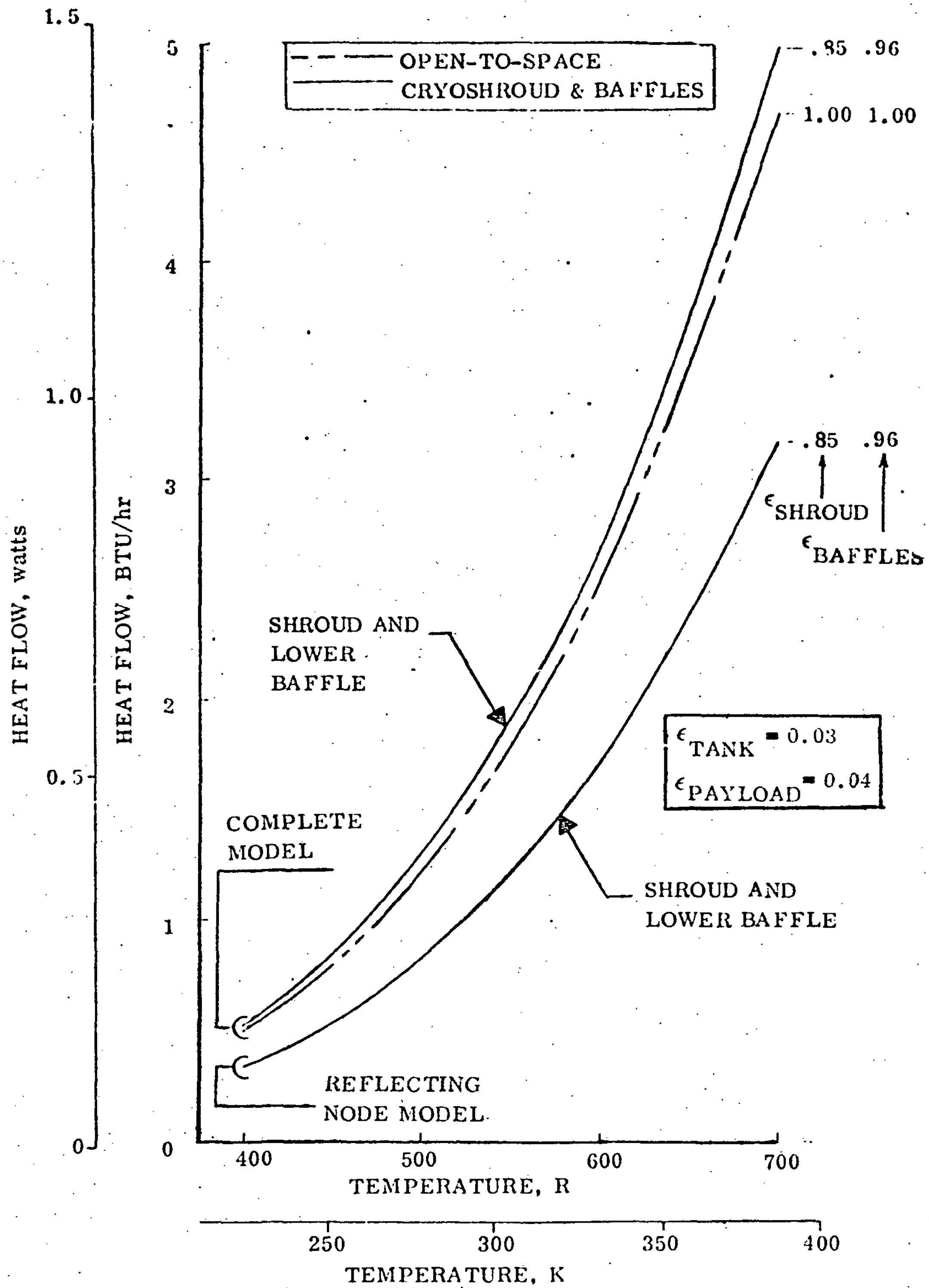

Figure 5-6. Heat Flow From Payload Simulator (Node 1) to Cryogenic Tank (Nodes 2, 3, 4) Versus Payload Surface Temperature

Table 5-2. Heat Transfer From Thermal Payload Simulator to Tank Bottom Hemisphere

Configuration	Model	ϵ shroud	ϵ baffle	$B_{ij} \times 10^{-4}$ Node 1 → 72	Node 1 → 73	Node 1 → 74	Total P/L → Tk
1. Open to Space	Complete	1.00	1.00	1.4230	5.3513	0.8165	7.5908
2. Shroud-Lower Baffle	Complete	0.85	0.96	1.4526	5.5456	1.0702	8.0684
3. Shroud-Lower Baffle	Reflecting	0.85	0.96	0.7147	3.2417	1.1883	5.1447

Heat Transfer, Watts (Btu/hr)

Configuration	$T_{P/L}$ K(R)	389 (700)	333 (600)	278 (500)	222 (400)	167 (300)	111 (200)
1. Open to Space	Complete	1.37 (4.68)	0.74 (2.54)	0.36 (1.22)	0.15 (0.50)	-	-
2. Shroud Lower Baffle	Complete	1.46 (4.98)	0.79 (2.69)	0.38 (1.29)	0.16 (0.53)	0.05 (0.17)	0.009 (0.03)
3. Shroud Lower Baffle	Reflecting	0.93 (3.17)	0.50 (1.71)	0.24 (0.83)	0.10 (0.34)	0.03 (0.11)	0.005 (0.02)

T_{TPS} = thermal payload simulator temperature (variable)

TT = tank insulation surface temperature, 28K (50R)

$\epsilon P/L$ = payload plate emissivity, 0.04

ϵ_{Tk} = tank insulation emissivity, 0.03

$Q = 15 \sigma B_{ij} (T_{P/L}^4 - T_{Tk}^4)$ Watts (BTU/hr)

15 = number model segments

σ = Stephan-Boltzman Constant

B_{ij} - $A\mathfrak{F}_{kj}$ script $\mathfrak{F}$x area

(0.077 Btu/hr) or 6.3%. Additional baffles within this narrow band are not justified or practical for such a small and largely indeterminate gain. The combined accuracy of the finite element analysis for radiation, the know accuracy of the surface emissivities and α/ϵ, and the test measurements are also not considered to be within the 6% band. It was therefore decided to use only one intermediate baffle between the top baffle and the thermal payload simulator.

5.3 BAFFLE DESIGN AND FABRICATION

The existing internal baffles which were furnished with the cryoshroud by NASA/LeRC were too small to accommodate the 1.52 m (60 in) diameter test tank. In order to enlarge this inside diameter it would have been necessary to remove the baffle surface cooling coil, making it impractical to rework these baffles into the design required for the test program. Three new annular-shaped liquid hydrogen cooled baffles for attachment to the internal surface of the cryoshroud were designed and fabricated.

5.3.1 BAFFLE LOCATION. The first baffle was located at the test tank equatorial plane and was rigidly attached to the cryoshroud. It intercepted and prevented thermal payload simulator radiant energy from entering into the region of the test tank upper hemisphere (Figure S-1). The lower baffle was aligned with its top surface approximately 0.025 m (1 in) above the top surface of the thermal payload simulator. This baffle was designed to move as a unit with the TPS and remain in that relationship at all positions of the thermal payload simulator to prevent back surface radiation emission and TPS-MLI interlayer tunneling radiation from entering into the tank lower hemisphere region. The intermediate baffle was rigidly connected to the lower baffle and moved with the lower baffle at a distance of 0.47 m (18.5 in).).

5.3.2 DESIGN. The fundamental baffle structure was a sandwich of annular shape whose main structural element was a flat, 6061-T 6 aluminum plate, 0.0032 m (0.125 in) thick. The annular aluminum base plate had 6061-T4 aluminum cooling coils welded to its upper surface. Aluminum honeycomb with 0.0032 m (0.125 in) cells was bonded with APCO 1252 urethane adhesive and additionally bolted to one or both surfaces. This configuration was selected to produce good thermal contacts allowing all baffle surfaces to attain the same temperature as the cryoshroud walls. The design is presented in Figures 5-7, 5-8 and 5-9.

The bottom surface of the honeycomb on the bottom baffle had a faceplate bonded to it to make a sandwich construction for stiffening. Six phenolic blocks were bolted to the lower surface of the movable baffle to provide support for the thermal payload simulator as well as reducing the load concentration of the baffle positioning mechanism. This mechanism allowed the lower two baffles to move with respect to the cryoshroud and the fixed upper baffle. Continuous LH_2 cooling flow was maintained by means

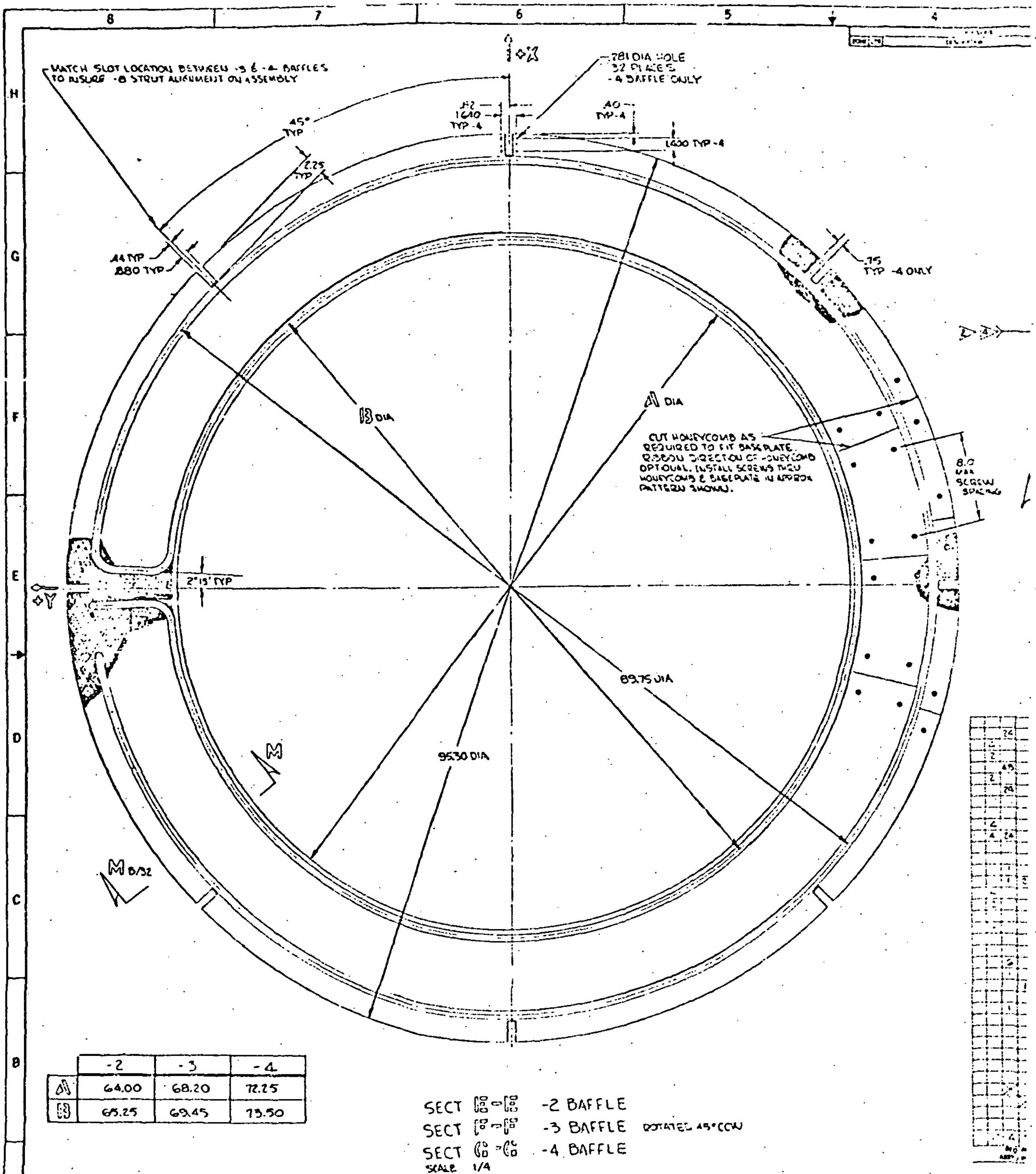

	-2	-3	-4
A	64.00	68.20	72.25
B	65.25	69.45	73.50

ORIGINAL PAGE IS OF POOR QUALITY

Figure 5-7. Baffle Assembly - Sandwich Construction

Dimensions: All dimensions are in inches

NOTES: UNLESS OTHERWISE SPECIFIED

1- WELD PER MIL-W-8604
2- DYE PENETRANT INSPECT WELDS NOTED PER MIL-I-6866. 100% INSPECTION REQUIRED. NO CRACKS PERMITTED
3- LEAK TEST LINES WITH HELIUM. MAX ALLOWABLE LEAKAGE 10^{-6} CC/SEC AT 15 PSIG
4- DO NOT ALLOW FLANGE FACE TEMPERATURE TO EXCEED 275°F DURING WELDING. USE EXTERNAL FLOOD COOL OR CHILL WITH LN2 AS REQUIRED
5- CLEAN BASEPLATE & HONEYCOMB PRIOR TO BONDING. FPL CLEAN BASEPLATE. SPRAY CLEAN HONEYCOMB WITH NAPHTHA
6- MAY BE FABRICATED BY CUTTING VARIOUS ARC LENGTHS OF THE REQUIRED ANNULUS. BUTT WELD SHEET STOCK INTO A CONTINUOUS ANNULUS. DO NOT WELD HONEYCOMB
7- PRODUCT OF HEXCEL AEROSPACE
8- BOND HONEYCOMB TO PLATE WITH CREST 1252. MIX & APPLY PER MFG INSTR TO APPROX 5 MIL THICKNESS. VACUUM BAG TO HOLD DURING CURE.

4 ONLY

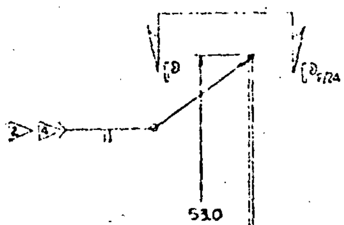

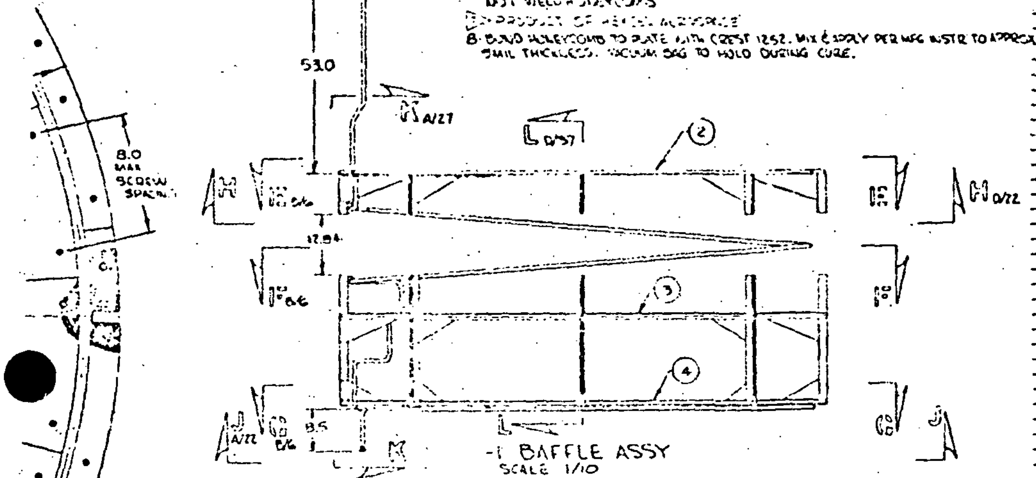

-1 BAFFLE ASSY
SCALE 1/10

PARTS LIST

Item	Part or Identifying Number	Nomenclature or Description
	[illegible]	SCREW
	[illegible]	NUT PLATE
	[illegible]	NUT
	[illegible]-4	NUT
	[illegible]	RIVET
	[illegible]	BOLT
	[illegible]	BOLT
	[illegible]	BOLT
	[illegible]	BOLT
	[illegible]	WASHER
	[illegible]	WASHER
21	-21	BRACKET
20	-20	BRACKET
	[illegible]	HONEYCOMB
	[illegible]	HONEYCOMB
	[illegible]	BOLT
	-19	CLAMP BLOCK
	-18	CLAMP PLATE
17	-17	CLAMP ASSY
	[illegible]	SETSCREW
	-16	U-CLAMP
15	-15	BLOCK
14	-14	BASE PLATE
13	-13	[illegible]
12	-12	[illegible]
11	-11	[illegible]
10	-10	TUBE
9	-9	CLAMP
8	-8	STRUT
7	-7	BRACKET
6	-6	BRACKET
5	-5	STRUT
4	-4	BAFFLE
3	-3	BAFFLE
2	-2	BAFFLE
	-1	[illegible]

CONVAIR AEROSPACE DIVISION OF GENERAL DYNAMICS
SAN DIEGO CALIFORNIA

BAFFLE ASSY

E | 14170 | PD73-0084

PD73-0084

FOLDOUT FRAME

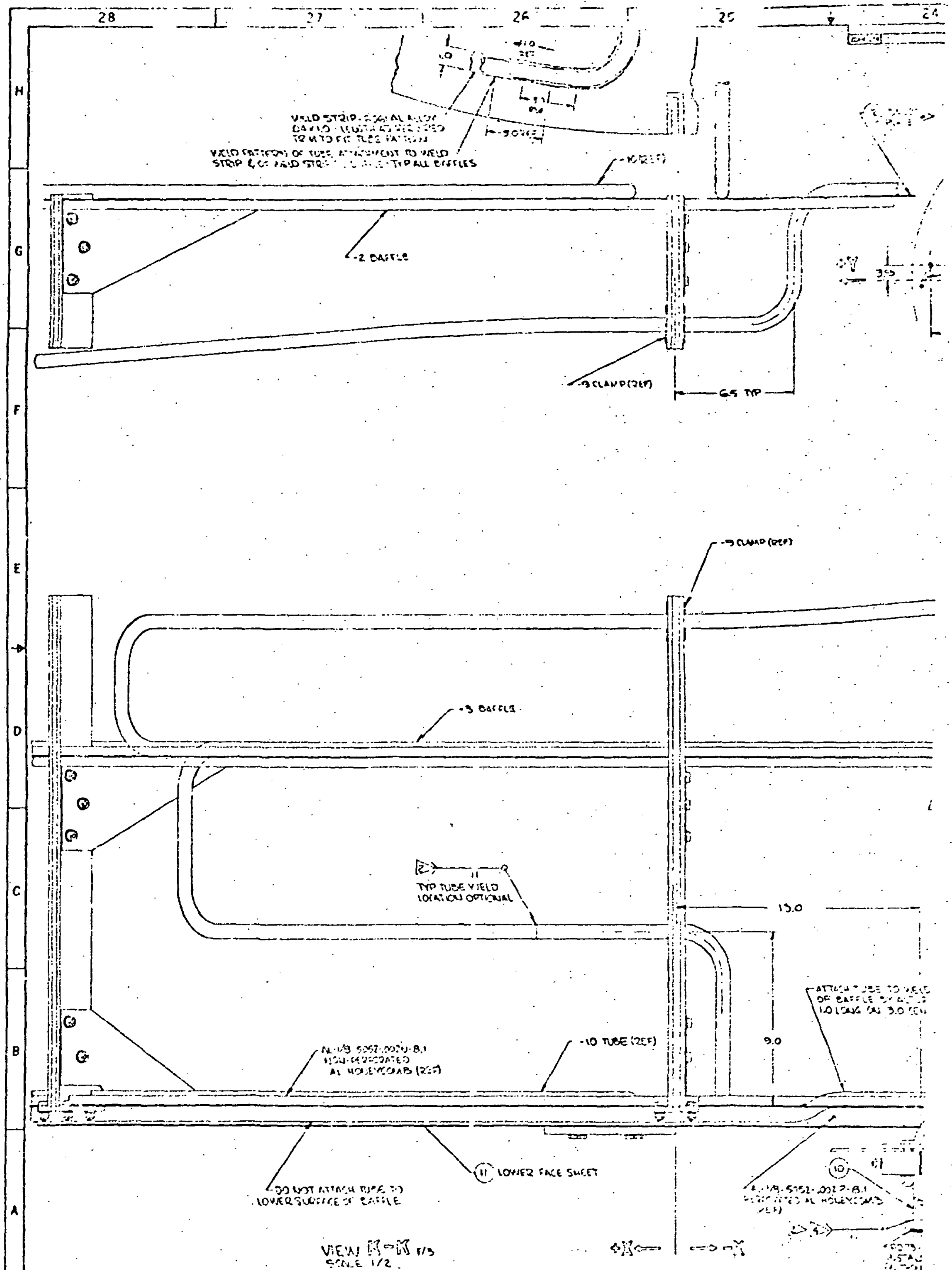

Figure 5-8. Baffle .

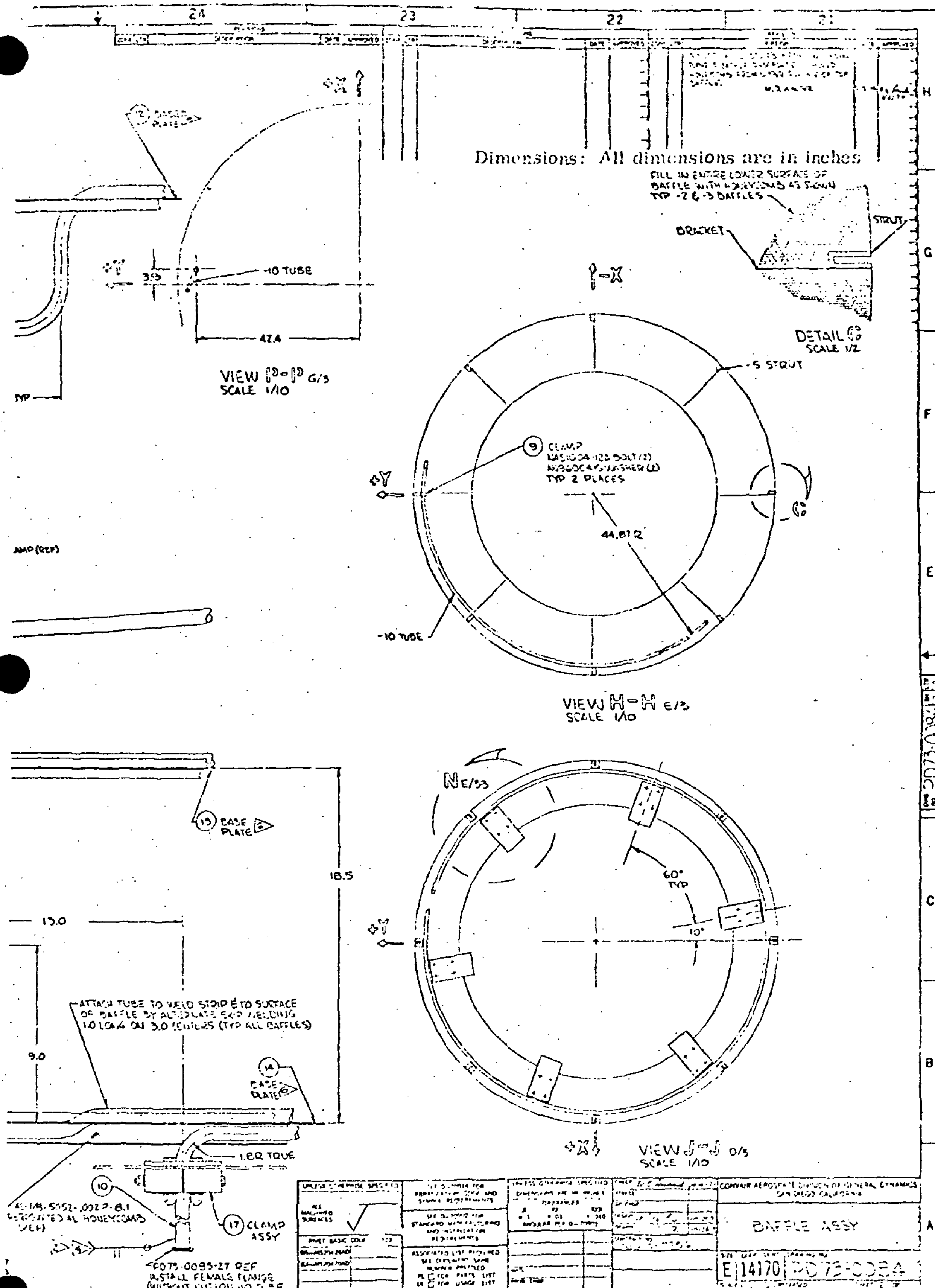

Figure 5-8. Baffle Assembly - Cooling Coil Arrangement

FOLDOUT FRAME 2

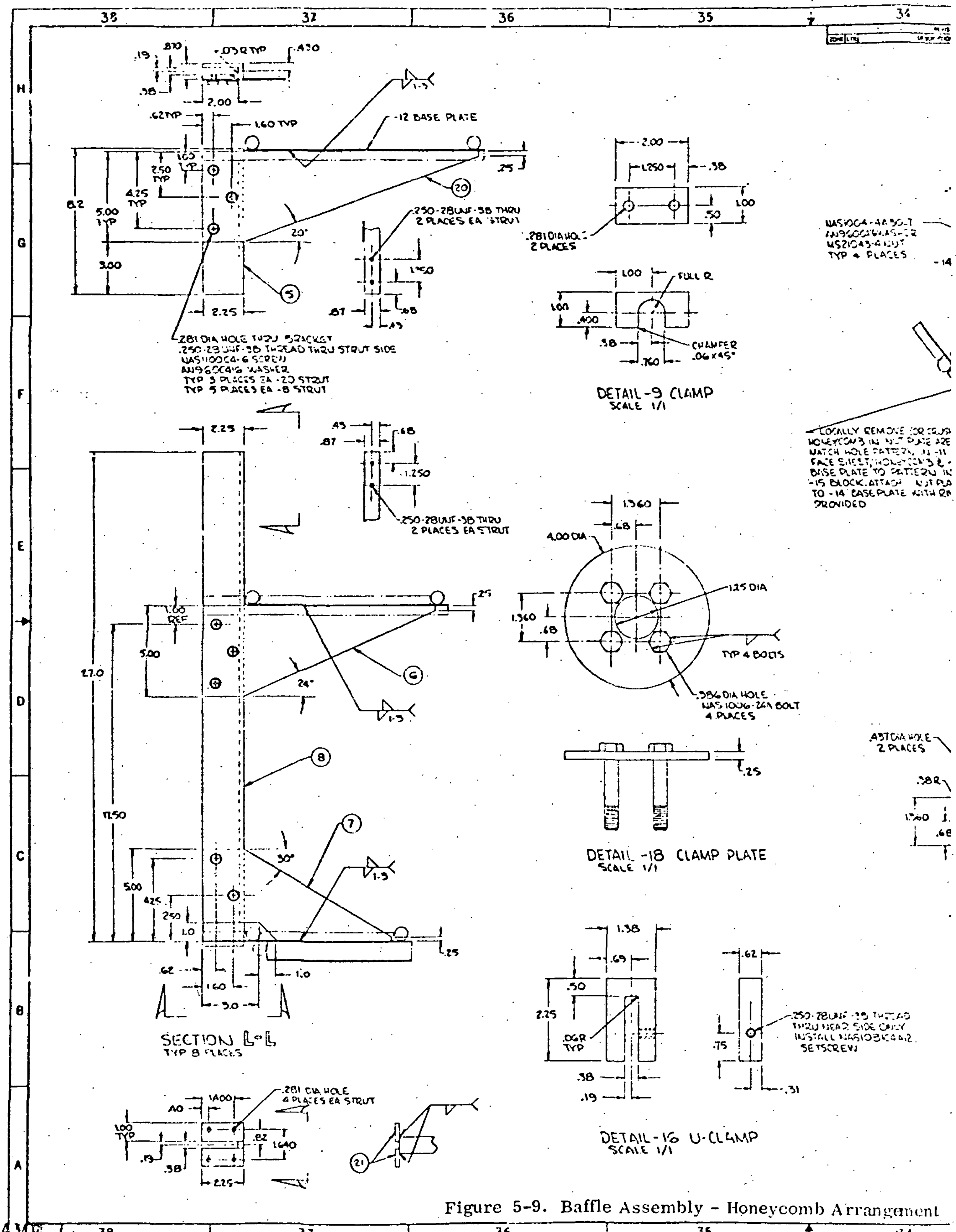

Figure 5-9. Baffle Assembly - Honeycomb Arrangement

FOLDOUT FRAME

Dimensions: All dimensions are in inches

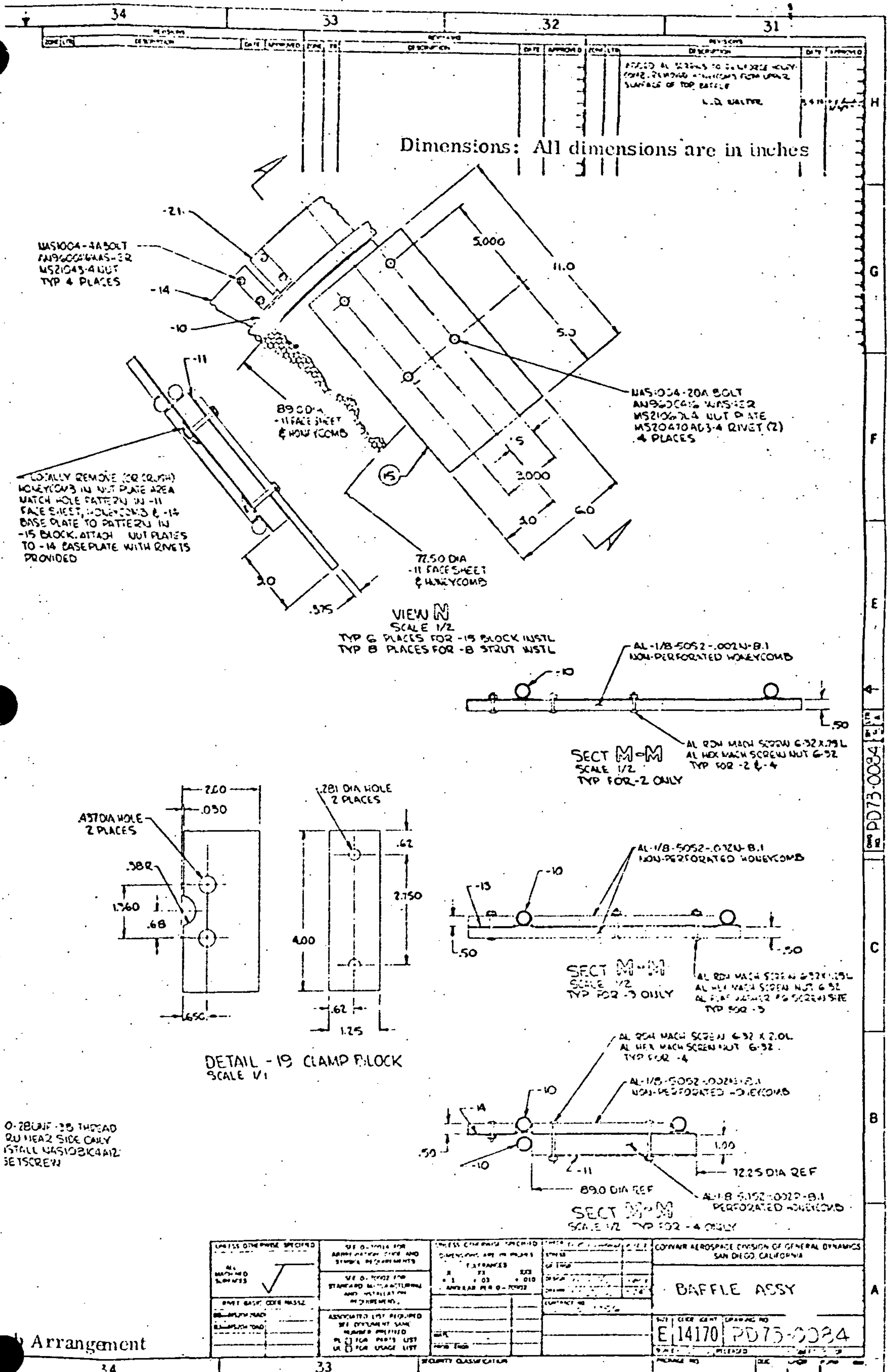

b Arrangement

FOLDOUT FR

of two cooling tube coils extending around the outside edge of the baffles. One of these coils was below the lower two movable baffles and the other coil was between the upper fixed baffle and the lower two movable baffles (Figures 5-7 and 5-8). These two coils extended and compressed like coils in a spring as the two movable baffles were adjusted up and down. With this method, there was no high spot in the cooling tubes for vapor entrapment. In the same manner, two coils were used between TPS and bottom of the cryoshroud to provide movement for the TPS. At the upper baffle, the tube was vented up through a hole in the cryoshroud upper cover. Eight slotted struts were provided at the outside edge of both the single upper fixed baffle and of the two lower movable baffles. These positioned and guided the baffles as they were moved in the shroud. "U" clamps locked the upper baffle in position and prevented the lower baffles from falling out during removal of the thermal payload simulator.

5.3.3 FABRICATION. Prior to fabricating the cryoshroud baffles, a sandwich sample consisting of 0.00102 m (0.040 in) thick 6061 aluminum with 1.587 m (0.625 in) honeycomb attached to both sides was immersed in liquid nitrogen for 2 minutes. The sample was removed from liquid nitrogen and allowed to return to ambient temperature. This test was repeated 19 times for a total of 20 cycles. Twenty additional tests of the same kind were conducted using liquid hydrogen. There was no apparent failure of the joint.

All base plate sections, tubing and honeycomb materials were cut and chemically cleaned. The tubing was provided with an additional 0.0254 m (1.0 in) wide aluminum base plate to avoid warping of the 2.44 m (96 in) O.D. annular baffle base plates. Welds of 0.0254 m (1.0 in) length at 0.076 m (3 in) centers were applied on each side of the tube to ensure good heat conduction between tubing and base plates. All liquid hydrogen tubing was leak checked and repaired as necessary after the welding operation. Unforeseen distortions of the 0.00102 m (0.040 in) aluminum baffle base plates were encountered during welding of the liquid hydrogen tubing onto the baffle sheet material. Since proper bonding of the honeycomb to the base plates could not be assured under these circumstances, the 0.00102 m (0.040 in) thick aluminum plate was replaced by 0.0032 m (0.125 in) thick plate material. Welding of the tubing to the new baffle sheet material was completed without distortions. The honeycomb material type AL-1/8-5052-002P-8.1 perforated, was purchased from HEXCEL Aerospace Company. This material was utilized on the lower surface of the upper baffle, on both surfaces of the intermediate baffle and on the top surface of the lower baffle (Figure 5-9). The honeycomb material on the lower surfaces of the bottom plate was Hexcel Type AL-1/8-5052-002 N-8.1 Non-Perforated. A face plate was bonded to it to make a rigid sandwich construction for the movable baffle. The plate was cut in sections and prefitted to blue print dimensions. It was then bonded to the baffle base plate under vacuum pressure for 18 hours utilizing APCO 1252 urethane adhesive. The honeycomb was additionally bolted to the plate with 6-32 aluminum bolts to achieve good thermal conductance and a better mechanical joint.

5.4 BAFFLE AND THERMAL PAYLOAD SIMULATOR POSITIONING MECHANISM

The thermal performance test of the customized multilayer insulation required that the spacing between test tank and thermal payload simulator could be adjusted from 0.457 m (18 in) to 0.151 m (6 in). The lower two baffles and the thermal payload simulator were designed to move together; the bottom baffle remaining in the same plane as the payload simulator as they were adjusted up and down. This was provided for by resting the thermal payload simulator on six phenolic blocks bolted to the bottom of the lowest baffle and resting three of the phenolic blocks on three 0.0254 m (1.0 in) diameter screw-jacks extending through the bottom of the cryoshroud, Figure S-1. The rotating nuts for the jack screws were fabricated from Teflon. A bicycle-chain sprocket was attached to the Teflon nut at the bottom of each of screw-jacks and all three sprockets were driven simultaneously by a single chain. By changing chain position on the sprocket, very minute adjustments to thermal payload simulator heights were made to level the thermal payload simulator during installation. The chain was driven by a small sprocket and hand crank on a shaft that passed through the bottom of the chamber. As a back up to the positioning transducer, the sprocket tooth ratio and jack screw threads/inch combined, required 166.5 turns of the hand crank to produce 0.152 m (6.0 in) of travel.

Drawings of the positioning mechanism with all details are shown in Figures 5-10 through 5-16. The selection of the material for the positioning mechanism parts was based on low heat transfer considerations.

5.5 GUARD TANK DESIGN AND FABRICATION

In order to prevent entry of extraneous heat to the test tank, fluid lines going to the test tank passed through the liquid hydrogen guard tank as shown in Figure S-1. The test tank was also suspended from the guard tank which was attached to a support ring in the top cover of the cryoshroud.

The guard tank was fabricated from 304 CRES material. Its construction (Figures 5-17 and 5-18) consisted of two formed 0.610 m (24 in) diameter tank heads connected by a 0.1422 m (5.6 in) high cylinder. The material gauge was 0.0032 m (0.125 in). A heavy mounting ring was welded to the top of the guard tank to transfer loads from the test tank to the cryoshroud structure. Three lugs were welded to the bottom of the tank at its periphery for attachment of the test tank support struts (Ref. 5-2).

The test tank fill/drain line and vent line, consisting of 0.051 m (2.0 in) O.D., 0.0009 m (0.035 in) wall, 304 CRES tubing, penetrated the guard tank. Both of these lines passed with a "U" bend through the guard tank to prevent radiation tunneling and to allow for thermal contraction. The guard tank fill and vent lines were fabricated from 0.0191 m (0.75 in) O.D. CRES-304 tubing. The instrumentation lines going into the test tank passed into the tank through the vent line. This eliminated an electrical pass-thru in the test tank door and an additional line through the guard tank.

-1, Basic Drawing
-3, Nut (3) - Teflon
-5, Washer (3) - 0.0032 m (0.125 in.) 6061 T6 Aluminum
-7, Angle (12) - 0.0032 m (0.125 in.) 6061 T6 Aluminum
-9, Adapter Ring (3) - 0.0032 m (0.125 in) 6061 T6 Aluminum
-11, Sprocket
-13, Jackscrew (3) - 1-8 NC, 0.406 m (16 in) Screw Thread 0.0254 m(1.0 in) Dia Epoxy Fiberglass
-15, Guide (3) - Teflon
-17, Angle (12) - 0.0032 m (0.125) 6061 T6 Aluminum

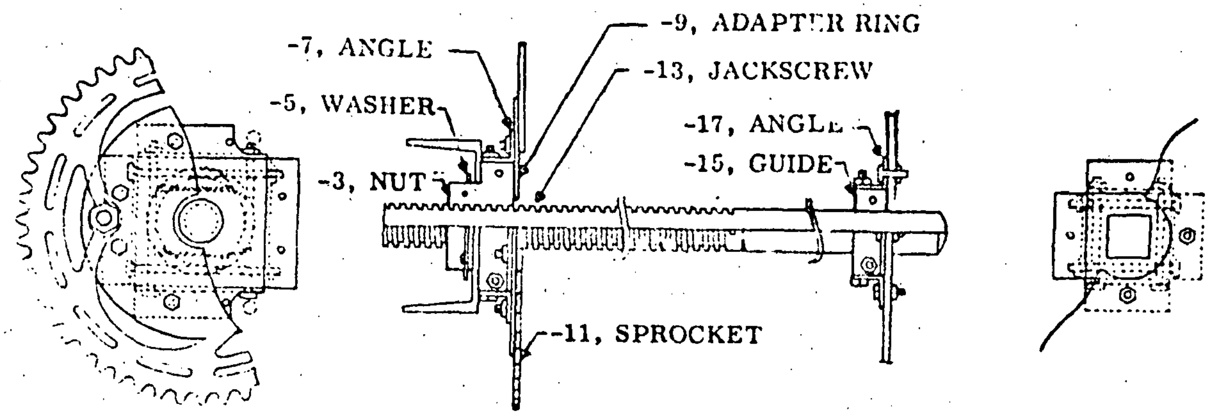

Figure 5-10 Thermal Payload Simulator and Cryoshroud Baffle Positioning Mechanism

NOTE: All dimensions are in inches

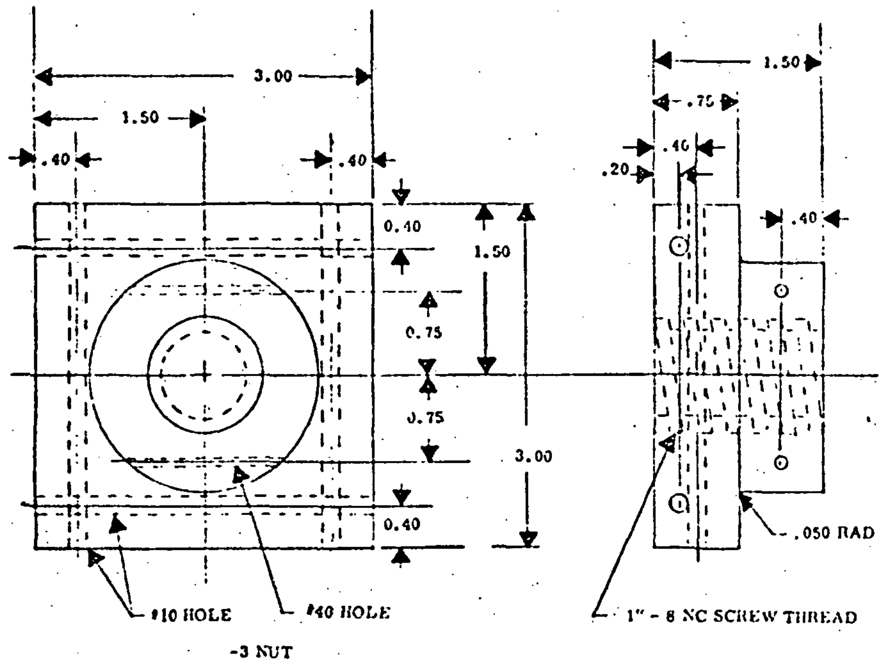

Figure 5-11. Positioning Screw-Nut

NOTE: All dimensions are in inches

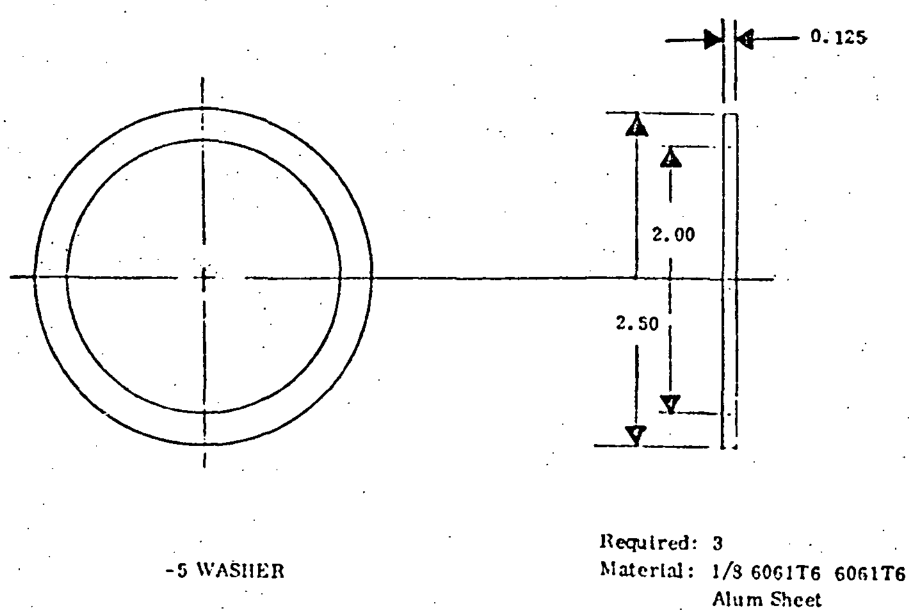

Figure 5-12. Positioning Screw-Washer

NOTE: All dimensions are in inches

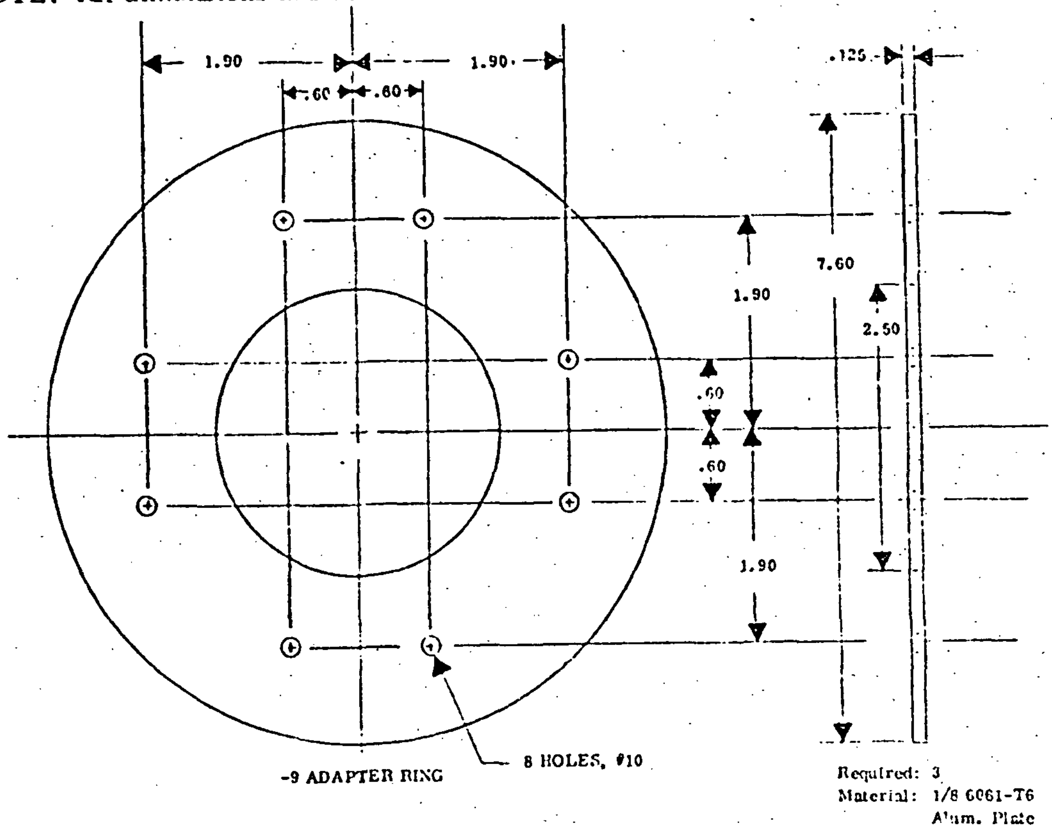

Figure 5-13. Positioning Screw - Adapter Ring

NOTE: All dimensions are in inches

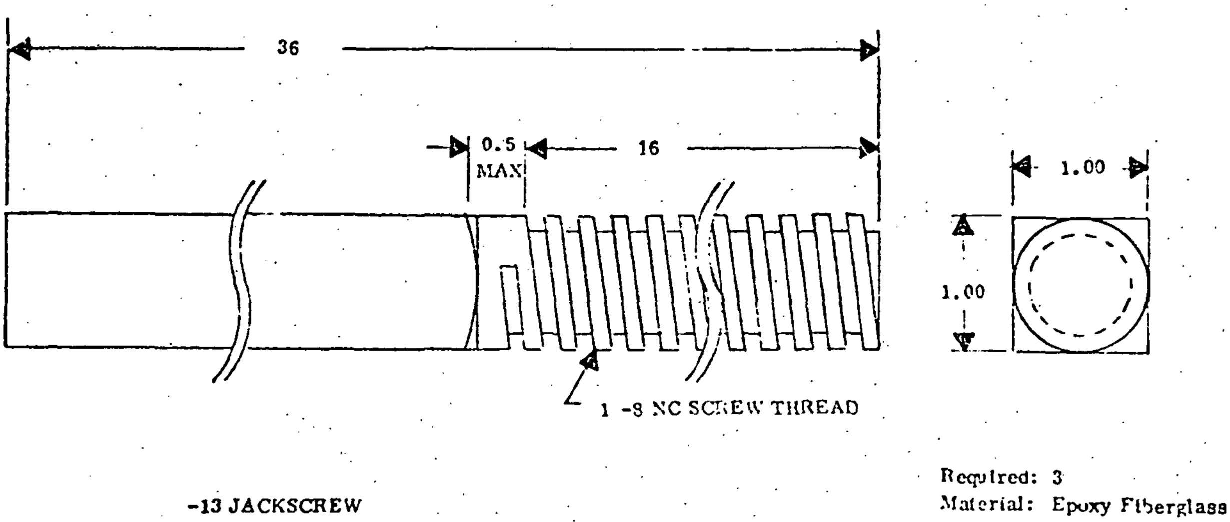

Figure 5-14. Positioning Mechanism - Jack Screw

NOTE: All dimensions are in inches

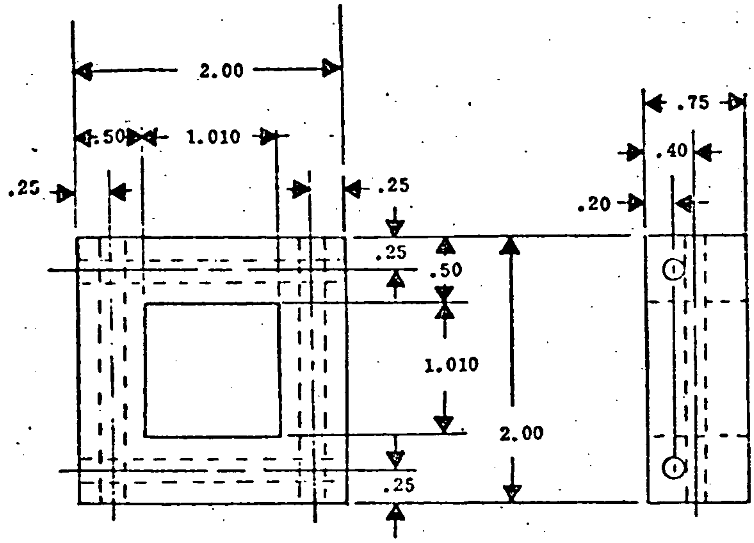

-15 GUIDE

Required: 3
Material: Teflon

Figure 5-15. Positioning Mechanism - Guide

NOTE: All dimensions are in inches

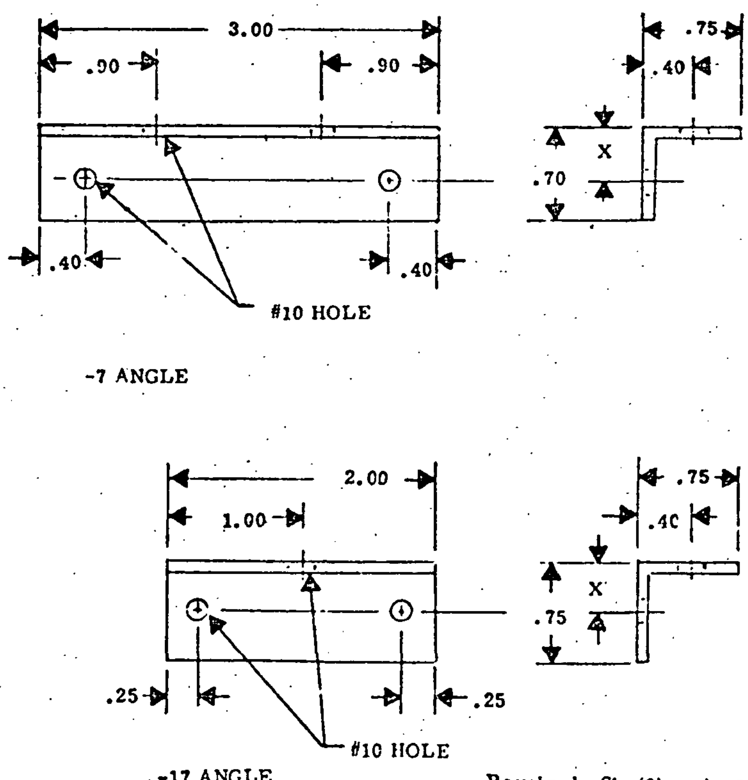

Required: Six (6) each -7 & -17 with x = .35
Six (6) each -7 & -17 with x = .55
Material: 3/4 × 3/4 × 3/32 or 1/8 6061 T6 Alum Angle

Figure 5-16. Positioning Mechanism - Angle

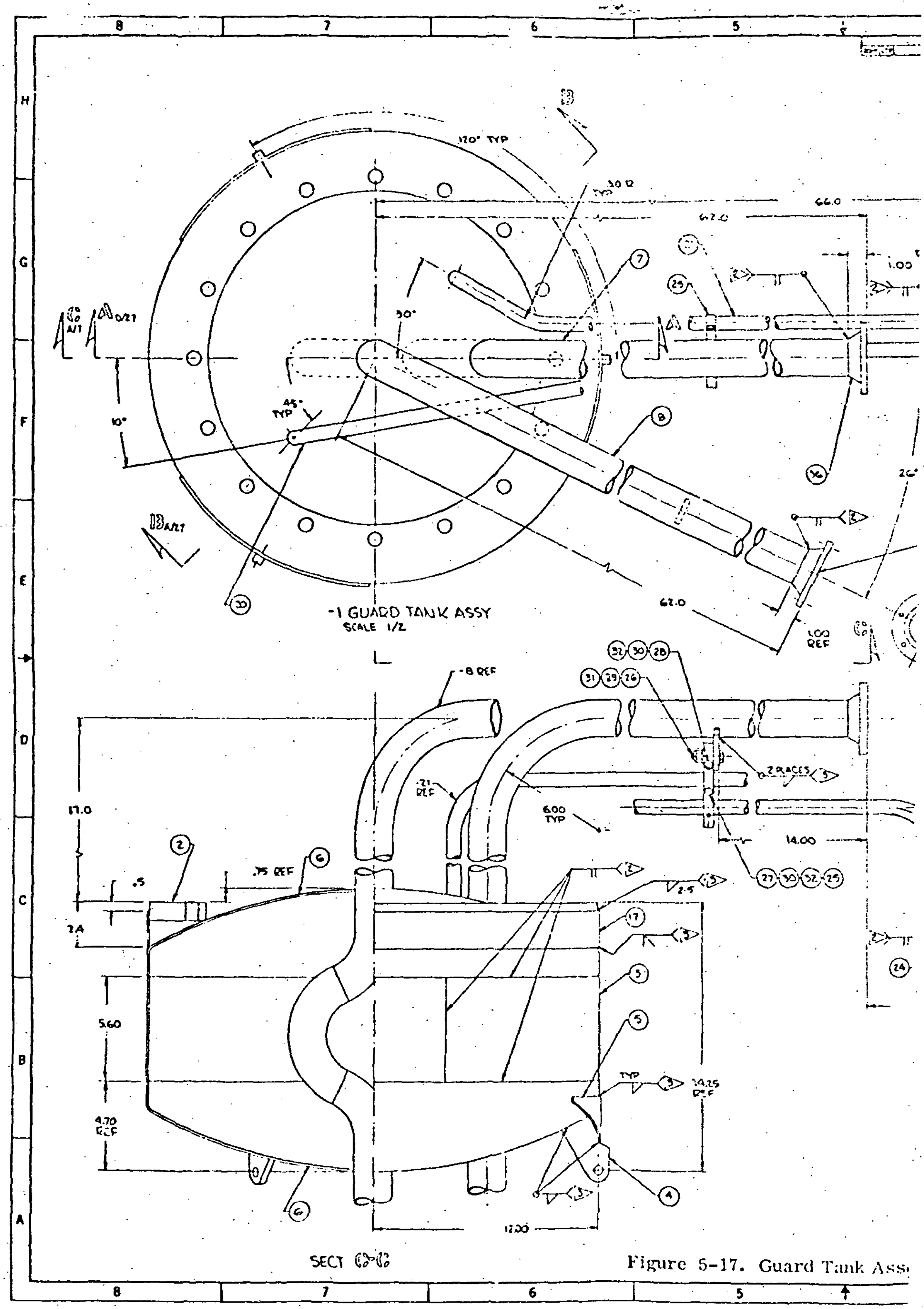

Figure 5-17. Guard Tank Ass[illegible]

IAL PAGE IS
OR QUALITY

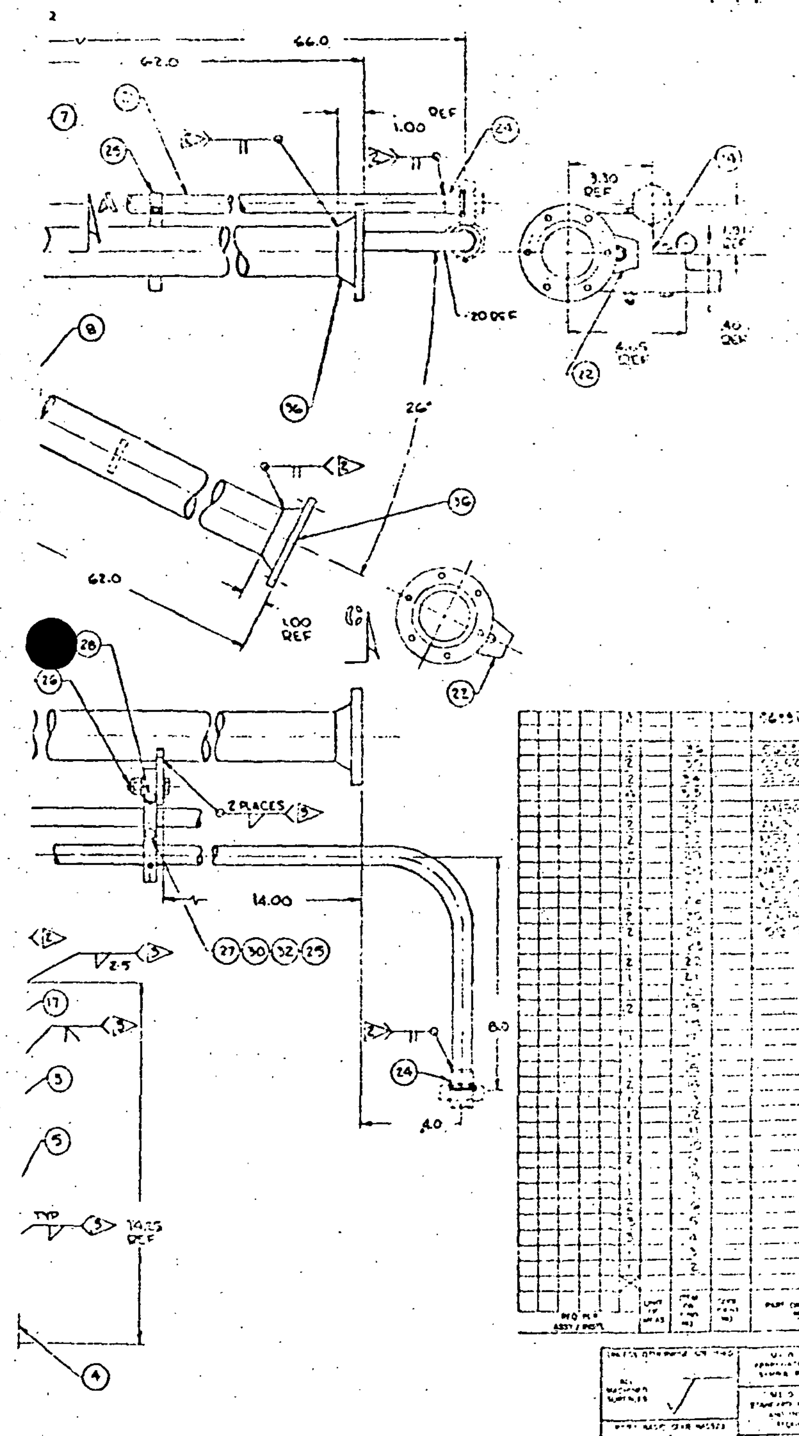

Dimensions: All dimensions are in inches.

NOTES: UNLESS OTHERWISE SPECIFIED

1- WELD PER MIL-W-8611
2- 100% RADIOGRAPHIC INSPECT WELDS NOTED PER MIL-STD-453. ACCEPTANCE STANDARD PER 0-77005
3- DYE PENETRANT INSPECT WELDS NOTED PER MIL-I-6866. 100% INSPECTION REQUIRED. NO CRACKS PERMITTED
4- IDENTIFY PER 0-10042 AS REQUIRED. LOCATION OPTIONAL
5- IMPRESSION MARKING OF PARTS NOT PERMITTED
6- WELD AFTER INSTALLATION OF GUARD TANK INTO CRYO-SHROUD COVER
7- PROOF PRESSURE TEST THE TEST TANK FILL & DRAIN (-5) AND VENT (-7) LINES TO [illegible] PSIG
8- PROOF PRESSURE TEST THE GUARD TANK ASSY TO 30 PSIG
9- LEAK TEST LINES & GUARD TANK ASSY WITH HELIUM. MAX ALLOWABLE LEAKAGE [illegible] CC/SEC AT [illegible] PSIG
10- PRODUCT OF MINI-FLEX CORP, VAN NUYS, CA
11- CLEAN TEST TANK FILL & DRAIN (-5) & VENT (-7) LINES TO 0-75192-2
12- CLEAN GUARD TANK & LINES TO REMOVE LARGE PARTICLES & CHIPS
13- PRODUCT OF AEROQUIP/MARMAN DIVISION
14- TEST FACILITY REQUIREMENTS
15- SIZE WELD BANDS & DUCT AS REQUIRED TO FIT SILICONE NECK
16- SEAM WELD & INSPECT PER 0-75751
17- CLEAN LOCALLY PRIOR TO RESISTANCE WELDING PER 0-73509-1
18- INSPECT INSIDE OF SMALL ELECTRICAL HARNESS TUBE AFTER WELDING FOR BURN THRU OR BLISTERS. REMOVE ANY PROTUBERANCES.
19 ALL DIMENSIONS IN ENGLISH UNITS
20- COORDINATE WELDING OF TUBES INTO GUARD TANK & TANK CLOSURE WELD WITH TEST ENGINEERING
21- FLARE END OF INNER TUBE TO 2.0 OD. FLARE ANGLE TO BE 30-50°.
22- FLARE END OF TUBE TO [illegible] X 45 [illegible]
23- PRODUCT OF ORANGE COUNTY [illegible] WORKS, ORANGE, CA. HEAD CONFIGURATION: [illegible] FLANGED, DIE FORMED, [illegible], 100% CROWN RADIUS. 24 IN. OD, NO 10 GAGE, 304 CRES
24- TRIM FLANGE SKIRT TO [illegible] .040 WALL THICKNESS. MAINTAIN INSIDE DIA

PART OR IDENTIFYING NUMBER	NOMENCLATURE OR DESCRIPTION			NOTES
76851-2005	FLANGE, MALE			SEE NOTES 13 & 14
[illegible]-2005	FLANGE, FEMALE		4	SEE NOTE 13
[illegible]-2005	FLANGE, MALE		[illegible]	SEE NOTE 13
[illegible]	[illegible]		27	SEE NOTE 10

PARTS LIST

TANK ASSY - GUARD

E 14170 PD73-0083

Figure 5-17. Guard Tank Assembly

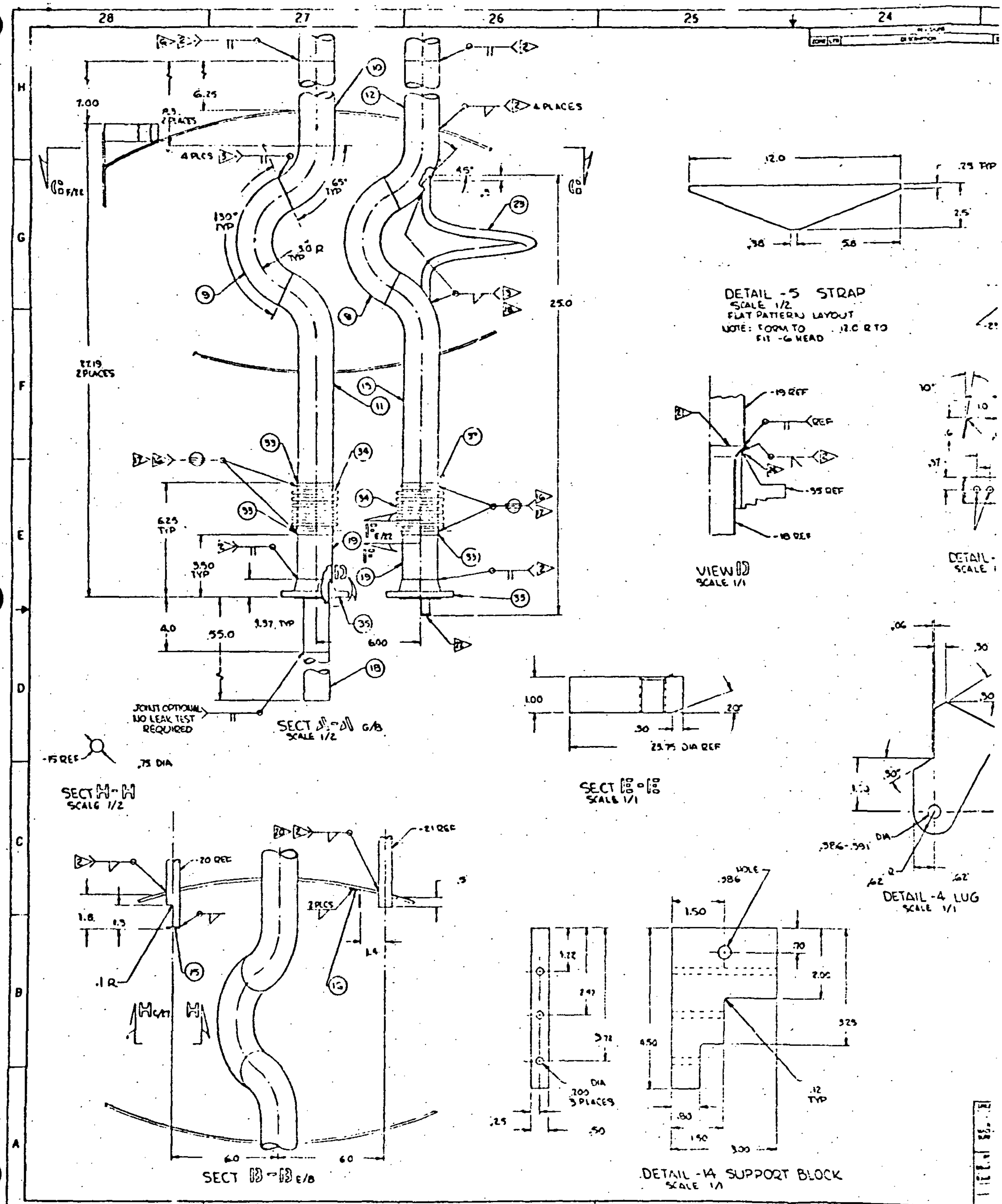

Figure 5.19 Guard Tor

Dimensions: All dimensions are in inches

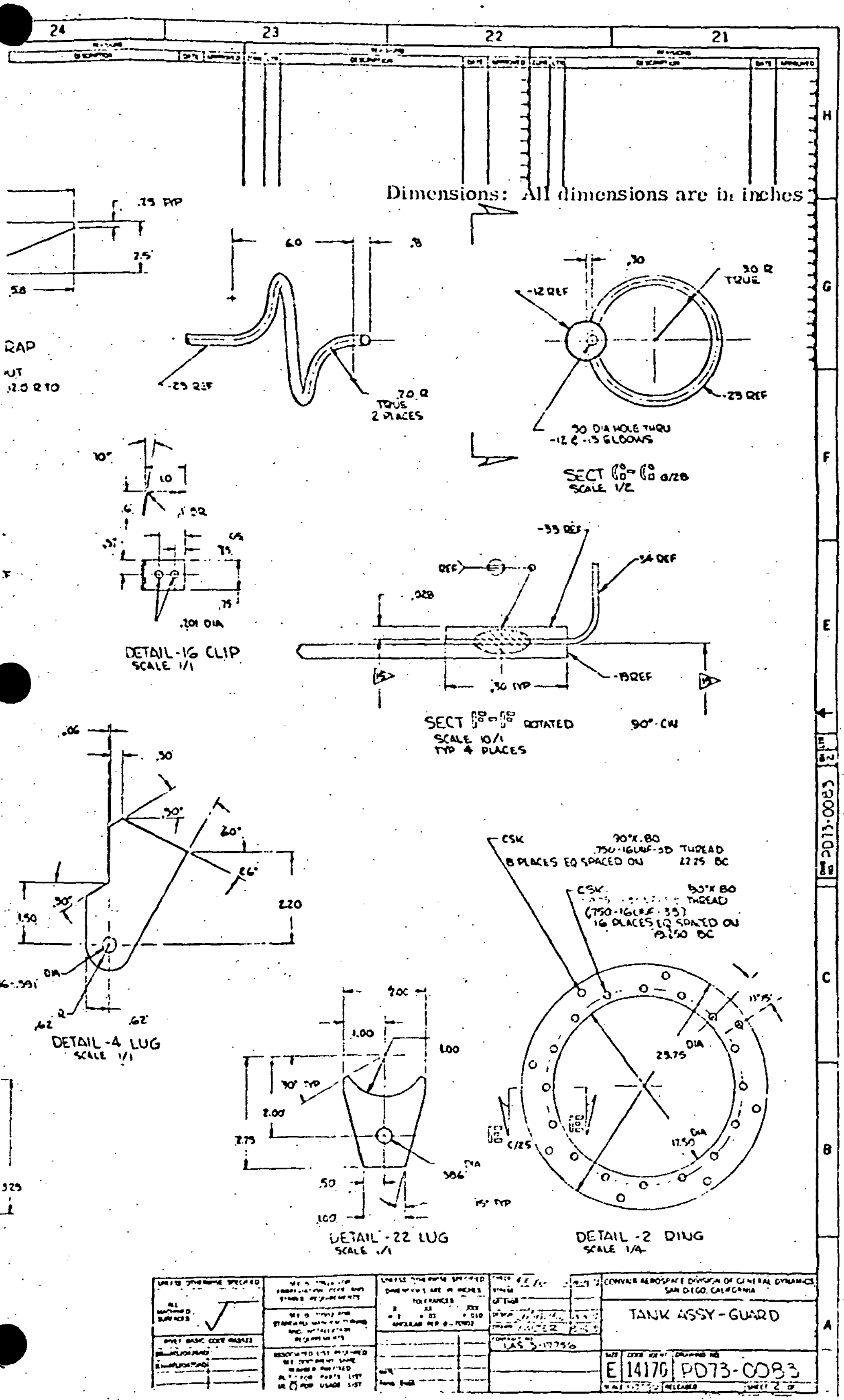

ORIGINAL PAGE IS
OF POOR QUALITY

The electrical harness was fed through a separate tube in the guard tank to provide good thermal contact and to assure complete heat removal. Bellows (SS-2000-120-85A, Mini-Flex Corp., Van Nuys, CA) were provided in both the lines between the test tank and guard tank for ease of installation and to assure that the loads caused by movement of the test tank were not transmitted through these lines.

5.6 MODIFIED CRYOSHROUD ASSEMBLY

5.6.1 ASSEMBLY SEQUENCE. Figure 5-19 shows the assembly of the cryoshroud cover including the fill/vent lines of the test tank, guard tank, thermal payload simulator, cryoshroud and baffles. The assembly of the cryoshroud and baffles with the guard tank, test tank, thermal payload simulator and Baffle/TPS positioning mechanism is presented in Figure 5-20. The assembly of the major components was initiated by mating the guard tank to the cryoshroud cover. The uninsulated test tank was attached to the guard tank/shroud cover (tank assembly) as shown in Figures 5-21 through 5-23. The tank assembly was leak checked with gaseous helium utilizing a helium mass spectrometer. After the installation of the baffles to the cryoshroud (Figure 5-24), the tank assembly was temporarily mounted to the cryoshroud/baffle assembly. The test tank supports were adjusted to obtain a concentric location of the test tank within the cryoshroud/baffle assembly.

Prior to mounting the baffles on the cryoshroud, all baffle supports were fabricated and attached to the wall as shown in Figure 5-9. The baffle cooling coils were externally cleaned with Freon solvent, then leak checked with helium and repaired as necessary.

As shown in Figure 5-20, the guard tank was supported from the cryoshroud lifting structure. This arrangement permitted assembly and installation of the cryoshroud cover and test tank as a unit.

The cryoshroud assembly support consisted of 6 micarta and aluminum legs, bolted to the cryoshroud and resting on the bottom of the vacuum chamber. The micarta material is used to minimize heat transfer.

5.6.2 THERMAL PAINT REQUIREMENTS. After assembly, all interior surfaces including the cryoshroud, baffles, and attachment hardware viewing the test package were completely covered with 3M "Nextel" Black Velvet (3M401C10) paint to achieve the highest emissivity possible. This paint is designed for surfaces requiring high emissivities and low outgassing in a vacuum.

5.6.3 FLUID TUBING. Single and double Conoseals were used for flange and tubing joints where welding was not feasible or desirable. Single Conoseals were utilized for stainless steel joints while double Conoseals were applied where a bi-metal (i.e., Al - Cres) joint could cause a possible leak. The Conoseals and Conoseal groove information were provided by Aeroquip Marman Corporation. The cryoshroud and baffle filling operation was accomplished through a single fill line at the bottom panel.

The electrical harness was fed through a separate tube in the guard tank to provide good thermal contact and to assure complete heat removal. Bellows (SS-2000-120-85A, Mini-Flex Corp., Van Nuys, CA) were provided in both the lines between the test tank and guard tank for ease of installation and to assure that the loads caused by movement of the test tank were not transmitted through these lines.

5.6 MODIFIED CRYOSHROUD ASSEMBLY

5.6.1 ASSEMBLY SEQUENCE. Figure 5-19 shows the assembly of the cryoshroud cover including the fill/vent lines of the test tank, guard tank, thermal payload simulator, cryoshroud and baffles. The assembly of the cryoshroud and baffles with the guard tank, test tank, thermal payload simulator and Baffle/TPS positioning mechanism is presented in Figure 5-20. The assembly of the major components was initiated by mating the guard tank to the cryoshroud cover. The uninsulated test tank was attached to the guard tank/shroud cover (tank assembly) as shown in Figures 5-21 through 5-23. The tank assembly was leak checked with gaseous helium utilizing a helium mass spectrometer. After the installation of the baffles to the cryoshroud (Figure 5-24), the tank assembly was temporarily mounted to the cryoshroud/baffle assembly. The test tank supports were adjusted to obtain a concentric location of the test tank within the cryoshroud/baffle assembly.

Prior to mounting the baffles on the cryoshroud, all baffle supports were fabricated and attached to the wall as shown in Figure 5-9. The baffle cooling coils were externally cleaned with Freon solvent, then leak checked with helium and repaired as necessary.

As shown in Figure 5-20, the guard tank was supported from the cryoshroud lifting structure. This arrangement permitted assembly and installation of the cryoshroud cover and test tank as a unit.

The cryoshroud assembly support consisted of 6 micarta and aluminum legs, bolted to the cryoshroud and resting on the bottom of the vacuum chamber. The micarta material is used to minimize heat transfer.

5.6.2 THERMAL PAINT REQUIREMENTS. After assembly, all interior surfaces including the cryoshroud, baffles, and attachment hardware viewing the test package were completely covered with 3M "Nextel" Black Velvet (3M401C10) paint to achieve the highest emissivity possible. This paint is designed for surfaces requiring high emissivities and low outgassing in a vacuum.

5.6.3 FLUID TUBING. Single and double Conoseals were used for flange and tubing joints where welding was not feasible or desirable. Single Conoseals were utilized for stainless steel joints while double Conoseals were applied where a bi-metal (i.e., Al + Cres) joint could cause a possible leak. The Conoseals and Conoseal groove information were provided by Aeroquip Marman Corporation. The cryoshroud and baffle filling operation was accomplished through a single fill line at the bottom panel.

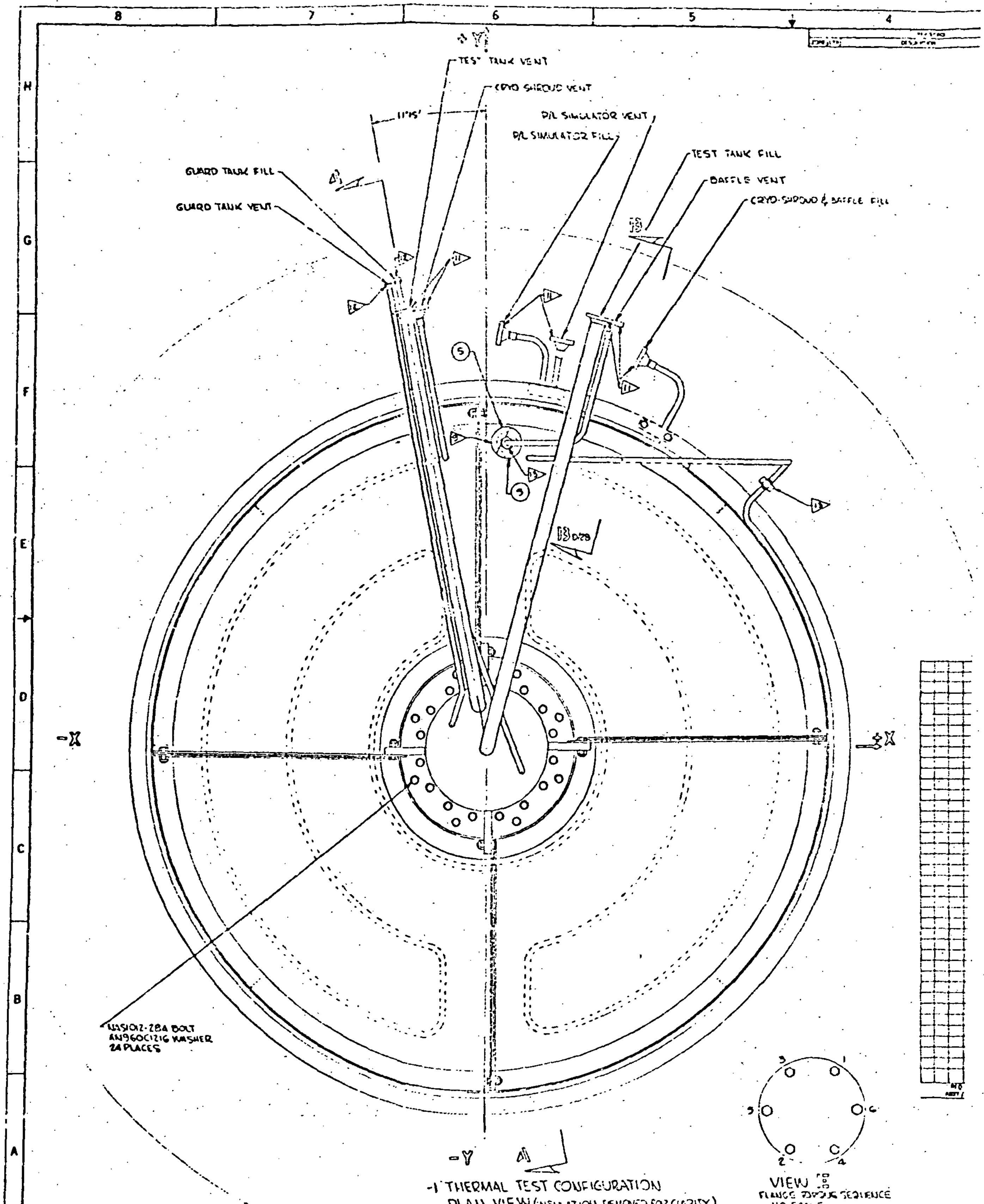

Figure 5-19. Cryoshroud Assembly

ORIGINAL PAGE IS OF POOR QUALITY

Dimensions: All dimensions are in inches

NOTES: UNLESS OTHERWISE SPECIFIED

1- DO NOT FILL TEST TANK WITH LH2 WITHOUT A STRUCTURAL ANALYSIS OF THE CRYO-SHROUD, GUARD TANK & TEST TANK

2- INSTALL MLI AS SHOWN IN SECTION A-A. USE ALUMINIZED MYLAR TAPE & VELCRO FASTENERS TO ATTACH INSULATION TO STRUCTURE & TO EFFECT CLOSURE OF BLANKETS. USE .125 THICK FOAM STRIPS FOR SEPARATORS

3- INSTALL TEST TANK ON CRYO-SHROUD COVER & LEAK TEST PRIOR TO INSTALLATION IN THE CRYO-SHROUD SHELL

4 LEAK TEST WITH HELIUM. MAX ALLOWABLE LEAKAGE IS 1X10⁻⁶ CC/SEC AT 15 PSIG

5 DIM 'D' IS NOMINALLY [illegible]. ON INSTALLATION OF TEST TANK (PD73-0012) TO GUARD TANK (PD73-0085), ADJUST STRUTS (PD73-0013) TO ADJUST BELLOWS IN PD73-0085 ASSY TO AS NEAR THEIR FREE LENGTH AS POSSIBLE WITH THE TANK LID PARALLEL TO THE CRYO-SHROUD COVER

6 ADJUST INDIVIDUAL STRUTS AS REQUIRED TO CENTER THE TEST TANK WITHIN THE CRYO-SHROUD SHELL. DIM 'C' (FROM TEST TANK TO WALL STIFFENER) SHOULD BE CONSTANT WITHIN ±.62 AT ALL STIFFENERS. DO NOT ALLOW DIM D TO DEVIATE MORE THAN ±.1 OVER THE SURFACE OF TANK COVER FROM THE BELLOWS FREE LENGTH POSITION ESTABLISHED IN NOTE 5

7- REMOVE -2 SHIPPING STRUTS & -7 CLAMP ON CRYOSHROUD VENT LINE PRIOR TO TEST

8 DO NOT ALLOW FLANGE FACE TEMPERATURE TO EXCEED 275°F DURING WELDING. USE EXTERNAL FLOOD COOL OR CHILL WITH LN2 AS REQUIRED

9 PAINT ONE SIDE OF -5 COVERS PER NOTES 10, 18 & 20

10 PREPARE UNPAINTED SURFACES WITH ANODIZ[illegible] METAL BRIGHTENER (PRODUCT OF A.C. FERGUSON CO. PHIL., PA). RINSE WITH DEIONIZED WATER. PROTECT TREATED SURFACES AGAINST CONTAMINATION. DO NOT HANDLE

11 TORQUE FLANGE BOLTS TO [illegible] IN-LB AS FOLLOWS: TIGHTEN ALL BOLTS FINGER TIGHT, THEN TIGHTEN ALL BOLTS 1/2 TURN IN SEQUENCE SHOWN IN VIEW E. CONTINUE IN THIS SEQUENCE UNTIL SPECIFIED TORQUE IS REACHED

12 TORQUE CRES TUBE FITTINGS TO 700-1050 IN-LB

13 TORQUE ALUMINUM TUBE FITTINGS TO 450-750 IN-LB

14- WELD PER MIL-W-8604

15- TEST FACILITY REQUIREMENT

16 5 STRUTS ARE USED FOR TEST & 3 STRUTS ARE USED FOR GROUND HANDLING. INSTALL ONE JAM NUT ON EACH STRUT USED FOR TEST, LOCK IN PLACE AFTER ADJUSTMENT

17 INSTALL -5 COVERS WITH PAINTED SURFACES DOWN. USE ALUMINIZED MYLAR TAPE TO ATTACH COVERS TO SHROUD

18 PRIME UNPAINTED SURFACES WITH 3M NEXTEL 901-T1 BLACK PRIMER

19 CLEAN PREVIOUSLY PAINTED SURFACES OF GREASE, WAX & SIMILAR STAINS WITH A NAPHTHA DAMPENED CLOTH OR SPONGE. RUB LIGHTLY & CHANGE CLOTHS FREQUENTLY TO REMOVE AS MUCH STAIN AS POSSIBLE WITHOUT SPREADING. REMOVE DIRT WITH A DAMP CLOTH, SPONGE OR SOFT BRISTLE BRUSH

20 PAINT INTERIOR SURFACES DESIGNATED WITH 3M NEXTEL VELVET COATING (3M 401-C10) MIX & APPLY PER MANUFACTURERS DIRECTIONS.

PART OR IDENTIFYING NUMBER	NOMENCLATURE OR DESCRIPTION	REMARKS
AN [illegible]	[illegible]	
3M [illegible]	PRIMER	PRODUCT OF 3M CO., ST PAUL, MINN
[illegible]	[illegible]	PRODUCT OF 3M CO., ST PAUL, MINN
[illegible]	[illegible]	[illegible]
[illegible]	ADAPTER	
[illegible]	BAFFLE ASSY	
[illegible]	TEST TANK	
[illegible]	[illegible]	PRODUCT OF A.C. FERGUSON CO., PHILADELPHIA, PA
[illegible]	[illegible]	[illegible] SEE NOTE 17
[illegible]	FLANGE	
[illegible]	[illegible]	[illegible] AL

PARTS LIST

CONVAIR AEROSPACE DIVISION OF GENERAL DYNAMICS SAN DIEGO, CALIFORNIA

THERMAL TEST CONFIGURATION CUSTOMIZED MLI

E 14170 PD73-0080

Shroud Assembly - Top View 3

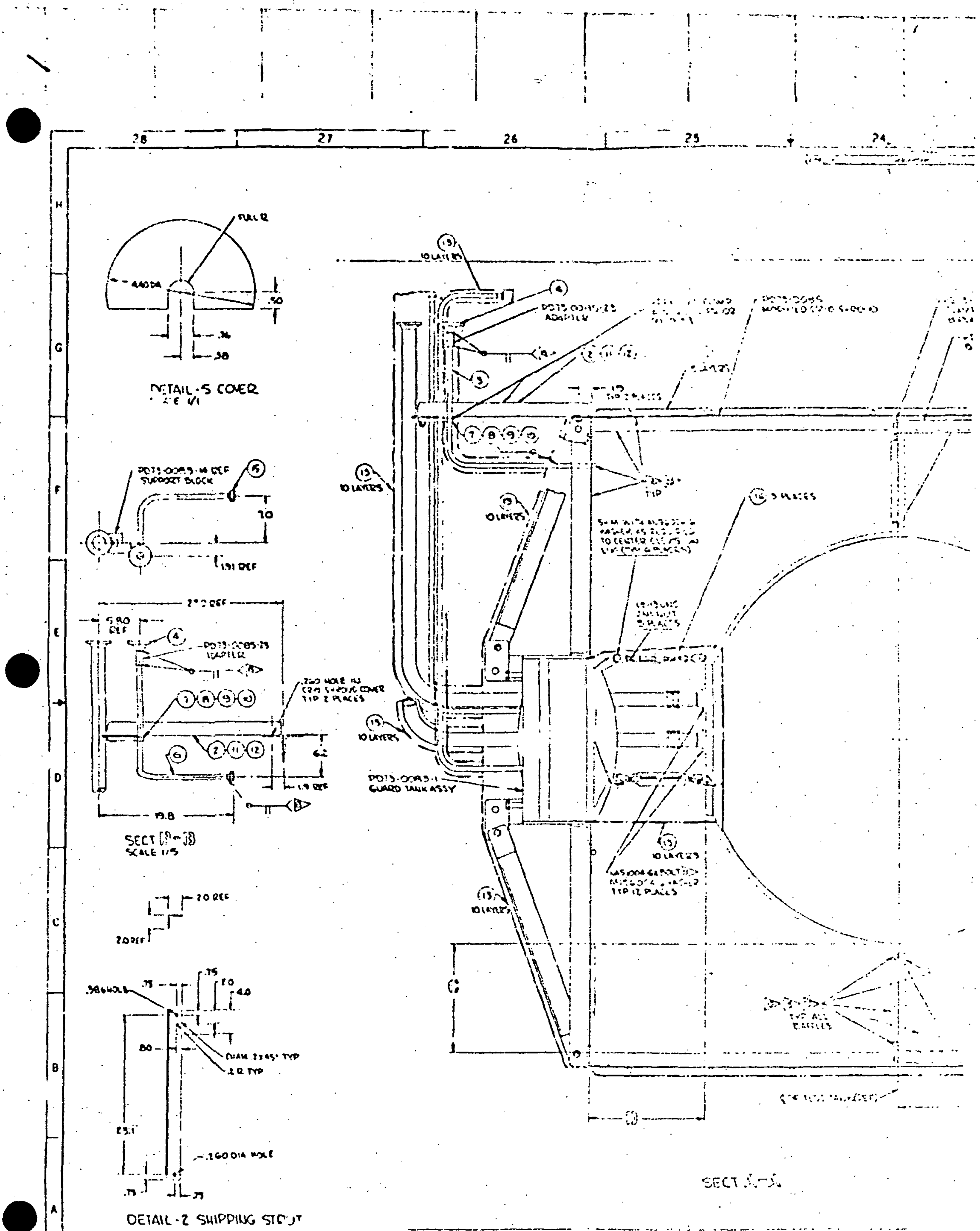

Figure 5-20. Cryoshroud Assembly - Side View

Dimensions: All dimensions are in inches

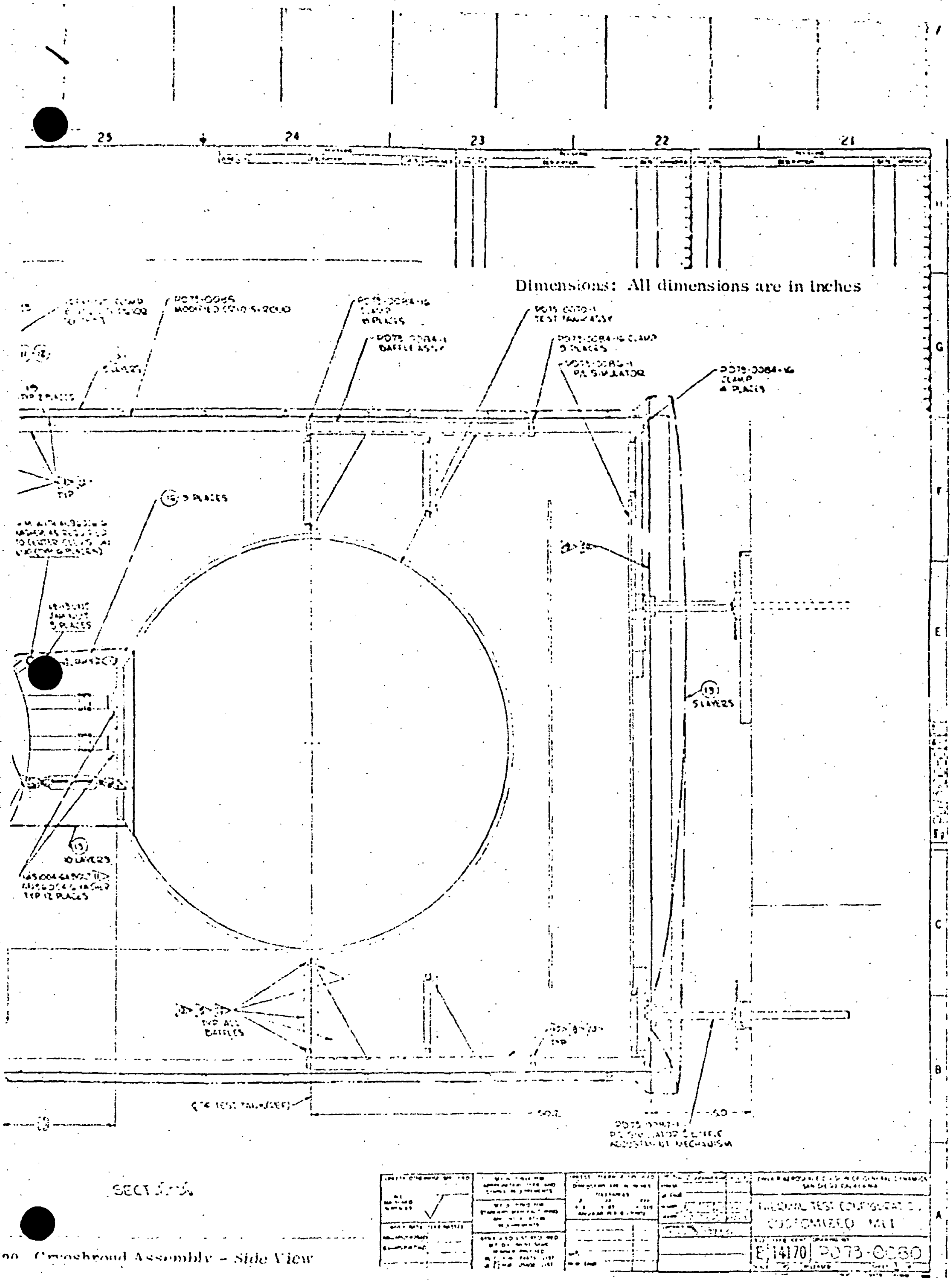

...00 Cryoshroud Assembly - Side View

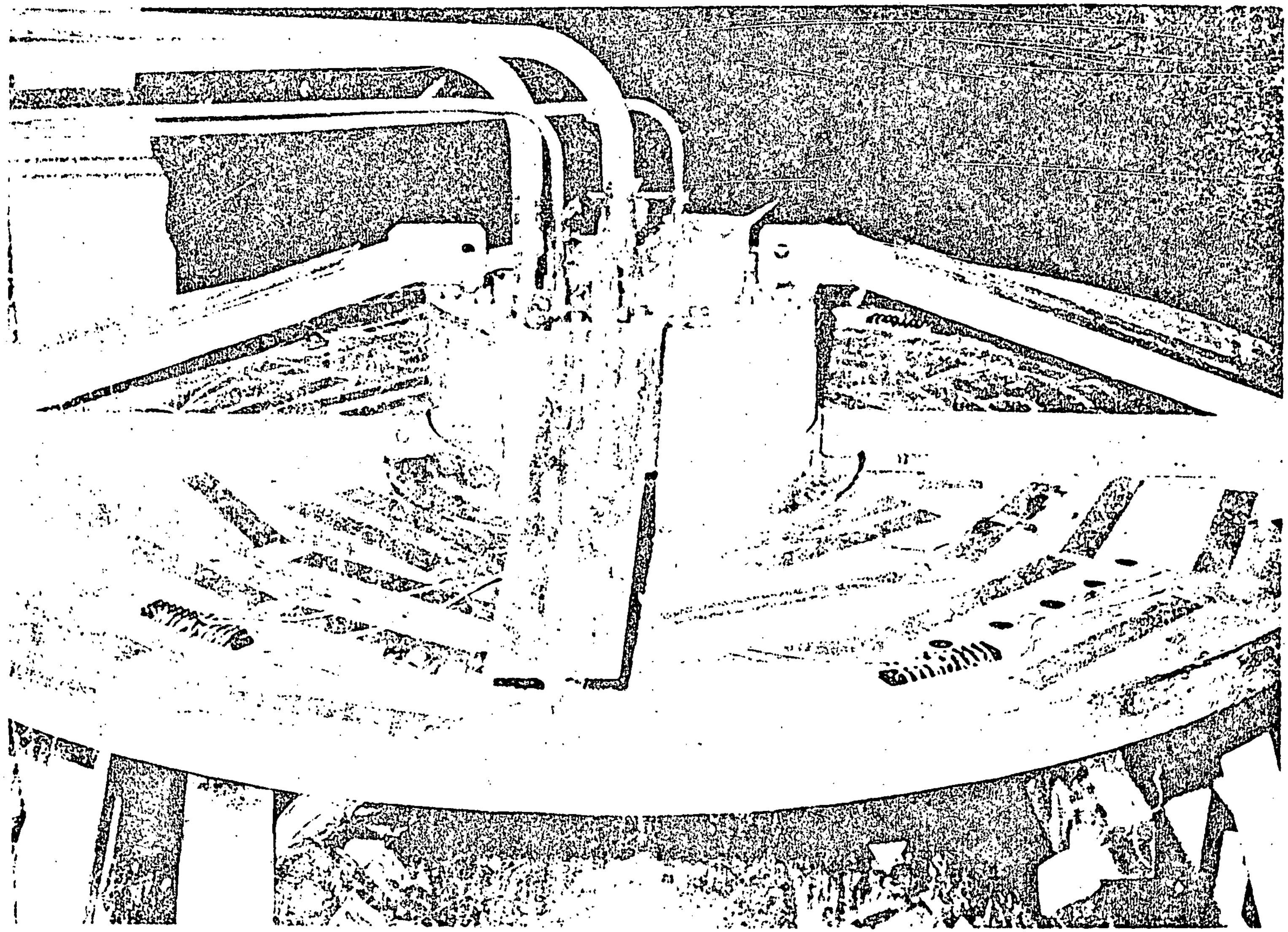

Figure 5-21. Assembly of the Guard Tank and Cryoshroud Cover

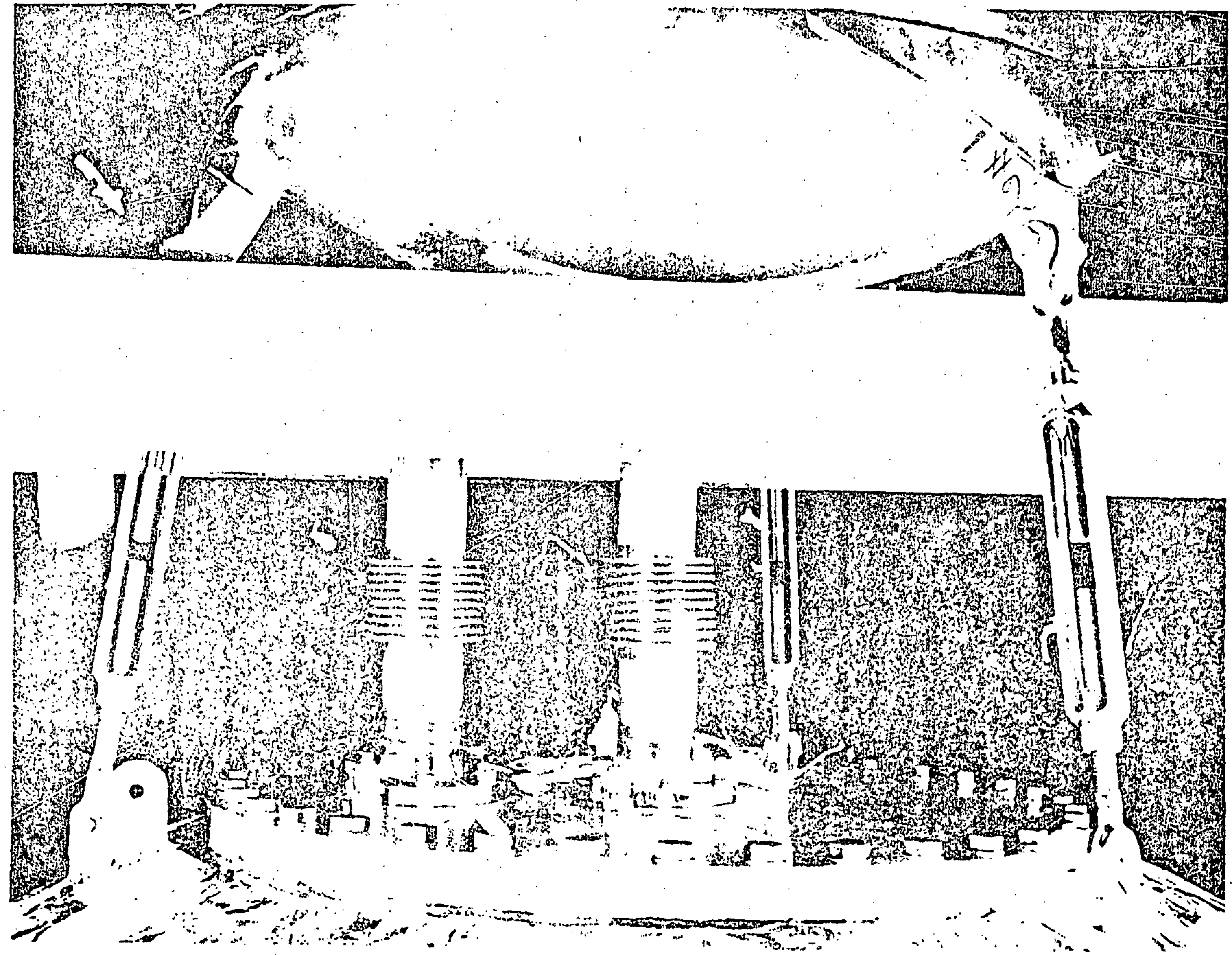

Figure 5-22. Assembly of Cryoshroud Cover/Guard Tank and Test Tank, Side View

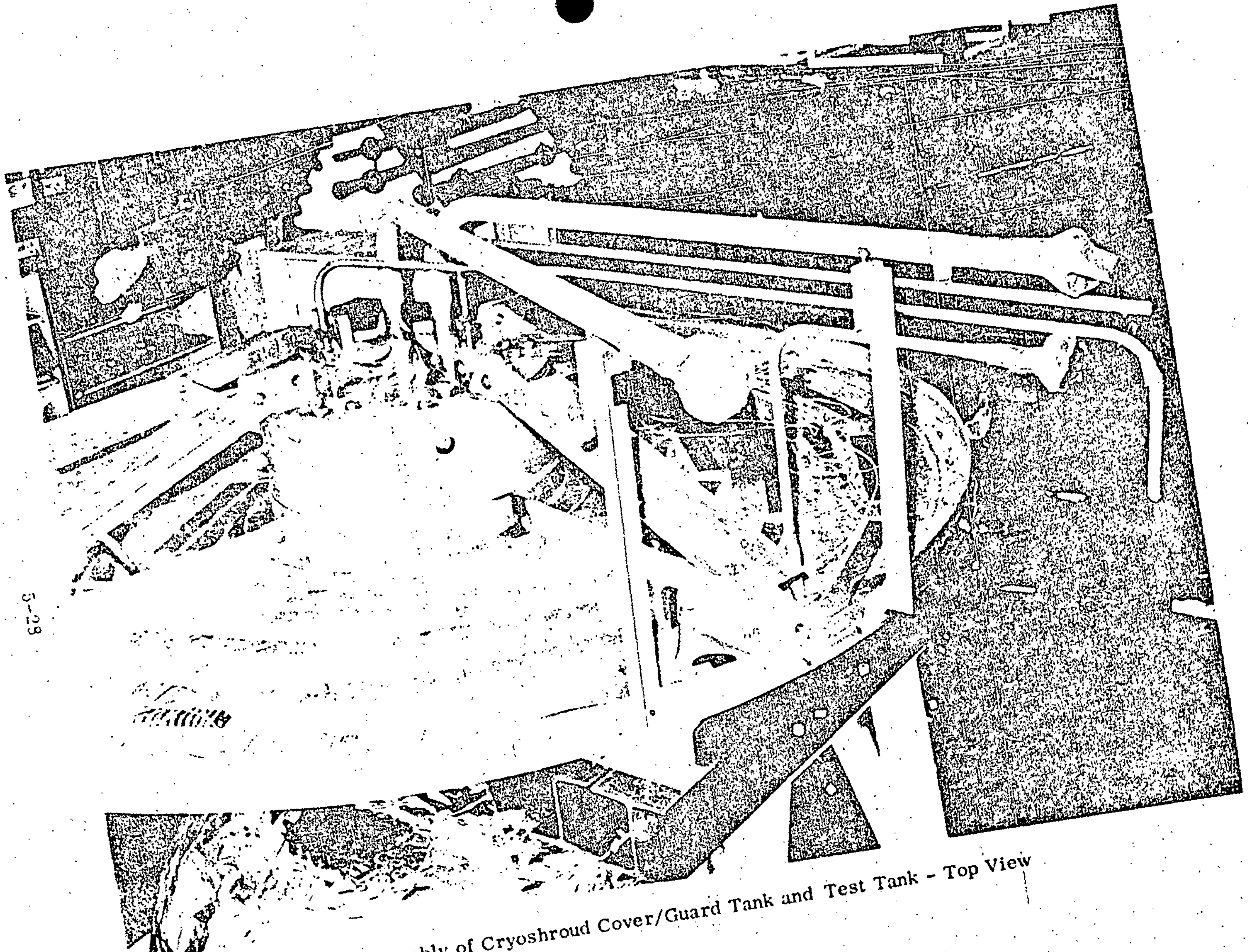

Figure 5-23. Assembly of Cryoshroud Cover/Guard Tank and Test Tank - Top View

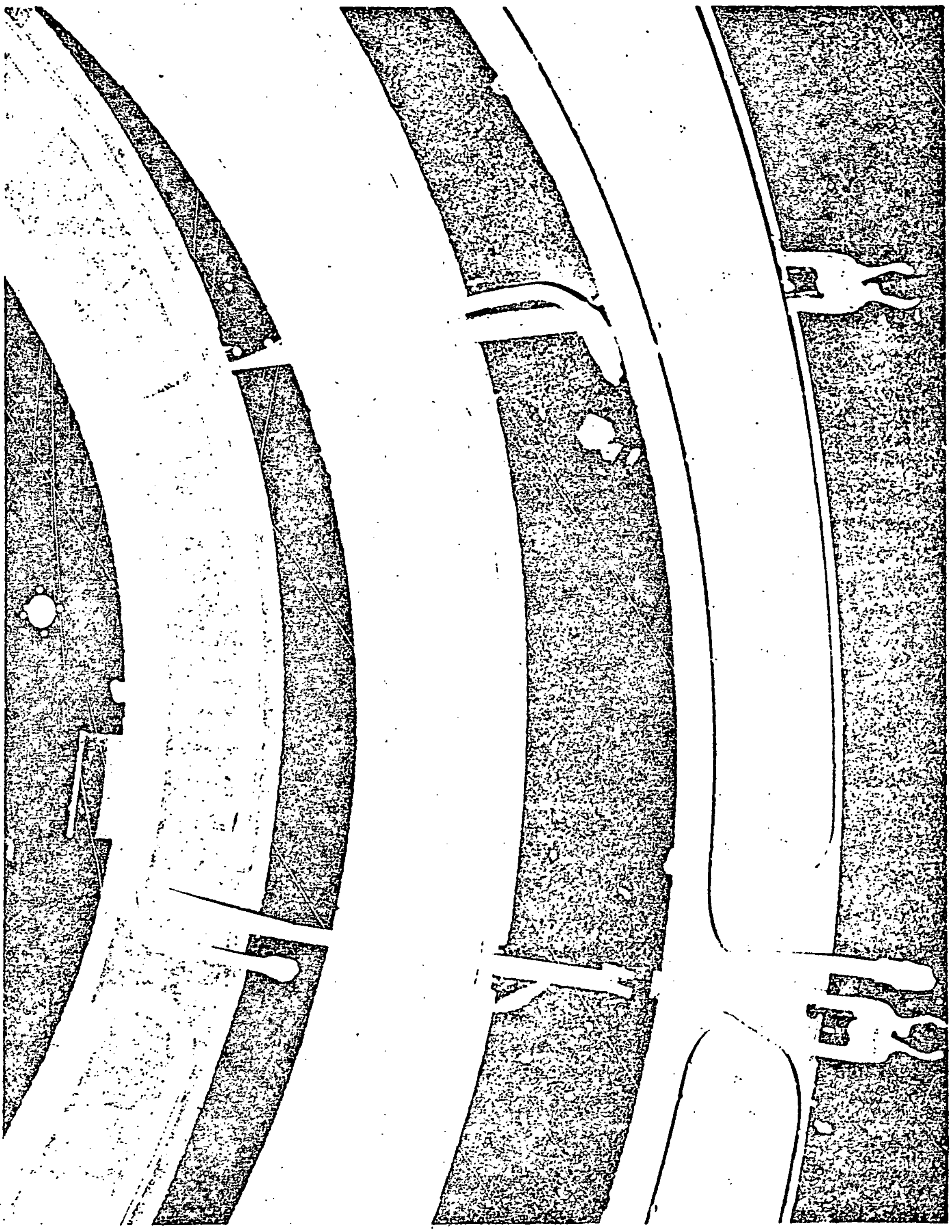

Figure 5-24. Cryoshroud and Baffle Assembly

The thermal payload simulator has its own fill and vent line. The baffle cooling line is a continuous aluminum tube which makes a circle around the baffle on the lower side (not attached), goes through the movable baffle plate and makes a double circuit on the upper surface of the movable baffle. It continues with a spiral around the cryoshroud from the lower movable baffle to the fixed baffle. The coil then exits through a hole in the shroud. The Conoseal flanges, tubing, joints and gaskets used for the cryoshroud assembly are shown in Table 5-3.

Table 5-3. Conoseal Flanges, Tubing Joints and Gaskets

Item	Location	Seal No.	No.	Material
Tube Joint	Guard Fill/Vent	59190-12SS	2	Cres
Double Seal Flange	TPS, Baffles Cryoshroud	59162-100S 59161-100A	5 5	Cres Male Al Female
Double Seal Flange	Test Tank Fill/Vent*	59162-200S	2	Cres Male
Single Seal Flange	Test Facility Test Tank Fill/Vent	56331-200S 56332-220S	2 2	Cres Male Cres Female
Gasket**		59307-12A 50887-100A 50887-150A 50887-200A 50887-250A		Al Alloy

* The mating female flange was machined as a part of the test tank lid.

** All gaskets were Teflon coated before installation.

6

DESIGN AND FABRICATION OF THE THERMAL PAYLOAD SIMULATOR MULTILAYER INSULATION

The Thermal Payload Simulator (TPS) is a 1.83 m (72 in) diameter disc, insulated over the entire surface on the side facing the test tank (Figure S-1). The objective of the TPS is to provide a constant temperature surface for the insulated tank to view. The thermal payload simulator surface viewing the tank is flat and free of penetrations and requires a total hemispherical emittance of less than 0.05. The perimeter of the thermal payload simulator is also shielded from an adjacent baffle by the application of three radiation shields attached to the baffle structure (Figure S-1).

6.1 BLANKET DESIGN

The multilayer insulation (MLI) of the thermal payload simulator is composed of three individual blankets to obtain the required constant thickness 60 shield MLI system over the entire surface area of the thermal payload simulator. A blanket arrangement schematic and the actual design drawing are presented in Figures 6-1 and 6-2 respectively.

Each blanket is a 1.83 m (72 in) diameter sandwich consisting of 20 radiation shields and 19 spacers. Two radiation shields are cover shields that establish high lateral thermal conductivity, act as protectors during handling and installation, and provide a stronger surface for attaching insulation fasteners. The blanket cover shields are laminates of 5.08×10^{-5} m (2 mil) Mylar and 2.54×10^{-5} m (1 mil) aluminum foil bonded together. The aluminum portion of the composite shield is located on the outside of the blanket. The cover shield of blanket No. 3, applied on the outer surface viewing the test tank is painted with 3M Black Velvet Paint (Section 6.2) in the area shown in Figure 6-1. The remaining 18 radiation shields are double aluminized 6.35×10^{-6} (1/4 mil) Mylar shields. Each shield requires between 300 and 500 Å of aluminized vapor deposited on both sides. The spacer is composed of two layers of silk net (silk netting No. 2772, Industrial Textile, Cleveland, Ohio).

All blanket layers are interconnected by Nylon button pin studs (ZYTEL 101 Nylon Resin) to control blanket thickness at a nominal dimension of 0.00793 m (0.312 in). The button pin stud set (Figure 6-3) consists of a 0.021 m (0.827 in) long pin integrally molded with a disc at one end and a notch located 0.00792 m (0.312) from the disc. The retaining button (Figure 6-4) slips into the pin notch. The button pins are distributed on 0.2032 m (8 in) centers throughout the blankets. Installation details of a typical section of the TPS blanket are shown in Figure 6-2.

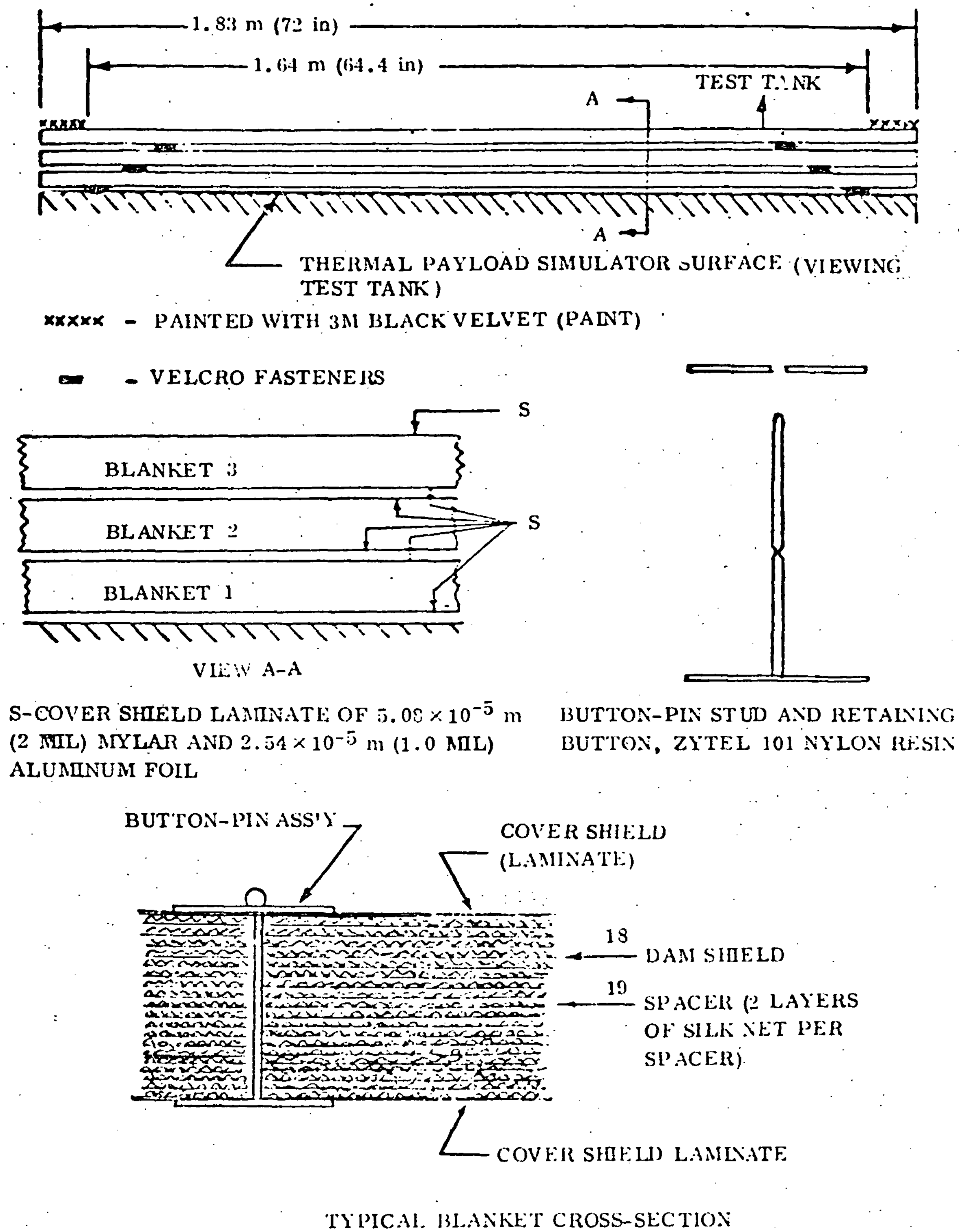

Figure 6-1. Thermal Payload Simulator MLI System

DET. NO.	BLANKET	[illegible] DESIGNATION	NO. REQD.	UPPER FACE SHT. COMPOSITE	NOTES
1	LOWER	A	1	2.0 MIL MYLAR [illegible] MIL ALUMINUM	DO NOT PAINT
2	CENTER	B	1	DITTO	DO NOT PAINT
3	UPPER	C	1	DITTO	[illegible]

TABLE I

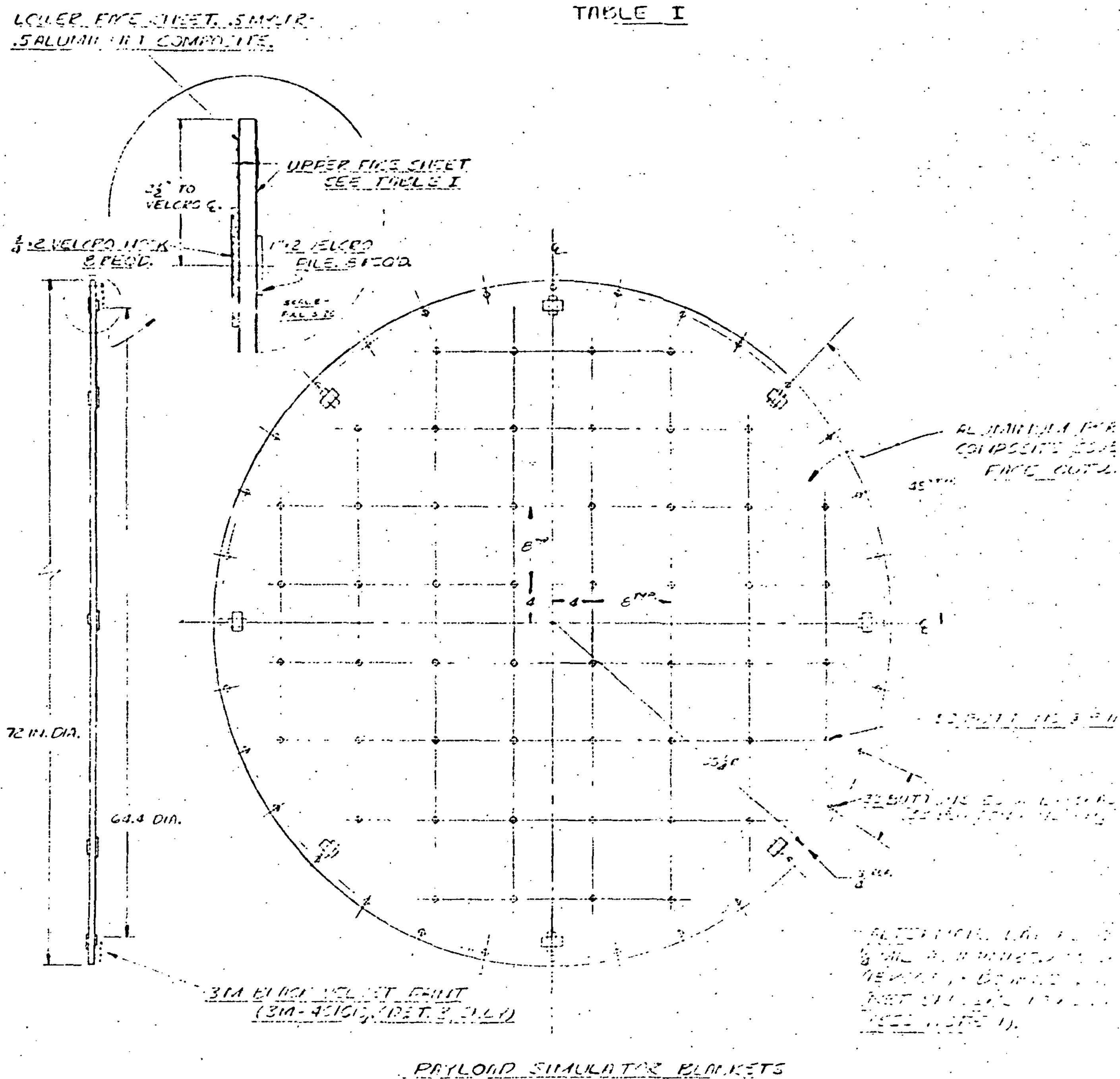

Figure 6-2. Thermal Payload Simulat

ORIGINAL PAGE IS

Dimensions: All dimensions are in inches

NOTES:

1. [illegible] MATERIAL

A. [illegible] SHIELD MATERIAL.

USE 15 LAYERS OF [illegible] MIL DOUBLE ALUMINIZED MYLAR. EACH SHIELD SHALL HAVE A MINIMUM [illegible] OF ALUMINUM VAPOR DEPOSITED ON EACH SIDE. BASE MATERIAL SHALL SHOW NO VISUAL EVIDENCE OF WRINKLES, CREASING, [illegible] ING & SHALL HAVE NO DEFECTS ON THE ALUMINUM COATING.

[illegible] WIDTH TAPE WITH 1" LONG SECTION OF ½" WIDE ALUMINIZED MYLAR TAPE AT 6" INTERVALS. OFFSET [illegible] BOTH LATERALLY & RADIALLY. TO [illegible]

B. SILK NETTING.

USE 15 [illegible] LAYERS OF SILK NET. [illegible] SILK NET [illegible] REQUIRED WIDTH. [illegible] SILK NET [illegible] MANUFACTURER'S [illegible] ASSEMBLY AND [illegible] BY [illegible] [illegible] SILK [illegible] WITH SILK [illegible] 3 PLACES.

2. [illegible] MATERIAL.

[illegible] COMPOSITE MATERIAL SPECIFIED IN [illegible]

[illegible] SHEETS TO OBTAIN REQUIRED WIDTH. [illegible] TAPE ON OUTSIDE WITH CONTINUOUS [illegible] ALUMINIZED MYLAR TAPE.

EMISSIVITY OF COVER SHEET MAT'L MUST BE LESS THAN [illegible]

3. BUTTON [illegible]

[illegible] BUTTON [illegible] THE BUTTON [illegible] SO THAT THE FLAT [illegible] SHIELDS. [illegible] THE BUTTON [illegible] INTO THE [illegible] THE MANUFACTURER'S [illegible] THE BUTTON.

4. [illegible]

[illegible]

[illegible]

ALUMINUM PORTION OF COMPOSITE COVER [illegible] MUST FACE OUTWARDS.

45°

℄

[illegible] BUTTONS [illegible] IN. [illegible]

(BUTTONS [illegible] SPACED. [illegible])

COVER SHEET [illegible]

BUTT [illegible] TOTAL [illegible]

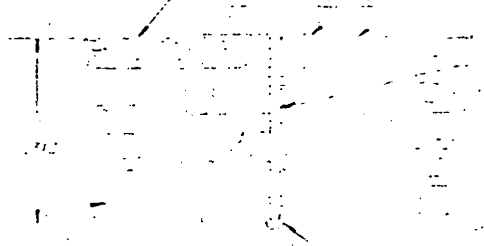

[illegible] LAYERS OF [illegible] ALUMINIZED MYLAR [illegible] SEE NOTE 1).

[illegible]

[illegible]	[illegible]
[illegible]	[illegible] BLANKETS [illegible]
[illegible]	14170 FD73

Thermal Payload Simulator Blankets

[illegible]

6.2 BLANKET ATTACHMENT DESIGN

The blankets are attached to each other and to the thermal payload simulator using Velcro hook-and-pile-type fasteners that conform to the specifications given in Figure 6-2.

For the first blanket assembly, facing the thermal payload simulator, the pile sections of the tapes are bonded to the simulator surface and the mating hook sections are bonded to the blanket cover shield using Teledyne Coast Pro-Seal 501 adhesive. This adhesive is designed for exceptionally high peel strength. Close tolerances for locating the fasteners are not required since the size of the fastener can be established to compensate for any mismatches between the pile and hook sections at assembly. The Velcro hooks and piles are arranged in a cross pattern as shown in Figure 6-2. This will permit easier installation of the blankets and will tolerate a slight mismatch in alignment.

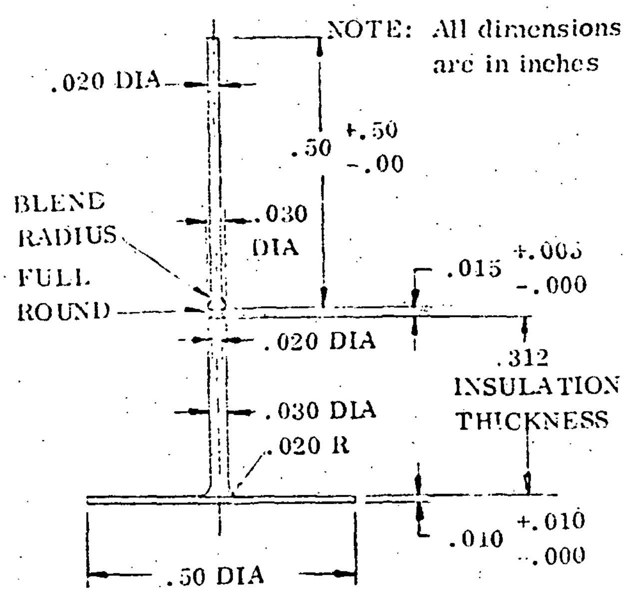

Figure 6-3. Button Pin Stud

NOTE: All dimensions are in inches

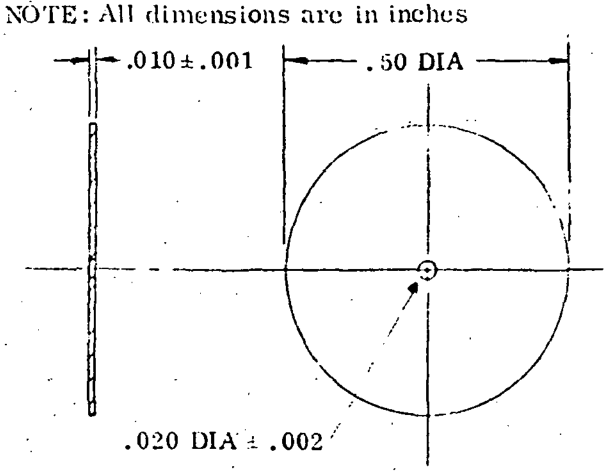

Figure 6-4. Retaining Button Detail

The second blanket is attached to the first by bonding the pile and hook sections to the adjacent face sheets between blankets. Similarly, the third blanket, which faces the test tank, is attached to the second blanket assembly. The location of the fasteners is common to all blankets. An annulus zone on the third blanket cover shield facing the test tank is painted with 3M "Nextel" Black Velvet Paint No. 3M-401C10. This paint is designed for spray application to surfaces requiring low gloss and low outgassing in vacuum.

6.3 BLANKET FABRICATION

Fabrication of the multilayer insulation blankets and components was conducted in the clean room facility in Building 51 at Convair's Lindbergh Field plant. The facility measures 13.4 m (529 in) wide, 20.1 m (792 in) long and 3.05 m (120 in) high. This environmental and particulate controlled facility is rated as a Class

C clean room in accordance with Federal Standard 209a "Clean Room and Work Station Requirements, Controlled Environment," dated 10 August 1966. The facility includes an air shower and foot scrubber unit in the entrance to assist in maintaining the environment with the referenced specification. The facility condition was checked at the beginning of the MLI production. It was found that the facility was controlled at a "Level of 10,000" which was superior to the level required by NASA.

6.3.1 MLI MANUFACTURING AID REQUIREMENTS. The manufacturing aids required for fabricating the thermal payload simulator blankets consisted of a frame to stretch-form the silk net spacer material and a MLI blanket manufacturing aid to lay up the blankets for the thermal payload simulator. The frame shown in Figure 6-5 is a wooden construction, with an inside width and length of 1.83 m (72 in) and 3.96 m (156 in), respectively. The silk netting which was purchased for this contract, 1.37 m (54 in) wide material, was stretch-formed with the aid of this tool. The stretch-form manufacturing aid was also provided with a trough to catch the access water during the wetting operation of the silk net. The design and a photo of the thermal payload simulator MLI blanket manufacturing aid are presented in Figures 6-6 and 6-7, respectively. This manufacturing aid was fabricated from two pieces of 0.0095 m (0.375 in) thick plywood. The tool was used for layup and assembly of blanket components, for trimming, as a hole pattern for attachment pins, and to locate the Velcro fasteners. The cover piece and base piece of the manufacturing aid are discs of 1.83 m (72 in) and 1.98 m (78 in) diameter, respectively. Both pieces are matched by locating pins. Fifty-two button pin drill holes are equally distributed at 0.203 m (8 in) centers over the surface of the disc. Thirty-two additional drill holes are located at the periphery of the disc.

6.3.2 SILK NET STRETCH-FORMING. The silk net spacers were first stretch formed in the frame described in Section 6.3.1. The 1.37 m (54 in) wide silk material was moistened and then dried for a minimum of 72 hours to remove inherent wrinkles and to provide shape stability. This production method resulted in a uniform layer density of the MLI system. The silk material, No. 2772, was manufactured in France and purchased through Industrial Textile, Cleveland, Ohio. Thirty-eight sheets of silk net were formed at a time. In order to obtain the required silk net spacer width, 2 pieces were butt jointed and taped with aluminized Mylar tape.

6.3.3 BLANKET COVER SHIELDS. The material which was used to fabricate the cover shields was Sheldahl GT-755 material. This material is a standard laminate, available in stock at G. T. Sheldahl Co., Northfield, Minnesota. It is composed of 2 mil Mylar Type A and 1 mil aluminum foil (1145-0 alloy), bonded together with a thermo setting polyester adhesive. It has a high lateral conduction and is impermeable to gas and moisture vapor. The properties are given in Table 6-1.

6.3.4 BLANKET LAY-UP AND ASSEMBLY. The thermal payload simulator MLI blanket assembly is shown in Figure 6-2. Since the reflective shields, silk net spacers and cover shields were oversize relative to the largest sheet materials available, the

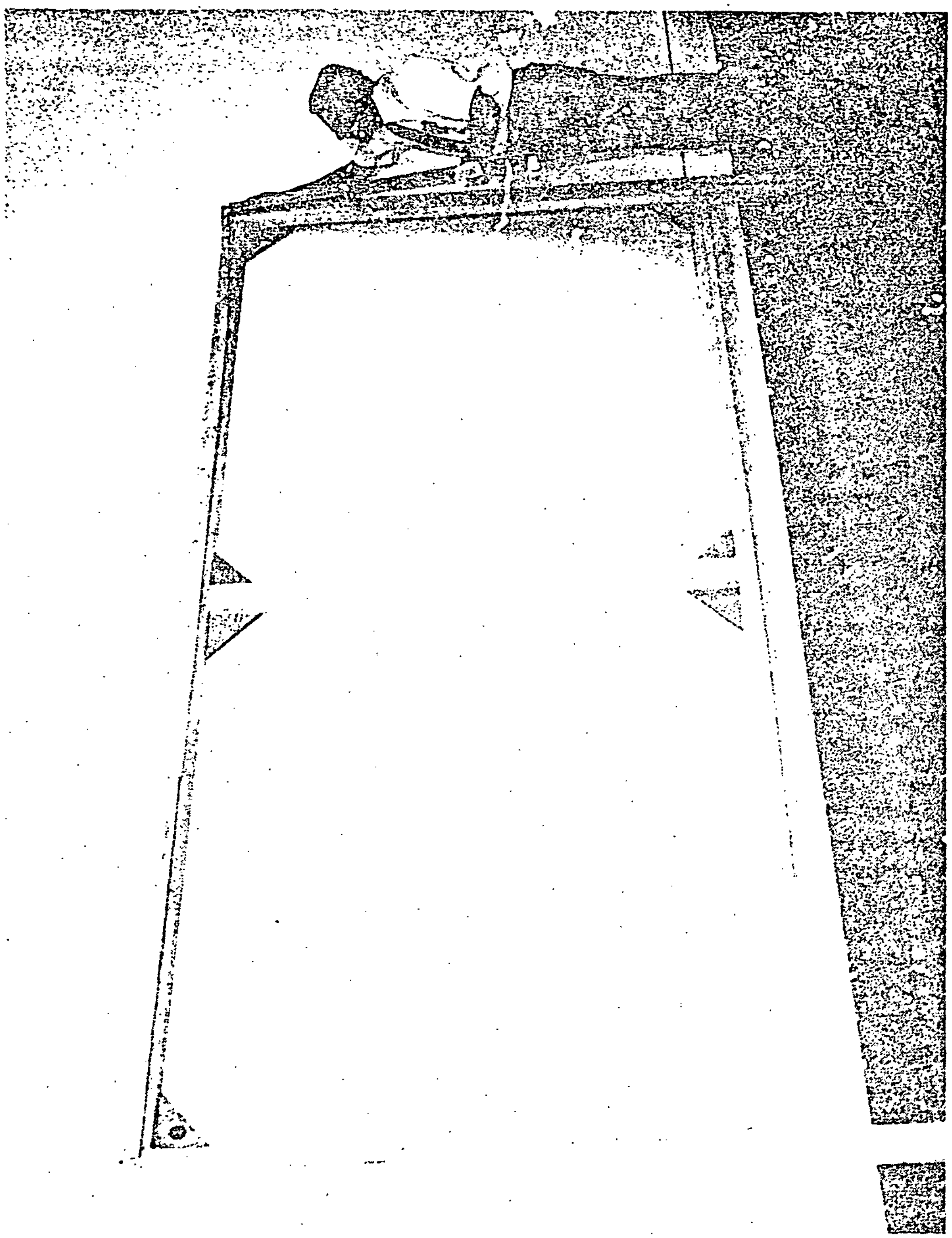

Figure 6-5. Silk Net Stretch Form Manufacturing Aid

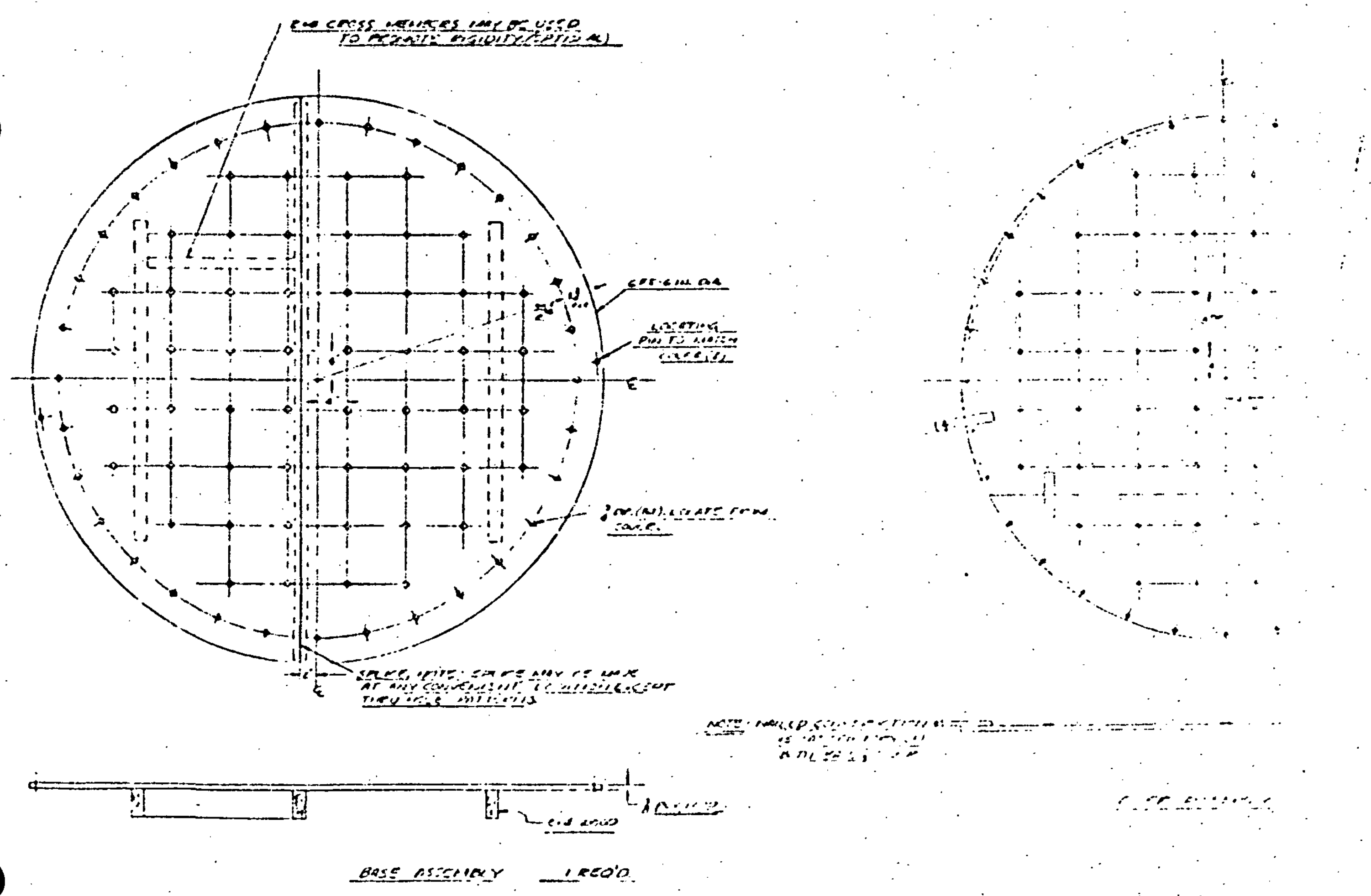

Figure 6-6. Thermal Payload Si

Dimensions: All dimensions are in inches

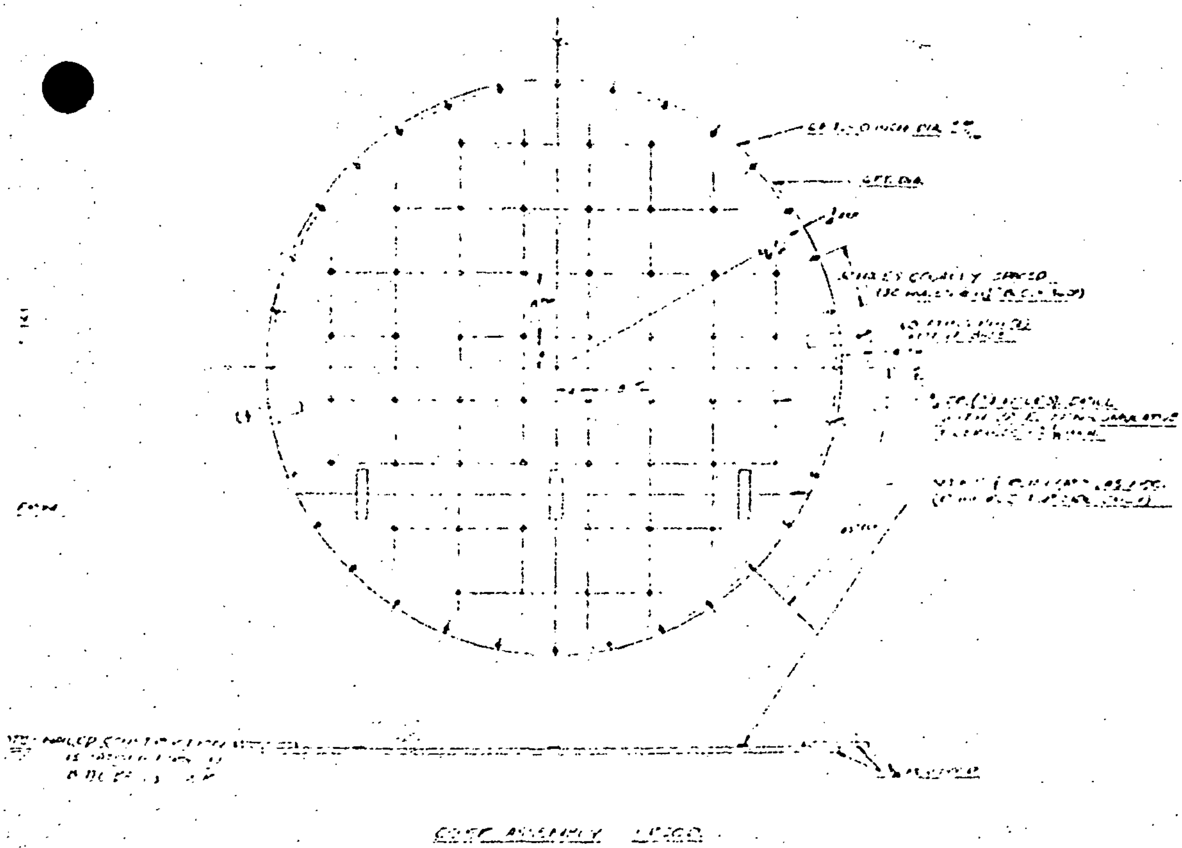

Figure 6-6. Thermal Payload Simulator MLI Blanket Manufacturing Aid

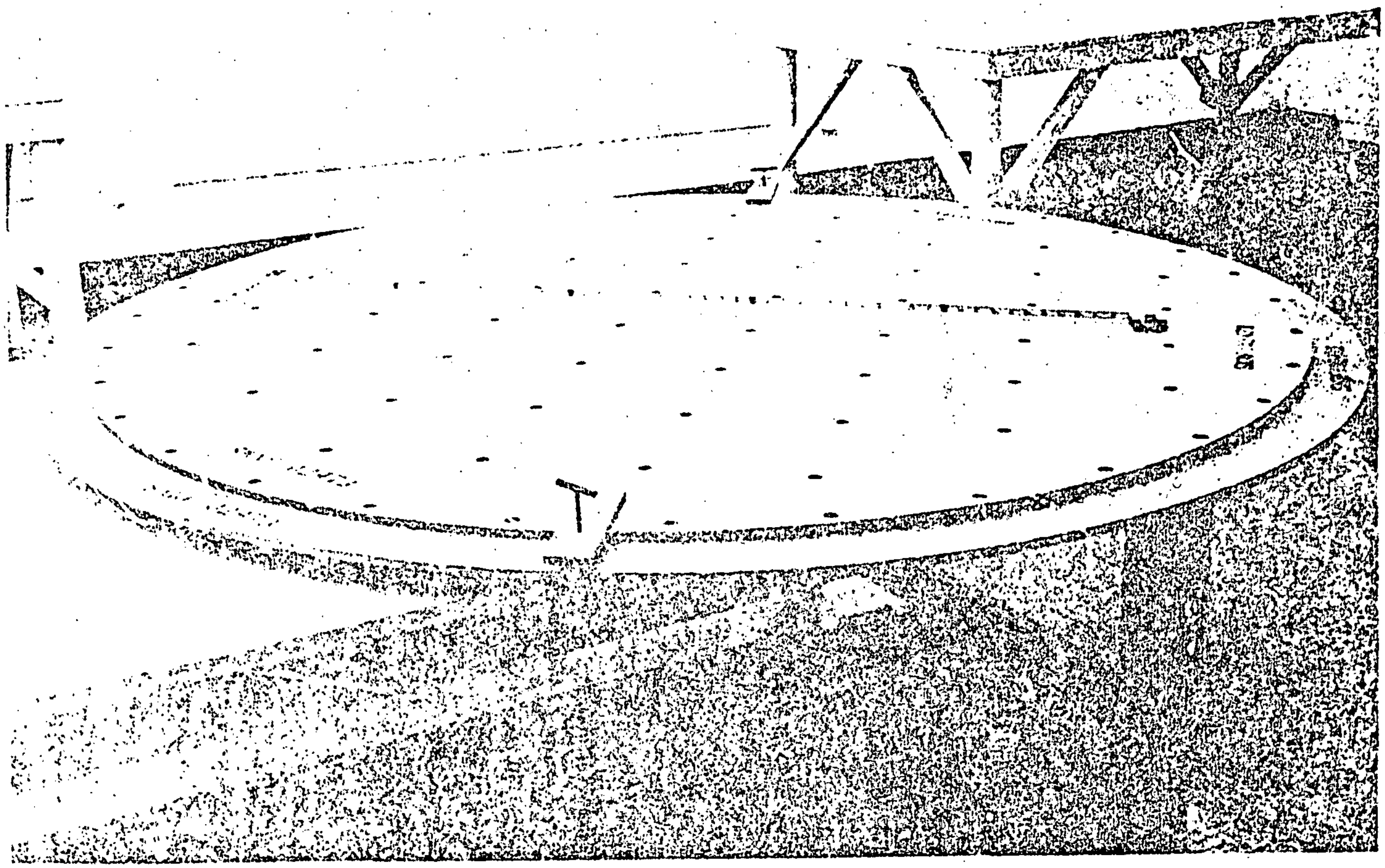

Figure 6-7. Thermal Payload Simulator MLI Blanket Manufacturing Aid

Table 6-1. Properties of Blanket Cover Shield Material

Tensile Strength:	Machine Direction:	7.9 kN/m (45 lb/in) of width
	Transverse Direction:	7.9 kN/m (45 lb/in)
Elongation:	Machine and Transverse Direction:	10%
Weight:		0.159 kg/m^2 (4.7 oz/yd^2)
Service Temperature:		213 to 383 K (383.4 to 689.4 R)
Permeability to H_2		Less than 0.01 $liters/m^2$/24 hours
Moisture Vapor Transmission Rate		nil

assembly/layup techniques included provisions for this condition to maintain satisfactory thermal characteristics. To meet these requirements, each blanket component was processed as described below.

Cover shields were fabricated with an overlap joint using a continuous strip of aluminized Mylar tape with the tape on the outside surface. Radiation shields were fabricated with a butt joint, and held together with short lengths of aluminized Mylar tape located at intervals along the joint. Silk netting was butt jointed, not overlapped. As an aid during layup, the silk net was held in place with masking tape attached to areas outside the finished trim periphery.

During assembly, the above described joints were offset from each other both laterally and radially to avoid material buildups.

The blanket layup was performed utilizing the manufacturing aid described in Section 6.3.1. The operation sequence following blanket layup was to pierce the pin holes with a hypodermic needle and insert button pins and buttons, apply heat to the portion of the extruding pin to form a balded head to keep the retaining button in place and finally trim the blanket periphery and remove the template at installation. Every other retaining button pin face was bonded to cover sheets with Pro-seal 501. No adhesive was allowed on any exposed surfaces around the buttons.

The next operation was the attachment of the Velcro fasteners to the blanket cover shields with Pro-seal 501 in the location provided on the tool template.

Since the Velcro fasteners are located near the edges of the blanket assembly (Figure 6-2), a normal pressure force between the bonding surfaces was easily applied using "clothspin type" clamps without gross disturbances of the blanket layers or the pin button assemblies. The final task was then the painting of the 0.056 m (3.3 in) wide annular zone on the third blanket with 3M-401C10 Black Velvet Paint. A photo of the three thermal payload simulator blankets is presented in Figure 2-8.

6.4 BLANKET INSTALLATION

The blanket installation was conducted as indicated in Section 6.2 and shown in Figure 6-2.

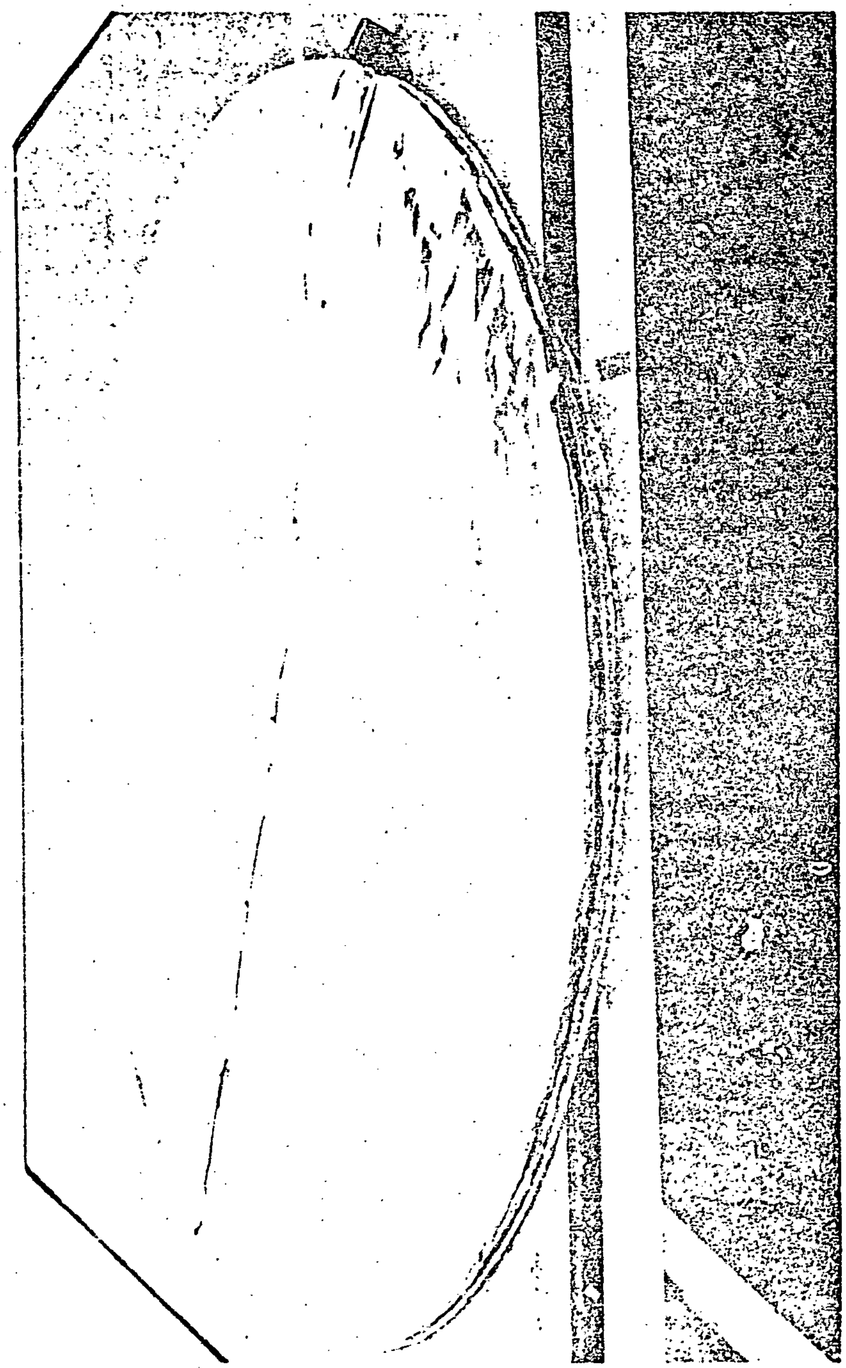

Figure 6-8. Thermal Payload Simulator Blanket Assembly

7

DESIGN AND FABRICATION OF THE TANK MOUNTED MULTILAYER INSULATION

During this task the tank mounted MLI, shown in Figure S-1 was designed and fabricated. This MLI system covers the entire area of the 1.52 m (60 in) test tank, except for the main tank door area. The system is composed of the inner and outer blankets, each containing 20 radiation shields. The blankets are supported from the tank wall using the Velcro fasteners described in Section 6.2. The design and fabrication of the MLI system is in accordance with the procedure used for the thermal payload simulator system. The primary differences from the payload mounted system are the requirements for forming all components to fit the spherical tank and installation methods to effectively minimize thermal leaks where the blankets join each other. Both items are critical to thermal performance.

7.1 VENTING CONSIDERATIONS

During vacuum chamber pumpdown, the MLI interstitial space is required to vent into the chamber. As the MLI interstitial pressure is reduced to the point where free molecular gas flow venting is predominant (approximately 1.33×10^{-3} kN/m^2)(10^{-2} Torr), the MLI venting becomes geometrically sensitive. That is, MLI venting of each interstitial gas molecule occurs along an unobstructed line-of-sight path. Thus the vent path area must be kept open and unobstructed, by minimizing the MLI interstitial vent path blockage resulting from blanket fasteners, supports and /or penetrations.

7.2 INNER BLANKET DESIGN

The inner blanket layup consists of six 1.043 rad (60 deg) gore sections and one 0.406 cm (16 in) diameter circular blanket. The circular blanket is located at the tank pole viewing the thermal payload simulator (Figure S-1). The gore sections are identical preformed assemblies running continuously from the access tank door area to the circular blanket. Three gore blankets are locally notched at assembly to clear the tank support lugs located at the access door ring. Butt joints are used between the gore and circular sections. All blankets are installed such that physical contact at these butt joints is achieved over the entire length of the joint. A schematic of the test tank inner blanket arrangement is presented in Figure 7-1. The actual design drawings of the gore section and circular blankets are shown in Figures 7-2 and 7-3, respectively. The MLI layups consist of 18 double aluminized, 6.35×10^{-6} m (1/4 mil) Mylar radiation shields and 19 double silk spacers sandwiched between two laminated cover shields. Each spacer is composed of two layers of silk netting, and the cover shields are

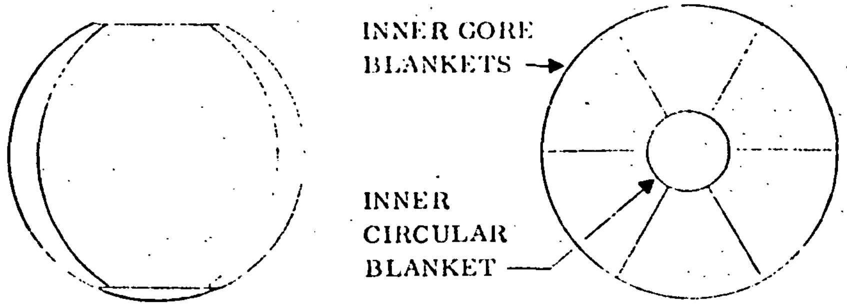

Figure 7-1. Test Tank Inner Blanket Arrangement

laminates consisting of 5.08×10^{-5} m (2 mil) Mylar and 2.54×10^{-5} m (1 mil) aluminum foil. Each of the eighteen radiation shields has between 300 and 500 Angstroms of aluminum vapor deposited on each side.

The blanket layers are interconnected with Zytel 101 Nylon resin button pin studs as shown in Figure 7-3. Forty three sets of button pin studs and retaining button assemblies per gore section are spaced at intervals not exceeding 0.203 m (8 in). The inner blanket gore sections are attached to the tank wall using 20 Velcro hooks per gore, 0.0254 m (1.0 in) wide and 0.076 m (3.0 in) long. The outer surface of each inner blanket gore section has 20 Velcro piles, 0.0254 m (1 in) wide and 0.0508 m (2.0 in) long to which the outer gore blanket will be attached. The inner circular blanket layup and materials are the same as those described for the inner blanket gore section. The radiation and cover shields are interconnected with 13 button-pin studs/button assemblies. Twelve 0.0254 m (1.0 in) × 0.0508 m (2.0 in) Velcro hook fasteners are used to attach the inner circular blanket to the tank. Eight Velcro pile sections of the same dimensions are attached to the outer surface of the inner circular blanket to fasten the outer circular blanket. (Figure 7-3).

7.3 OUTER BLANKET DESIGN

A schematic of the outer blanket arrangement is presented in Figure 7-4. The outer blanket layup and materials are the same as those outlined for the inner blankets, Section 7.2, except for the addition of cover shield strips applied over the butt joints between the gore sections and an annulus cover shield applied over the butt joints between the circular blankets and gores. The girth area is coated with 3M Black Velvet paint No. 401C10. The butt joints are staggered relative to the inner blanket sections (Figure 7-5). The outer circular blanket diameter is 0.305 m (12 in) which provides the butt joint offset at the tank outlet cap. The actual designs of the outer blanket gore section and the circular blanket are shown in Figures 7-2 and 7-3, respectively.

7.4 BLANKET ATTACHMENT DESIGN

The outer blankets are attached to the inner blanket cover shields using Velcro fasteners bonded to the cover shields as shown in the schematic Figure 7-5 and

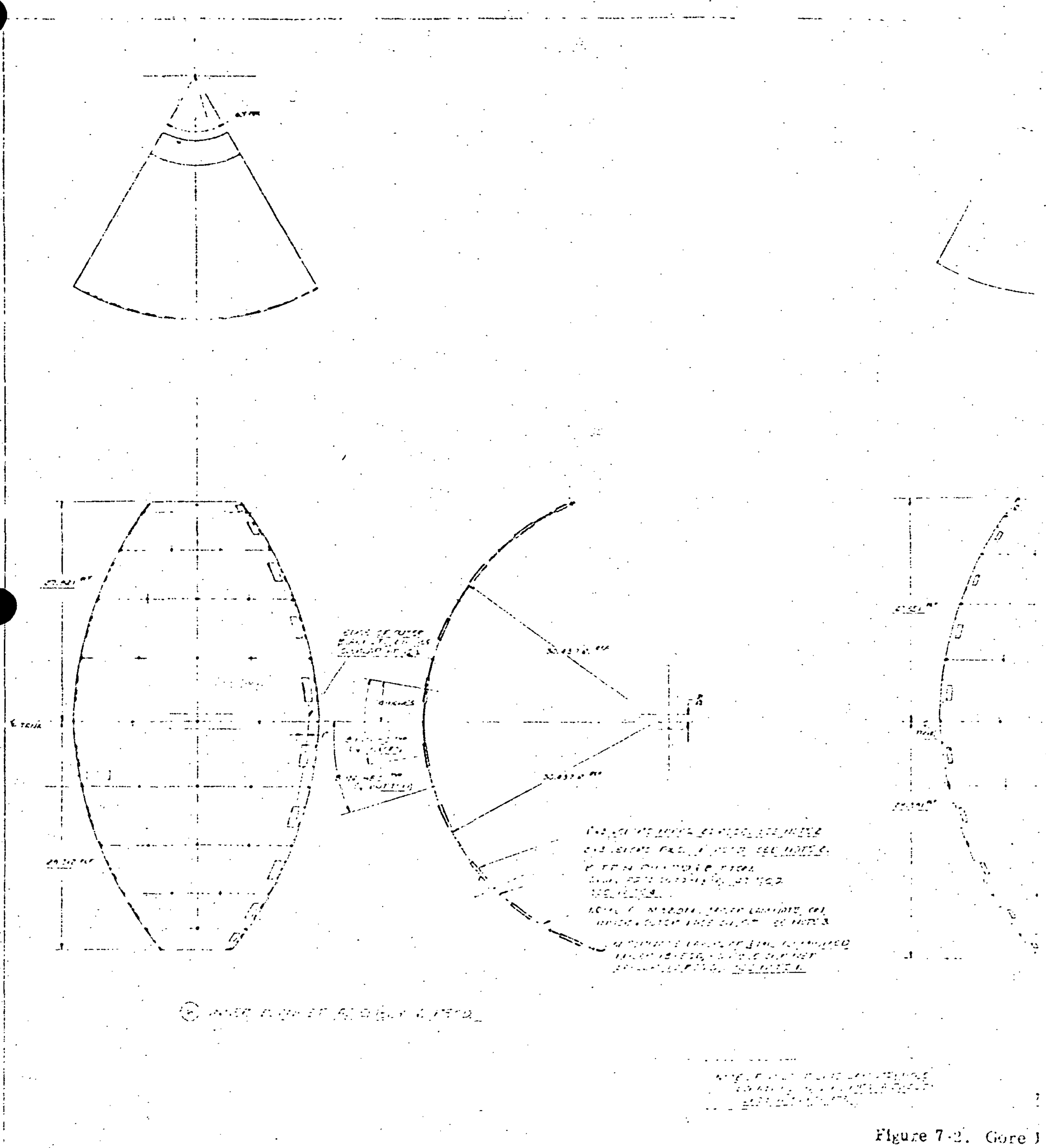

Figure 7-2. Gore I

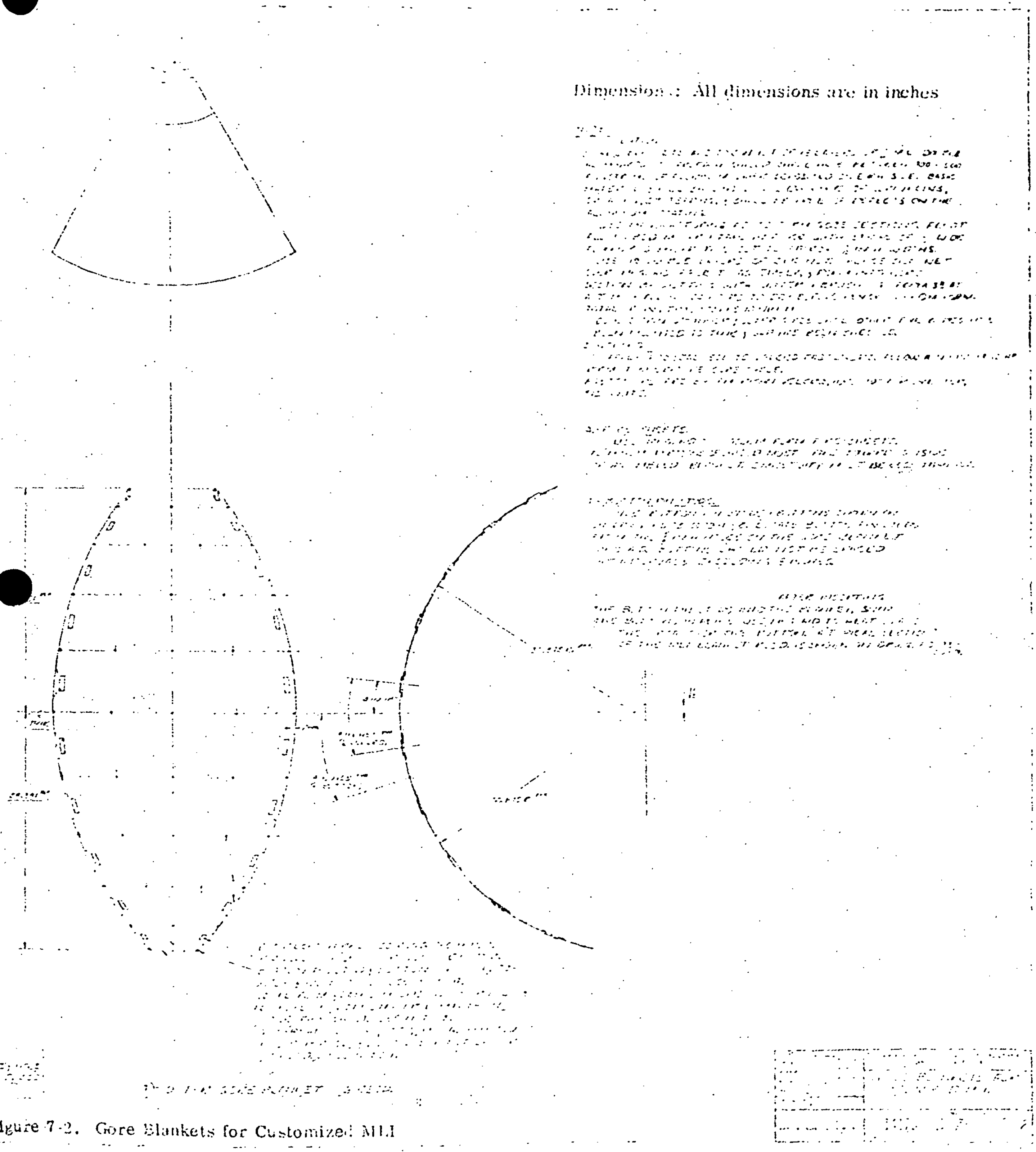

Figure 7-2. Gore Blankets for Customized MLI

FOLDOUT FRAME

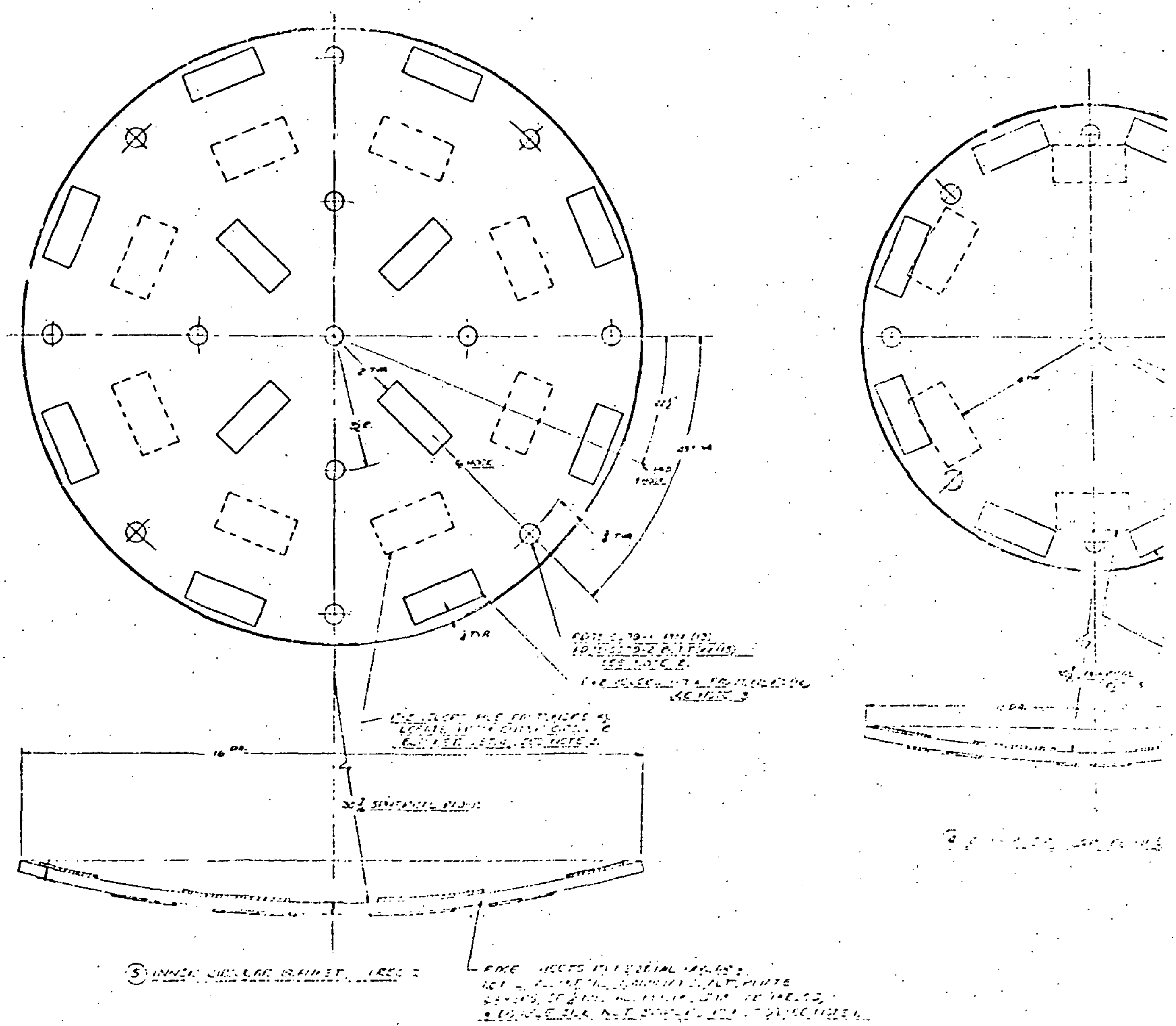

Figure 7-3. In

ORIGINAL PAGE IS
OF POOR QUALITY

Dimensions: All dimensions are in inches

NOTES:

1. INSULATION.

2. BUTTON INSTALLATION.

3. VELCRO FASTENERS.

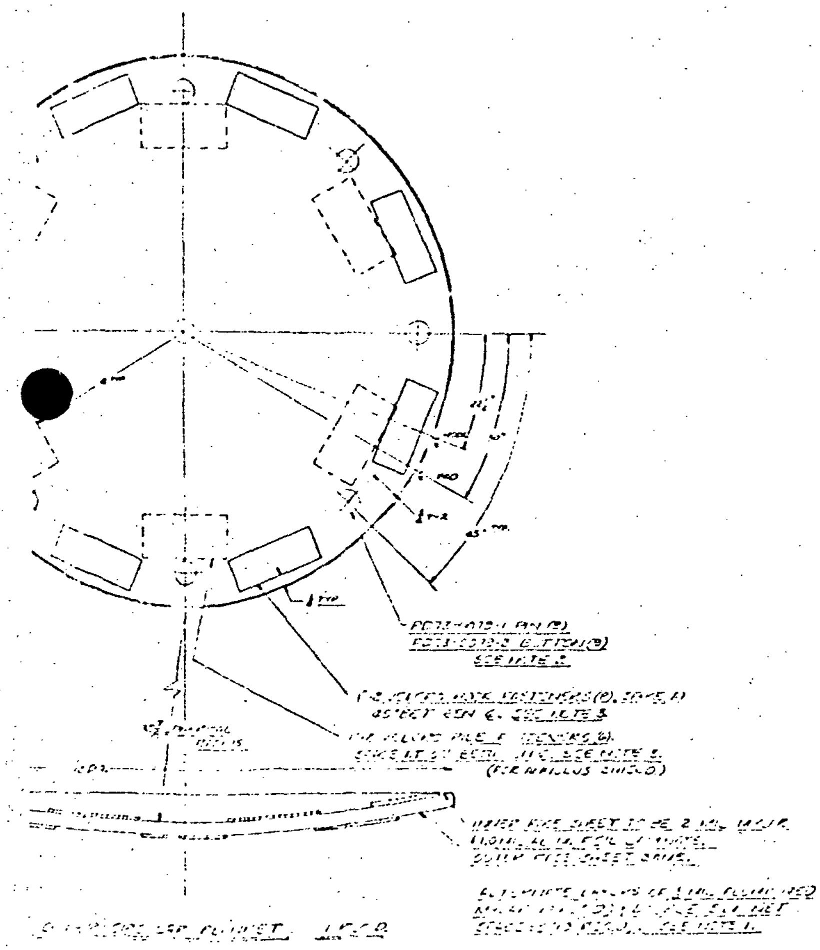

Figure 7-3. Inner and Outer Circular Blankets, Customized MLI

FOLDOUT FRAME 2

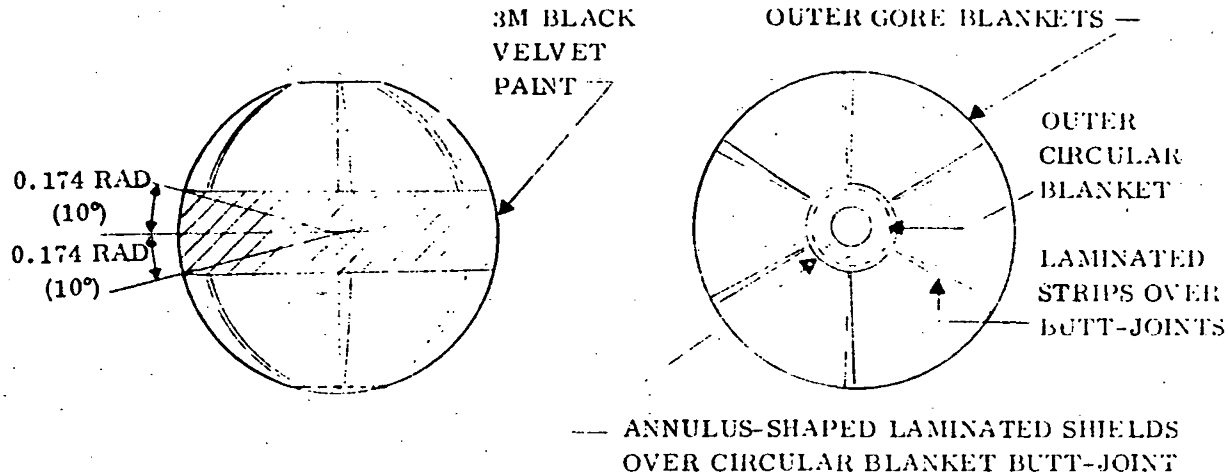

Figure 7-4. Test Tank Outer Blanket Arrangement

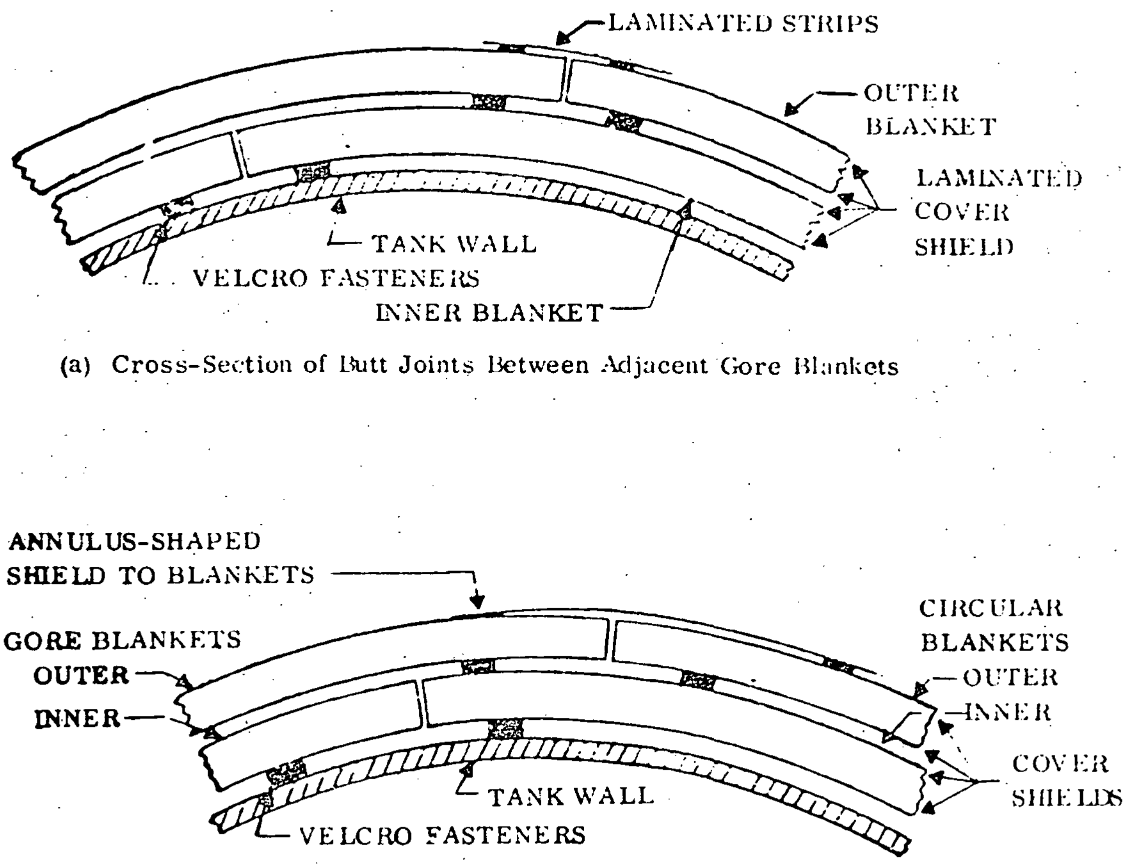

(a) Cross-Section of Butt Joints Between Adjacent Gore Blankets

(b) Cross-Section of Butt Joints Between Gore Blankets and Circular Blankets

Figure 7-5. Butt Joint Sections of Tank Mounted MLI System actual design drawing Figure 7-6. The inner blankets are mounted to the tank utilizing Velcro fasteners which are bonded to the tank wall. All butt joints at the gore lines are covered with 5.08×10^{-5} m (2 mil) Mylar and 2.54×10^{-5} m (1 mil) aluminum foil laminated strips attached to the blanket cover shields with Velcro fasteners as shown in Figure 7-6. The spacing between these fasteners provides vent paths and facilitates installation and removal. For the joints between the gores and circular blanket, a similar arrangement is used, except that an annulus-shaped shield provides a 0.102 m (4 in) overlap at the seam.

7.5 BLANKET FABRICATION

The tank mounted multilayer insulation system was fabricated in the Convair clean room described in Section 6.3. The fabrication was comprised of six inner and outer gore blankets, an inner and outer circular blanket for the tank outlet cap area, the laminated strips for the gore butt joints and the annular shaped shields over the circular blanket butt joints. The insulation system was fabricated in accordance with the assembly drawing shown in Figure 7-6. Inspection of each part, process, subassembly and assembly was performed and recorded at each operation as required by the drawing.

7.5.1 <u>MANUFACTURING AID REQUIREMENTS</u>. The fabrication of the MLI system for the tank mounted insulation required the manufacturing of the following tooling aids:

1. Inner gore blanket layup aid.
2. Outer gore blanket layup aid.
3. Inner circular blanket layup aid.
4. Outer circular blanket layup aid.
5. Cover shield vacuum forming tooling aid.

The design drawing of the inner and outer gore and circular blanket is shown in Figure 7-7. The inner gore blanket layup, a fiberglass-reinforced blanket shell, was fabricated utilizing the surface of the 1.52 m (60 in) test tank. The fabrication process of the gore and circular blanket layup aids is schematically demonstrated in Figure 7-8. The surface of the tank was first cleaned and then coated with Dow Chemical Company X-100 wax before applying fiberglass. This section was face coated with Poly-Resin GEL Coat 111. Seven layers of 1534 Fiber Glass Cloth with 204 Poly Resin were added to form the first inner gore (Figures 7-8, 7-9 and 7-10). After a 24 hour cure, a 0.016 m (0.625 in) thick layer of wax was applied to the top of the gore to obtain the representative 0.016 m (0.625 in) blanket thickness (Figure 7-11). The outer shell of the inner blanket was then built up over the wax to form the outer shell of the inner gore manufacture aid. After a 24 hour cure, this outer shell was removed and fabrication of the outer layup aid was started. Using wax as a spacer turned out to be a very time consuming operation. In order to reduce the fabrication time, fiberglass covered with a thin sheet of Mylar held by a vacuum, was used as a spacer. In accordance with the design drawing shown in Figure 7-7, for each inner and outer gore and circular blanket manufacturing aid, one base and one cover plate was required. The base plate extended

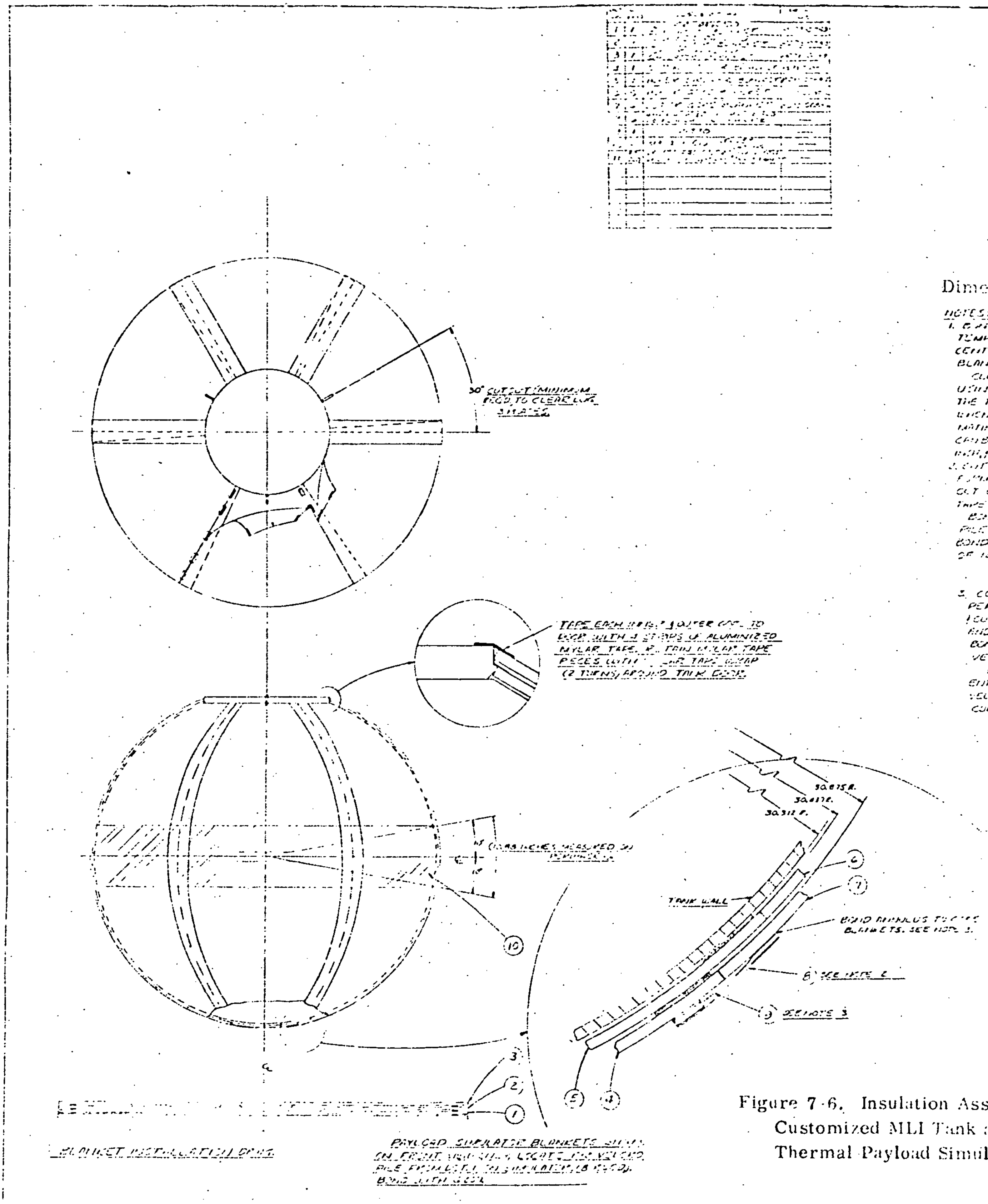

Figure 7-6. Insulation Asse
Customized MLI Tank a
Thermal Payload Simula

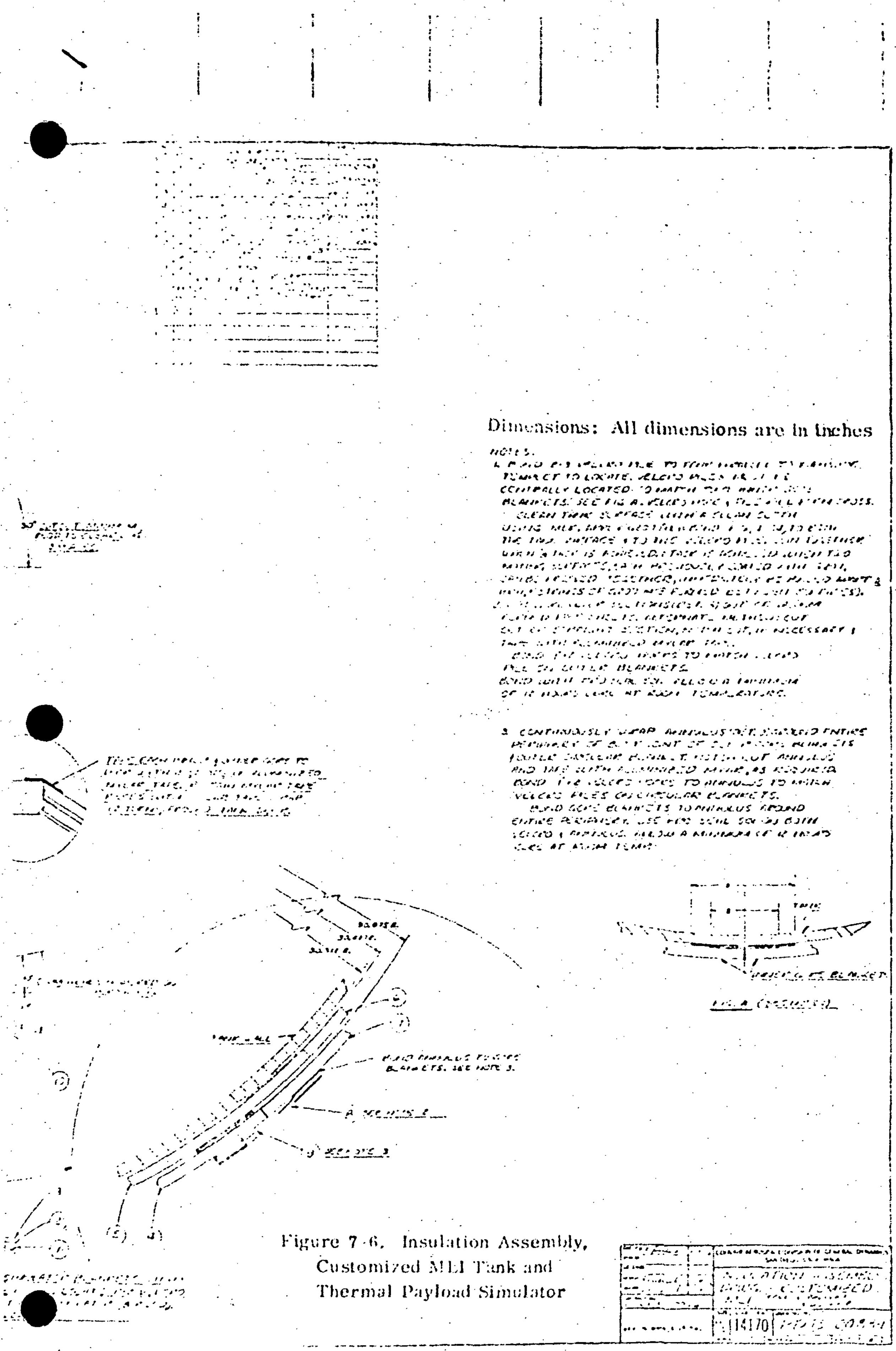

Dimensions: All dimensions are in inches

Figure 7-6. Insulation Assembly, Customized MLI Tank and Thermal Payload Simulator

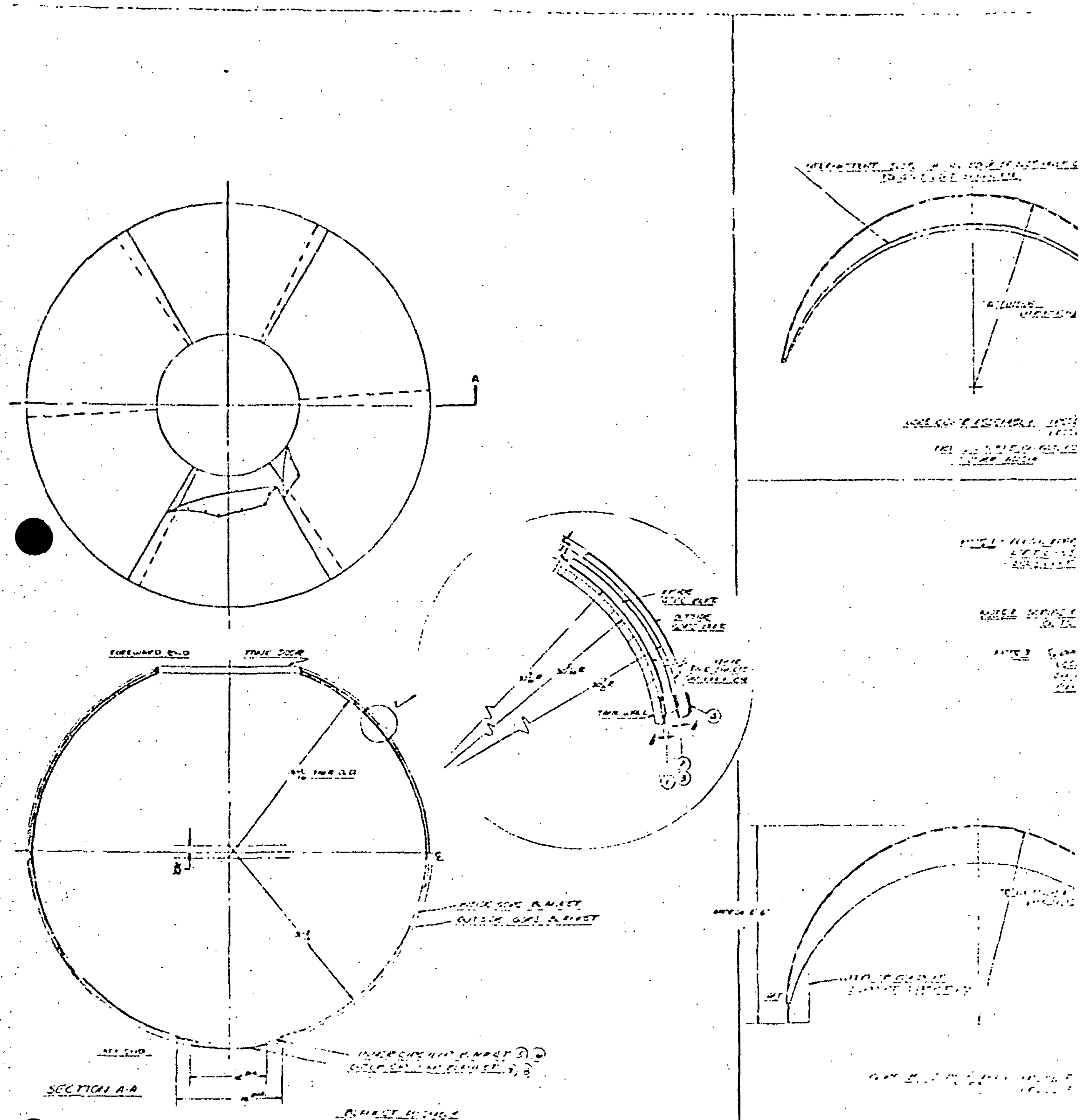

Figure 7-7. Blanket Manufacturing

Dimensions: All dimensions are in inches

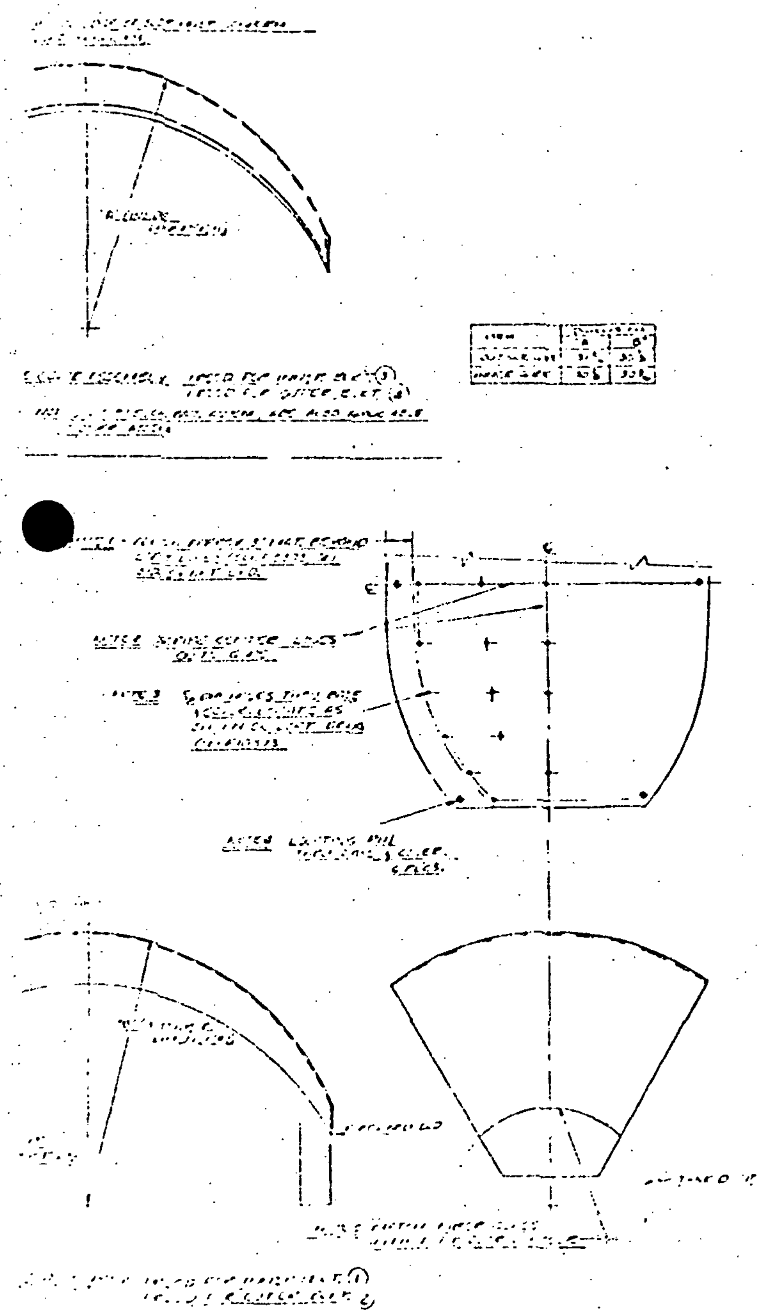

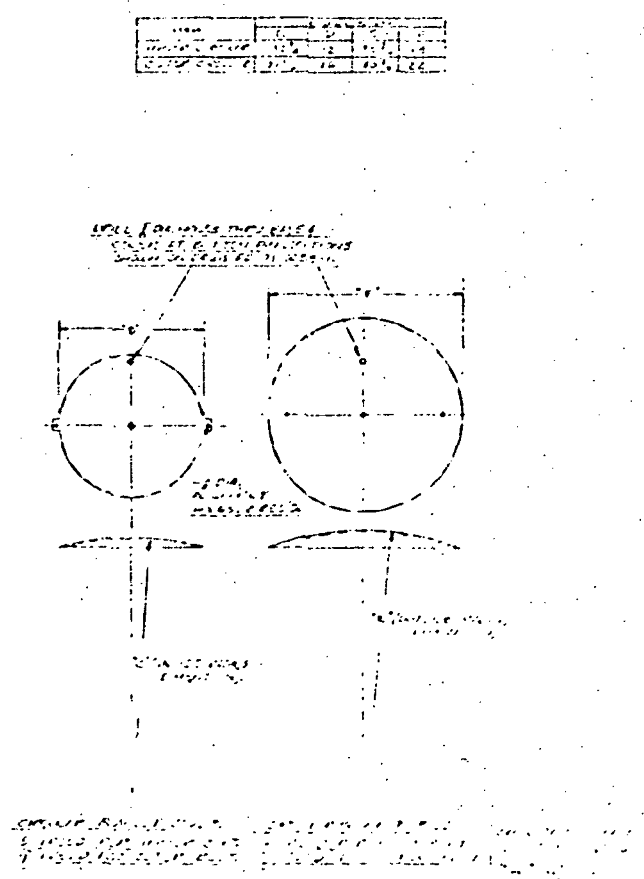

Manufacturing and Lay-out Aids

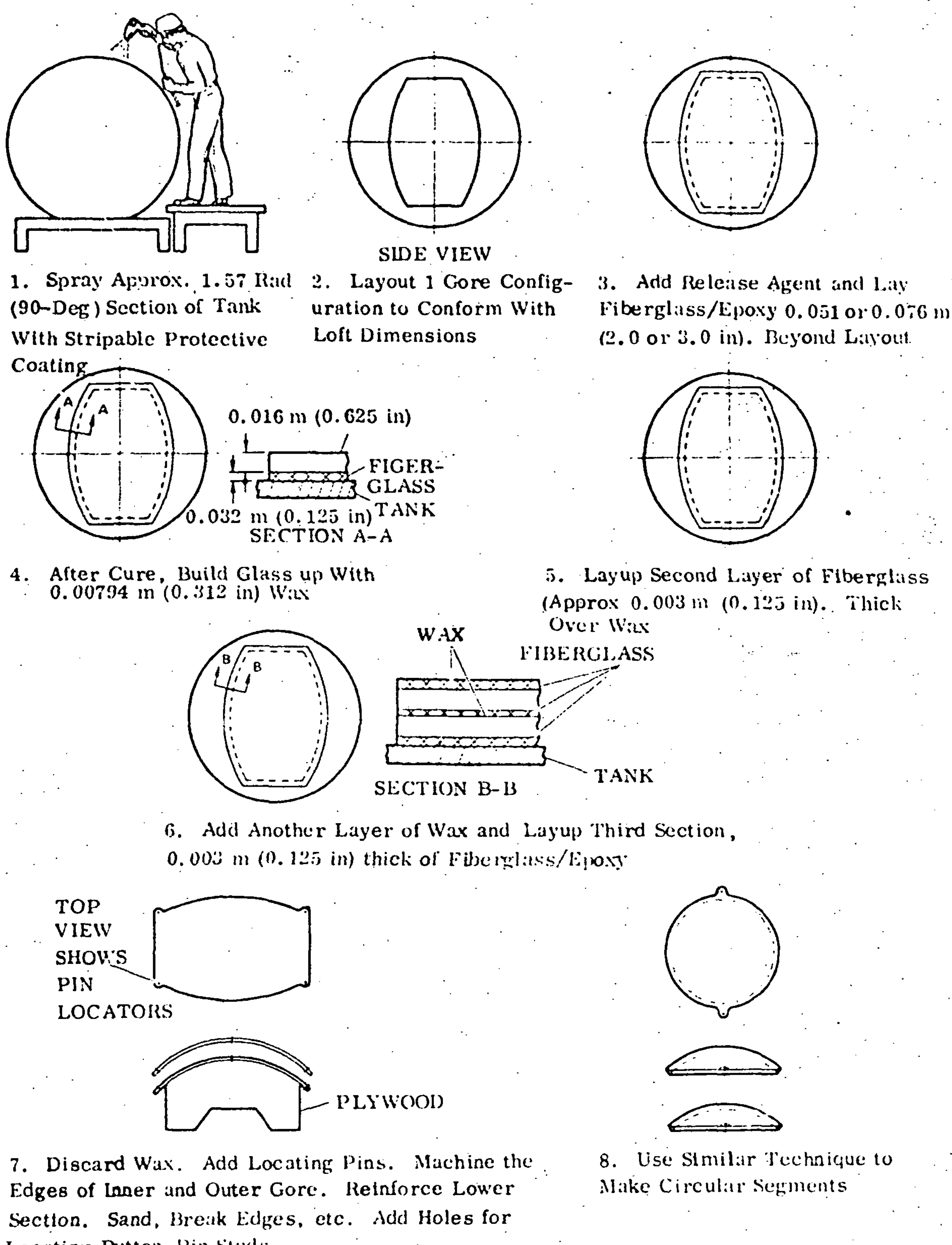

Figure 7-8. Schematic of Fabrication Process of Gore and Circular Blanket Layup Aids

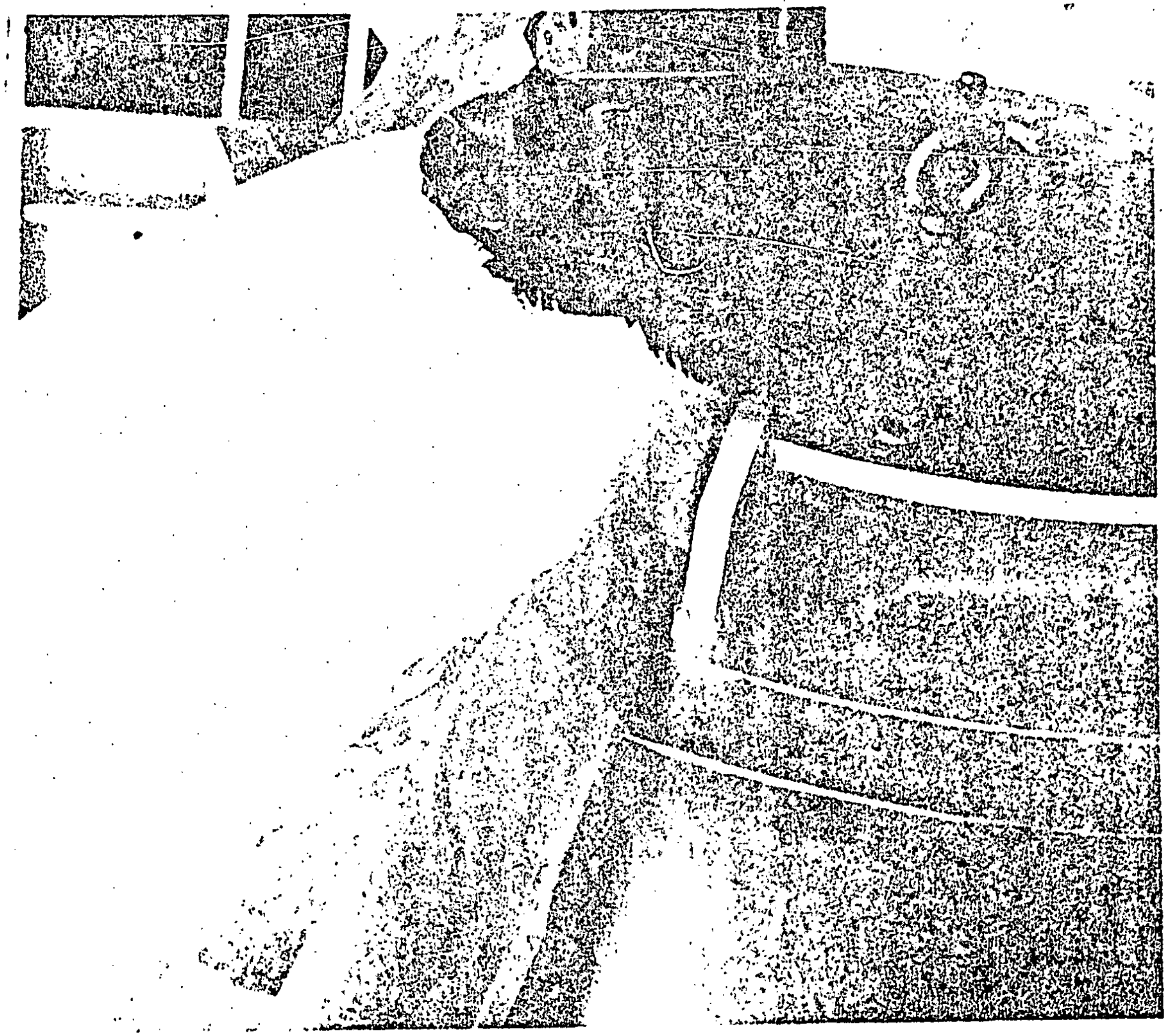

Figure 7-9. Inner Gore Blanket Manufacturing Aid - First Layer of Fiberglass Cloth on Tank

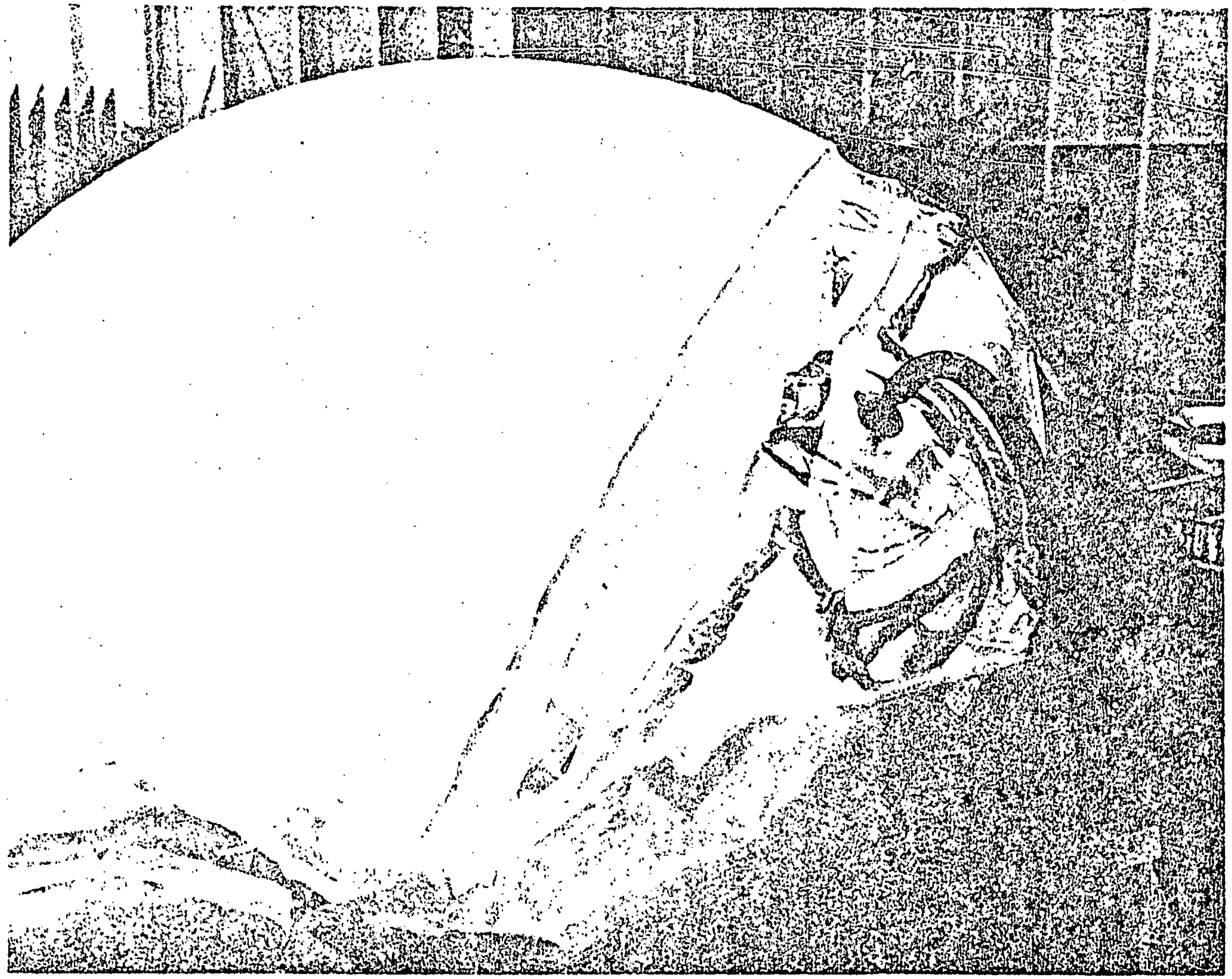

Figure 7-10. Inner Gore Blanket Manufacturing Aid - Gore Layup With Seven Layers of Fiberglass Cloth on Tank

Figure 7-11. Inner Gore Blanket Manufacturing Aid With Wax Spacer

approximately 0.076 m (3.0 in) beyond the cover plate to provide sufficient support of the blanket during the edge-trimming operation. 0.016 m (0.625 in) diameter holes were drilled through base and cover plates at all button-pin locations. Figure 7-12 shows a photo of the finished manufacturing aids.

The blanket cover shields consisting of a laminate of 5.08×10^{-5} m (2 mil) Mylar and 2.54×10^{-5} m (1 mil) aluminum foil were formed with a vacuum tool. This tool was fabricated by applying fiberglass shells directly to the tank in a manner similar to that used on the gore layup manufacturing (Figures 7-13 and 7-14). Figure 7-15 presents a photo of the completed vacuum form tooling aid.

7.5.2 SILK NET STRETCH FORMING. The silk net spacer material for each blanket was stretch-formed using the appropriate blanket layup aid. The silk net was first moistened with water to provide the needed drape characteristics and then draped over the manufacturing aid, followed by air drying for a minimum of 72 hours. The sizing of the material becomes rigid during the drying process, thus the spacer material assumes the contour of the manufacturing aid. Approximately 18 layers of silk net were formed at the same time, dried on the manufacturing aid and trimmed oversize, preparatory to blanket assembly.

7.5.3 BLANKET COVER SHIELD FABRICATION. The MLI blanket cover shield material, a Sheldahl GT-755 standard laminate material, was vacuum stretch formed using the vacuum form tooling aid, (Section 7.5.1). This material is composed of 2 mil Mylar Type A and 1 mil 1145-0 alloy aluminum foil, bonded together with a thermosetting polyester adhesive. The emissivity of the material as received was measured to be 0.0213 at a temperature of 300K (540°R) and a wavelength of 9.65×10^{-6} (9.65μ). It was necessary to fabricate fourteen (14) cover shields with the aluminum surface and fourteen (14)with the Mylar surface located on the outside of the curvature to meet the design requirement (figure 7-2) that the aluminum portion of each cover shield must face toward the outside of each assembled blanket.

Five cover shields with the aluminum surface on the outside of the shield curvature were vacuum stretch formed with good results. All shields were of high quality. The manufacturing procedure that had been used to make the cover shields was as follows: (1) pull partial vacuum to hold the shield material in place in the tooling aid. (2) heat in oven to 450K (810°R)-hold for 8 minutes, (3) pull full vacuum, (4) remove from oven, cool to room temperature, (5) remove vacuum. The stretch forming of cover-shields No. 6, 7 and 8, however, was not successful. The shields became porous using the same manufacturing methods. It was observed that the defective cover shields were produced after a splice of the roll of the stock material. The problem was investigated by Convair's Material and Process Department.

The objectives of the investiagion were: (1) to determine the cause of cracking and tearing during forming of laminated Mylar/aluminum foil obtained from the spliced end of the supply roll, and (2) recommend corrective action.

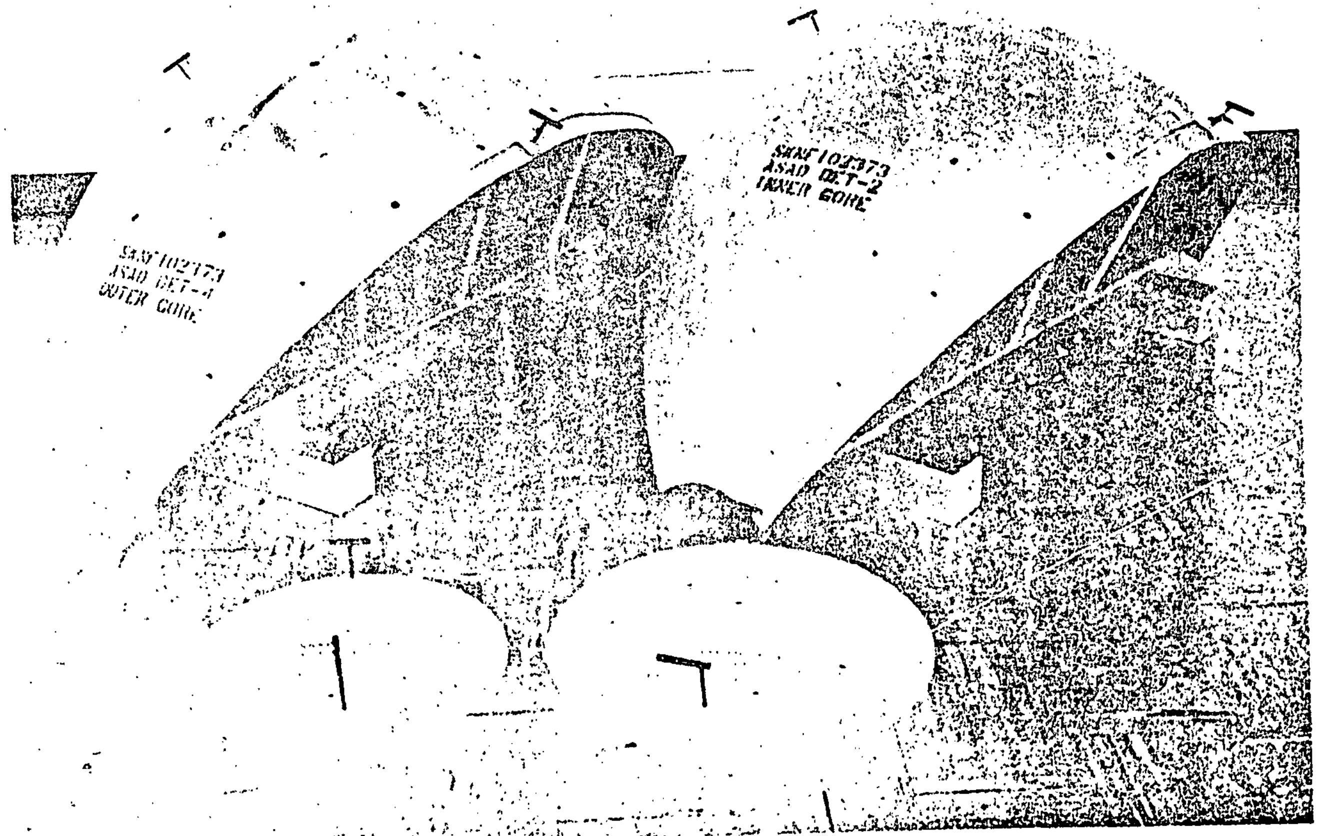

Figure 7-12. Inner and Outer Gore and Circular Blanket Manufacturing Aids

Figure 7-13. Cover Shield Vacuum Form Tooling Aid - Layup on Tank

Figure 7-14. Cover Shield Vacuum Form Tooling Aid - Ready for Mounting

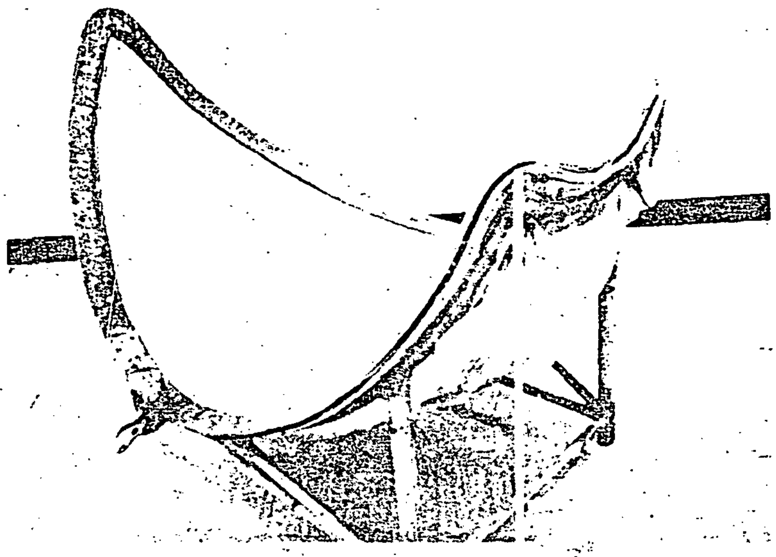

Figure 7-15. Vacuum Form Tooling Aid for Cover Shield Manufacturing

Samples of laminated Mylar/aluminum foil from the start of the roll and from the spliced end were examined. The aluminum was removed from samples of each material type and measured to see if differences existed in the relative thicknesses of the Mylar and aluminum foil. The two materials were examined metallographically along with material from a vacuum formed gore segment containing many minute cracks and tears. In addition, tensile coupons were cut from material from the start of the roll and the spliced end. Three specimens each were tested to failure and one specimen of each was strained to 14% total elongation (10% permanent set) and relaxed. The tensile specimens were examined at 7×, 20×, and 30× to determine any differences in strain behavior. No differences existed in the relative thickness of the Mylar and aluminum between the two materials. The results of the tensile tests are shown below:

		Thickness				Breaking Strength (Load in kN/m (lb/in) of width)		Elongation
		Mylar		Aluminum				
	Spec No.	m	in	m	in	kN/m	lb/in	% in 0.051 m
Material from start of roll	A1	0.000063	0.0025	0.000033	0.0013	7.94	45.4	22.5
	A2	0.000061	0.0024	0.000033	0.0013	7.84	44.6	17.0
	A3	0.000061	0.0024	0.000036	0.0014	8.90	51.0	41.0
Material from spliced end of roll	B1	0.000061	0.0024	0.000033	0.0013	8.04	45.8	65.0
	B2	0.000061	0.0024	0.000033	0.0013	7.84	44.8	10.0*
	B3	0.000058	0.0023	0.000038	0.0015	7.74	44.4	60.0

* Specimen B2 failed by tearing which started at an edge of the reduced section. The relatively low elongation is attributed to the tearing which may have been caused by a notch effect on the edge.

The results of tests showed that the breaking strength of both materials was equivalent. The high elongation of material from the spliced end of the roll indicated that material elongation was not the problem and suggested that the forming temperature for the B material should not be higher than that used for the A material to make good parts. The specimens strained to 10% permanent set showed no difference in material texture. Examinations at 100× and 200× of cross sections of the material did not reveal any differences. However, the specimen from the vacuum formed segment indicated that the polyester adhesive had softened considerably. This also suggested lower forming temperatures.

Vacuum forming the laminated Mylar/aluminum part at room temperature prior to exposing it to heat is desirable whereas heating it first would soften the adhesive and allow slippage to take place between the Mylar and aluminum. The unsupported aluminum is vulnerable to tearing. To conserve material, forming tests were conducted on a smaller "Liberty Bell" vacuum form die. Three forming tests were conducted as follows: (1) Vacuum form - at ambient temperature, then heat to 394K (710R) (2) heat to 394K (710R), then vacuum form at this temperature, (3) vacuum form at ambient temperature, then heat to 478K (860R).

Tests 2 and 3 resulted in tears and cracks in an area of the die with high material elongation. It is felt that test 3 resulted in cracks after exposure to the 478K (860R) temperature because of residual stresses in the material. The stresses caused relative movement between the Mylar and aluminum when the adhesive was softened at the high temperature. Test 1 resulted in a good part without cracks. Gore segments were then formed with the same procedure.

Based on the tests, the following sequence was recommended to the shop: (1) after setting the sealing clamp on the laminated material push the material into the center of the die. This will prevent excessive stretching of the material as it is formed. Allow the material to wrinkle at the edges, (2) pull full vacuum, (3) put into oven set at 394K (710R)-hold 8 minutes total time, (4) remove from oven and let cool to room temperature, (5) release vacuum.

7.5.4 <u>BLANKET LAYUP AND ASSEMBLY</u>. The blanket layup and assembly operation consisted of joining the prefabricated components into the required multilayer layup of cover shields, radiation shields and silk net spacers. First, the inner gore blanket was laid up onto the base plate of the blanket tooling manufacturing aid (Figure 7-16), beginning with the inner cover shield, followed by alternate layers of 18 radiation shields and 19 double silk net spacers, and the outer cover shield. The radiation shields were cut to rough size with electric scissors and then pleated to shape on the base plate. The pleats were held in place with aluminized Mylar pressure sensitive adhesive tape. This was a manual operation which employed a two-tined fork to form the pleats. The layup procedure is shown in Steps 1, 2 and 3 of Figure 7-17. To keep the layers correctly positioned, masking tape was used as required to fasten the layers to the manufacturing aid during layup. The tape was fastened outside the form line, and discarded as the blanket edges were trimmed.

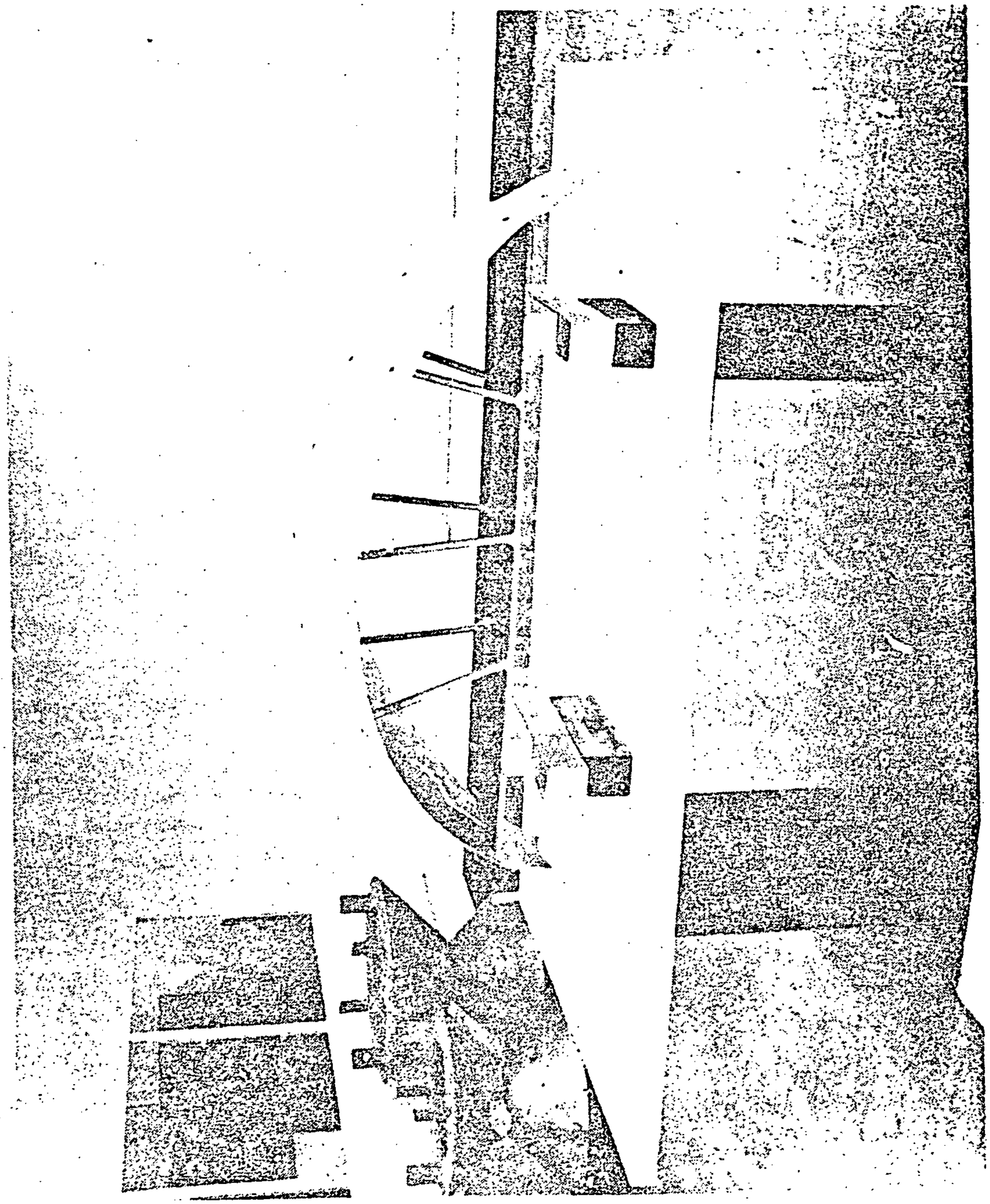

Figure 7-16. Base Plate for Gore Blanket Manufacturing Aid

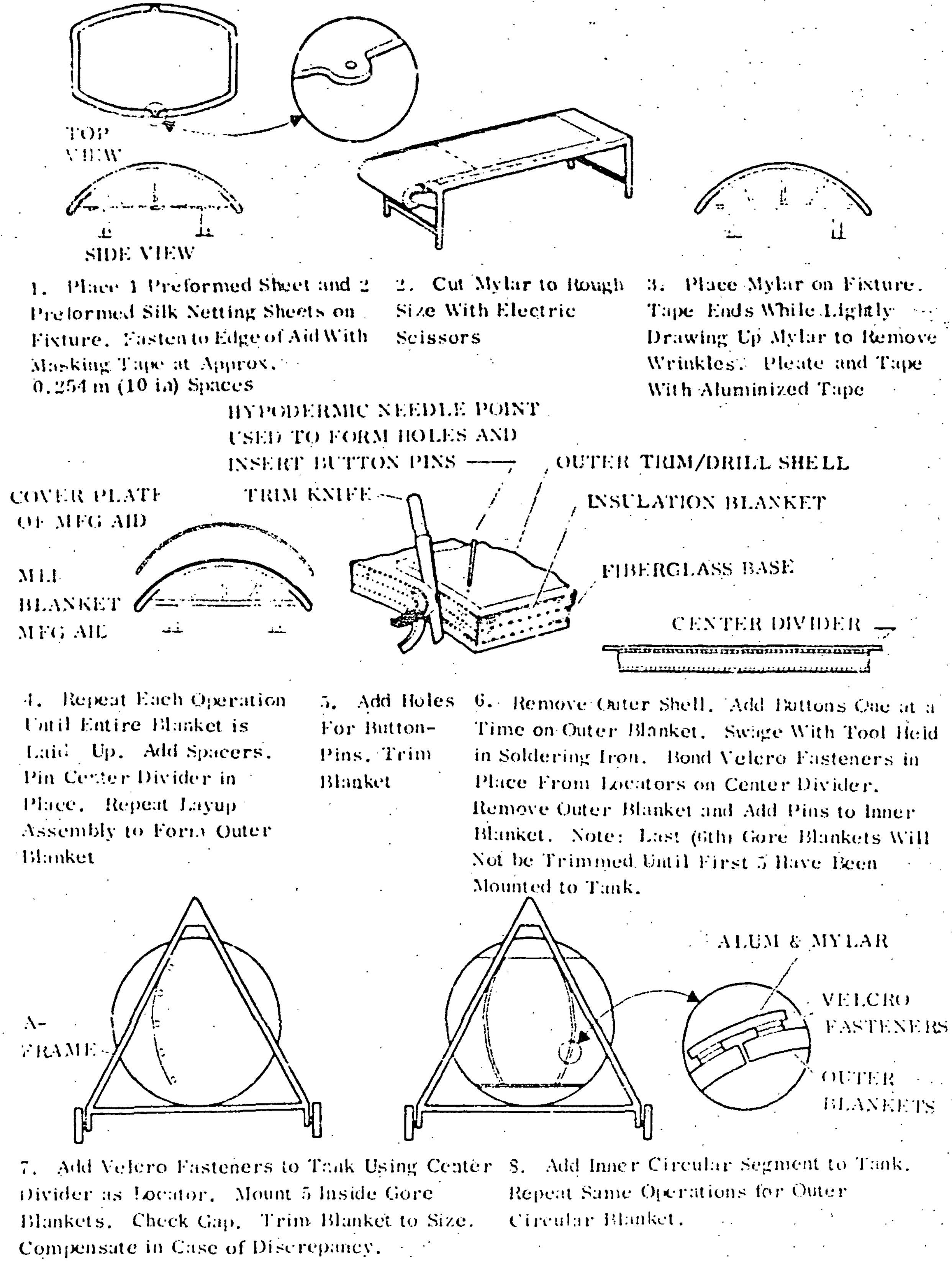

Figure 7-17 Blanket Layup and Assembly Sequential Operation

Next, all layers were covered with the female cover plate of the blanket manufacturing aid (Step 4). The female cover plate was used as both a hole template and, in combination with the male base plate as a guide for trimming the blanket periphery. The blanket sandwich was pierced for the button pins, button pins were installed and the blanket was trimmed to size (Step 5). The buttons were added one at a time. The pin was swaged with a soldering iron (Step 6). Finally, the Velcro fasteners were bonded to the cover shields with Pro-Seal 501 adhesive. Twenty four hours of curing time were allowed for the room temperature curing cycle. All these operations were repeated on the inner and outer gore and circular blanket manufacturing aids until all blankets were fabricated. All gore blankets were trimmed net size except one each of the inner and outer gore blankets. These were tailored as required to fit the tank, during the final installation operation.

7.6 BLANKET INSTALLATION

The inner blankets of the customized MLI system were preliminarily attached to the tank (Figure 3-18) at the clean room assembly area, using #12 white polyester Velcro fasteners manufactured by American Velcro Company. The sizes and location of the fasteners are indicated in the detailed design, shown in Figures 3-2 and 3-3. Before installation of the Velcro fasteners, the tank surface was cleaned with MEK (methyl, ethyl, ketone). A template was used to locate the Velcro positions. A prime coat of Plyobond 4001/4004 was applied to these positions and was allowed to cure for 24 hours. The pile section of each fastener was bonded to the tank wall with Plyobond and was held in place with masking tape for 24 hours during the room temperature curing period. Velcro hooks, 0.0254 m (1 in) × 0.0508 m (2 in), were bonded onto the outer blanket surfaces to match the Velcro piles on the tank and the outer blanket surfaces. The hooks were bonded with Pro Seal 501 adhesive and also cured for 24 hours at room temperature. The use of local patch type fasteners rather than continuous strips provided venting paths and aided in the alignment of the blanket sections at installation. Opposite each fastener, located at the manhole access door, the outer cover shield of each gore blanket was attached to the tank door ring using Mylar tape strips as shown in Figure 3-3. This arrangement provided support for the blankets.

The inner blanket installation started with the centering and attachment of the circular blanket to the pole region of the tank by engaging the fasteners. A gore blanket was next positioned with one end butted firmly to the circular blanket and the fasteners engaged. The blanket was then lightly rolled onto the tank while engaging the fasteners near the gore lines and at the end near the tank door. The above technique was repeated for the remaining gore sections while carefully aligning the butt joints. Figure 7-19 is a photo which shows the tank partially insulated and the mounting of the inner blanket Velcro fasteners.

Standard procedure at Convair is to trim the final gore blankets at assembly. At this time, if there are any discrepancies, the final gore blanket will be altered to ensure that there are no gaps or overlaps at the seams. Very little alteration was required

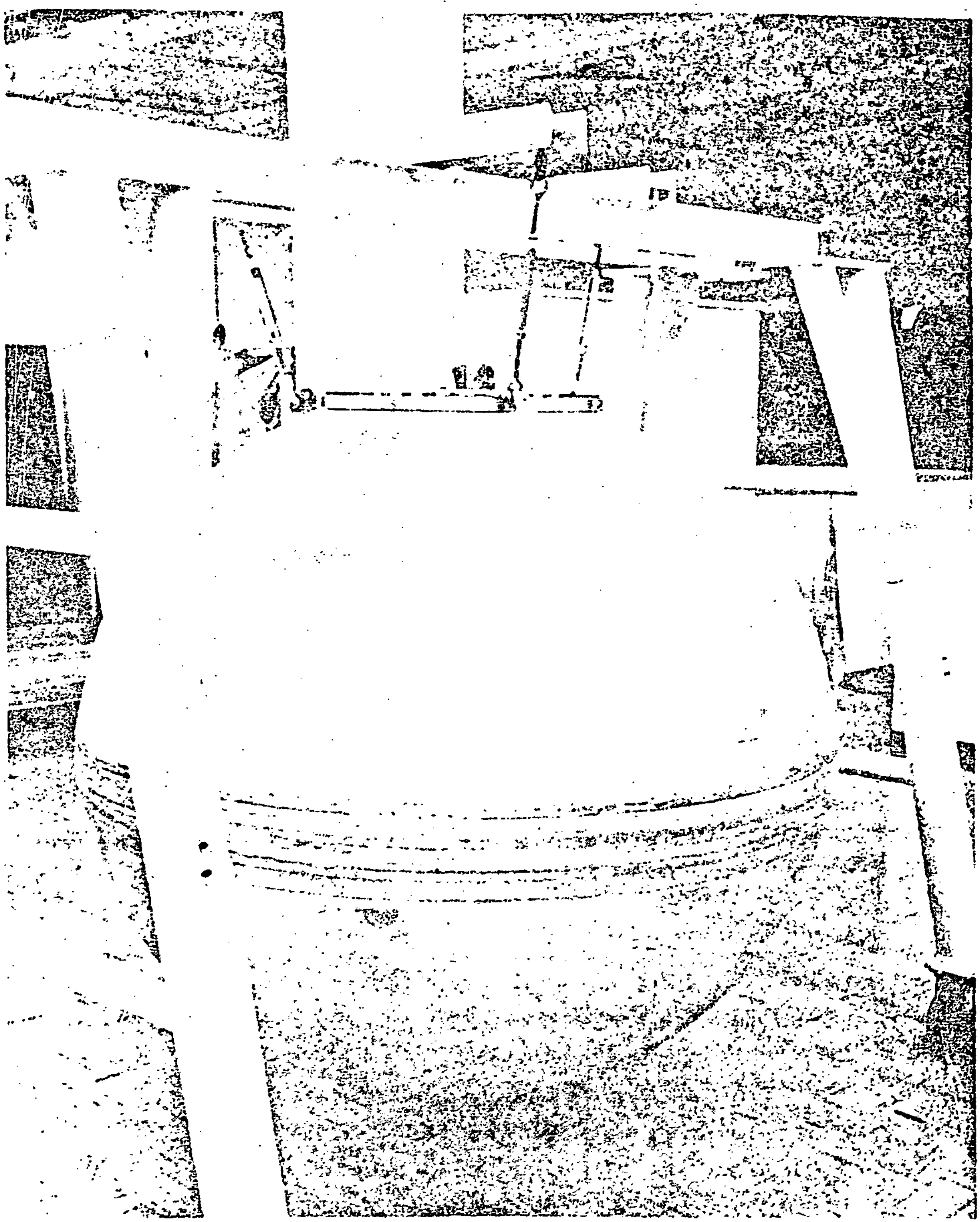

Figure 7-18. The Modified 1.52 m (60 in) Tank

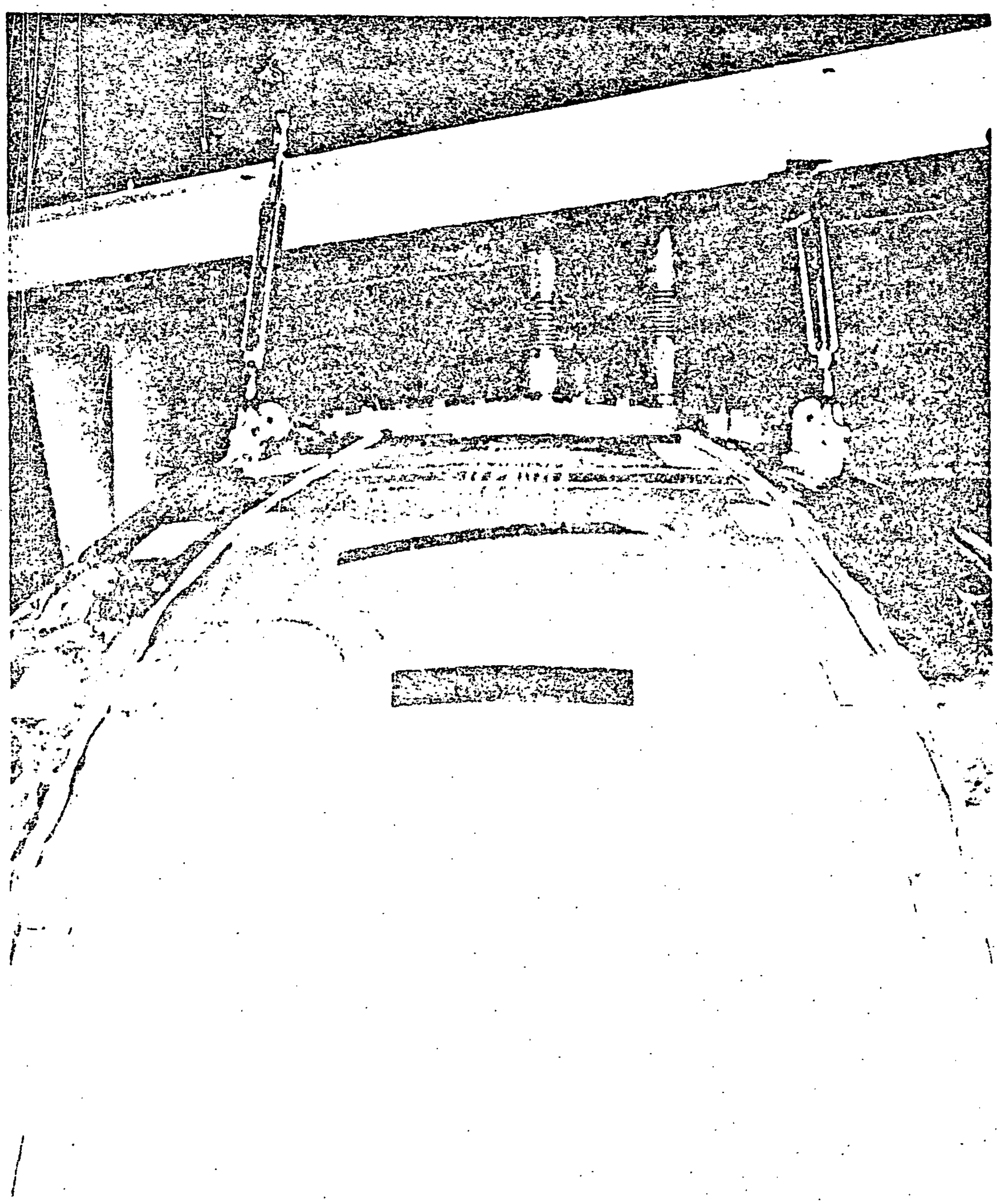

Figure 7-19. Inner Gore Blanket Layup and Velcro Fastener Mounting

on the 6th and final inner gore. The outer blankets were then fitted over the inner, but it was decided to trim the 6th and final outer blanket at the test site. After fitting, the blankets were removed from the tank, stored in sealed plastic bags containing dessicant, and purged with dry nitrogen.

Although the blankets were assembled in a clean room having an average humidity of 35, it was decided to place the blankets in a heated vacuum chamber and outgassed at a temperature of 339K (610R) before the blankets were attached to the tank. This extra precaution was taken in the event that any moisture remained in the silk net.

After removal from the vacuum chamber, the blankets were re-bagged and moved to Sycamore Canyon Test Site.

At final assembly, it was discovered that the blankets had shrunk approximately 0.0032 m (0.125 in) in width. Since the final inner blanket had already been trimmed, it was necessary to take corrective action. The possibility of stretching the blankets tightly over the Velcro fasteners and allowing gaps approximately 0.0008 m (0.03 in) wide to exist was discarded as thermodynamically undesirable. The problem was corrected by splicing sections of aluminized Mylar and silk net with aluminized tape onto one of the existing gores. The gore was retrimmed so the gap would be closed.

The inner circular blanket was completely rebuilt and was custom fitted. Although these techniques were time consuming, complete closure of the seams was attained without creating thermodynamic shorts caused by having excessive tension on the gores.

Strips of 0.0190 m (0.75 in) wide and 0.038 m (1.5 in) long aluminum Mylar tape were placed horizontally on approximately 0.1524 m (6 in) centers on all of the seams to further minimize gaps and to provide additional strength. Final assembly of the inner gores is presented in Figure 7-20.

Installation of the outer gore blankets was the same as that outlined for the inner blankets except for the addition of the butt joint shields, painting at the girth zone, and the angular orientation to assure an offset between the inner and outer butt joints. Three gore blankets were locally notched to clear the tank support lugs.

Since the final outer gore was not pre-trimmed, it was possible to trim this gore to obtain complete closure (Figure 7-21).

The vertical seams were covered with vacuum formed 0.1015 m (4 in) wide strips of laminated sheet material 0.000051 m (0.002 in) Mylar bonded to 0.000025 m (0.001 in) aluminum]. The strips were held in three places with Velcro fasteners. A similar annulus strip was placed over the circular gap and was continuously adhesively bonded to the outer gore blankets on the forward side only. Both the inner and outer blankets were taped to the access door ring at the forward section. Final assembly of the outer blankets is shown on Figure 7-22. Finally, after completion of the MLI installation, a 3M-401-C10 velvet coating was applied as shown in Figure 7-4.

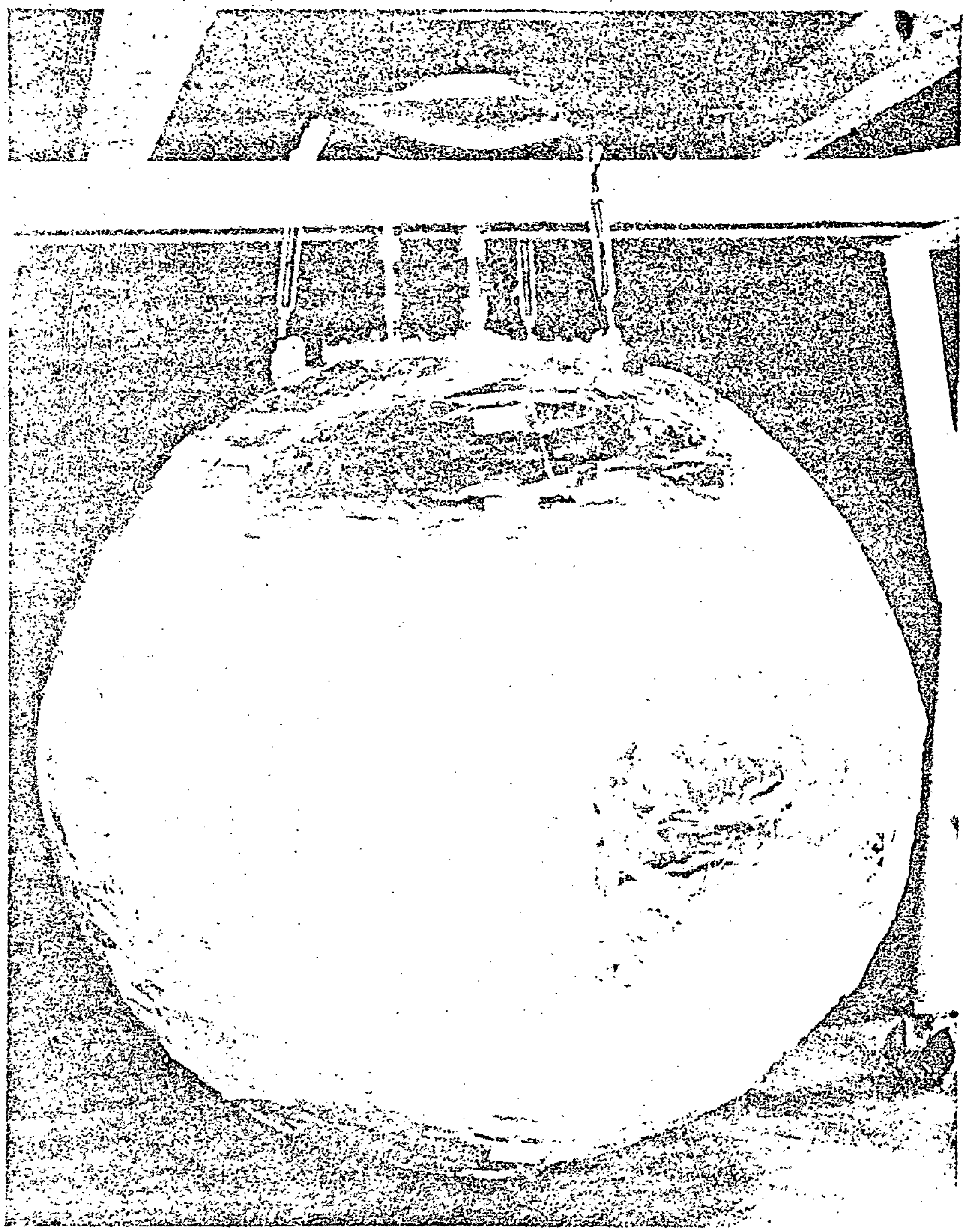

Figure 7-20. Inner Gore Blanket Assembly

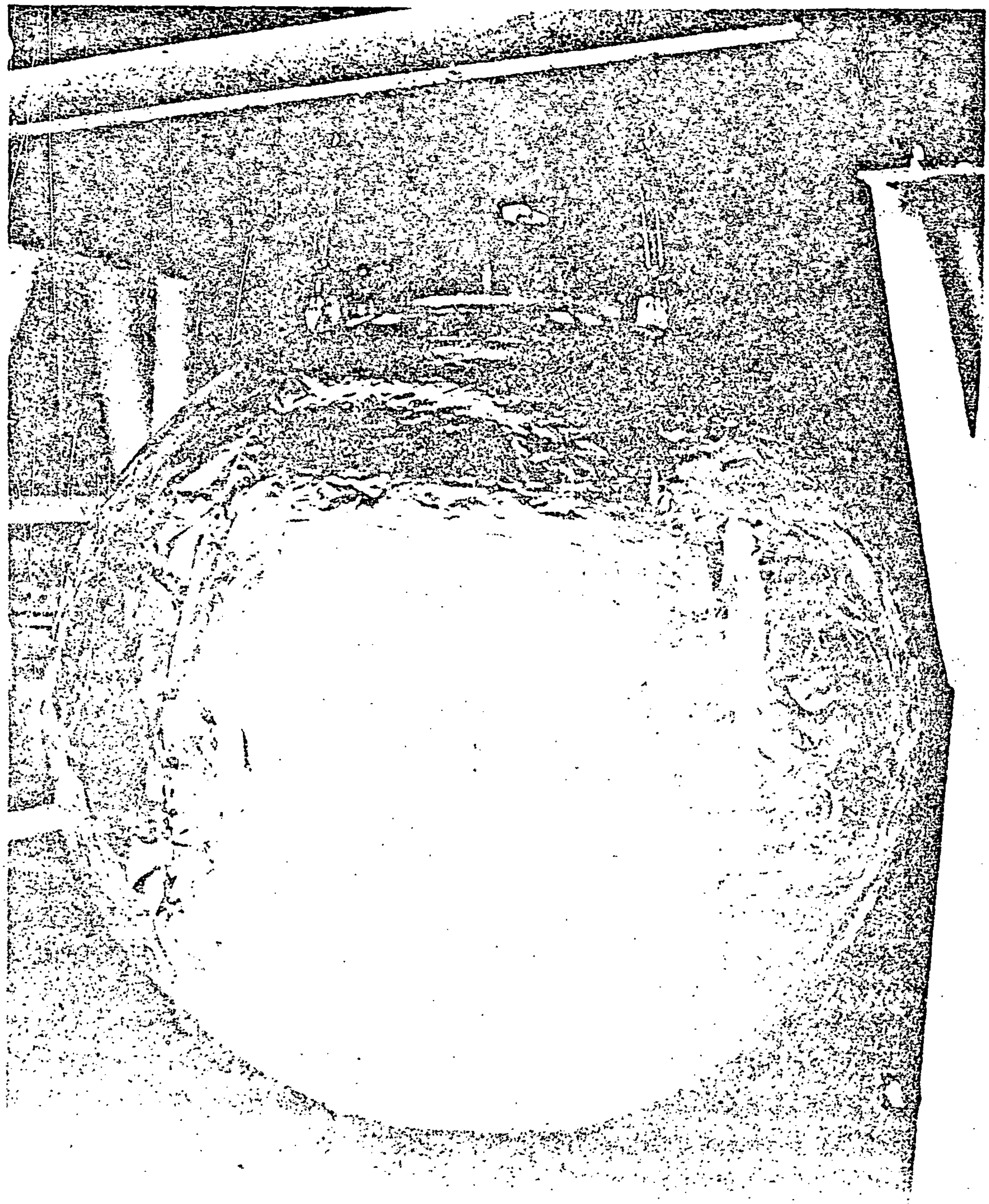

Figure 7-21. Outer Core Blanket With Velcro Fastener Mounting

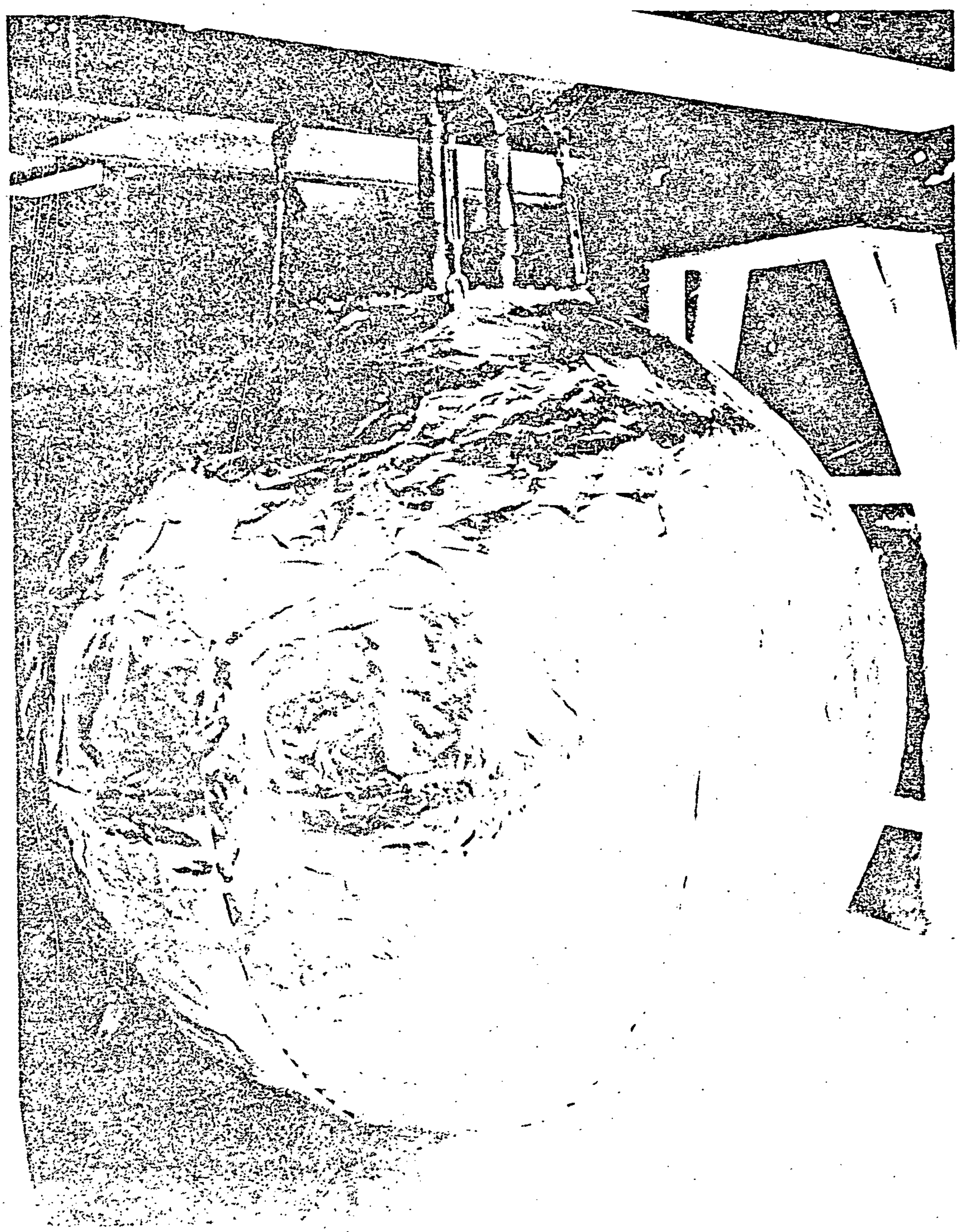

Figure 7-22. Superinsulated, 1.52 m (60 in) Tank

8

TEST FACILITIES

All system tests were conducted at the Convair Liquid Hydrogen Test Center Site "B" thermal vacuum facility. This site lies on a 2400-acre parcel of land located 19.3 × 10^3 m (12 miles) north of the Kearny Mesa plant, approximately 32.2 × 10^3 m (20 miles) north of downtown San Diego. The site test complex has the capability of testing a wide variety of aerospace systems, components, and materials using liquid hydrogen or liquid nitrogen as a working fluid, thus providing a complete testing environment.

8.1 VACUUM CHAMBER

The test chamber (Figures 8-1 and 8-2) was a 3.66 m (144 in) diameter by 4.9 m (192 in) water jacketed vacuum chamber and was serviced by a 0.813 m (32 in) oil diffusion pump, a LN_2 cold trap, and backed by two 14.2 m^3/min (500 ft^3/min) Kinney mechanical vacuum pumps. Controls for these pumps, along with all fluid system controls and the data acquisition equipment, were located in a blockhouse approximately 23 m (900 in) from the test pad.

8.2 TEST TANK PRESSURE CONTROL SYSTEM

The pressure control system shown in Figures 8-3 through 8-8 was used during testing to control the ullage pressure in the liquid hydrogen test tank. The system was designed to maintain the test tank pressure within ± 1.38 N/m^2 (0.0002 psi) of the set point. The MKS Baratron, differential capacitance manometer, Model 145 AH-1 (± 1 mm Hg diff.) was utilized to sense very small positive or negative pressure variations in the test tank relative to a constant reference pressure of a fixed volume of gas, maintained at a constant temperature. The electrical output of the Baratron system was fed to the pressure controller, Dahl Model C601B, which actuates the Hammel-Dahl vent valves Model A40A located in the test tank vent line. Figure 8-9 is a randomly selected 15 minute segment of the test tank pressure recording. A brief description of the major components is given in the following paragraphs.

8.2.1 CAPACITANCE MANOMETER MKS BARATRON NO. 145 AH-1, ± 1 mm Hg DIFFERENTIAL - The MKS Baratron Type 145A capacitance manometer head is a tensioned diaphragm pressure gauge with the bridge circuit and preamplifier inside the diaphragm case. The head was mounted inside a temperature controlled chamber and attached to a 5454 kg (12000 lb) mass block to eliminate vibrations. The MKS Baratron Head mounting is shown in Figure 8-6.

8.2.2 SIGNAL CONDITIONER, MKS MODEL 170 M-7A - This electronic unit provided excitation to the Head, and converted the Head output to a proportional DC output of ± 10 VDC full scale.

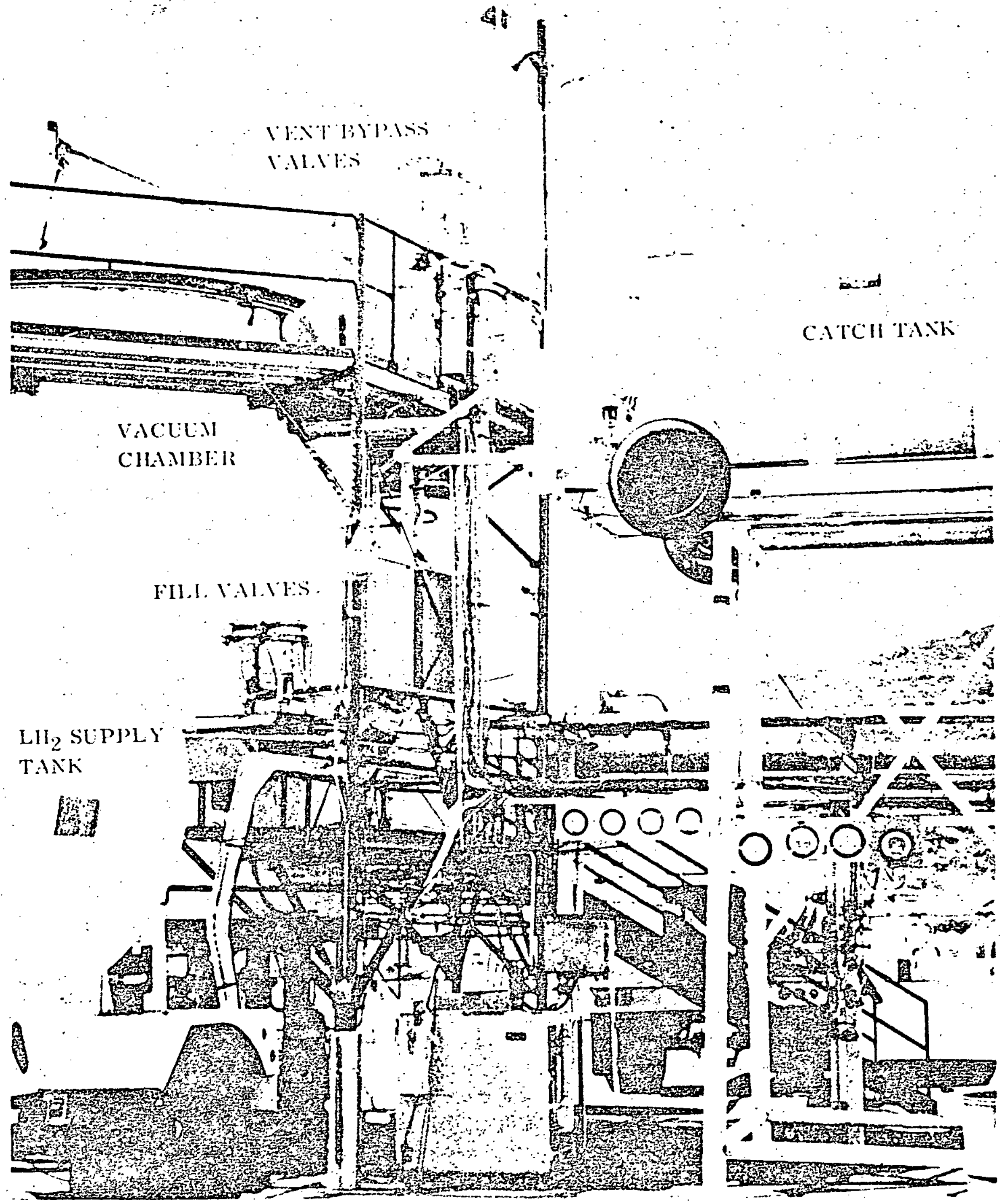

14-9486

Figure 8-1. Test Facility - South View

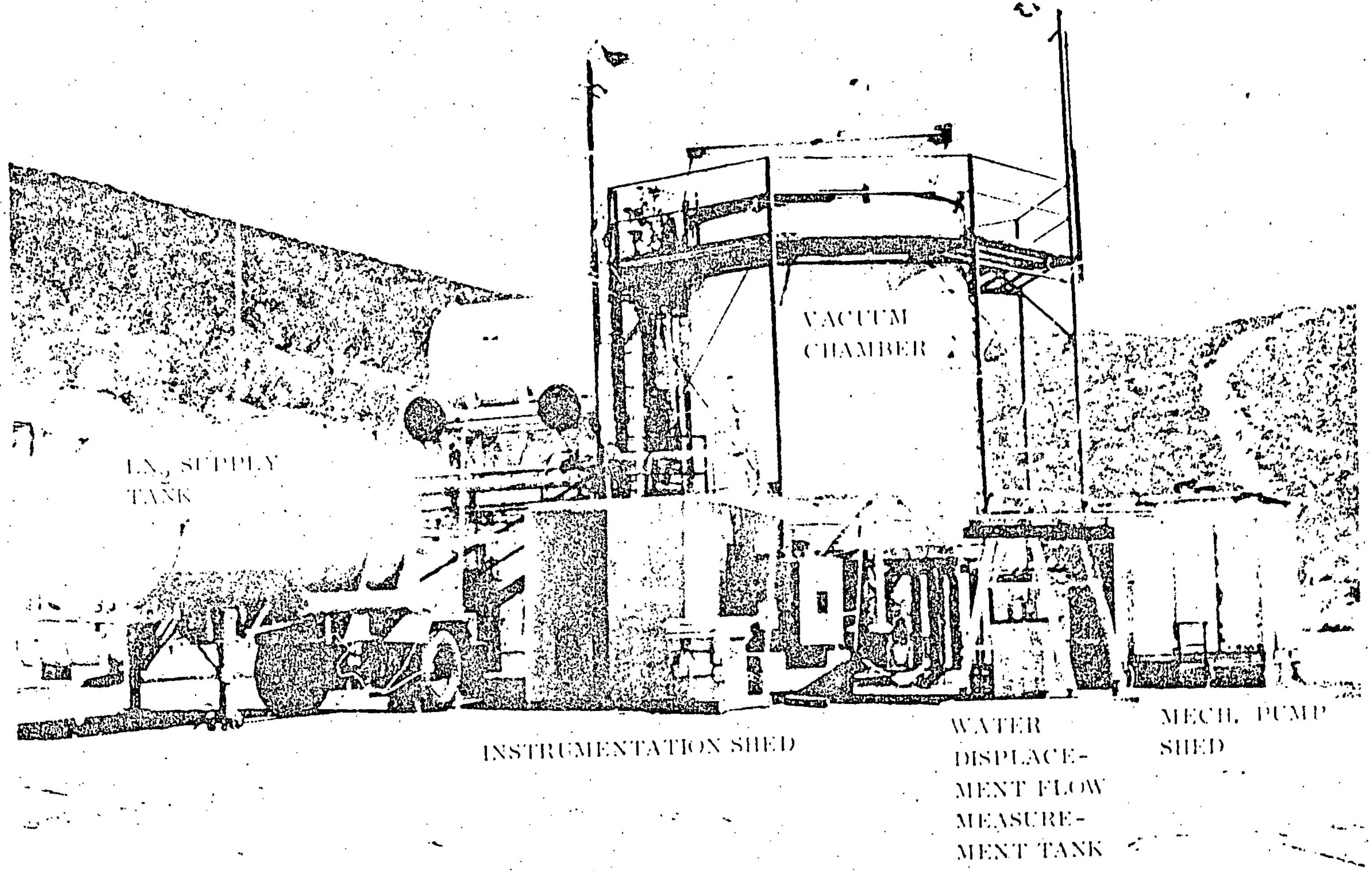

14-9483

Figure 8-2. Test Facility, North View

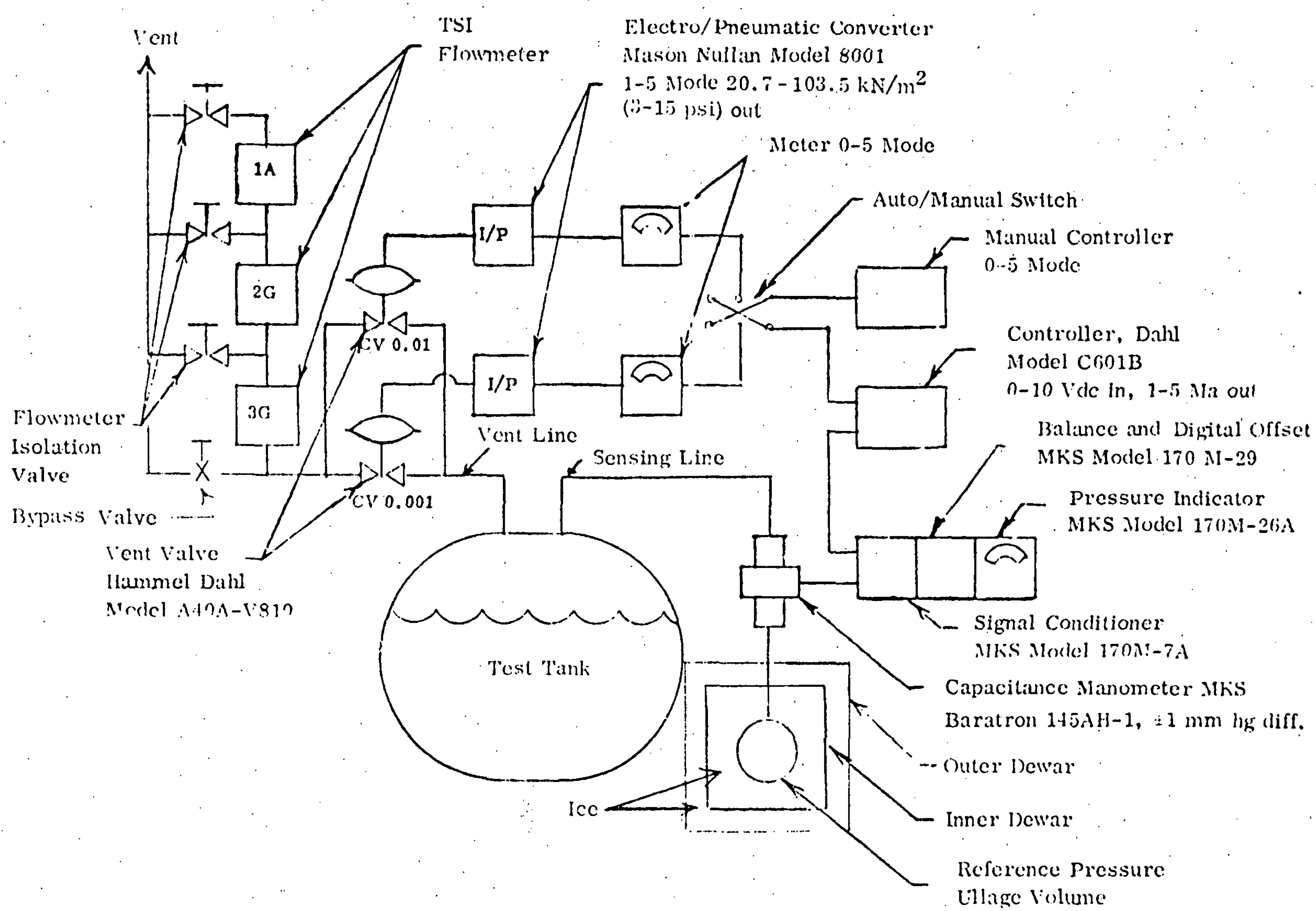

Figure 8-3. Test Tank Pressure Control System Schematic

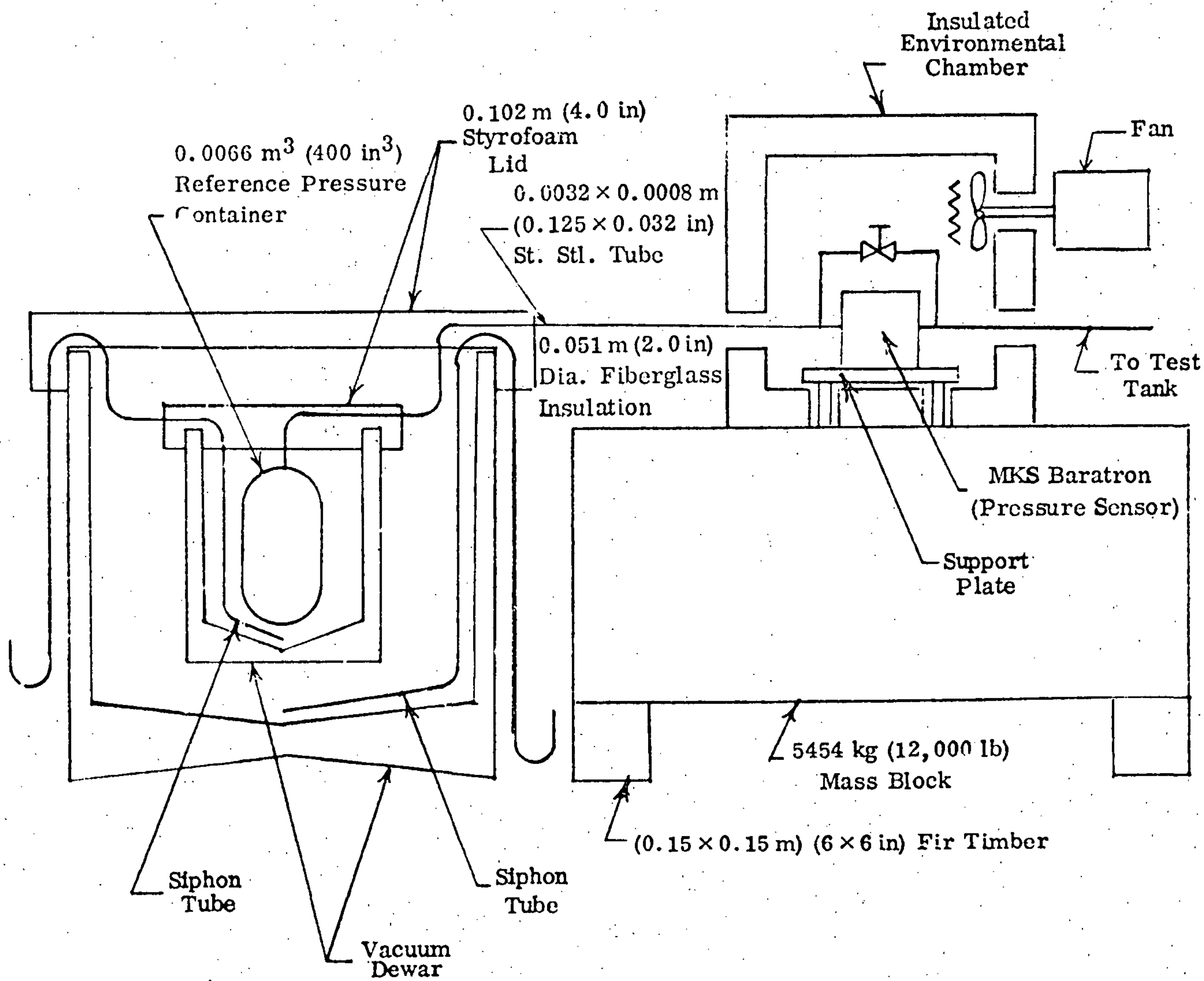

Figure 8-4. MKS Baratron Head Mounting and Reference Pressure Container

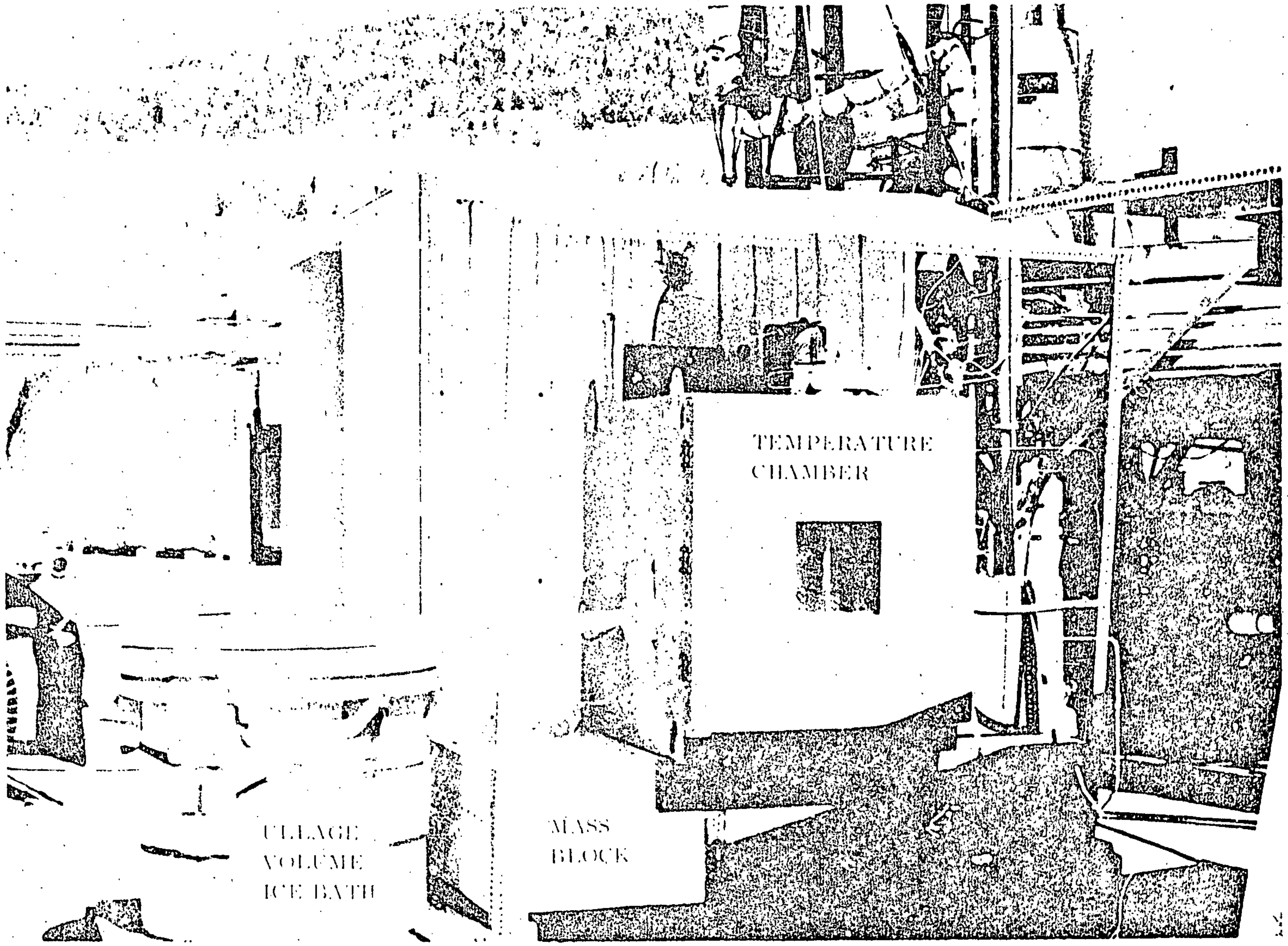

14-9494

Figure 8-5. Test Tank Pressure Control System

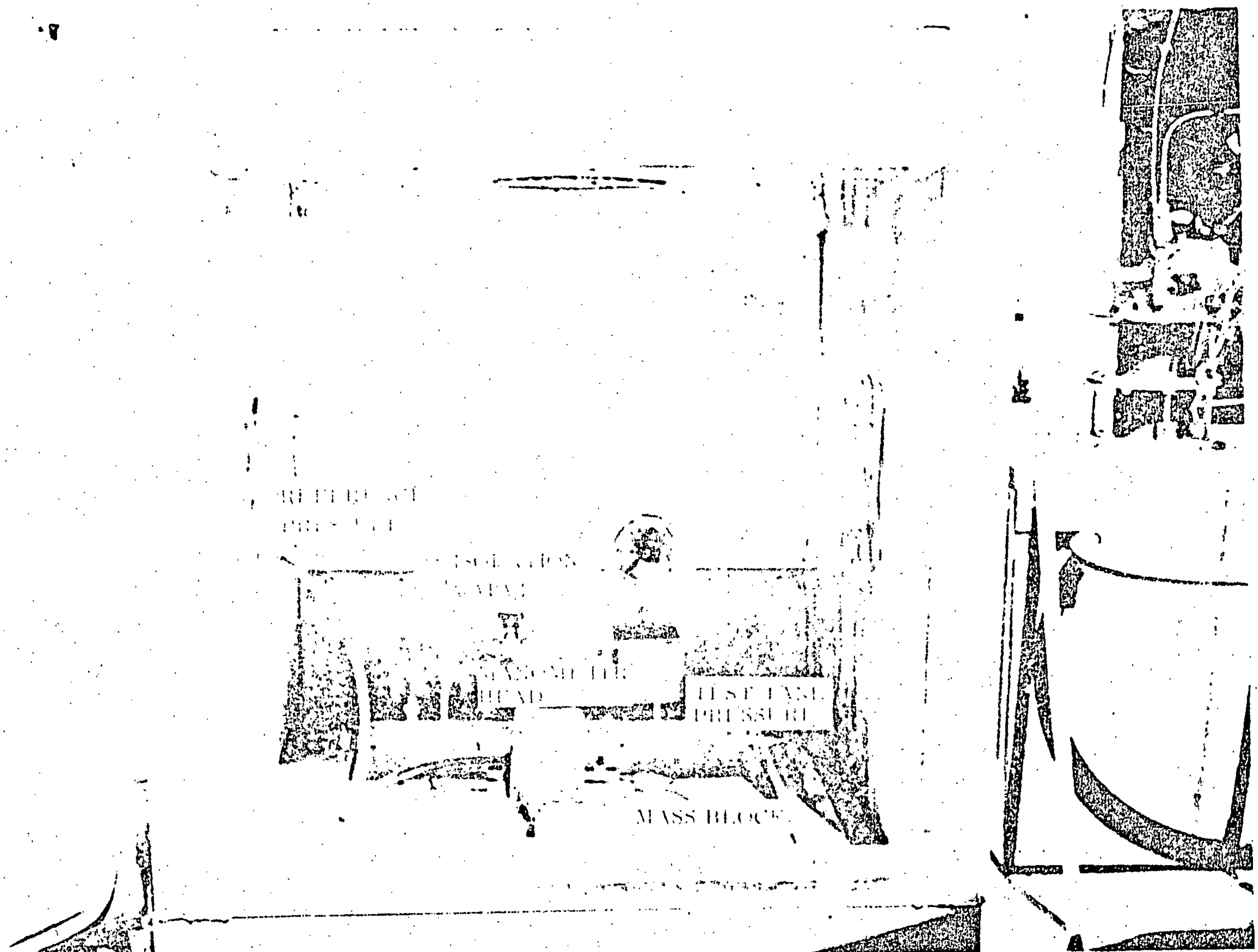

14-9493

Figure 8-6. MKS Baratron Capacitance Manometer Head Mounting

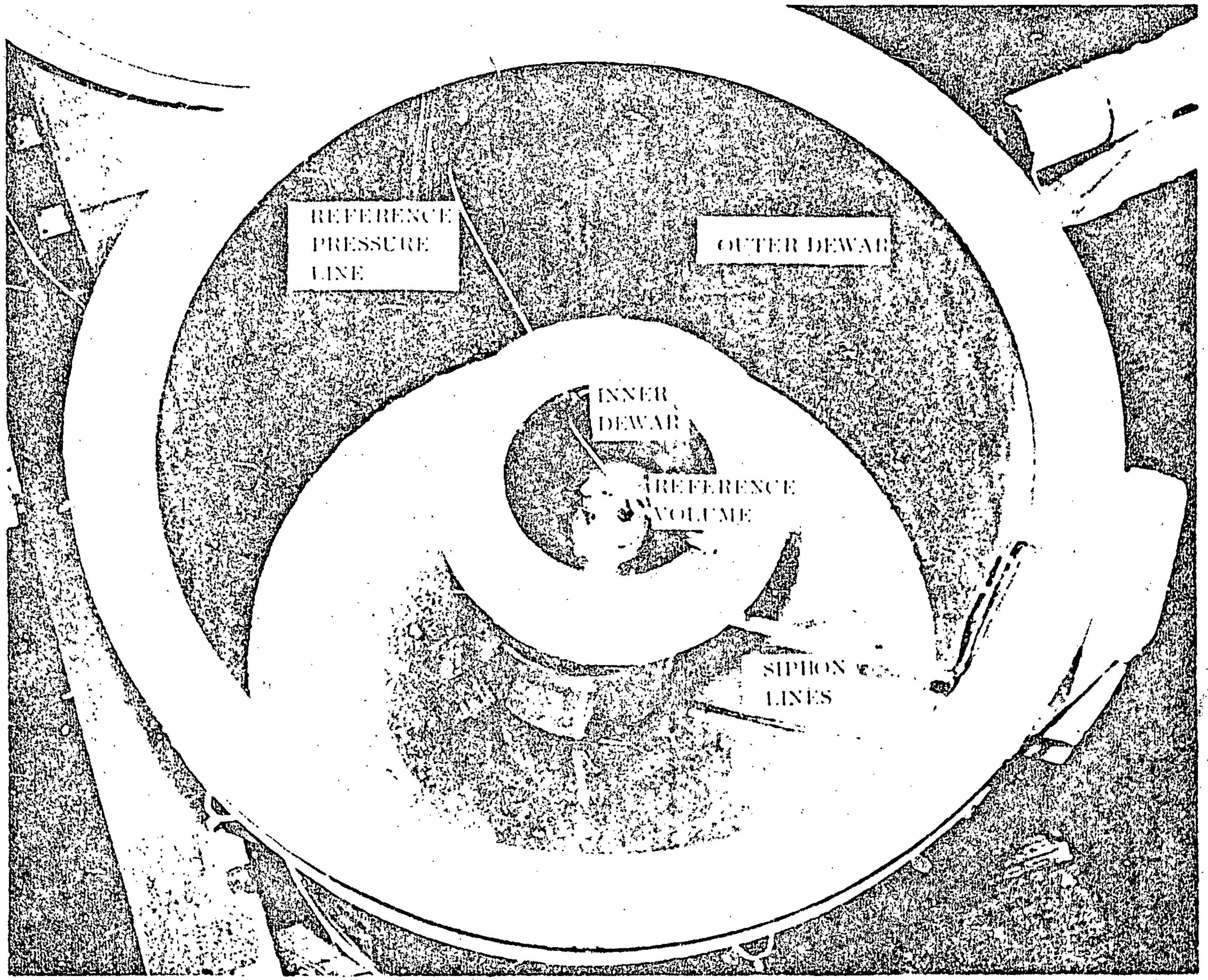

Figure 8-7. Reference Pressure Volume and Ice Bath   14 6986

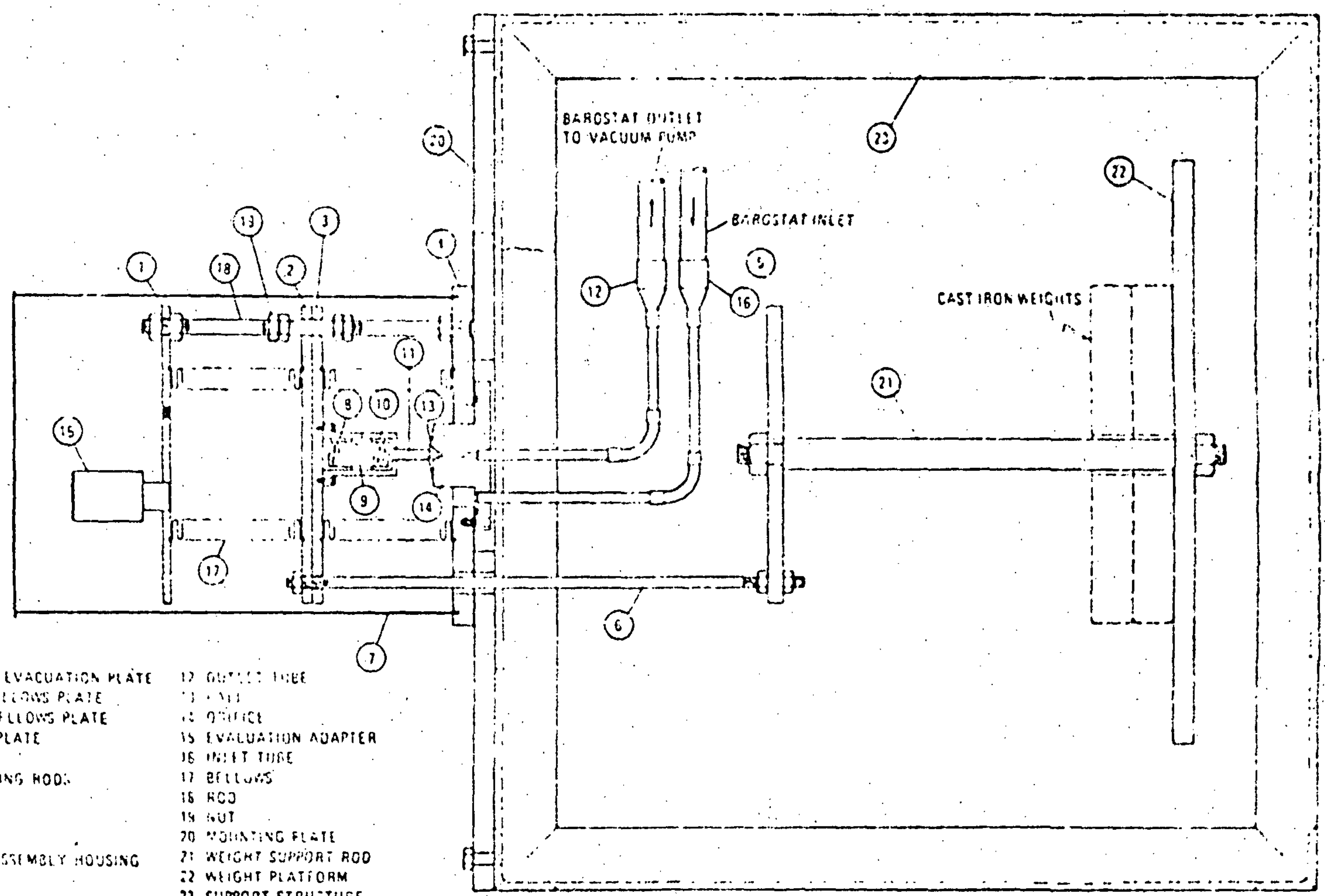

1 BELLOWS EVACUATION PLATE
2 UPPER BELLOWS PLATE
3 LOWER BELLOWS PLATE
4 ORIFICE PLATE
5 PLATE
6 CONNECTING RODS
7 COVER
8 CUP
9 SPRING
10 SPRING ASSEMBLY HOUSING
11 PLUNGER
12 OUTLET TUBE
13 [illegible]
14 ORIFICE
15 EVALUATION ADAPTER
16 INLET TUBE
17 BELLOWS
18 ROD
19 NUT
20 MOUNTING PLATE
21 WEIGHT SUPPORT ROD
22 WEIGHT PLATFORM
23 SUPPORT STRUCTURE

Figure 8-8. NBS Barostat Assembly

ORIGINAL PAGE IS
OF POOR QUALITY

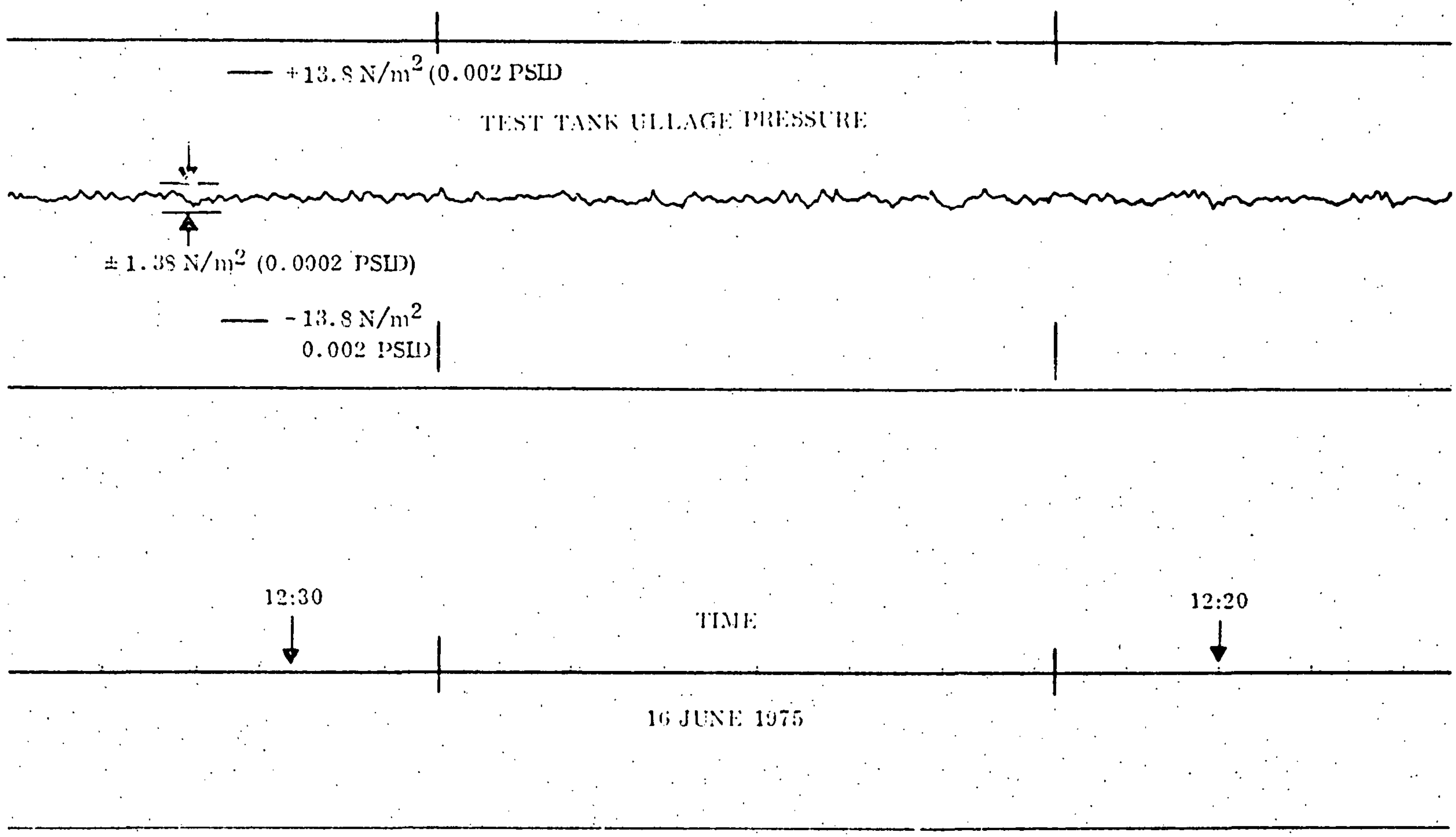

Figure 8-9. Test Tank Ullage Pressure Versus Time

8.2.3 PRESSURE INDICATOR, MKS MODEL 170M-26A - This unit was a 0.13 m (5 in) precision mirror scale meter readout unit, calibrated directly in pressure units. It had a center-zero meter for reading both positive and negative pressures.

8.2.4 BALANCE DIGITAL OFFSET MKS MODEL 170 M-29 - This unit provided for setting the manometer head output null point anywhere within ± 1 mm HG of the reference pressure.

8.2.5 CONTROLLER, DAHL MODEL C-601B - The C-601B is a three mode analog controller which permits full time automatic control. It accepts all standard transmitter and remote set-point signals.

8.2.6 HAMMEL-DAHL VALVE CV 0.001, MODEL NO. A10A/V810/DGE42/P4SG8 - This was a 316 stainless steel, spline trim, globe valve with an air to open actuator, manual open limit stop, plain bonnet, teflon packing, and a micro positioner.

8.2.7 HAMMEL-DAHL VALVE, CV 0.01, MODEL NO. A40A/V810/DGE42/PWSG8 - Same as Spec. No. 8.2.6.

8.2.8 REFERENCE PRESSURE CONTAINER ICE BATH - The reference pressure volume ice bath (Figures 8-4 and 8-7) consisted of a 0.15 m (6 in) diameter, 0.305 m (12 in) long stainless steel vessel containing hydrogen gas. This vessel was mounted within the inner vacuum jacketed dewar, 0.254 m (10 in) diameter and 0.457 m (18 in) deep. This assembly was contained within an outer dewar, 0.762 m (30 in) diameter and 0.772 m (30 in) deep. Both dewars were filled with ice, covered with 0.10 m (4 in) thick foam lids and equipped with tubes to siphon water away. The reference pressure vessel was connected with the Baratron Head by a 0.0032 m (0.125 in) diameter, 0.0008 m (0.032 in) wall, 2.44 m (96 in) long stainless steel tube. The outer dewar siphon tube was designed to keep the water level below the bottom of the inner dewar, and the inner dewar siphon tube was designed to keep the water level below the bottom of the reference pressure vessel. The outer dewar held approximately 182 kg (400 lb) of ice and required an additional 45 to 68 kg (100 to 150 lb) of ice every 3 to 4 days. The inner dewar held approximately 0.9 kg (2 lb) of distilled water ice and required an additional 0.09 kg (0.2 lb) every 3 to 4 weeks.

8.3 GUARD TANK PRESSURE CONTROL

The NBS barostat device was used to control the pressure of the guard tank during the null and thermal tests. The NBS barostat was developed by the National Bureau of Standards (NBS), Washington, to maintain constant tank back pressure with small variations in vent gas flow rate. The barostat was used successfully at NASA/MSFC and at Convair on a 2.21 m (87 in) diameter test tank thermal test program (Ref. 8-1). Convair's experience in calibration of the unit indicates that with an 0.00254 m (0.1 in) diameter orifice, pressure control was maintained over a band of ± 13.8 N/m^2 (± 0.002 psi) provided the flow rate does not change more than ± 0.000094 m^3/sec (± 0.2 scfm).

The initial predicted guard tank boiloff rate was approximately 0.014 m^3/sec (30 scfm). Because of this, the Barostat was set up with a larger 0.013 m (0.5 in) diameter orifice.

Figure 8-8 is a schematic of the NBS barostat. The basic principle of operation of the unit is balance between the pressure in the lower cavity and weights suspended from this bellows assembly. In order to reach equilibrium, the bellows respond to the pressure from the tank and open or close the orifice by moving the ball and plunger assembly. This plunger is spring loaded to prevent damage to the lapped orifice seat when the unit closes. The amount of weight placed on the weight platform determines the pressure at which the unit will control. The upper bellows section is evacuated to provide a constant pressure reference for the controlling bellows that is not affected by changes in atmospheric pressure.

During the null test, the guard tank boiloff was found to vary from a high of greater than 0.0047 m^3/sec (10 scfm) immediately after filling to a low of less than 0.00024 m^3/sec (0.5 scfm) after the temperature had stabilized (approx. 12 hours). After temperature stabilization there still remained a large day to night to day variation in the boiloff. This resulted in the need for constant adjustments of the Barostat control weights to maintain the required narrow guard tank pressure band. Before the start of the customized MLI tests, the Barostat was replaced with a pressure transducer/closed loop controller/flow control valve system.

In this system a Statham Model PD-822 34.5 kN/m^2 (5 psid) pressure transducer was used to sense the guard tank ullage pressure relative to the test tank ullage pressure. The output of the transducer was fed into a Foxboro Model M62 closed loop controller with variable rate and reset. The process control signal from the controller was then used to position an Annen Domotor valve with a 0.013 m (0.5 in) proportional plug. Except for the first few minutes after filling, this system maintained the proper guard tank pressure without the need of constant adjustment.

8.4 FLUID SYSTEM

Figure 8-10 is an overall schematic of the fluid systems required for the thermal test.

The systems for the guard tank, payload simulator, cryoshroud, and baffles were fabricated and leak checked before test tank installation. Welding and silver brazing were used as the principal means of joining parts of the system. All the aluminum to stainless steel transitions were made using double seal Conoseal flanges with the interseal cavity vacuum pumped to less than 1.33 N/m^2 (0.01 torr). After assembly and installation of the test tank a complete section by section leak check was performed.

To assure adequate performance of the vacuum system during the testing phase, a total systems leak check was performed. Several leaks were found and repaired after which no leakage could be measured by the mass spectrometer leak detector.

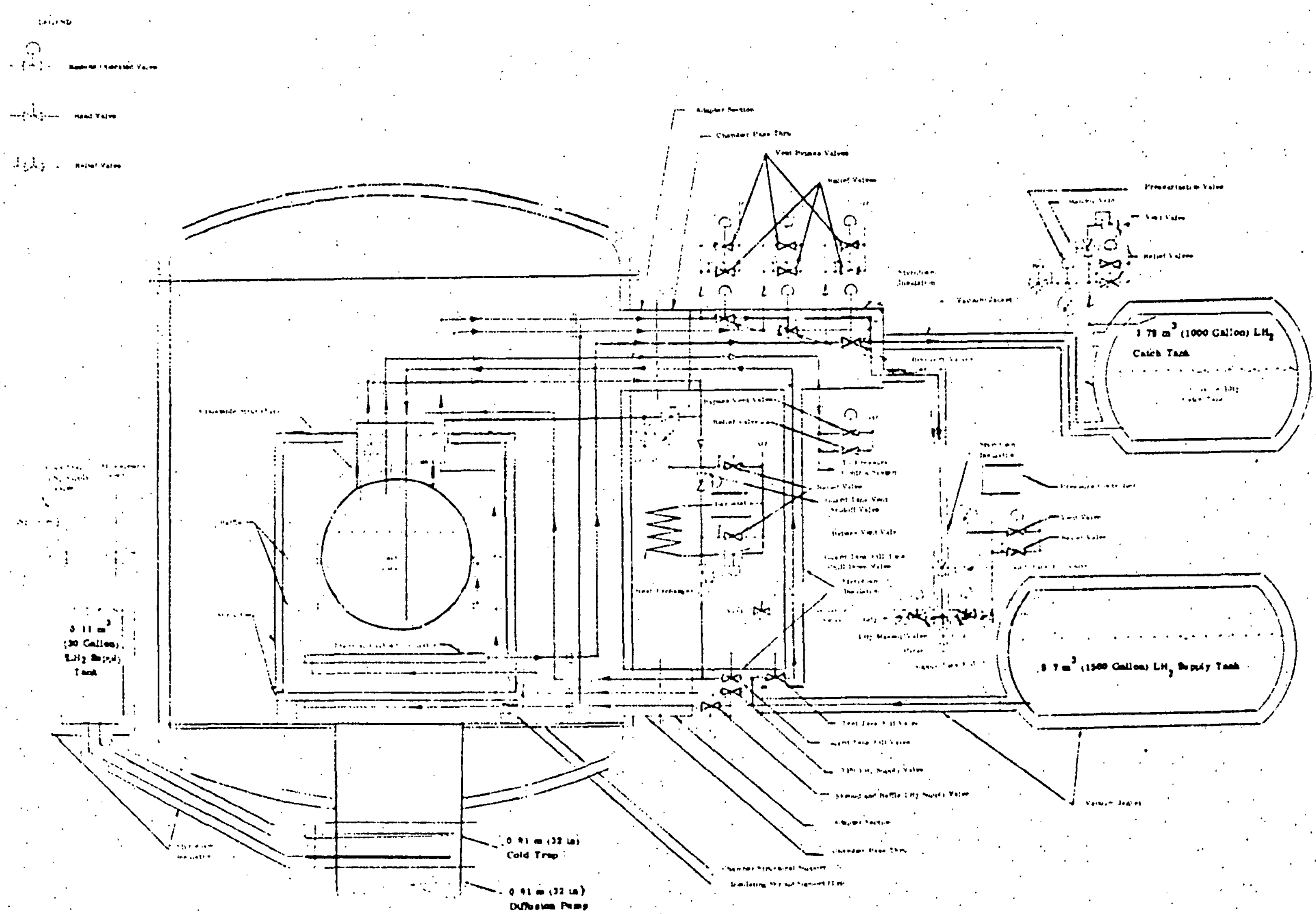

Figure 8-10. Schematic of Test Apparatus and Fluid System

The fill line for the test tank extended to the bottom of the tank primarily as a safety measure. Since the fill line was guarded at LH_2 temperature, there was no need to terminate the line in the ullage space. In an emergency, the tank could have been emptied through the fill line by pressurizing the tank, opening the fill valve, and forcing the liquid back into the site storage tank. The fill valve was located immediately outside the chamber wall. This valve was a proportionally controlled globe valve permitting metering of the LH_2 supply during filling operations.

The vent line terminated at the tank door. This line was also guarded and penetrated the chamber wall at a level just above the cryoshroud. The primary tank vent valve that was used during filling and initial chilldown was also a proportionally controlled valve. After the filling transients disappeared and the test tank boiloff had dropped to less than 0.000472 m^3/sec (1.0 scfm), the large primary vent valve was isolated from the vent line and vent gases were passed through the test tank pressure control system (8.2).

The majority of the components shown in Figure 8-10 were remotely operated from the blockhouse. A 5.7 m^3 (1500 gal) LH_2 supply tank was maintained at an approximate pressure of 41.4 kN/m^2 (6 psig) all the time by a pneumatic pressure controller and vent valve. When empty, the supply tank was filled with liquid hydrogen through the LH_2 make-up valve from the 49.2 m^3 (13,000 gal) site LH_2 storage tank or from the 3.78 m^3 (1000 gal) catch tank through the LH_2 recovery valve. The fill rate was limited to prevent pressure surges in the tank. The catch tank was vented to the atmosphere while acting as a liquid vapor separator for the cryoshroud, baffles and TPS vents. When full, it was isolated from the cryoshroud, baffles and TPS vents, pressurized to approximately 172.5 kN/m^2 (25 psig), and drained into the supply tank.

In normal operation the system was able to run for a minimum of 15 hours before the supply tank needed to be filled or for 5 hours before the catch tank needed to be emptied. Transfer from the catch to supply tank took less than 15 minutes. Therefore, the vents were "recovered" about 95% of the time. Flow through the cryoshroud, baffle, and the TPS (when required by the procedure) was continuous. Vent flow was normally through the vent shutoff valves into the catch tank. During LH_2 filling and transfer operations the vent shutoff valves were closed and the vent flow dumped to atmosphere through the vent bypass valves.

The guard tank, once it was cold and the temperature stabilized, needed refilling only once every five days. The guard tank vent bypass was used only during filling. At other times the guard tank venting was controlled by the guard tank pressure control. The schematic in Figure 8-10 shows that each tank and line segment was protected by a relief valve and that no liquid or cold gas could be trapped in an unprotected cavity.

Most of the valves which were operated from the blockhouse required manipulation during test operations. Since the LH_2 Supply Tank pressure was constant throughout the test, manual stops on the LH_2 supply valves were initially adjusted to provide the appropriate LH_2 flow to each segment of the system and remained set during test operations. Platinum resistance thermometers and thermocouples installed on all surfaces were monitored during test operations and used to measure and control system performance.

8.5 TEST TANK HEATER

An electrical heater (Figures 8-11 and 8-12) was used to simulate payload thermal input to the test tank during the null test. The heater was designed to provide a maximum heat flow of one watt into the tank. In order to provide a large enough area to eliminate nucleate boiling on the heater surface, the heater was fabricated from Nichrom Ribbon 1.194 m (47 in) long, 0.00005 m (0.002 in) thick by 0.00317 m (0.125 in) wide. The ribbon was mounted on two pieces of terminal board as shown in Figure 8-11. The ribbon was divided into eight segments and connected in a parallel/series circuit with a total resistance of approximately one ohm.

The terminal board was mounted to the lower end of the instrumentation tree as shown in Figure 8-12. The transition from heater ribbon to a minimum 16-gauge power lead was made at the bottom of the tank.

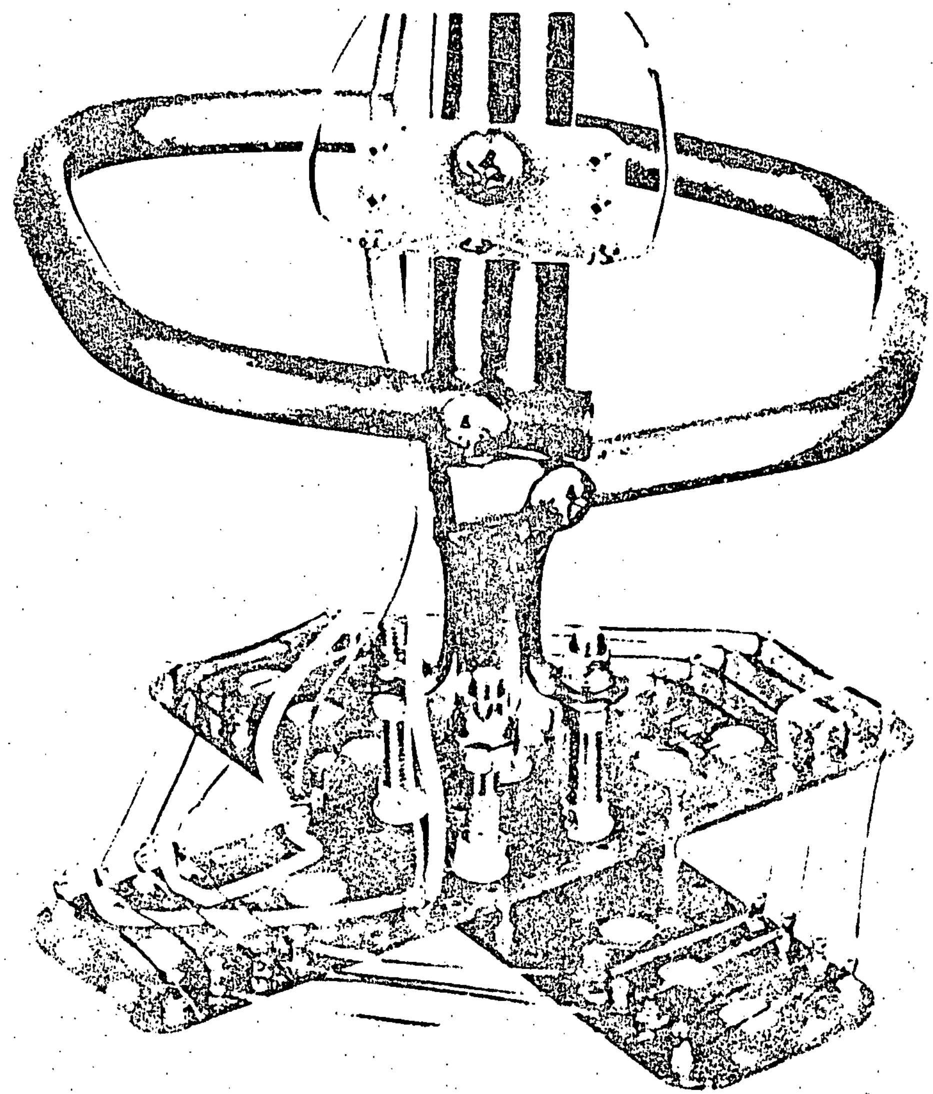

Figure 8-11. Test Tank Heater

14 0290

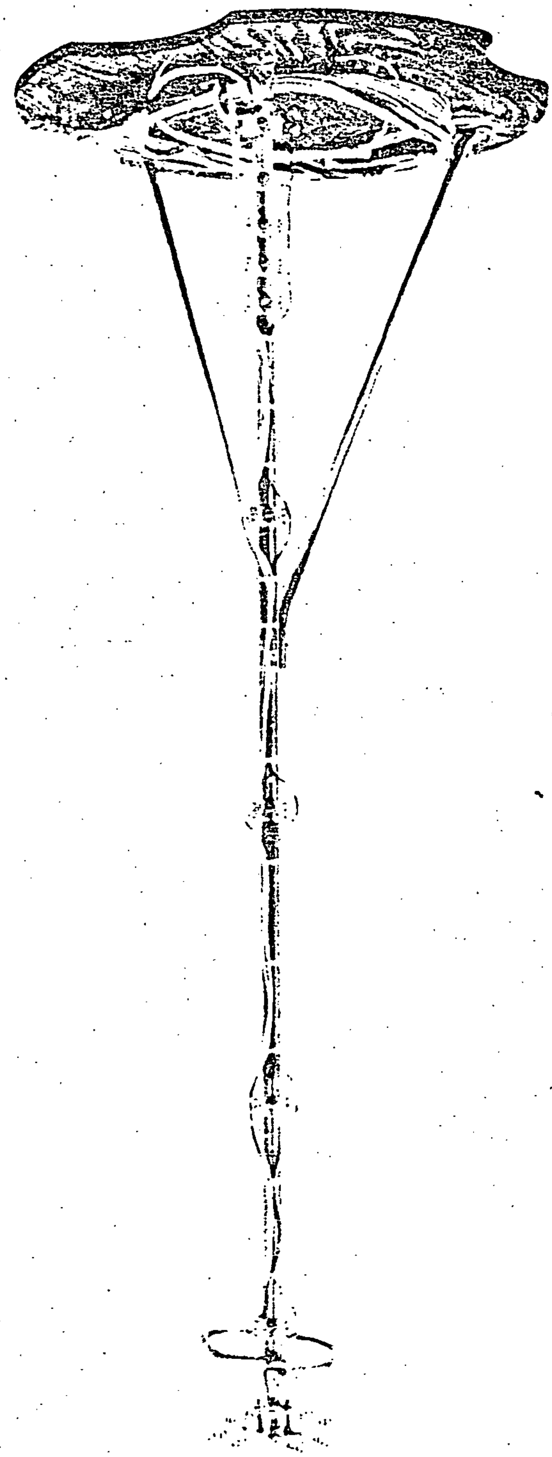

Figure 8-12 Test Tank Heater - Attached to Instrumentation Tree

9

TEST INSTRUMENTATION

9.1 INSTRUMENTATION DEFINITION

Instrumentation selection for the full scale test specimen was based upon measurement of the independent and dependent variables required for demonstration of system overall thermal performance, system efficiency, and system component operation. Independent variables included hydrogen liquid level, chamber pressure and ullage pressure. Dependent variables included temperature distribution, MLI thermal gradients and LH_2 boiloff rate. The instrumentation tree platinum resistors within the tank permitted LH_2 level as well as temperature measurement. Chromel/Constantan thermocouples were used for all other temperature measurements. Chamber and shroud pressure measurements were made with hot filament ion gages (Bayard-Alpert) in their respective ranges. Liquid hydrogen boiloff flow rates were measured with TSI hot-film anemometers and a water displacement apparatus. Pressures other than the test tank pressure were measured with Statham Strain gage transducers. Test specimen instrumentation locations are presented in Figures 9-1 through 9-6. Table 9-1 summarizes measurement description and location definition.

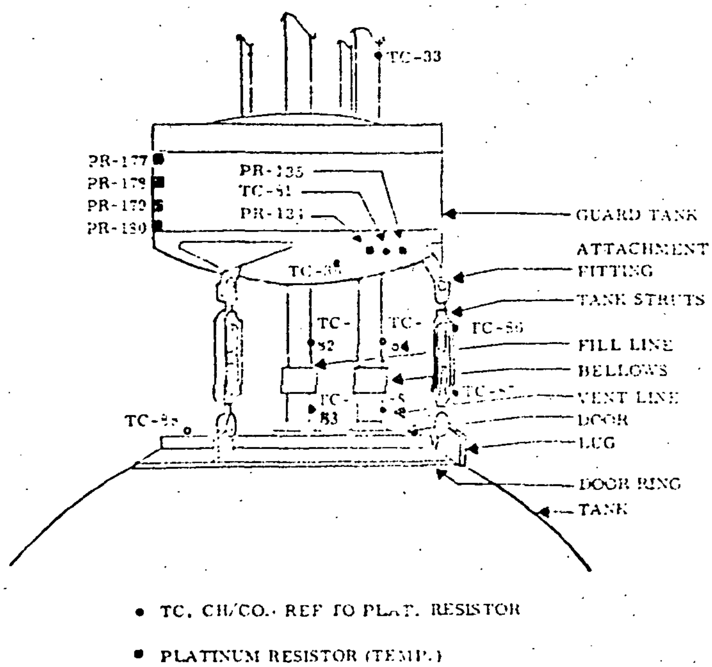

Figure 9-1. Guard Tank, Support, Fill Line and Vent Line Instrumentation

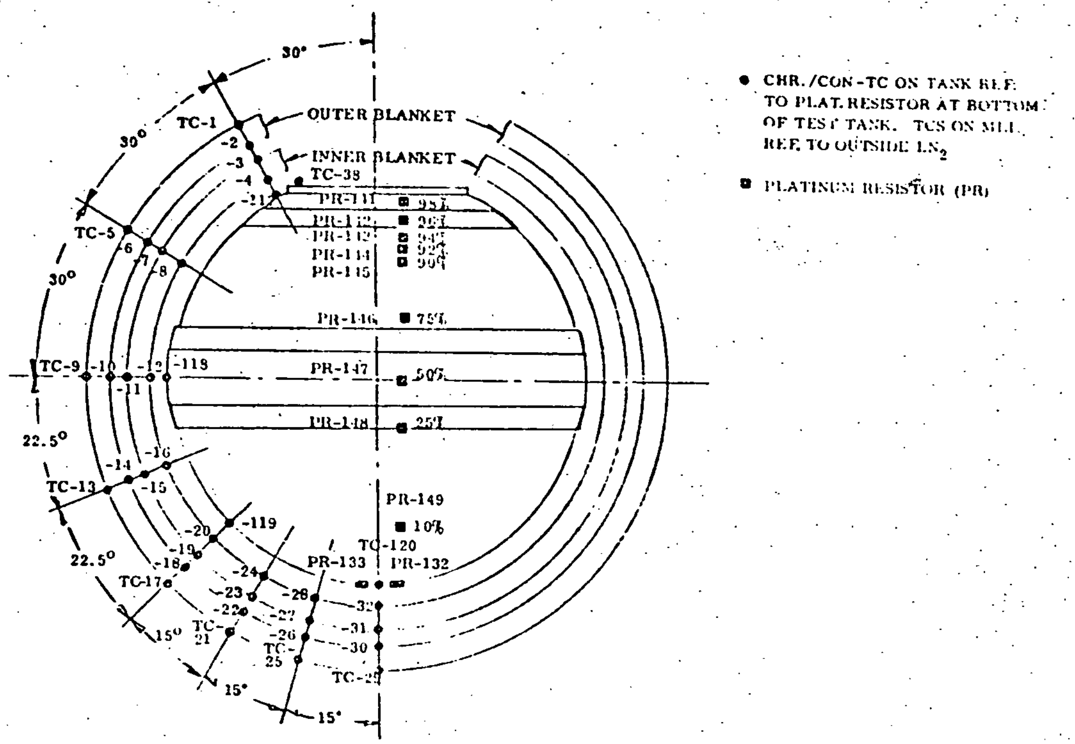

Figure 9-2. Test Tank and MLI Instrumentation

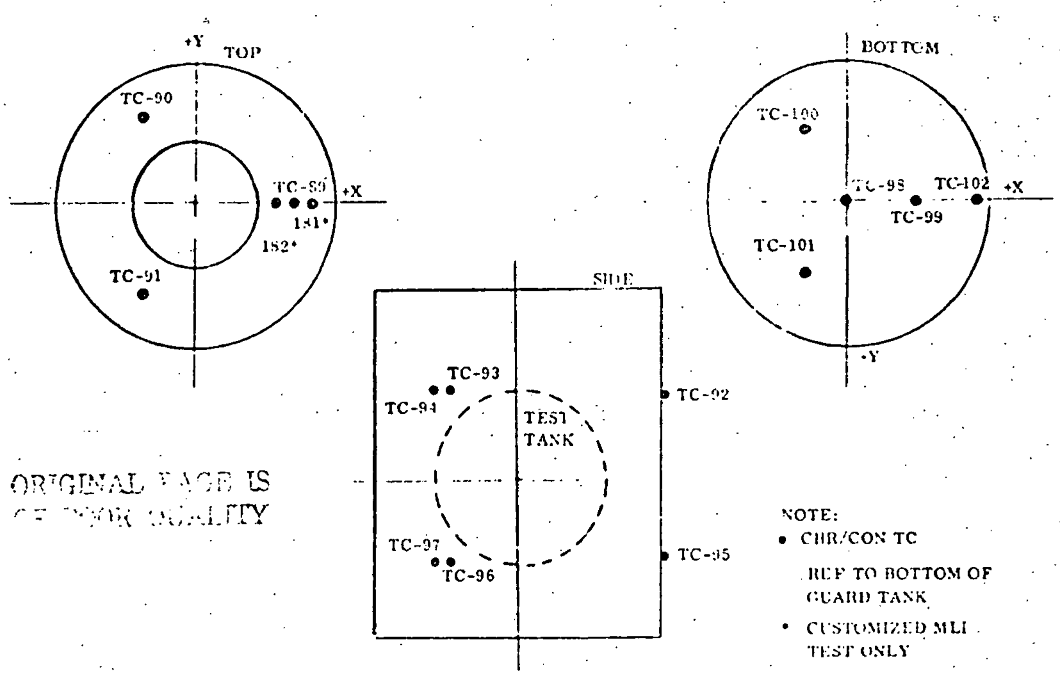

Figure 9-3. Shroud Thermocouple Location

NOTE: Dimensons of thermocouple locations are shown in Table 9-1

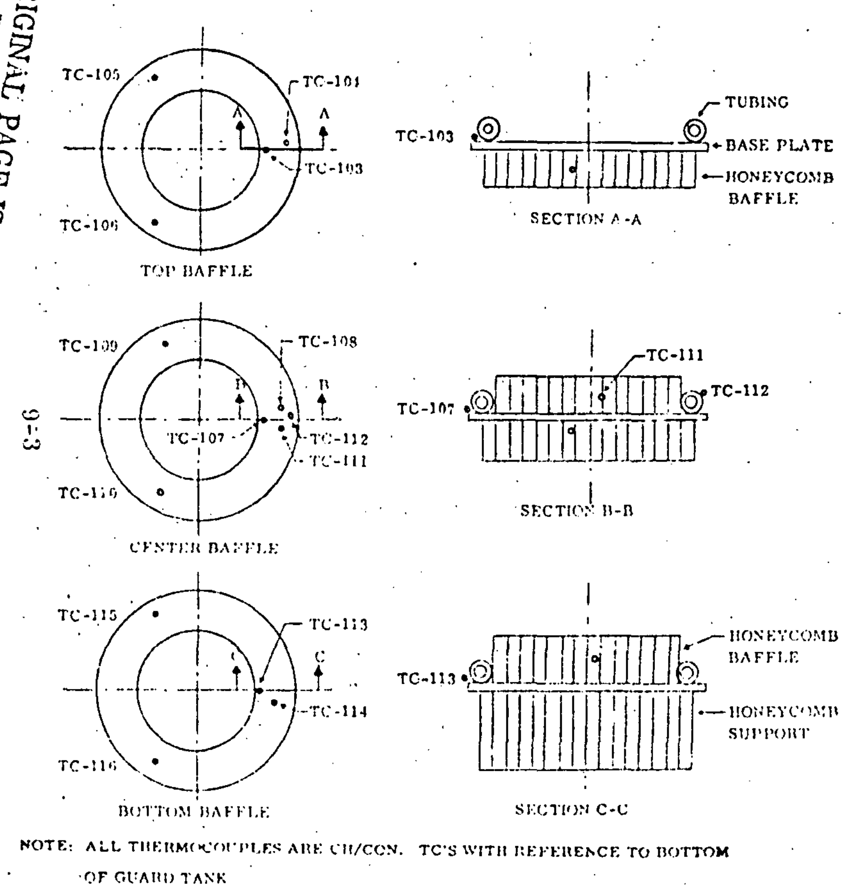

Figure 9-4. Baffle Thermocouple Location

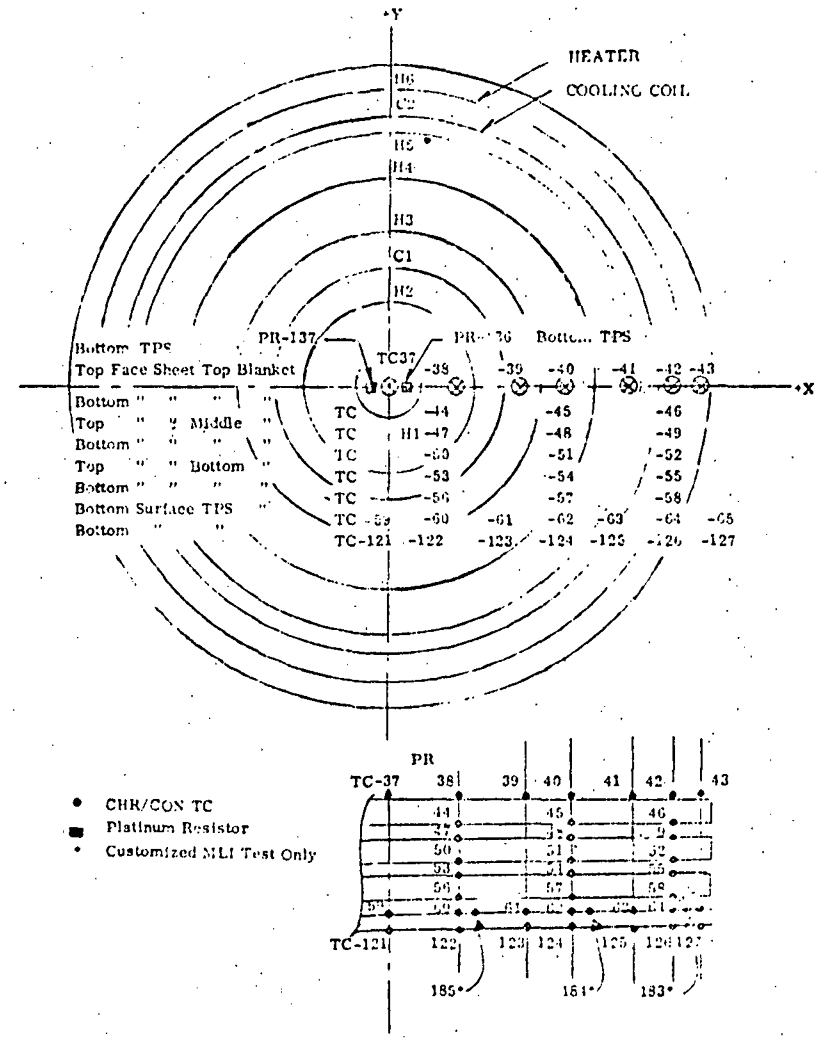

Figure 9-5. Thermal Payload Simulator Instrumentation Location

ORIGINAL PAGE IS OF POOR QUALITY

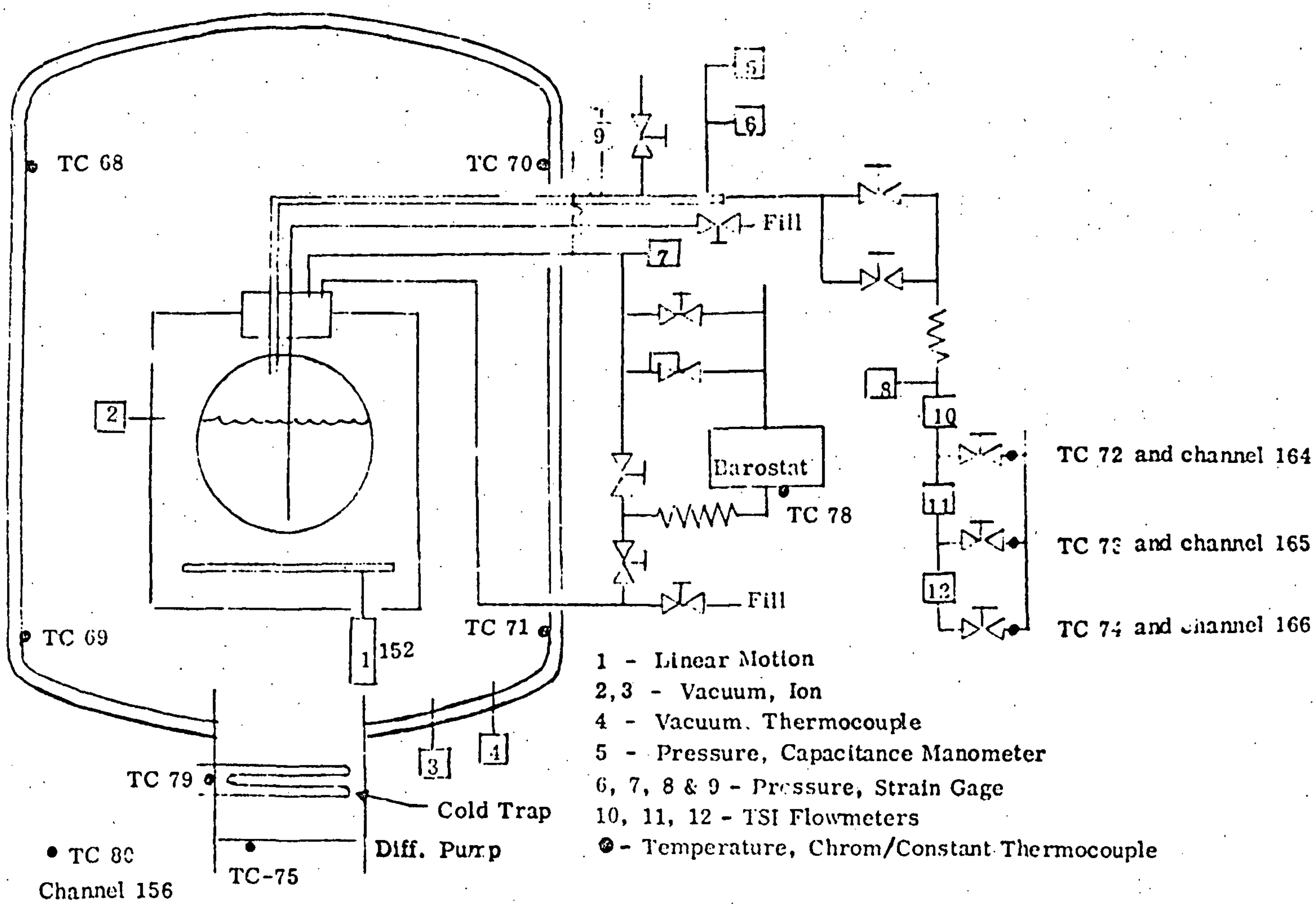

Figure 9-6. Instrumentation for Auxiliary Hardware

Table 9-1. Measurement Description Summary

Note: ** Azimuth is measured from test tank fill line, * Inclination, altitude and radius are measured from center of tank.

Channel No.	Identification		Physical Location ※				Type of Instr.	Fig. No.	Reference Junction	Measurement Description
	Instr.	Location	Component	** AZIM(0)	*INC(0) * ALT (in)	* RAD (in)				
1	TC-1	TT-1A	Outer Facesheet - Outer Blanket	0	+60		CHR/CON	9-2	Outside LN_2 Bath	Thermal Gradient Through Tank MLI
2	TC-2	TT-1B	Inner " " "	0	+60		"	"	"	"
3	TC-3	TT-1C	Outer " Inner "	0	+60		"	"	"	"
4	TC-4	TT-1D	Inner " " "	0	+60		"	"	"	"
5	TC-5	TT-2A	Outer Facesheet - Outer Blanket	0	+30		"	"	"	"
6	TC-6	TT-2B	Inner " " "	0	+30		"	"	"	"
7	TC-7	TT-2C	Outer " Inner "	0	+30		"	"	"	"
8	TC-8	TT-2D	Inner " " "	0	+30		"	"	"	"
9	TC-9	TT-3A	Outer Facesheet - Outer Blanket	0	0		"	"	"	"
10	TC-10	TT-3B	Inner " " "	0	0		"	"	"	"
11	TC-11	TT-3C	Outer " Inner "	0	0		"	"	"	"
12	TC-12	TT-3D	Inner " " "	0	0		"	"	"	"
13	TC-13	TT-4A	Outer Facesheet - Outer Blanket	0	-22.5		"	"	"	"
14	TC-14	TT-4B	Inner " " "	0	-22.5		"	"	"	"
15	TC-15	TT-4C	Outer " Inner "	0	-22.5		"	"	"	"
16	TC-16	TT-4D	Inner " " "	0	-22.5		"	"	"	"
17	TC-17	TT-5A	Outer Facesheet - Outer Blanket	0	-45		"	"	"	"
18	TC-18	TT-5B	Inner " " "	0	-45		"	"	"	"
19	TC-19	TT-5C	Outer " Inner "	0	-45		"	"	"	"
20	TC-20	TT-5D	Inner " " "	0	-45		"	"	"	"
21	TC-21	TT-6A	Outer Facesheet - Outer Blanket	0	-60		"	"	"	"
22	TC-22	TT-6B	Inner " " "	0	-60		"	"	"	"
23	TC-23	TT-6C	Outer " Inner "	0	-60		"	"	"	"
24	TC-24	TT-6D	Inner " " "	0	-60		"	"	"	"
25	TC-25	TT-7A	Outer Facesheet - Outer Blanket	0	-75		"	"	"	"
26	TC-26	TT-7B	Inner " " "	0	-75		"	"	"	"
27	TC-27	TT-7C	Outer " Inner "	0	-75		"	"	"	"
28	TC-28	TT-7D	Inner " " "	0	-75		"	"	"	"
29	TC-29	TT-8A	Outer Facesheet - Outer Blanket	0	-90		"	"	"	"

All dimensions are in inches

Table 9-1. Measurement Description Summary (Continued)

Note: ** Azimuth is measured from test tank fill line. * Inclination, altitude and radius are measured from center of tank.

Channel No.	Identification		Physical Location *				Type of Instr.	Fig. No.	Reference Junction	Measurement Description
	Instr.	Location	Component	** AZIM (0)	* INC (0) * ALT (in)	* RAD (in)				
30	TC-30	TT-8B	Inner Facesheet - Outer Blanket	0	-90		CHR/CON	9-2	Outside LN_2 Bath	Thermal Gradient Thru Tank MLI
31	TC-31	TT-8C	Outer " Inner "	0	-90		"	"	"	"
32	TC-32	TT-8D	Inner " " "	0	-90		"	"	"	"
33	TC-33	GT-Vent	Tank Vent-Line, 2 ft FR from Top of G.T.				"	9-1	"	Temp. of Test Tank Vent Line
34	TC-34	S/ST-Vent	Shroud/Side Top-Vent Line				"	9-6	"	Temp. of Shroud Vent Line
35	TC-35	S/BB-Vent	Shroud/Baffle Vent Line				"	9-6	"	Temp. of Baffle Vent Line
36	TC-36	GT-R	Bottom of Guard Tank				"	9-1	Outside of Chamber	Reference Measurement
37	TC-37	TPS-1A	Top Facesheet, Top MLI Blanket	0		0	CHR/CON	9-5	Outside LN_2 Bath	Thermal Gradient Thru TPS-MLI
38	TC-38	TPS-2A	" " " " "	0		6.5	"	"	"	"
39	TC-39	TPS-3A	" " " " "	0		13.0	"	"	"	"
40	TC-40	TPS-4A	" " " " "	0		18.0	"	"	"	"
41	TC-41	TPS-5A	" " " " "	0		25.5	"	"	"	"
42	TC-42	TPS-6A	" " " " "	0		30.0	"	"	"	"
43	TC-43	TPS-7A	" " " " "	0		34.5	"	"	"	"
44	TC-44	TPS-2B	Bottom " " " "	0		6.5	"	"	"	"
45	TC-45	TPS-4B	" " " " "	0		18.0	"	"	"	"
46	TC-46	TPS-6B	" " " " "	0		30.0	"	"	"	"
47	TC-47	TPS-2C	Top " Middle " "	0		6.5	"	"	"	"
48	TC-48	TPS-4C	" " " " "	0		18.0	"	"	"	"
49	TC-49	TPS-6C	" " " " "	0		30.0	"	"	"	"
50	TC-50	TPS-2D	Bottom " " " "	0		6.5	"	"	"	"
51	TC-51	TPS-4D	" " " " "	0		18.0	"	"	"	"
52	TC-52	TPS-6D	" " " " "	0		30.0	"	"	"	"
53	TC-53	TPS-2E	Top " Bottom " "	0		6.5	"	"	"	"
54	TC-54	TPS-4E	" " " " "	0		18.0	"	"	"	"
55	TC-55	TPS-6E	" " " " "	0		30.0	"	"	"	"
56	TC-56	TPS-2F	Bottom " " " "	0		6.5	"	"	"	"
57	TC-57	TPS-4F	" " " " "	0		18.0	"	"	"	"

All dimensions are in inches

Table 9-1. Measurement Description Summary (Continued)

Note: ** Azimuth is measured from test tank fill line, * Inclination, altitude and radius are measured from center of tank.

Channel No.	Identification: Instr.	Identification: Location	Physical Location *: Component	** AZIM(θ)	*INC(θ) * Alt.Tank	*RAD (in)	Type of Instr.	Fig. No.	Reference Junction	Measurement Description
58	TC-58	TPS-6F	Bottom Facesheet Bottom MLI Blanket	0		30.0	CHR/CON	9-5	Outside LN_2 Bath	Thermal Gradient Thru TPS-MLI
59	TC-59	TPS-1G	Top Surface of TPS			0.0				
60	TC-60	TPS-2G	Top Surface of TPS	0		6.5	"	"	"	"
61	TC-61	TPS-3G	Top Surface of TPS			13.0			"	"
62	TC-62	TPS-4G	Top Surface of TPS	0		18.0	"	"	"	"
63	TC-63	TPS-5G	Top Surface of TPS			25.5		"	"	"
64	TC-64	TPS-6G	Top Surface of TPS	0		30.0	"	"	"	"
65	TC-65	TPS-7G	Top Surface of TPS			34.5		"	"	"
66	TC-66	TPS-R	Bottom of Therm. Payload Simulator	0	-	0	"			Reference TC
67	TC-67	TPS-Vent	TPS- Vent Line Outside Shroud				"	9-6	"	Temp. of TPS Vent Gas
68	TC-68	CHAM-NT	Top of Chamber, Internal				"	9-7	"	Defines Enclosure Boundary Temp.
69	TC-69	CHAM-NB	Bottom of Chamber, Internal				"	9-7	"	"
70	TC-70	CHAM-ST	Side of Chamber, Top Internal				"	9-7	"	"
71	TC-71	CHAM-SB	Side of Chamber, Bottom Internal				"	9-7	"	"
72	TC-72	FM	Instrument Console Flowmeter 1A				"	9-7	"	Temp. of Boiloff Meter
73	TC-73	FM	" " " 2G				"	9-7	"	"
74	TC-74	FM	" " " 3G				"	9-7	"	"
75	TC-75	DIFF	Diffusion Pump				"	9-6	"	Diffusion Pump Oil Temperature
76	TC-76	ICE-OUT	ICE Bath - Outer Container				"			Monitor ICE Bath Temperature
77	TC-77	MKS-Capacitor	Capacitance Manometer MKS				"	9-7		Temperature of Head (Sensing Element)
78	TC-78		Barostat (Equip. Rack)				CHR/CON	9-7	"	Temperature of Barostat
79	TC-79		Cold Trap				"	9-7	"	Temp. of Cold Trap (Feedline)
80	TC-80		Ambient Temperature				"	9-7	"	Ambient Air Temperature
81	TC-81	GT-A	Guard Tank Bottom, 6" From Fill Line				"	9-1	Guard Tank Bottom	Check of Guard Tank Temperature
82	TC-82	FL-T	Fill Line, 6" Above Test Tank Lid				"	9-1	"	Evaluation of Fill Line Heat Leak

All dimensions are in inches

Table 9-1. Measurement Description Summary (Continued)

Note: ** Azimuth is measured from test tank fill line, * Inclination, altitude and radius are measured from center of tank.

Channel No.	Identification: Instr.	Identification: Location	Physical Location*: Component	** AZM(0)	*INC(0) * ALT(in)	*RAD (in)	Type of Instr.	Fig. No.	Reference Junction	Measurement Description
83	TC-83	FL-B	Fill Line, 2" Above Test Tank Lid				CHR/CON	9-1	Guard Tank Bottom	Evaluation of Fill Line Heat Leak
84	TC-84	VL-T	Vent " 6" " " " "				"	9-1	"	" Vent " " "
85	TC-85	VL-B	" " 2" " " " "				"	9-1	"	" " " " "
86	TC-86	SR-T	Support, 1/2" From Turn Buckle End				"	9-1	"	" Support Rod Heat Leak
87	TC-87	SR-B	" " " " " " (nearest vent line)				"	9-1	"	" " " " "
88	TC-88	TT-L	Tank Lid, 2" From Rim				"	9-1	"	Sink Temp. of Tank Lid
89	TC-89	ST-A	Top Surface of Shrouc Top	0		37	"	9-3	"	Sink Temp. of Shroud
90	TC-90	ST-B	" " " "	120		37	"	9-3	"	"
91	TC-91	ST-C	" " " "	240		37	"	9-3	"	"
92	TC-92	SS-1A	Outside Surface of Shroud Wall	0	Alt = +24"		"	9-3	"	"
93	TC-93	SS-1B	" " " "	120	Alt = +24"		"	9-3	"	"
94	TC-94	SS-1C	" " " "	240	Alt = +24"		"	9-3	"	"
95	TC-95	SS-2A	" " " "	0	Alt = -30"		"	9-3	"	"
96	TC-96	SS-2B	" " " "	120	Alt = -30"		"	9-3	"	"
97	TC-97	SS-2C	" " " "	240	Alt = -30"		"	9-3	"	"
98	TC-98	SB-1	Bottom Surface of Shroud Bottom	0		0	"	9-3	"	"
99	TC-99	SB-2A	" " " "	0		24	"	9-3	"	"
100	TC-100	SB-2B	" " " "	120		24	"	9-3	"	"
101	TC-101	SB-2C	" " " "	240		24	"	9-3	"	"
102	TC-102	SB-3	" " " "	0		49	"	9-3	"	"
103	TC-103	BT-1	Top Baffle Alt. = 0.0 in.	0		32.25	"	9-4	"	Evaluation of Radiation Effects
104	TC-104	BT-2A	" " " -0.5 in.	0		40	"	9-4	"	"
105	TC-105	BT-2B	" " " -0.5 in.	120		40	"	9-4	"	"
106	TC-106	BT-2C	" " " -0.5 in.	240		40	"	9-4	"	"
107	TC-107	BM-1	Center Baffle Alt. = 0.0 in.	0		34.5	"	9-4	"	"
108	TC-108	BM-2A	" " " -0.5 in.	0		41	"	9-4	"	"
109	TC-109	BM-2B	" " " -0.5 in.	120		41	"	9-4	"	"
110	TC-110	BM-2C	" " " -0.5 in.	240		41	"	9-4	"	"
111	TC-111	BM-2D	" " " +0.5	0		41	"	9-4	"	"

All dimensions are in inches

Table 9-1. Measurement Description Summary (Continued)

Note: ** Azimuth is measured from test tank fill line, * Inclination, altitude and radius are measured from center of tank.

Channel No.	Identification: Instr.	Identification: Location	Physical Location *: Component	** AZIM(0)	*INC(0) * ALT(in)	*RAD (in)	Type of Instr.	Fig. No.	Reference Junction	Measurement Description
112	TC-112	BM-3	Center Baffle Alt. = 0.0"	0		47	CHR/CON	9-4	Guard Tank Bottom	Evaluation of Radiation Effects
113	TC-113	BB-1	Bottom " " 0.0"	0		36.5	"	9-4	"	"
114	TC-114	BB-2A	" " " +0.5"	0		42	"	9-4	"	"
115	TC-115	BB-2B	" " " +0.5"	120		42	"	9-4	"	"
116	TC-116	BB-2C	" " " +0.5"	240		42	"	9-4	"	"
117	TC-117	TT-1E	Outer Surface of Test Tank	0	+60		"	9-2	Bottom of Test Tank at TT-8F&G	Test Tank Wall Temperature
118	TC-118	TT-3E	" " " " "	0	0		"	9-2	"	"
119	TC-119	TT-5E	" " " " "	0	-45		"	9-2	"	"
120	TC-120	TT-8E	" " " " "	0	-90		"	9-2	"	"
121	TC-121	TPS-1H	Bottom Surface of TPS	0		0.0	"	9-5	TPS - 1J & K	TPS Bottom Temperature
122	TC-122	TPS-2H	" " "	0		6.5	"	9-5	"	"
123	TC-123	TPS-3H	" " "	0		13.0	"	9-5	"	"
124	TC-124	TPS-4H	" " "	0		18.0	"	9-5	"	"
125	TC-125	TPS-5H	" " "	0		25.5	"	9-5	"	"
126	TC-126	TPS-6H	" " "	0		30.0	"	9-5	"	"
127	TC-127	TPS-7H	" " "	0		34.5	"	9-5	"	"
128			Not Used							
129			"							
130			"							
131	EXC-T1	-	-							Excitation Voltage (to reduce data)
132	PR-132	TT-8F	Outer Surface Test Tank	0	-89		Plat-Res	9-2		Temp. of Test Tank Wall - Bottom
133		TT-8G	" " " "	180	-89		"	9-2		" " " " "
134	PR-134	GT-B	Guard Tank Bottom, 1" From Fill Line				"	9-1		" Guard " " "
135	PR-135	GT-C	" " " " " " "				"	9-1		" " " " "
136	PR-136	TPS-1G	Bottom Surface - TPS	0		0.5	"	9-5		
137	PR-137	TPS-1K	" " "	180		0.5	"	9-5		
138		ICE-IN	Inner ICE Container							Check of Inner Ice Container Temp.
139			Not Used							
140	EXCT2									Excitation Voltage

All dimensions are in inches

Table 9-1. Measurement Description Summary (Continued)

Note: ** Azimuth is measured from test tank fill line, * Inclination, altitude and radius are measured from center of tank

Channel No.	Identification: Instr.	Identification: Location	Physical Location *: Component	** AZIM(0)	*INC(0) * ALT(in)	*RAD (in)	Type of Instr.	Fig. No.	Reference Junction	Measurement Description
141	PR-141	TT-L1	Test Tank Volume 98%				Plat. Res.	9-2		Temp. and Liquid Level of Test Tank
142	PR-142	TT-L2	" " " 96%				"	9-2		"
143	PR-143	TT-L3	" " " 94%				"	9-2		"
144	PR-144	TT-L4	" " " 92%				"	9-2		"
145	PR-145	TT-L5	" " " 90%				"	9-2		"
146	PR-146	TT-L6	" " " 75%				"	9-2		"
147	PR-147	TT-L7	" " " 50%				"	9-2		"
148	PR-148	TT-L8	" " " 25%				"	9-2		"
149	PR-149	TT-L9	" " " 10%				"	9-2		"
150			Not Used							
151	-	Exc 5vdc								Excitation
152		TPS POS	Therm. Payload Simulator				Linear Potenti-ometer	9-7		Indicates Position of TPS
153		TT-PRES	Test Tank				Strain	9-7		Indicates Test Tank Pressure
154	-	GT-PRES	Guard Tank				"	9-7		Indicates Guard Tank Pressure
155		FLOW-PRES	Flowmeter Inlet Pressure				"	9-7		Flowmeter Inlet Pressure
156		ATM PRES	Atmosphere				"	9-7		Atmospheric Pressure
157		TT/GTΔP	Test Tank/Guard Tank				"	9-7		Test Tank/Guard Tank ΔP
158			Not Used							
159			Not Used							
160			Not Used							
161		TT-PRES	Test Tank				Baratron			Monitor Change in Tank Pressure
162		C.V. 1	Not Used							
163		C.V. 2	Not Used							
164		TT-FLOW	TSI Flowmeter				Hot Film	9-7		LH_2 Boiloff Rate Measurement (1A)
165		"	TSI Flowmeter				" "	9-7		" " " " (2G)

All dimensions are in inches

Table 9-1. Measurement Description Summary (Concluded)

Note: ** Azimuth is measured from test tank fill line, * Inclination, altitude and radius are measured from center of tank. All dimensions are in inches

Channel No.	Identification: Instr.	Identification: Location	Physical Location*: Component	Physical Location*: ** AZIM(0)	Physical Location*: *INC(0)* ALT(in)	Physical Location*: *RAD (in)	Type of Instr.	Fig. No.	Reference Junction	
166		TT-FLOW	TSI Flowmeter				Hot Film	9-7		LH_2 Boiloff Rate Measurement (3G)
167		SHR. VAC	Shroud				Ion Tube	9-6		Shroud Vacuum in Torr
168		SHR. VAC	Shroud				Ion Tube			Decade - Multiplier
169		CHAM-VAC	Vacuum Chamber				Ion Tube			Chamber Vac. Press (Torr)
170		CHAM-VAC	Vacuum Chamber				Ion Tube			" " " (Decade)
171		CHAM-VAC	Vacuum Chamber				TC Tube			" " " (TC)
172		TT-HEAT	Test Tank Heater							Voltage of Test Tank Heater
173		TT-HEAT	" " "							Amps of " " "
174			Not Used							
175			Not Used							
176			Not Used							
177		GT-L1	Guard Tank Vol. 80%				PL. Res.	9-1		Temp. & Liq. Level of Guard Tank
178		GT-L2	Guard Tank Vol. 60%				"	9-1		" " " " "
179		GT-L3	Guard Tank Vol. 40%				"	9-1		" " " " "
180		GT-L4	Guard Tank Vol. 20%				"	9-1		" " " " "
181	TC-181	ST-X1	Shroud Lid	0	-	35.0	Chr/Con	9-3	Outside LN_2Bath	Thermal gradient in shroud lid
182	TC-182	ST-X2	Shroud Lid	0	-	33.0	" "	9-3	"	Thermal gradient in shroud lid
183	TC-183	TPS-X1	TPS Top Surface	0	-	32.5	" "	9-5	"	Thermal gradient in TPS
184	TC-184	TPS-X2	TPS Top Surface	0	-	26.6	" "	9-5	"	Thermal gradient in TPS
185	TC-185	TPS-X3	TPS Top Surface	0	-	9.0	" "	9-5	"	Thermal gradient in TPS

All dimensions are in inches

9.2 MEASUREMENTS AND ACCURACIES

9.2.1 THERMOCOUPLES - All thermocouples were fabricated from Chromel/Constantan teflon insulated thermocouple wire. Thirty-six gage wire was used on the MLI, on the test tank outer skin, and on the upper surface of the TPS. All other measuring thermocouples were fabricated from 28 gage or heavier wire. All of the MLI thermocouples (Channels 1 thru 58, Ref. Table 9-1) were fabricated with the 36 gage wire extending from the measuring junction to outside of the shroud where they were spliced to a 22 gage Chromel/Constantan chamber harnesses that connected them to the vacuum chamber passthrough. The seven thermocouples on the upper surface of the TPS (Channels 59 through 65 Table 9-1) were fabricated with the 36 gage wire extending from the measuring junction to a point approximately 0.305 m (12 in) from the edge of the TPS where they were spliced to an intermediate Chromel/Constantan harness fabricated from 28 gage wire that led to the outside of the shroud. The intermediate extension wire was then spliced to the 22 gage chamber harness leading to the chamber passthrough. A large but unknown part of the ambient to 22K (40R) thermal gradient existed in this 28 gage extension wire. With the TPS at LH_2 temperature this resulted in a maximum lower temperature reading in these channels (59-65) of approximately 4.4K (8R) when compared with the readings of thermocouples 183, 184, and 195 (figure 9-5 and Table 9-1). These three thermocouples were added to the top surface of the TPS when the vacuum chamber was open between the thermal performance testing of the tank installed MLI and the customized MLI thermal performance test. With the TPS at approximately 289K (520R) the approximate errors were as follows:

TPS-Radius m (in)	0.23 (9)	0.66 (26.6)	0.83 (32.5)
+ Reading K (R)	2.1 (3.8)	1.5 (2.7)	0.94 (1.7)
- Reading K (R)	0.0 (0.0)	0.28 (0.5)	1.06 (1.9)

These values were obtained by comparing the readings of thermocouples No. 60/61, 63 and 64/65 with the readings of thermocouples 185, 184 and 183 at the comparable location during the customized MLI thermal performance test.

All the thermocouples with Channel Numbers 1 thru 80 and 181 thru 185 had their Chromel/copper and Constantan/copper reference junctions located outside the vacuum chamber in a liquid nitrogen bath. All the thermocouples with Channel Nos. 81 thru 127 (Table 9-1) were referenced to the bottom surface of the test tank, the guard tank, or the TPS and copper wire run out of the chamber. The primary objective of referencing these thermocouples inside the vacuum chamber was to reduce errors by having the large ambient to liquid hydrogen temperature gradient in the pure element (copper) wires instead of in the alloy (Chromel and Constantan) wires. Since only one junction in each channel can be grounded, these thermocouples were installed with the reference junctions electrically insulated from the metal surfaces with one mil Mylar tape. At the prevailing temperature, 21K (38R) and pressure 1.33×10^{-5} N/m^2 (10^{-7} torr) in the shroud, this electrical insulation turned out to have an extremely low thermal conductance. This allowed the thermal conduction in the chamber harness wires to heat the reference junctions enough to make these channels unusable. Between the thermal performance of the test tank installed MLI and the customized MLI thermal performance test, thermocouples No. 92 thru 116 were rewired with their reference junctions outside the vacuum chamber in the liquid nitrogen bath, after which they read correctly. At this time TC No. 68 thru 71 (Table 9-1) were disconnected since the number of Chromel and Constantan pins in the chamber wall pass-through was limited.

During the warm-up following the customized MLI tests, all the thermocouples were monitored and there was an indication that channels 36, 48, 52, 102 and 115 might not have maintained good thermal contact. After the warm-up, the circuits were resistance checked and channels 10, 33 and 97 were found to be open circuit or shorted. Except as noted, all the thermocouples had a usable range of 232K (418R) to 478K (860R). The absolute accuracies were:

22K (40R) to 61K (110R)	±1.7K (3R)
61K (110R) to 117K (210R)	±1.1K (2R)
117K (210R) to 200K (360R)	±0.55K (1R)
200K (360R) to 533K (960R)	±0.28K (0.5R)

The repeatability of relative accuracy for any one channel was:

22K (40R) to 61K (110R)	±1.7K (3R)
61K (110R) to 117K (210R)	±1.1K (2R)
117K (210R) to 200K (360K)	±0.55K (1R)
200K (360R) to 533K (960R)	±0.28K (0.5R)

9.2.2 RESISTANCE THERMOMETERS - All the resistance thermometers were Rosemount Engr. Co. Model 118F or 118L platinum film resistors. Each resistor was wired in one of three series circuits as follows:

a. The first circuit consisted of the nine combination liquid level/temperature probes inside the test tank.

b. The second circuit consisted of the four liquid level probes in the guard tank.

c. The third circuit consisted of seven probes, two each of the bottom surface of the test tank, guard tank, and the TPS, and one on the surface of the reference volume in the inner ice bath.

The nine probes inside the test tank (Channels 141 thru 149) and the four probes inside the guard tank (Channels 177 thru 180) were fluid measurements and had the following ranges and accuracy. As temperature probes, their range was 19K (35R) to ambient with an absolute accuracy of ±0.055K (0.1R) from 19K (35R) to 33K (60R) and ±0.03K (0.05R) from 33K (60R) to ambient. As liquid levels their range was go/no go with an accuracy of ±0.00254 m (0.1 in). The seven probes in the third circuit (Channels 132 thru 138) were all skin probes and all except the reference volume temperature were inside the shroud. As with the thermocouple reference junctions, the prevailing temperature, 22K (40R) and pressure 1.33×10^{-5} N/m^2 (10^{-7} torr) inside the shroud resulted in a low thermal conductance between the ceramic coating on the probe and the metal surface. Because of this, thermal conduction through the instrumentation lead wires made these (Channel 132 to 138) unusable.

9.2.3 PRESSURE - Six pressure data channels were recorded:

Channel No.	Range, Full Scale	Measurements
153	0-137.88 kN/m^2 (0-20 PSIA)	Test Tank Ullage (Secondary)
154	0-172.35 kN/m^2 (0-25 PSIA)	Guard Tank Ullage
155	0-241.29 kN/m^2 (0-35 PSIA)	Flow Meter Inlet
156	0-172.35 kN/m^2 (0-25 PSIA)	Atmosphere
157	±34.5 kN/m^2 (± 5 PSID)	Test Tank/Guard Ullage Differential
161	±0.133 kN/m^2* (±1 TORR)	Test Tank Ullage (primary)

* Relative to the reference volume pressure.

Channels 153 thru 157 were recorded using Statham Model PA822 bonded film strain gage pressure transducers with a total system absolute accuracy of ± 0.5% FS and a repeatability or relative accuracy of ±0.1% FS. The primary test tank ullage pressure measurement (Channel No. 161) was the output from the MKS Baratron Model 145 AH-1 Capacitance Manometer as described in Section 8.2. This unit has an absolute accuracy, as stated by the manufacturer, of 1.33×10^{-3} N/m^2 (1×10^{-5} mm hg) and a repeatability of 1.33×10^{-4} N/m^2 (1×10^{-6} mm hg).

9.2.4 VACUUM - The chamber vacuum was measured using a Veeco Model RG-840 ionization gage controller and a Veeco Model RG 45 ionization gage tube. The gage tube filament was operating continuously throughout the test and the tube was degassed approximately once a day. In the range from 1.33×10^{-1} N/m^2 to 1.33×10^{-5} N/m^2 (1×10^{-3} to 1×10^{-7} torr), the accuracy was better than ± 10% of the scale reading.

The shroud vacuum was measured using a Veeco Model RG-21A ionization gage controller with a Veeco Model RG 45 ionization gage tube. This gage tube filament was turned on only while the gage was being read, and the accuracy was therefore degraded to an estimated ± 30% of the scale reading. The recorder outputs on these two gage controllers were not connected to the digital recorder (Channels 167 thru 171) but were read and logged manually. The chamber pressure was read at 30 minute intervals throughout the entire test. The shroud pressure was read at 30 minute intervals during the first null test, then roughly daily for the remainder of the testing.

9.2.5 FLOW - The test tank boiloff flow measurements were taken with a Thermo Systems Inc. Model 1053B-A1 constant temperature anemometer (Channels 164 thru 166). A sudden eight to one increase in the test tank boiloff during the first null test (Paragraph 10.1.3) destroyed the sensor and the back up unit was not available. At this time a water displacement flow measurement was substituted using a five gallon glass water bottle inverted over a stainless steel open top tank as shown in Figure 9-7 and 9-8. The H_2 boiloff flowed continuously through the bubble tube which could be slid back and forth approximately one inch thereby allowing the gas bubbles to rise either inside or outside the neck of the bottle. After each reading, the gas siphon and aspirator were used to remove the gas and refill the bottle with water. The plexiglas plate supporting the bottle was not quite horizontal with one edge 0.005 m (0.2 in) higher than the other. The bottle surface of this plate was the reference for the tank water level which was maintained so that the bottom of the plate was partially but not completely wetted. A Meylan stop watch (±0.1 minute) was used to time the interval between moving the bubble tube under the bottle neck and when the first bubble broke outside the bottle neck. The water volume of the bottle (±0.05%) was determined by weighing the bottle empty and then filled with distilled water at 295.6K (532R). The temperature of the water in the tank and the air surrounding the bottle were measured ±0.55K (1.0R). Since the "stay time" of the gas in the bottle was large (15 to 60 min), it was very nearly in equilibrium with the outside air temperature. Using a correction factor of 532/1.8K (532/R), the error is less than 0.3%. Two other sources of error considered were the solubility of GH_2 in H_2O and the creation of H_2O vapor in the dry GH_2. At 294K (530R) both these effects could cause a maximum error of less than 2%, however, since they are of approximately equal magnitude but opposite sign, their total error will probably be much less than 1%.

9.2.6 POWER - The test tank heater power was determined from separate recordings of the voltage across the heater leads in the test tank (Channel 172), and the voltage drop across a 1.10 ohm shunt in series with the heater (Channel 173).

9.2.7 POSITION - The TPS position (Channel 152) was recorded using a Waldale Research Co. Model LTD-160-140 linear motion transducer with a range of 0 to 1.27m (50 in). As installed in the setup the total system accuracy was ±0.0013m (0.05 in).

9.3 DATA ACQUISITION

Test data for this MLI test program was recorded by using a Dymec digital recorder. Raw analog data from each measuring device was sampled by the Dymec at various rates depending upon the test conditions and data requirements. Data was recorded as raw voltages printed out on paper tape. The decks of paper tape were labeled at the beginning and end of each test period and assigned a deck number corresponding to a numerical listing recorded in the test engineering data log of test operations. The Dymec paper tape decks were then transported from Test Site B to the Kearny Mesa Plant.

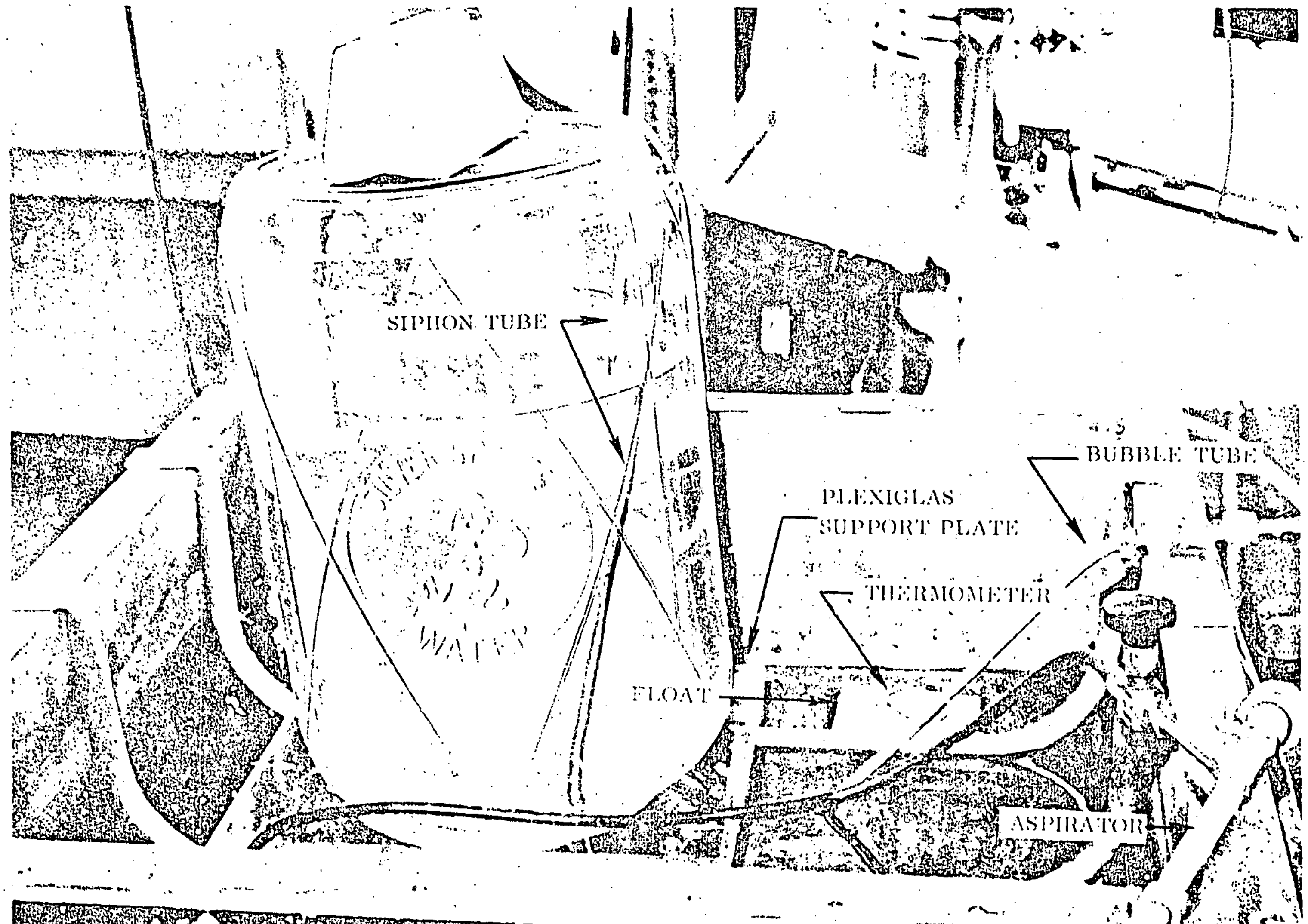

Figure 9-7. Water Displacement Flow Setup

14-9490

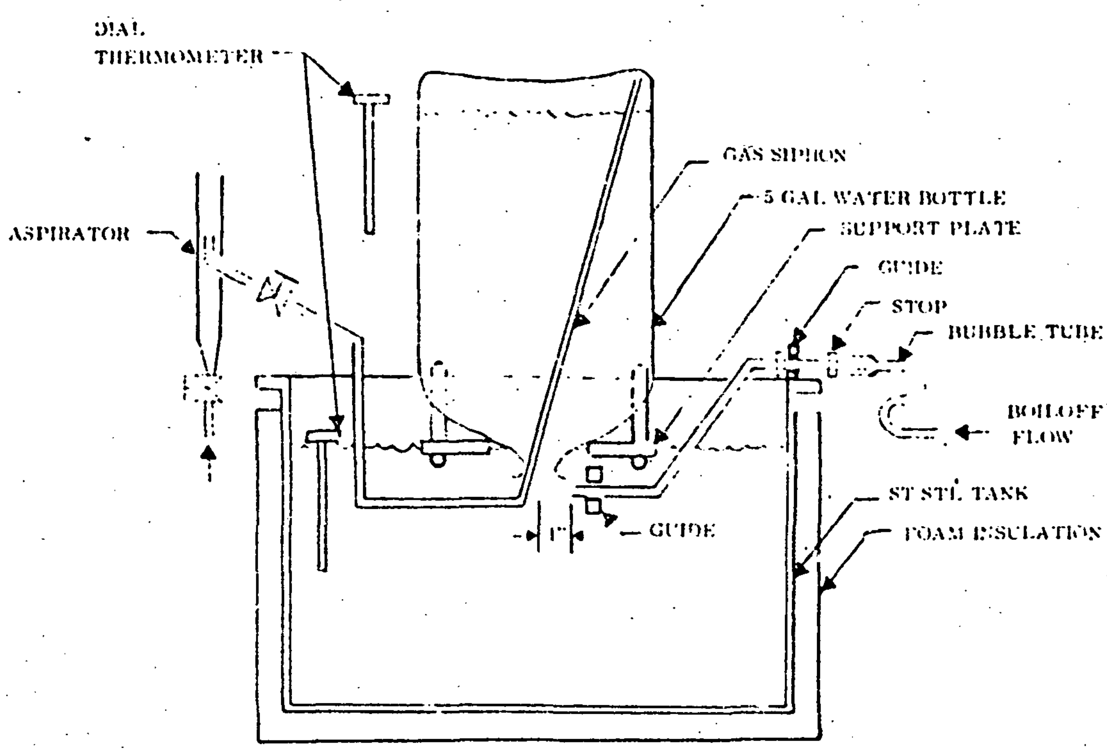

Figure 9-8. Water Displacement Flow Setup

10

TESTING

The test program included three major test categories, (1) null testing, (2) thermal testing of the tank installed MLI system, and (3) thermal testing of the customized MLI configuration. Table 10-1 outlines the objectives and conditions of the test program. The null tests are systems operation functional tests. These tests were performed to verify satisfactory operation of all hardware components including cryoshroud, thermal payload simulator (TPS), test tank pressure control system and guard tank and to determine extraneous heat flow into the test tank. The thermal payload simulator was not insulated during these tests.

The purpose of the tank installed MLI test was to determine the thermal performance of the tank insulation at a TPS temperature of 289K (520R). The thermal payload simulator surface remained uninsulated.

The objective of the customized MLI test was to determine the thermal performance of the tank insulation at a TPS temperature of 289K (520R) and three different distances (Table 10-1) between tank and TPS. The TPS was insulated.

Figure 10-1 is a simple schematic which shows the test article installed within the cryoshroud. The test facility is discussed in Section 8. The test article consisted of the test tank (Sections 2 and 3), associated insulation (Section 7), tank support system (Section 2.2 and 3.2), guard tank (Section 5.5), fill/drain and vent lines (Section 5.5) between test and guard tank, and the double seal leakage pumpout line (Section 2.1.1). A detailed schematic of the test article, installed within the cryoshroud assembly (Section 5) including TPS (Section 4) is shown in Figure 10-2. The

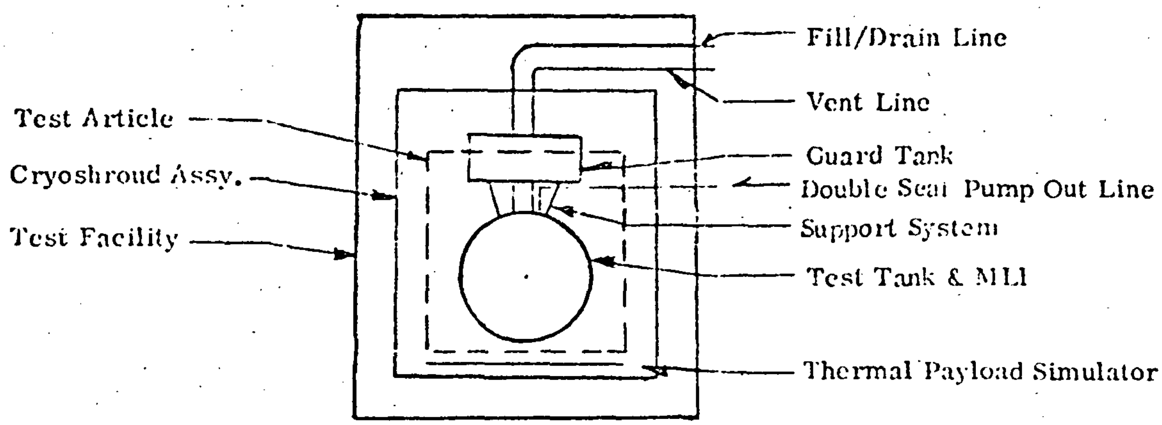

Figure 10-1. Test Set-Up Definition

Table 10-1. Test Objectives and Conditions

Test Category	Objectives	Test Conditions
1. Null Test	1. Establish the correct functioning of the tank pressure control system. 2. Verify required cryoshroud baffle and TPS temperatures. 3. Correlate between measured boiloff and a known heat input internal to the tank obtained with the heater element. 4. Determine heat flow into the test tank through supports, instrumentation leads and tank penetrations by radiation and/or conduction from the cryoshroud and baffles.	1. Liquid hydrogen in test tank. 2. Environmental vacuum pressure less than 1.33×10^{-4} N/m^2 (1×10^{-6} Torr). 3. Test tank pressure within ± 1.38 N/m^2 (0.0002 psia) of set point 4. Test tank insulated. 5. Cryoshroud and baffle surface temperature less than 27.8K (50 R). 6. TPS uninsulated. 7. TPS/test tank spacing 0.457 m (18 in). 8. TPS temperature less than 27.8K (50R). 9. Test tank heater power input as indicated in Section 10.1.1.
2. Tank Installed MLI Sys.	1. Determine thermal performance of the MLI system installed on the tank using a TPS temperature of 289K (520R) without MLI on the TPS.	1. Same as Null Test steps 1 through 7. 2. TPS temperature at 289K (520R). 3. Test tank heater power input 0.2 watts.
3. Customized MLI Configuration	1. Determine thermal performance of the customized MLI at 289K (520R) with TPS mounted MLI and 0.152 m (6 in) distance between tank and TPS. 2. Determine thermal performance of the customized MLI at 289K (520R) with TPS mounted MLI and 0.305 m (12 in) distance between tank and TPS. 3. Determine thermal performance of the customized MLI at 289K (520R) with TPS mounted MLI and 0.457 m (18 in) distance between tank and TPS.	1. Same as Null Test steps 1 through 5. 2. TPS insulated. 3. TPS temperature at 289K (520R). 4. TPS/test tank spacing as shown in objectives. 5. Test tank heater power input 0.2 watts.

Note: All fill and vent lines are insulated with 10 layers of MLI.

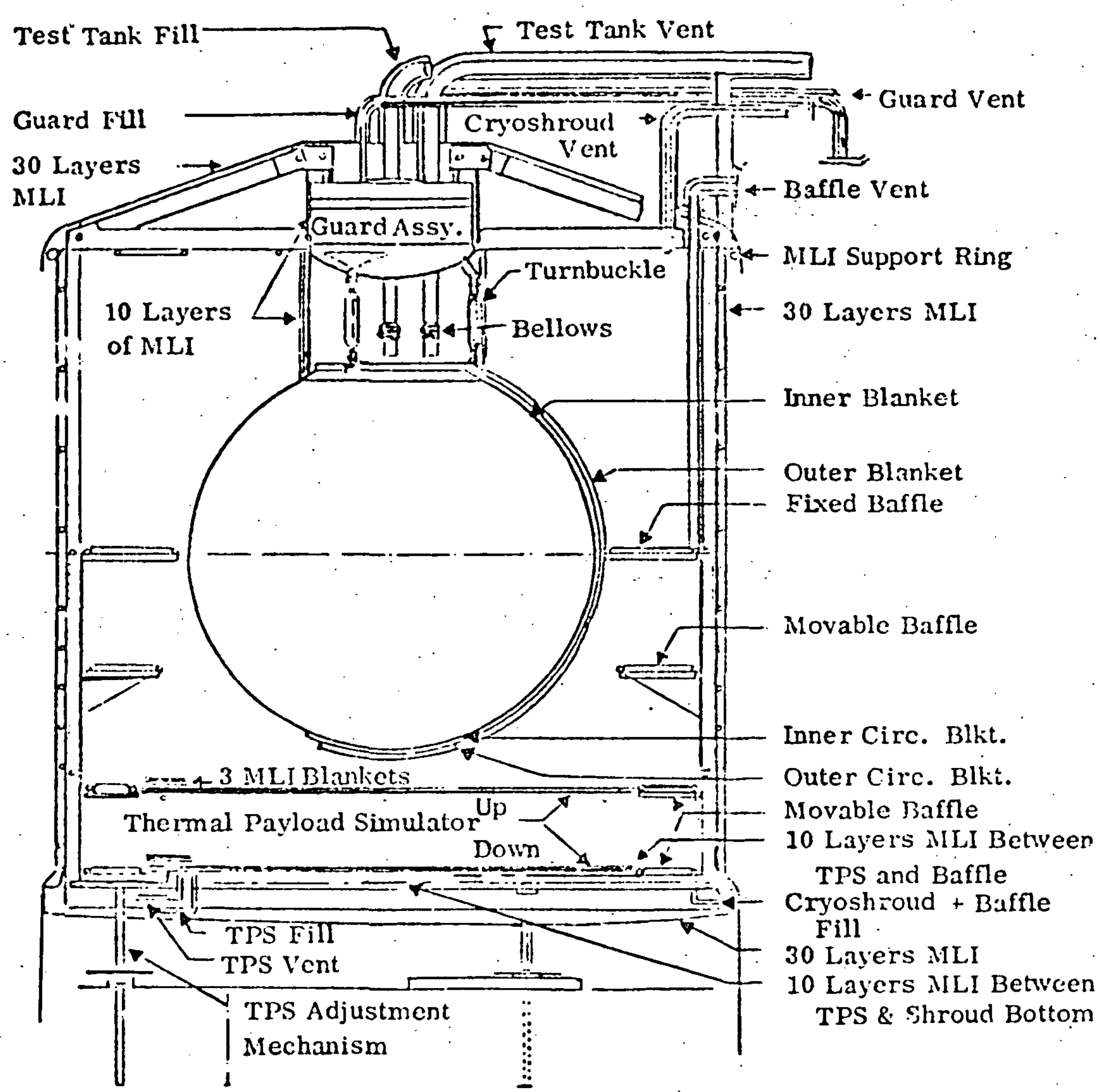

Figure 10-2. Schematic of Test Article and Cryoshroud Assembly

assembly of the cryoshroud with the baffles, guard tank and the test tank was discussed in Section 5.6.1. The assembly sequence of the test setup was as follows:

1. Installation of the MLI on test tank.

2. Installation of the instrumentation on test tank assembly.

3. Installation of plumbing on baffle/shroud-side assembly and leak checking of the assembly.

4. Installation of the instrumentation on baffle/shroud-side assembly, shroud bottom, and thermal payload simulator.

5. Mating of TPS to baffle/shroud-side assembly.

6. Installation of the MLI on bottom of TPS.

7. Mating of shroud-bottom to TPS/baffle/shroud-side assembly (shroud assembly).

8. Installation of plumbing on shroud assembly and leak checking of the assembly.

9. Mating of test tank assembly to shroud assembly (test assembly).

10. Installation of test assembly in chamber and mounting of support legs.

11. Installation of plumbing between test assembly and chamber, and leak checking of assembly.

12. Installation of baffle and TPS positioning mechanism.

All liquid hydrogen fill and vent lines between the test configuration and the vacuum chamber were wrapped with ten layers of MLI fastened with aluminized Mylar tape. The top of the guard tank and the top, sides, and bottom of the cryoshroud were insulated with 30 layers of MLI. As shown in Figure 10-2, the MLI on top of the shroud and guard tank was supported directly by the guard tank and the angle of braces, and overlapped the sidewall MLI approximately 0.25 m (10 in). The sidewall MLI was sewn onto a tubular support structure approximately 0.05 m (2 in) from the outer edge of the shroud cover. It was applied to the sidewall and extended 0.30 m (12 in) below the shroud bottom. The shroud bottom MLI was supported 0.10 m (4 in) below the bottom surface of the shroud by a layer of wire mesh stretched between the shroud support legs. Figure 10-3 presents a photo of the test article prior to installation into the vacuum chamber.

The test tank and guard tank back pressure control system, instrumentation and auxiliary hardware including the pneumatic and electric valve control systems were checked out. The plumbing lines of the test apparatus were leak checked with the vacuum chamber open and the chamber closed. Several leaks were found and repaired. An operational check of the total system was performed after an initial pumpdown of the vacuum chamber.

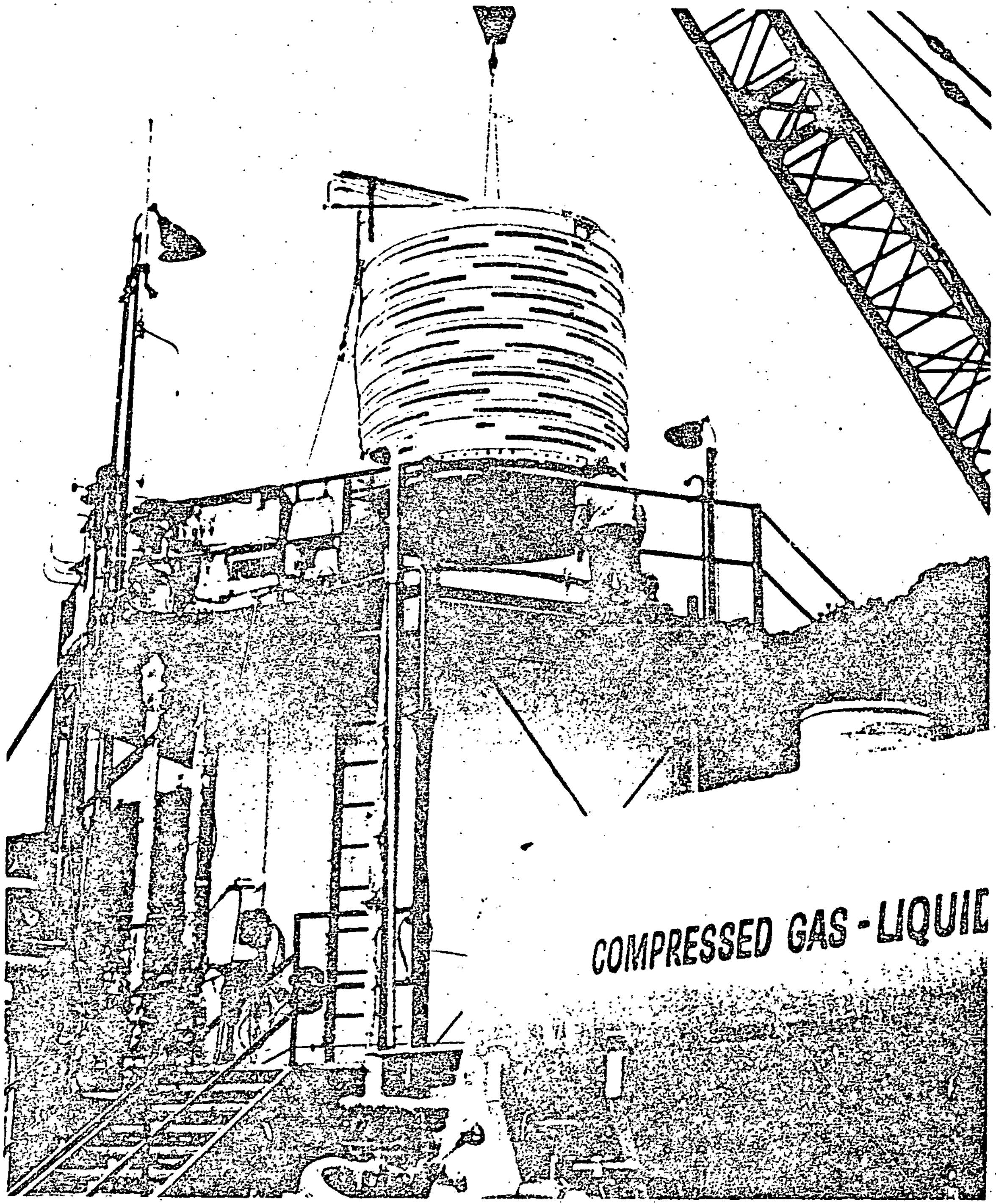

1 4 6 9 8 1

Figure 10-3. Cryoshroud Assembly Ready for Installation Into the Vacuum Chamber

10.1 NULL TESTING

Objectives and conditions of the null testing are shown in Table 10-1. The test program was initiated on 30 May 1975. The following sections present the null test procedures, test specimen preparation, test results and evaluation of the results.

10.1.1 NULL TEST PROCEDURES - The null test procedures were as follows:

1. Adjustment of test tank/TPS spacing to 0.46 m (18 in).
2. Closing of environmental vacuum chamber.
3. Evacuation of environmental vacuum chamber to 6.65×10^{-3} N/m^2 (5×10^{-5} torr).
4. Purging of vacuum chamber with GHe.
5. Purging of test tank with hot GN_2 for 6 hours at a temperature of 333K (600R) maximum.
6. Evacuation of environmental vacuum chamber to 6.65×10^{-3} N/m^2 (5×10^{-5} torr).
7. Supplying of cold trap with LN_2 and evacuation of chamber to below 1.33×10^{-4} N/m^2 (1×10^{-6} torr).
8. Cooling of baffles, cryoshroud, and TPS surface temperatures below 27.8 K (50R) and maintaining of these temperatures.
9. Filling of test tank with LH_2.
10. Approach of thermal equilibrium at a constant test tank pressure level. Equilibrium conditions are achieved when the temperature readings of test tank thermocouples TC-3, -11, and -31 (Figure 9-2) vary not more than $\pm$ 0.56K ($\pm$ 1F) in 10 hours and the LH_2 boiloff rate changes not more than 0.5% per hour.
11. Maintaining of the environmental chamber pressure at less than 1.33×10^{-4} N/m^2 (1×10^{-6} torr).
12. Maintaining of baffle, cryoshoud, and TPS surface temperatures at less than 27.8K (50R).
13. Verification of a hydrogen boiloff rate from the test tank of less than 0.00024 Kg/hr (0.00052 lb/hr) which correlates with the NASA required heat leak of less than 0.0293W (0.1 BTU/hr).

14. Application of 0.2W (0.683 BTU/hr) to test tank heater, allowing the tank to reach equilibrium and checking that the total boiloff rate (heat input plus leakage) of 0.00185 Kg/hr (0.00408 lb/hr) agrees with the known energy input. Boiloff rate corresponding to the 0.2W heat input is 0.00161 Kg/hr (0.00356 lb/hr).

15. Repeating of Step 14 with the following heat inputs to the test tank heater:

<u>Heat Input 0.5W (1.7065 BTU/hr)</u>	
Total predicted boiloff rate:	0.00428 Kg/hr (0.00941 lb/hr)
Boiloff rate corresponding to 0.5W:	0.00404 Kg/hr (0.00889 lb/hr)
<u>Heat input 0.4W (1.3652 BTU/hr)</u>	
Total predicted boiloff rate:	0.00347 Kg/hr (0.00763 lb/hr)
Boiloff rate corresponding to 0.4W:	0.00323 Kg/hr (0.00711 lb/hr)
<u>Heat input 0.2W (0.683 BTU/hr)</u>	
Total predicted boiloff rate:	0.00185 Kg/hr (0.00408 lb/hr)
Boiloff rate corresponding to 0.2W:	0.00161 Kg/hr (0.00356 lb/hr)

10.1.2 TEST SPECIMEN PREPARATION - A series of purging and evacuation cycles were initiated to remove condensible gases from the MLI and vacuum facility. Pump down of the chamber was initiated on Friday, 30 May 1975, utilizing the mechanical pumping system. Pumping was continued over the weekend. Chamber pressure was 199.5 N/m^2 (1.5 torr) on Monday, 2 June 1975. It was necessary to back fill the chamber with air to repair a leak in the second stage of the diffusion pump. Mechanical pumping was resumed after completion of the repair work. The chamber pressure was 13.3 N/m^2 (0.1 torr) on 3 June 1975. The main diffusion pump was turned on and reduced the pressure to 5.32×10^{-3} N/m^2 (4×10^{-5} torr) within 3 hours. At this time number 2 mechanical pump failed. The chamber was locked up until 4 June 1975 while the pump was repaired. The chamber was back filled with a mixture of 50% air and 50% helium. After a renewed pump down to 33.25 N/m^2 (0.25 torr), gaseous nitrogen was introduced through the fill line into the test tank at a temperature of 344K (620R). The hot purging operation was continued for 6 hours. On 5 June 1975, the chamber was evacuated and back filled three times with gaseous nitrogen to a pressure of 266 N/m^2 (2.0 torr). Utilizing the diffusion pumping system on 6 June 1975, heavy outgassing of the system was observed in the pressure range between 4.65×10^{-2} and 6.92×10^{-3} N/m^2 (3.5×10^{-4} and 5.2×10^{-5} torr). During the weekend days, June 7 and 8, the chamber was left at a vacuum pressure 39.9 N/m^2 (0.3 torr).

On Monday, 9 June 1975, mechanical and diffusion pumping reduced the pressure to 2.39×10^{-3} N/m^2 (1.8×10^{-5} torr) when chilling of the cold trap was initiated. The Cosmodyne supply tank, the catch tank, cryoshroud and baffles were filled with LH_2 at an approximate vacuum pressure of 1.33×10^{-4} N/m^2 (1.0×10^{-6} torr). Thermal payload simulator (TPS), guard tank and test tank were supplied with LH_2 on 10 June 1975. At the beginning of filling the test tank the pressure was 2.39×10^{-5} N/m^2 (1.8×10^{-7} torr) and 1.73×10^{-5} N/m^2 (1.3×10^{-7} torr) in the vacuum chamber and within the cryoshroud respectively. The pressure within the recovery tank was set at 34.7 kN/m^2 (5 psig). Filling of the test tank was intentionally performed over a 4 hour and 20 minute period to avoid leaks caused by the cooldown process. The pressures of the vacuum chamber and shroud at the end of the filling operation (98% full) were 1.73×10^{-5} N/m^2 (1.3×10^{-7} torr) and 10.4×10^{-6} N/m^2 (7.8×10^{-8} torr), respectively. Pressures of the test tank and guard tank were set 113.08 kN/m^2 (16.4 psia) and 114.11 kN/m^2 (16.55 psia). A pressure differential of 1.03 kN/m^2 (0.15 psid) between guard tank and test tank was maintained with a tolerance of 0.344 kN/m^2 (0.05 psid) through the entire test operation.

During June 11 the LH_2 boiloff rates were still high therefore no flow rate data were recorded.

10.1.3 NULL TEST RESULTS - The actual test activity started on June 12, 1975. The null test was conducted over a period of 218 continuous test hours. Boiloff flow rates and temperature readings of MLI thermocouples TC-3, TC-11, TC-31 (Table 9-1 or Figure 9-2) and TC-62 (Table 9-1 or Figure 9-5) are plotted in Figures 10-4, Sheet 1 through 3. At 0-time the guard tank was 80% full. An unexpected rise of the vacuum chamber pressure to 1.33×10^{-2} N/m^2 (1×10^{-4} torr) after 12 hours reduced the temperature of the test tank insulation by gaseous conduction to near the liquid hydrogen temperature level (Figure 10-4, Sheet 1). The sudden rise in pressure was caused by a loss of oil in the diffusion pump. Fifteen hours after 0-time the vacuum chamber pressure was recovered. The test and guard tanks were refilled.

10.1.3.1 Null Test No. 1, Zero Power Input - The first null test was performed to establish the extraneous heat leak into the test article. The tank pressure was controlled within ±0.68947 N/m^2 (± 0.0001 psia) of the set point. A typical plot of the tank pressure control is shown in Figure 8-9. The vacuum pressure achieved within the cryoshroud was approximately 1×10^{-7} torr. The thermal equilibrium period began 51 hours after 0-time. Test data of the thermal equilibrium period are shown in Table 10-2. All measured hydrogen boiloff rates were corrected as discussed in Section 10.1.5. An average equilibrium boiloff rate of 0.00055 Kg/hr (0.00121 lb/hr)

Table 10-2. Null Test No. 1, Zero Watt Power Input Boiloff Data During The Thermal Equilibrium Period

Equil. Hour	Total Elapsed Time, hr	LH_2 Boiloff kg/hr	LH_2 Boiloff lb/hr	Equil. Hour	Total Elapsed Time, hr	LH_2 Boiloff kg/hr	LH_2 Boiloff lb/hr
0	51	0.000545	0.00120	5	56	0.000545	0.00120
1	52	0.000545	0.00120	6	57	0.000636	0.00140
2	53	0.000545	0.00120	7	58	0.000500	0.00110
3	54	0.000545	0.00120	8	59	0.000500	0.00110
4	55	0.000545	0.00120	9	60	0.000591	0.00130

Average Boiloff: 0.00055 kg/hr (0.00121 lb/hr)

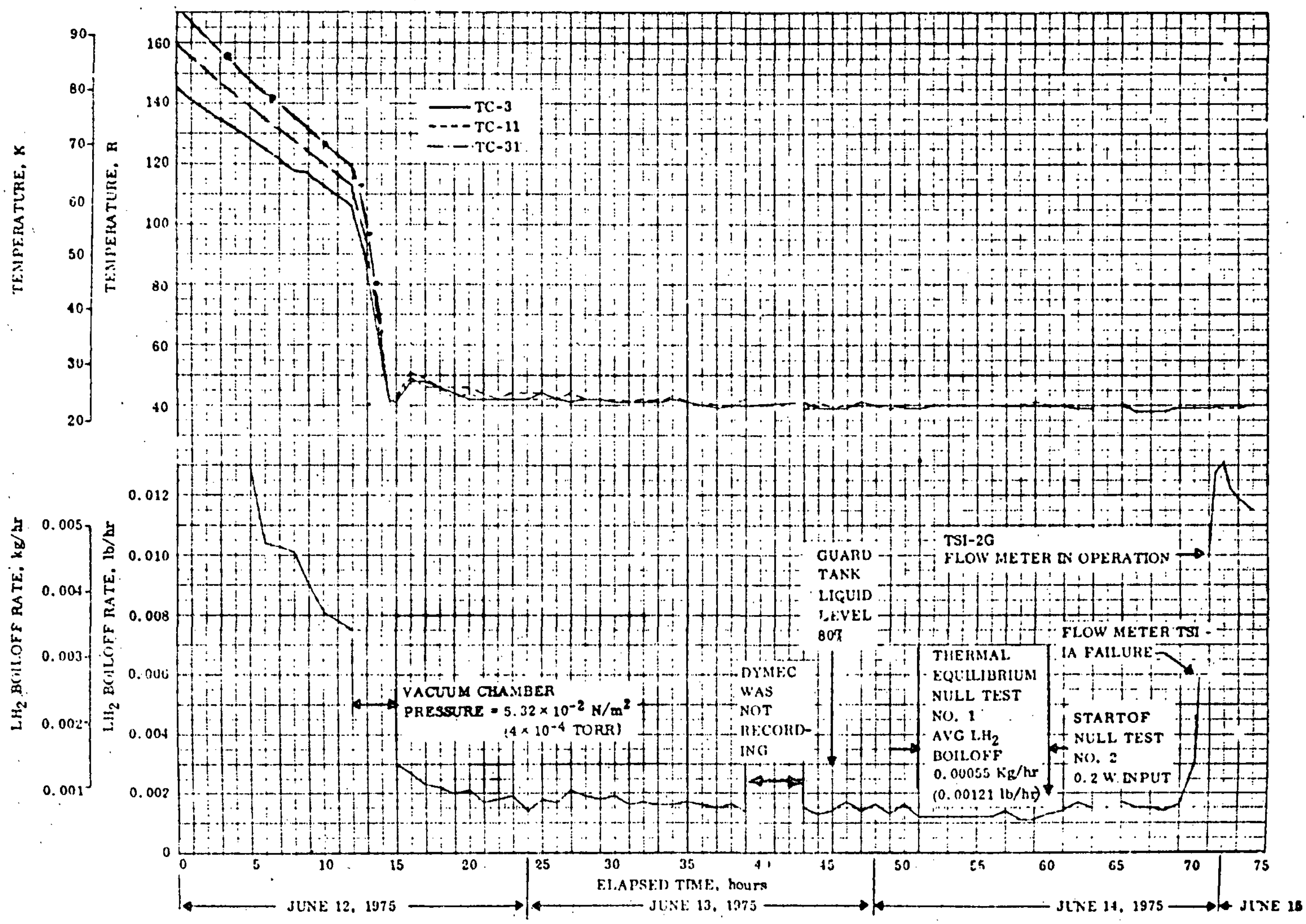

Figure 10-4. Null Test No. 1, Zero Power Input (Elapsed Hours: 0 to 73) - Sheet 1 of 3

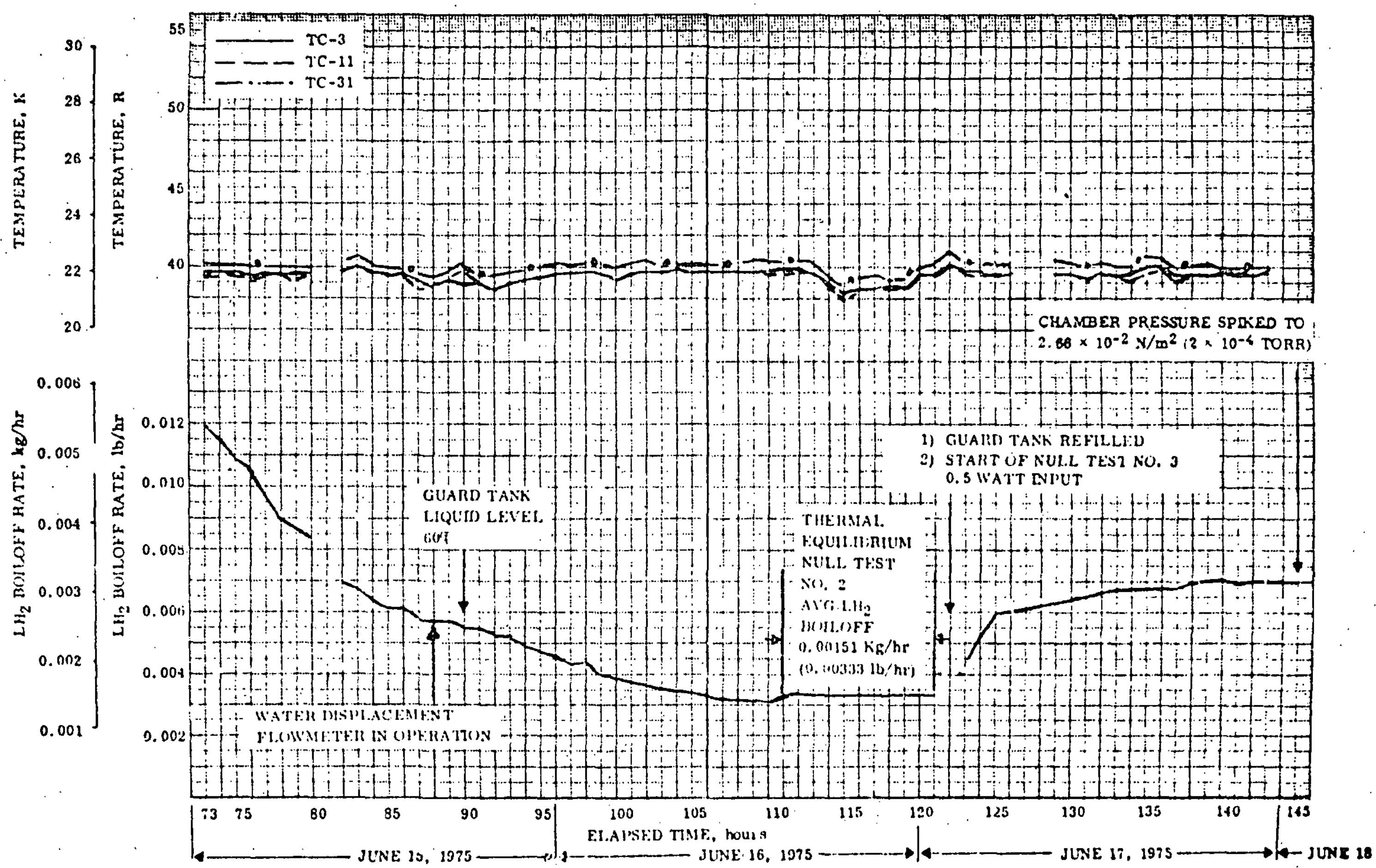

Figure 10-4. Null Test No. 2, 0.2 Watt Power Input (Elapsed Hours: 73 to 145) - Sheet 2 of 3

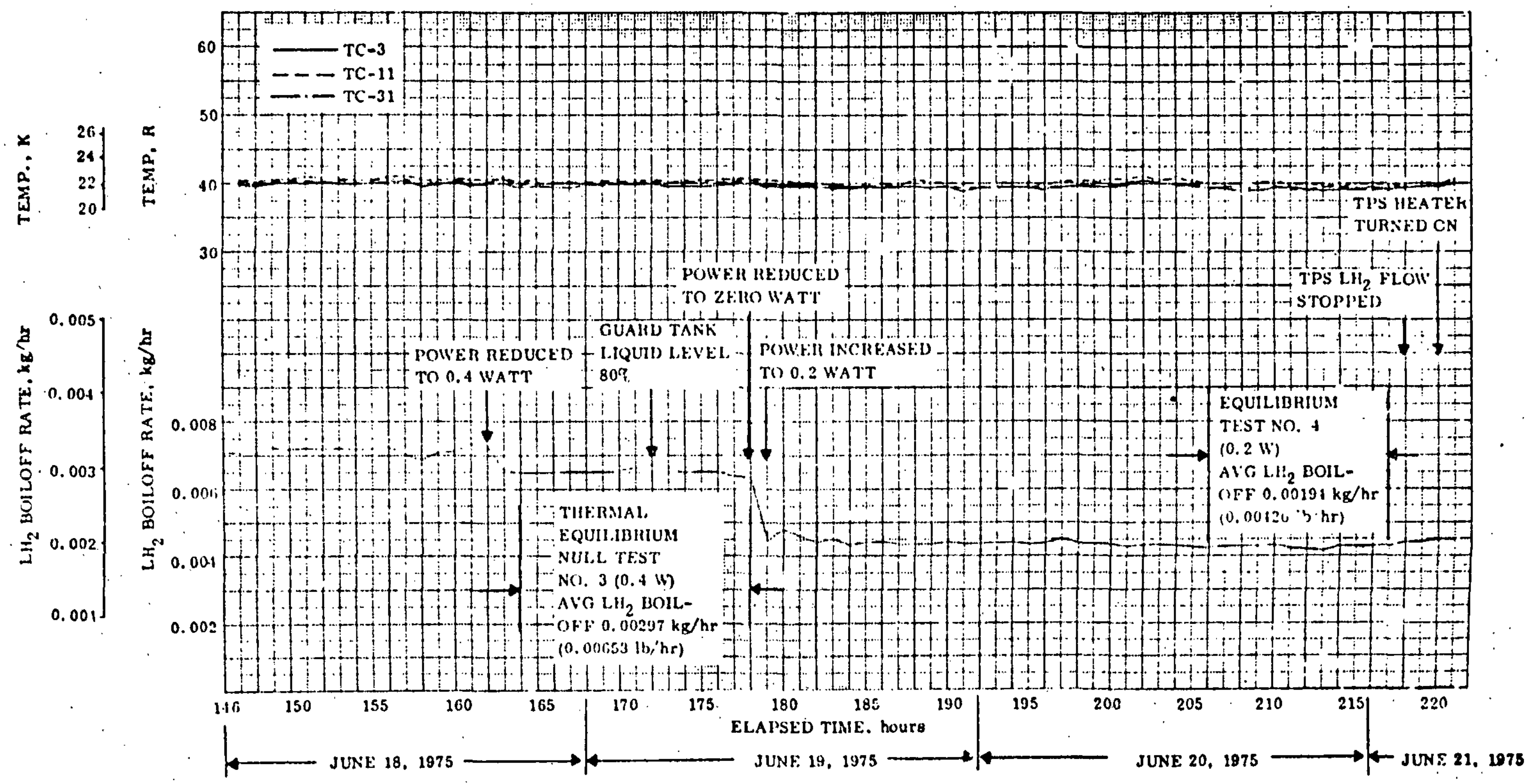

Figure 10-4. Null Test No. 3 (0.4 Watt)and No. 4 (0.2 Watt) Power Input (Elapsed Hours: 146 to 221) - Sheet 3 of 3

was measured during the nine hour equilibrium period. MLI temperatures of thermocouples TC-3, 11 and 31 are plotted in Figure 10-4 (Sheet 1). During the entire null test equilibrium period there was no significant change in the test tank MLI temperatures as shown in Table 10-3. The results are discussed in Section 10.1.4.1.

10.1.3.2 Null Test No. 2, 0.2 Watt Power Input - The second null test (Step 14, Section 10.1.1) was the application of 0.2 watt to the test tank heater to verify a known heat input into the test tank. The boiloff rate (Figure 10-4, Sheet 1) was increasing slowly to approximately 0.00068 Kg/hr (0.00150 lb/hr) when a rapid increase in flow rate to 0.00273 Kg/hr (0.006 lb/hr) damaged the TSI-IA flowmeter, 69 hours after 0-time. For the following 19 hours boiloff readings were taken with the TSI-2G flowmeter (Table 9-1, Channel 165). These readings were below the operating range of the TSI-2G meter after 88 hours after 0-time. A water displacement flowmeter (Section 9.2.5) was then introduced and it was kept in use for the remainder of the test operation. Test tank pressure oscillations occurred after the change of the flowmeter. They were reduced by adjusting the sensitivity and reset rate of the Dahl controller (C_V = 0.010).

The thermal equilibrium period began 51 hours (111 hours after 0-time) after the 0.2 watt power application (Figure 10-4, Sheet 2). Test data of the second null test are listed in Table 10-4. MLI temperatures (TC-3, 11 and 31) are plotted in Figure 10-4, Sheet 2. A measured average boiloff rate of 0.00151 Kg/hr (0.00333 lb/hr) was obtained during 10 hours of equilibrium conditions. During the entire null test equilibrium period there was no significant change of the test tank MLI temperature (Table 10-5). At the end of the test the guard tank was approximately 40% full. The results of null test no. 2 are discussed in Section 10.1.4.2.

10.1.3.3 Null Test No. 3, 0.5 to 0.4 Watt Power Input - The third null test (Section 10.1.1, Step 15) was the application of 0.5 watt to the test tank heater. The predicted hydrogen boiloff at this power level was 0.00428 Kg/hr (0.00941 lb/hr). The test was started 122 hours after 0-time when the guard tank was refilled (Figure 10-4, Sheet 2). The increase in flowrate was extremely small. During a 24 hour period (138 to 162 hours after 0-time) the boiloff rate increased only by 0.00027 Kg/hr (0.0006 lb/hr). It was decided after 40 hours of total test time to reduce the power level to 0.4 watts due to the long time projected as being required to reach thermal equilibrium. The thermal equilibrium period begun after 2 hours. A measured average boiloff of 0.00297 kg/hr (0.00653 lb/hr) was obtained during the following 14 hours of thermal equilibrium (164 hours to 178 hours after 0-time). Boiloff rates are presented in Table 10-6. MLI temperatures (TC-3, -11 and -31) and boiloff rates are plotted in Figure 10-4, Sheet 3. The results of null test no. 3 are discussed in Section 10.1.4.3.

10.1.3.4 Null Test No. 4, 0.2 Watt Power Input - During the fourth null test (Section 10.1.1, Step 15), the power level was reduced to the original 0.2 watt case (second null test), to establish the repeatability of the boiloff measurements. The test was started 178 hours after 0-time. The thermal equilibrium began 26 hours after the 0.2 watt power input. A measured average boiloff rate of 0.00194 Kg/hr (0.00426 lb/hr)

Table 10-3. Test Data at Beginning and End of the Thermal Equilibrium Period of Null Test No. 1

	Beginning-51 Hrs After 0-Time				End - 60 Hrs After 0-Time			
	°F	°R	°C	°K	°F	°R	°C	°K
TC-1	-419.4	41.6	-250.1	23.1	-417.5	42.5	-249.6	23.6
TC-2	-420.8	39.2	-251.4	21.6	-420.3	39.7	-251.1	22.1
TC-3	-420.6	39.4	-251.3	21.9	-420.0	40.0	-251.0	22.2
TC-4	-421.8	38.2	-252.0	21.2	-421.2	38.8	-251.6	21.6
TC-5	-418.4	41.6	-250.1	23.1	-417.8	42.2	-249.8	23.4
TC-6	-419.7	40.3	-250.8	22.4	-419.3	40.7	-250.6	22.6
TC-7	-420.5	39.5	-251.3	21.9	-419.8	40.2	-250.9	22.3
TC-8	-422.0	38.0	-252.1	21.1	-421.2	38.8	-251.6	21.6
TC-9	-417.8	42.2	-249.8	23.4	-416.9	43.1	-249.3	23.9
TC-10	-420.6	39.4	-251.3	21.9	-419.8	40.2	-250.9	22.3
TC-11	-420.6	39.4	-251.3	21.9	-419.8	40.2	-250.9	22.3
TC-12	-421.6	38.4	-251.9	21.3	-420.8	39.2	-251.4	21.8
TC-13	-419.1	40.9	-250.5	22.7	-418.4	41.6	-250.1	23.1
TC-14	-421.4	38.6	-251.8	21.4	-420.5	39.5	-251.3	21.9
TC-15	-420.0	40.0	-251.0	22.2	-419.5	40.5	-250.7	22.5
TC-16	-422.0	38.0	-252.1	21.1	-421.0	39.0	-251.5	21.7
TC-17	-419.7	40.3	-250.8	22.4	-418.5	41.5	-250.1	23.1
TC-18	-421.2	38.8	-251.6	21.6	-420.6	39.4	-251.3	21.9
TC-19	*				-420.6	39.4	-251.3	21.9
TC-20	-422.0	38.0	-252.1	21.1	-421.2	38.8	-251.6	21.6
TC-21	-418.1	41.9	-249.9	23.3	-417.8	42.2	-249.6	23.6
TC-22	-420.5	39.5	-251.3	21.9	-420.2	39.8	-251.1	22.1
TC-23	-420.0	40.0	-251.0	22.2	-419.7	40.3	-250.8	22.4
TC-24	-421.0	39.0	-251.5	21.7	-420.5	39.5	-251.3	21.9
TC-25	-418.2	41.8	-250.0	23.2	-417.7	42.3	-249.7	23.5
TC-26	-420.5	39.5	-251.3	21.9	-420.0	40.0	-251.0	22.2
TC-27	-419.8	40.2	-250.9	22.3	-419.5	40.5	-250.7	22.5
TC-28	*				*			
TC-29	-418.9	41.1	-250.4	22.8	-418.7	41.3	-250.3	22.9
TC-30	-420.0	40.0	-251.0	22.2	-419.8	40.2	-250.9	22.3
TC-31	-419.7	40.3	-250.8	22.4	-419.5	40.5	-250.7	22.5
TC-32	-422.3	37.7	-252.3	20.4	-421.6	38.4	-251.9	21.3
TC-33	*							
TC-34	-420.6	39.4	-251.3	21.9	-418.4	41.6	-250.1	23.1
TC-35	-413.7	46.3	-247.5	25.7	-412.8	47.2	-247.0	26.2
TC-36	*				*			
TC-37	NO TPS BLANKETS USED ↓							
TC-38								
TC-39								
TC-40								

	Beginning - 51 Hrs After 0 - Time				End - 60 Hrs After 0 - Time			
	°F	°R	°C	°K	°F	°R	°C	°K
TC-41	NO TPS BLANKETS USED ↓							
TC-42								
TC-43								
TC-44								
TC-45								
TC-46								
TC-47								
TC-48								
TC-49								
TC-50								
TC-51								
TC-52								
TC-53								
TC-54								
TC-55								
TC-56								
TC-57								
TC-58								
TC-59	*				-417.8	42.2	-249.8	23.4
TC-60	*				-418.7	41.3	-250.3	22.9
TC-61	-423.0	37.0	-252.6	20.6	-417.0	43.0	-249.3	23.9
TC-62	-423.0	37.0	-252.6	20.6	-417.6	42.4	-249.6	23.6
TC-63	*				-420.5	39.5	-251.3	21.9
TC-64	*				-418.5	41.5	-250.1	23.1
TC-65	*				-419.1	40.9	-250.5	22.7
TC-66	-419.7	40.3	-250.8	22.4	-416.2	43.8	-248.9	24.3
TC-67	-410.7	49.3	-245.8	27.4	-406.3	53.7	-243.4	29.8
TC-68	53.8	513.8	12.2	285.4	52.3	512.3	11.4	284.6
TC-69	52.2	512.2	11.4	284.6	50.9	510.9	10.6	283.8
TC-70	53.5	513.5	12.1	285.3	51.9	511.9	11.2	284.4
TC-71	51.2	511.2	10.8	284.0	50.1	510.1	10.2	283.4
TC-72	58.2	518.2	14.7	287.9	64.8	524.8	18.4	291.6
TC-73	58.8	518.8	15.0	288.2	68.3	[illegible]	20.3	293.5
TC-74	57.3	517.3	14.2	287.4	67.2	527.2	19.7	292.9
TC-75	DIFFUSION PUMP							
TC-76	59.7	519.7	15.5	288.7	59.7	519.7	15.5	288.7
TC-77	102.6	562.6	39.4	312.6	104.3	564.3	40.3	313.5
TC-78	58.5	518.5	14.9	288.1	65.4	525.4	18.7	291.9
TC-79	-317.0	143.0	-193.8	79.4	-316.7	143.3	-193.6	79.6
TC-80	55.2	515.2	13.0	286.2	63.8	523.8	17.8	291.0

* Incorrect Reading

ORIGINAL PAGE IS
OF POOR QUALITY

Table 10-4. Null Test No. 2, 0.2 Watt Power Input Boiloff Data During The Thermal Equilibrium Period

Equil. hour	Total Elapsed Time, hrs	LH_2 Boiloff kg/hr	LH_2 Boiloff lb/hr	Equil. Hour	Total Elapsed Time, hrs	LH_2 Boiloff kg/hr	LH_2 Boiloff lb/hr
0	111	0.00151	0.00333	5	116	0.00150	0.00330
1	112	0.00154	0.00339	6	117	0.00152	0.00334
2	113	0.00152	0.00335	7	118	0.00151	0.00332
3	114	0.00151	0.00333	8	119	0.00153	0.00336
4	115	0.00150	0.00330	9	120	0.00149	0.00329
				10	121	0.00151	0.00333

Average Boiloff: 0.00151 kg/hr (0.00333 lb/hr)

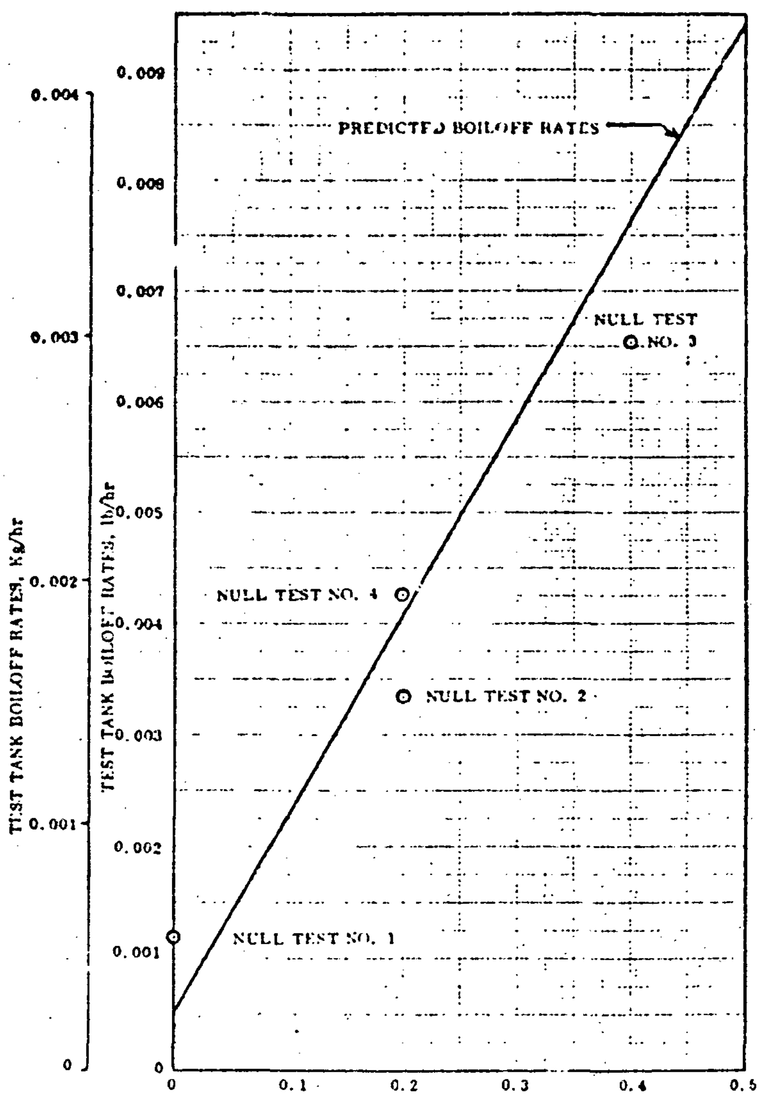

Figure 10-5. Test Tank Heater Power Input Vs Test Tank Boiloff Rates During Null Testing

was obtained during 12 hours of equilibrium conditions (205 to 217 hours after 0-time, Table 10-7, and Figure 10-4, Sheet 3 of 3). Thermocouple temperature data at the beginning and at the end of the thermal equilibrium period are presented in Table 10-8.

10.1.4 EVALUATION OF NULL TEST RESULTS - The results of null tests no. 1, 2, 3 and 4 are summarized in Table 10-9 and plotted in Figure 10-5.

The results include the maximum extraneous heat flow of 0.0293 watt (0.1 Btu/hr) into the test tank when the internal heater element was turned off. The test apparatus was designed to meet this NASA requirement. A system thermal performance analysis and the analytical determination of all extraneous heat flows were beyond the scope of this work. Utilizing test data, the heat leakage was re-estimated. The components which were investigated and their contribution to heat leakage are listed in Table 10-10.

The heat leak through the MLI was determined by using the equation which describes the thermal performance of

Table 10-5. Test Data at Beginning and End of the Thermal Equilibrium Period of Null Test No. 2

	Beginning - 111 Hrs After 0 - Time				End - 121 Hrs After 0 - Time			
	°F	°R	°C	°K	°F	°R	°C	°K
TC-1	-417.8	42.2	-249.8	23.4	-418.0	42	-249.9	23.3
TC-2	-420.5	39.5	-251.3	21.9	-420.8	39.2	-251.4	21.8
TC-3	-420.3	39.7	-251.1	22.1	-420.6	39.4	-251.3	21.9
TC-4	-421.4	38.6	-251.8	21.4	-421.6	38.4	-251.9	21.3
TC-5	-420.3	39.7	-251.1	22.1	-420.3	39.7	-251.1	22.1
TC-6	-419.5	40.5	-250.7	22.5	-419.8	40.2	-250.9	[illegible]
TC-7	-420.6	39.4	-251.3	21.9	-420.5	39.5	-251.3	21.9
TC-8	-421.4	38.6	-251.9	21.4	-421.8	39.2	-252.0	21.2
TC-9	-419.5	40.5	-250.7	22.5	-419.7	40.3	-250.8	22.4
TC-10	-420.3	39.7	-251.1	22.1	-420.5	39.5	-251.3	21.9
TC-11	-420.0	40.0	-251.0	22.2	-420.5	39.5	-251.3	21.9
TC-12	-421.2	38.8	-251.6	21.6	-421.4	38.6	-251.8	21.4
TC-13	[illegible]	39.4	-251.3	21.9	-418.9	41.1	-250.4	22.8
TC-14	-421.2	38.8	-251.6	21.6	-421.4	38.6	-251.8	21.4
TC-15	-420.0	40.0	-251.0	22.2	-420.2	39.9	-251.1	22.1
TC-16	-421.6	38.4	-251.9	21.3	-421.8	39.2	-252.0	21.2
TC-17	-419.0	42.0	-249.9	23.3	-419.5	40.5	-250.7	22.5
TC-18	-420.6	39.4	-251.3	21.9	-421.2	38.8	-251.6	21.6
TC-19	*				*			
TC-20	-421.2	38.8	-251.6	21.6	-421.6	38.4	-251.9	21.3
TC-21	-417.8	42.2	-249.8	23.4	-418.2	41.8	-250.0	23.2
TC-22	-420.5	39.5	-251.3	21.9	-420.6	39.4	-251.3	21.9
TC-23	-420.0	40.0	-251.0	22.2	-420.6	39.4	-251.3	21.9
TC-24	-420.5	39.5	-251.3	21.9	-420.6	39.4	-251.3	21.9
TC-25	-419.0	42.0	-249.9	23.3	-418.2	41.8	-250.0	23.2
TC-26	-420.3	39.7	-251.1	22.1	-420.3	39.7	-251.1	22.1
TC-27	-419.7	40.3	-250.8	22.4	-419.8	40.2	-250.9	22.3
TC-28	-423.3	36.7	-252.8	20.4	*			
TC-29	-418.9	41.1	-250.4	22.8	-418.9	41.1	-250.4	22.9
TC-30	-419.8	40.2	-250.9	22.3	-420.3	39.7	-251.1	22.1
TC-31	-419.6	40.4	-250.8	22.4	-419.8	40.2	-250.9	22.3
TC-32	-422.0	38.0	-252.1	21.1	-421.9	38.1	-252.0	21.2
TC-33	*							
TC-34	-418.5	41.5	-250.1	23.1	-419.8	40.2	-250.9	22.3
TC-35	[illegible]	47.0	-247.1	26.1	-413.0	47.0	-247.1	26.1
TC-36	*				*			
TC-37	NO TPS BLANKETS USED							
TC-38	↓							
TC-39	↓							
TC-40	↓							

	Beginning - 111 Hrs After 0 - Time				End - 121 Hrs After 0 - Time			
	°F	°R	°C	°K	°F	°R	°C	°K
TC-41	NO TPS BLANKETS USED							
TC-42	↓							
TC-43	↓							
TC-44	↓							
TC-45	↓							
TC-46	↓							
TC-47	↓							
TC-48	↓							
TC-49	↓							
TC-50	↓							
TC-51	↓							
TC-52	↓							
TC-53	↓							
TC-54	↓							
TC-55	↓							
TC-56	↓							
TC-57	↓							
TC-58	↓							
TC-59	-422.0	38.0	-252.1	21.1	*			
TC-60	-423.5	36.5	-252.9	20.3	-423.5	36.5	-252.9	20.3
TC-61	-422.9	37.1	-252.6	20.6	-422.7	37.3	-252.5	20.7
TC-62	-422.5	37.5	-252.4	20.8	-422.3	37.7	-252.3	20.9
TC-63	*				*			
TC-64	-423.5	36.5	-252.9	20.3	-423.5	36.5	-252.9	20.3
TC-65	*				*			
TC-66	-419.3	40.7	-250.6	22.6	-419.0	41.1	-250.4	22.8
TC-67	-410.8	49.2	-245.9	27.3	-410.3	49.7	-245.6	27.6
TC-68	51.4	511.4	10.8	284.1	51.0	511.0	10.7	283.9
TC-69	50.0	510.0	10.1	283.3	49.5	509.5	9.9	283.1
TC-70	51.0	511.0	10.7	283.9	50.6	510.6	10.5	283.7
TC-71	49.1	509.1	9.6	282.8	48.6	508.6	9.4	282.6
TC-72	63.3	523.3	17.5	290.7	58.8	518.8	15.0	288.2
TC-73	64.8	524.8	18.4	291.6	59.5	519.5	15.4	288.6
TC-74	63.3	523.3	17.5	290.7	57.9	517.9	14.5	287.7
TC-75	DIFFUSION PUMP							
TC-76	59.9	519.9	15.6	288.8	60.0	52.0	15.7	288.9
TC-77	102.3	562.3	39.2	312.4	105.5	565.5	41.0	314.2
TC-78	61.5	521.5	16.5	289.7	57.0	517.0	14.0	287.2
TC-79	-316.6	143.4	-193.6	79.7	-316.9	143.1	-193.7	79.5
TC-80	59.2	519.8	15.6	288.8	54.2	514.2	12.5	285.7

* Incorrect Reading

Table 10-6. Null Test No. 3, 0.4 Watt Power Input Boiloff Data During the Thermal Equilibrium Period

Equil. hour	Total Elapsed Time, hr	LH_2 Boiloff		Equil. hour	Total Elapsed Time, hr	LH_2 Boiloff	
		kg/hr	lb/hr			kg/hr	lb/hr
0	164	0.002945	0.00648	8	172	0.003055	0.00672
1	165	0.002955	0.00650	9	173	0.003023	0.00665
2	166	0.002959	0.00651	10	174	0.002945	0.00648
3	167	0.002973	0.00654	11	175	0.002959	0.00651
4	169	0.002973	0.00654	12	176	0.002955	0.00650
5	169	0.002977	0.00655	13	177	0.002905	0.00639
6	170	0.002986	0.00657	14	178	0.002882	0.00634
7	171	0.003036	0.00668				

Average Boiloff: 0.00297 kg/hr (0.00653 lb/hr)

Table 10-7. Null Test No. 4, 0.2 Watt Power Input Boiloff Data During the Thermal Equilibrium Period

Equil. hour	Total Elapsed Time, hr	LH_2 Boiloff		Equil. hour	Total Elapsed Time, hr	LH_2 Boiloff	
		kg/hr	lb/hr			kg/hr	lb/hr
0	205	0.001941	0.00427	7	212	0.001909	0.00420
1	206	0.001932	0.00425	8	213	0.001886	0.00415
2	207	0.001945	0.00428	9	214	0.001950	0.00429
3	208	0.001941	0.00427	10	215	0.001941	0.00427
4	209	0.001950	0.00429	11	216	0.001945	0.00428
5	210	0.001973	0.00434	12	217	0.001959	0.00431
6	211	0.001918	0.00422				

Average Boiloff: 0.00194 kg/hr (0.00426 lb/hr)

Table 10-8. Test Data at Beginning and End of Thermal Equilibrium Period of Null Test No. 4

	Beginning - 205 Hrs After 0-Time				End - 217 Hrs After 0-Time			
	°F	°R	°C	°K	°F	°R	°C	°K
TC-1	-418.4	41.6	-250.1	23.1	-418.4	41.6	-250.1	23.1
TC-2	-420.6	39.4	-251.3	21.9	-420.8	39.2	-251.4	21.8
TC-3	-420.8	39.2	-251.4	21.8	-421.0	39.0	-251.5	21.7
TC-4	-421.6	38.4	-251.9	21.3	-421.6	38.4	-251.9	21.3
TC-5	-418.7	41.3	-250.3	22.9	-418.7	41.3	-250.3	22.9
TC-6	-419.9	40.1	-250.9	22.3	-419.9	40.1	-250.6	22.6
TC-7	-420.5	39.5	-251.3	21.9	-420.5	39.5	-251.3	21.9
TC-8	-421.6	38.4	-251.9	21.3	-421.8	38.2	-252.0	21.2
TC-9	-418.0	42.0	-249.9	23.3	-418.0	42.0	-249.9	23.3
TC-10	-420.6	39.4	-251.3	21.9	-420.8	39.2	-251.4	21.8
TC-11	-420.6	39.4	-251.3	21.9	-420.8	39.2	-251.4	21.8
TC-12	-421.2	38.8	-251.6	21.6	-421.6	38.4	-251.9	21.3
TC-13	-419.1	40.9	-250.5	22.7	-419.7	40.3	-250.8	22.4
TC-14	-421.2	38.8	-251.6	21.6	-421.6	38.4	-251.6	21.6
TC-15	-420.3	39.7	-251.1	22.1	-420.5	39.6	-251.3	21.9
TC-16	-421.6	38.4	-251.9	21.3	-421.8	38.2	-252.0	21.2
TC-17	-420.0	40.0	-251.0	22.2	-420.3	39.7	-251.1	22.1
TC-18	-421.4	38.6	-251.0	21.4	-421.2	39.8	-251.6	21.6
TC-19	*				*			
TC-20	-421.4	38.6	-251.8	21.4	-421.4	38.6	-251.8	21.4
TC-21	-418.7	41.3	-250.3	22.9	-418.7	41.3	-250.3	22.9
TC-22	-420.6	39.4	-251.3	21.9	-420.8	39.2	-251.4	21.8
TC-23	-420.3	39.7	-251.1	22.1	-420.3	39.7	-251.1	22.1
TC-24	-420.5	39.5	-251.3	21.9	-420.5	39.5	-251.3	21.9
TC-25	-418.5	41.5	-250.1	23.1	-418.7	41.3	-250.3	22.9
TC-26	-420.5	39.5	-251.3	21.9	-420.5	39.5	-251.3	21.9
TC-27	-419.8	40.2	-250.9	22.3	-420.0	40.0	-251.0	22.2
TC-28	-421.6	38.4	-251.9	21.3	*			
TC-29	-419.3	40.7	-250.6	22.6	-419.5	40.5	-250.7	22.5
TC-30	-420.5	39.5	-251.3	21.9	-420.5	39.5	-251.3	21.9
TC-31	-419.8	40.2	-250.9	22.3	-420.0	40.0	-251.0	22.2
TC-32	-422.0	38.0	-252.1	21.1	-422.0	38.0	-252.1	21.1
TC-33	*				*			
TC-34	-418.1	41.9	-249.9	23.3	-420.0	40.0	-251.0	22.2
TC-35	-412.6	47.4	-246.9	26.3	-412.8	47.2	-247.0	26.2
TC-36	*				*			
TC-37	NO TPS BLANKETS USED							
TC-38								
TC-39								
TC-40								

	Beginning - 205 Hrs After 0-Time				End - 217 Hrs After 0-Time			
	°F	°R	°C	°K	°F	°R	°C	°K
TC-41	NO TPS BLANKETS USED							
TC-42								
TC-43								
TC-44								
TC-45								
TC-46								
TC-47								
TC-48								
TC-49								
TC-50								
TC-51								
TC-52								
TC-53								
TC-54								
TC-55								
TC-56								
TC-57								
TC-58								
TC-59	*				*			
TC-60	*				*			
TC-61	-423.0	37.0	-252.6	20.6	-423.0	37.0	-252.6	20.6
TC-62	-423.0	37.0	-252.6	20.6	-423.0	37.0	-252.6	20.6
TC-63	*				*			
TC-64	*				*			
TC-65	*				*			
TC-66	-421.2	38.8	-251.6	21.6	-421.4	38.6	-251.8	21.4
TC-67	-415.6	41.4	-248.5	24.7	-416.0	44.0	-248.8	24.4
TC-68	45.6	505.6	7.7	280.9	46.7	506.7	8.3	281.5
TC-69	41.3	501.3	7.0	280.2	45.5	505.5	7.6	280.8
TC-70	45.3	505.3	7.5	280.7	46.3	506.3	9.1	281.3
TC-71	43.4	503.4	6.5	279.7	44.0	504.0	6.8	280.0
TC-72	65.7	525.7	18.9	292.1	50.4	510.4	10.4	283.6
TC-73	66.9	526.9	19.5	292.7	51.2	511.2	10.8	284.0
TC-74	65.6	525.6	18.8	292.0	49.7	509.7	10.0	283.2
TC-75	DIFFUSION PUMP							
TC-76	59.6	519.6	15.5	288.7	59.6	519.6	15.5	288.7
TC-77	103.8	563.8	40.0	313.2	102.6	562.6	39.4	312.6
TC-78	64.0	524.0	17.9	291.1	48.9	508.9	9.5	282.7
TC-79	-316.7	143.3	-193.6	79.6	-316.7	143.3	-193.6	79.6
TC-80	60.5	520.5	16.0	289.2	45.5	5[illegible]5	7.6	280.8

* Incorrect reading.

ORIGINAL PAGE IS OF POOR QUALITY

preconditioned silk net spacer system (Reference 10-1)

$$q = \frac{C_S (\bar{N})^{2.56} T_m}{N_S + 1} (T_H - T_C) + \frac{C_r \epsilon_{TR}}{N_S} (T_H^{4.67} - T_C^{4.67}) \qquad (10\text{-}1)$$

where

$C_S = 8.95 \times 10^{-6}$ and $C_r = 5.39 \times 10^{-8}$ for $\bar{N}$ in layers/m, T in °K, and q in W/m^2

or $C_S = 8.06 \times 10^{-10}$ and $C_r = 1.10 \times 10^{-11}$ for $\bar{N}$ in layers/in, T in °R, and q in BTU/hr ft^2

$\epsilon_{TR} = 0.031$

The equation does not include any heat transfer through insulation attachments. The temperature $T_H = 23.2$K (41.75R) was determined by averaging all TC temperatures at the outer face sheet of the outer blanket shown in Table 10-3. The temperature $T_H = 20.6$K (37.12R) is the saturation temperature of the hydrogen at the test tank pressure of 113.08 kN/m^2 (16.4 psia). The heat leak through the test tank door (not insulated) was estimated by performing a simple radiation exchange calculation between guard tank and test tank. A maximum ΔT of 0.55K (1.0R) was assumed because the guard tank was controlled at a pressure of 114.11 kN/m^2 (16.55 psia). The value of the emissivity for both tanks was assumed to be 0.5.

Table 10-9. Summary of Null Test Results

Null Test Number	1	2	3	4
1. Tank Heater Power Input (watts)	Zero	0.2	0.4	0.2
2. Elasped Test Time Range (Figure 10-4) (hours)	0-60	60-121	122-178	179-217
3. Thermal Equilibrium Period (Figure 10-4) (hours)	3	10	14	11
4. Predicted Boiloff Rate, Kg/hr (lb/hrs)	0.00024 (0.00052)*	0.00185 (0.00408)	0.00347 (0.00763)	0.00185 (0.00408)
5. Average Measured Boiloff, Kg/hr (lb/hrs)	0.00055 (0.00121)	0.00151 (0.00333)	0.00297 (0.00655)	0.00194 (0.00426)
6. Predicted Heat Leakage, Watts (BTU/hr)	0.0293 (0.1)	0.2293 (0.7826)	0.4293 (1.4652)	0.2293 (0.7826)
7. Average Measured Heat Leakage, Watts (BTU/hr)	0.068 (0.2321)	0.187 (0.6387)	0.367 (1.2524)	0.239 (0.8170)
8. % Deviation Between Predicted and Measured Boiloff Rates	-133	-18.3	-14.4	-4.4
9. Chamber Pressure, N/m^2 (Torr)	1.33×10^{-5} (1.0×10^{-7})	9.31×10^{-6} (7.0×10^{-8})	2.4×10^{-4} (1.8×10^{-4})	10.8×10^{-5} (8.0×10^{-7})
10. Shroud Pressure, N/m^2 (Torr)	2.4×10^{-5} (1.9×10^{-7})	2.0×10^{-5} (1.5×10^{-7})	3.32×10^{-5} (2.5×10^{-7})	2.13×10^{-5} (1.6×10^{-7})

* Based on 0.0293 watts (0.1 BTU/hr) heat leakage into the test tank.

Table 10-10. Estimated Extraneous Heat Flow Into the LH_2 Test Tank

Component	Rpt Sect.	Heat Leakage		Boiloff Rate	
		Watt	BTU/hr	Kg/hr	lb/hr
1. MLI	7.2	0.00412	0.01406	0.000033	0.000073
2. Test Tank Door	2.1.1	0.00033	0.00112	0.000003	0.000006
3. Leakage Evacuation Line	2.1.1	0.00361	0.01232	0.000029	0.000064
4. 16 TC's to Outside Tank Wall (Bottom)	9.1	0.00795	0.02713	0.000064	0.000141
5. 3 Tank Supports	3.2.1	0.00769	0.02625	0.000062	0.000137
6. Vent Line	5.5	0.00300	0.01025	0.000024	0.000053
7. Fill Line	5.5	0.00300	0.01025	0.000024	0.000053
8. H_2 Gas in Fill Line	5.5	0.00004	0.00015	0.0000004	0.000001
Total		0.02974	0.10153	0.000239	0.000529

The gas leakage evacuation line which was intended to reduce leakage from the door bleed ports shown in Figure 2-2, Section B-B, F/7 consisted of a 304 stainless steel tube, 0.00635 m (0.25 in) diameter and 0.0005 m (0.020 in) wall thickness. The length of the tube between door and guard tank where it was attached to the outside wall was 1.52 m (60 in). The temperature of the tube at the guard tank location was estimated to be 51K (110R).

Sixteen thermocouple wires, 28 gauge, were attached to the outside wall of the lower end of the test tank. Each wire was 6.1 m (240 in) long. The temperature at the hot end of the wire was approximately 116.7K (210R).

The length of the three stainless steel tank supports between guard and test tank was 0.381 m (15 in). The diameter was 0.013 m (0.5 in). The temperature difference between the cold and warm end of the support was 0.55K (1.0R).

Both the vent and fill line consisted of 304 stainless steel tubing, 0.051 m (2.0 in) diameter and a wall thickness of 0.0009 m (0.035 in). The length between guard and test tank was 0.356 m (14 in). The ΔT was assumed to be 0.55K (1.0R).

Finally, the contribution to heat leakage of the stagnant hydrogen gas within the fill line was analyzed. The contribution is insignificant as shown in Table 10-10. Heat leakage through the instrumentation wires leading to the liquid level sensors was also insignificant. The electrical harness was fed through a separate tube in the guard tank to provide good thermal contact and to assure complete heat removal.

10.1.4.1 Null Test No. 1 - Zero Power Input - Table 10-9 indicates that the measured LH_2 boiloff rate was 2.3 times higher than the estimated boiloff rate. There are several reasons for the large discrepancy between measured and estimated boiloff rates. Reason number one is that the predicted boiloff rates were only estimates. A re-evaluation of the heat leaks after the testing was not completely successful because of the guard tank thermocouple failures (Section 9.2.1). No allowance was made for heat transfer through MLI attachments. The second reason for the discrepancy was the incomplete outgassing of the MLI. An extremely slow outgassing of the system is not surprising at the low temperature levels which were maintained throughout this test. Gas conduction heat transfer through composite MLI systems such as the silknet/DAM MLI becomes significant at interstitial pressures above 1.33×10^{-4} N/m^2 (10^{-6} torr) (Ref. (Ref. 10-1, page 8-1). Interstitial pressures up to three orders of magnitude higher than those maintained within the surrounding vacuum environment can exist in composite MLI systems for relatively long times (i.e., for days or even weeks) due to continued outgassing of water vapor. However, it must be realized that the estimated heat leakage through the MLI is only 14 percent of the total heat leakage into the tank (table 10-10).

A third and major reason for the discrepancy between the predicted and measured boiloff rate may be the additional heat transfer through the vent and fill line caused by thermal acoustic oscillations. Such thermal acoustic oscillations produce large heat leaks to stored cryogens (Ref. 10-2). Pressure oscillations also occurred during these tests.

In general, the temperature and boiloff measurements taken during the equilibrium period were stable and within the selected thermal equilibrium criteria (Section 10. 1. 1).

10.1.4.2 Null Test No. 2 - 0.2 Watt Power Input - The power application of 0.2 watt during the first eight hours (Figure 10-4) resulted in an average LH_2 boiloff rate of approximately 0.00068 kg/hr (0.0015 lb/hr). After eight hours (69 hours after 0-time) the boiloff rate increased sharply to 0.0059 kg/hr (0.013 lb/hr). The rapid rise of the boiloff rate was caused by a sudden onset of convective currents which destroyed the inverse stratification where the fluid layers on the bottom of the tank were hotter than those on the top. The inverse stratification was created by the internal tank heater located at the bottom of the tank. The tank fluid was capable of storing the incoming energy from the heater for a period of eight hours. The energy was then suddenly released through the top surface of the fluid causing the sharp increase in LH_2 boiloff. As shown in Table 10-9, the average measured boiloff rate was 18.3% lower than the predicted rate. Since the operation and the performance of the test equipment and fluid system remained unchanged, the lower boiloff rate can only be explained by assuming that a portion of the energy created by the internal heater was stored within the bulk of the fluid, waiting for convective currents to be carried through the liquid/gas interface.

During the thermal equilibrium time of 10 hours, insulation temperatures (Table 10-5) and hydrogen boiloff rates (Table 10-4) were very stable and within the equilibrium criteria. A comparison between insulation temperatures of null test no. 1 (Table 10-3) with those of null test no. 2 indicates that the temperatures of test no. 2 are higher only by a fraction of a degree.

10.1.4.3 Null Test No. 3 - 0.5 to 0.4 Watt Power Input - The objective of this test was to determine the LH_2 boiloff rate for a power input of 0.5 watt. The predicted boiloff rate at this power level was 0.00428 kg/hr (0.00941 lb/hr), (Section 10. 1. 1). A boiloff rate (Figure 10-4, Sheet 3) of approximately 0.00318 kg/hr (0.007 lb/hr) was achieved after 16 hours (122 to 138 hours after 0-time). An additional 24 hours (138 to 162 hours after 0-time) of testing increased the boiloff rate to 0.00332 kg/hr (0.00730 lb/hr). At this rate increase (1.25×10^{-5} lb/hr/per hour) the predicted boiloff rate would have been achieved in 221 hours, not considering the asymptotic behavior of the curve to achieve thermal equilibrium. In order to obtain a thermal equilibrium in a reasonable amount of time the power level was reduced from 0.5 watt to 0.4 watt. Thermal equilibrium was achieved after two hours. As shown in Table 10-6, the predicted boiloff rate at this power level was 14.4% above the average measured boiloff rate. This indicates again that a portion of the incoming energy was absorbed by the LH_2 storage system. The mixing process was not complete. An assumption that energy was absorbed by the LH_2 fluid during the ortho to para conversion process was ruled out after a discussion with Air Products Company. This company assured that liquid hydrogen is delivered to NASA and guaranteed to be 99.5% para hydrogen.

10.1.4.4 Null Test No. 4 - 0.2 Watt Power Input - For the Null Test No. 4 the power level was reduced again to 0.2 watt to determine the repeatability of boiloff measurements at this power level. The average measured LH_2 boiloff rate (Figure 10-4, Sheet 3) during the thermal equilibrium period was 4.4% above the predicted boiloff.

10.1.5 FLOW RATE CORRECTIONS - Theoretically the null test was to provide the correction for any constant offset in the flow rate. It was therefore assumed that any flow measurement made under some standard set of environmental conditions would be inherently correct and that any further corrections would be made only for deviations from this standard environment. After the thermal performance test (Section 10.2) it was obvious that there was a 24 hour cycle in the measured flow rate. During the customized MLI testing (Section 10.3) it became obvious that there was a second periodic variation that coincided with the guard tank liquid level. An effort was made to derive an exact theoretical equation for correcting the flow rate. Three main sources of errors and the factors that might affect them were considered.

1. Real changes in the liquid to gas transition rate inside the test tank.

   a. Creation and destruction of liquid stratification.
   b. Variations in test tank pressure.
      (1) Temperature of Baratron gage.
      (2) Temperature of Reference volume.
      (3) Leakage from Reference volume.
   c. Test tank heater power.
   d. Guard tank/test tank Δtemperature.
   e. Conduction through -
      (1) Instrumentation wires outside test tank.
      (2) Instrumentation wires inside test tank.
      (3) Leakage evacuation.
      (4) Metal walls of, and gas inside, fill and vent lines.
   f. Radiation through fill and vent lines.
   g. Thermal acoustic oscillations of gas in fill and vent lines.
   h. Variations in chamber pressure.

2. Leakage in or out of test tank.

   a. To vacuum chamber.
   b. From guard tank.
   c. To atmosphere.
   d. Apparent leakage due to temperature expansion and contraction of the gas in the plumbing outside the vacuum chamber.

3. Measurement errors.

   a. Effective volume of water displacement bottle.
   b. Temperature of gas in water displacement bottle.
   c. Pressure of gas in water displacement bottle.
   d. Solubility of hydrogen in H_2O.
   e. Creation of water vapor in water displacement bottle.

A number of these factors can be eliminated as being,

1. Non-cyclic.

2. Too small to be meaningful.

3. Highly improbable.

The correction functions for some of the remaining factors can be derived exactly. For others, the form of the correction function can be closely approximated but there is no way to evaluate the constants. For the remaining terms, even the form of the correction function cannot be determined with any certainty. It was therefore decided to derive the simplest empirical correction that would minimize the periodic variations. The resulting correction was of the form

$$Q_c = Q_M \left[\frac{532}{°R} \right]^{\approx 1.5} - A \left[t - t_{GTF} \right] \qquad (10\text{-}2)$$

where

Q_c = flow rate corrected, (SCFH)

Q_M = flow rate measured, (SCFH)

t = time (hour) Q_M was taken

t_{GTF} = time (hour) at last guard tank filling

R = ambient air temperature near water bottle at t-1

A = constant = 0 for $0 < (t - t_{GTF}) \leq 40$ hours

A = constant = 0.000025 for $40 < (t - t_{GTF})$ hours

Of all the environmental conditions and test setup operations, the outside air temperature had the overwhelming correlation with the 24 hour cycle. Because of thermal inertia, a term containing the time derivative of the air temperature might have provided more consistent results. For simplicity a time offset in the air temperature was investigated and indeed consistent results were obtained by using the air temperature from one hour previous. In actual use, the exponent in this term was never evaluated, but instead a table of F_T (Flow Correction Factor) versus Air Temperature (Table 10-11) was generated so that

$$Q_c = Q_M F_T - A (t - t_{GTF}) \qquad (10\text{-}3)$$

Since the guard tank liquid level sensors were discreet point go-no go, the liquid level was known only at the instant it was 20, 40, 60 or 80%. However, these points in time were found to be highly repeatable functions of time following guard tank fill. Therefore, the empirical correction factor for the guard tank liquid level was generated directly as a function of time. The change in the correction factor constant at 40 hours was because the fill and vent line thermal traps and the contact with the instrumentation wires on the outside surface did not extend all the way to the top of the guard tank. As such, the guard tank liquid level could drop to approximately 85% before any significant increase in heat leak occurred. The standard conditions ($Q_c = Q_M$) were at an air temperature of 295.6K (532R) and with the guard tank liquid level greater than 85%.

10.2 THERMAL TESTING OF TANK INSTALLED MLI SYSTEM

Objectives and conditions of the thermal test of the tank installed MLI system are presented in Table 10-1. This test was initiated on June 21, 1975, 220 hours after the beginning of the null test program.

The following sections present the test procedures, test specimen preparation, test results and evaluation of the results.

10.2.1 TANK INSTALLED MLI TEST PROCEDURE-

The procedure was as follows:

1. Test tank/TPS spacing: 0.457 m (18 in).
2. Maintain environmental chamber pressure at less than 1.33×10^{-4} N/m^2 (10^{-6} torr).
3. Apply 0.2 W (0.683 BTU/hr) to the test tank heater and maintain this power level.

Table 10-11. Flow Correction Factor (F_T) for Air Temperature °K (°R)

R	K	F_T	R	K	F_T
510	283.3	1.070	532	295.6	1.000
511	283.9	1.066	533	296.1	0.997
512	284.4	1.063	534	296.7	0.994
513	285.0	1.060	535	297.2	0.991
514	265.6	1.057	536	297.8	0.988
515	286.1	1.054	537	298.3	0.985
516	286.7	1.051	538	298.9	0.982
517	287.2	1.047	539	299.4	0.979
518	[illegible]	1.044	540	300.0	0.976
519	288.3	1.041	541	300.6	0.973
520	255.9	1.038	542	301.1	0.970
521	259.4	1.035	543	301.7	0.967
522	290.0	1.032	544	302.2	0.964
523	290.6	1.029	545	302.8	0.962
524	291.1	1.025	546	303.3	0.959
525	291.7	1.022	547	303.9	0.956
526	292.2	1.019	548	304.4	0.953
527	292.8	1.016	549	305.0	0.950
528	293.3	1.013	550	305.6	0.947
529	293.9	1.009	551	306.1	9.944
530	294.4	1.006	552	306.7	0.941
531	295.0	1.003	553	307.2	0.939

4. Maintain baffles and cryoshroud temperature at less than 27.8K (50R).
5. Heat TPS to 289K (520R).
6. Allow test tank to reach thermal equilibrium at a constant pressure level. Equilibrium conditions are achieved when the temperature reading of test tank thermocouples TC-3, -11 and -31 vary not more than ±1F in 10 hours and the liquid hydrogen boiloff rate changes not more than 0.5% per hour.
7. Measure LH_2 boiloff rate of the test tank.
8. Shutdown test facility.

10.2.2 TEST SPECIMEN PREPARATION - Test specimen preparation was not required. The thermal test of the tank installed MLI system was conducted immediately after the null tests without increasing the vacuum chamber pressure or refilling the LH_2 test tank. The thermal payload simulator heater was turned on 220 hours after 0-time.

10.2.3 THERMAL TEST RESULTS - Liquid hydrogen boiloff and temperatures of the tank insulation thermocouples TC-3, -11, -31 (Figure 9-3 and Table 9-1) are plotted in Figure 10-6, Sheet 1 and 2. The specified thermal payload simulator temperature (TC-62) of 289K (520R) was achieved after 18 hours (238 hours after 0-time). The test continued for 134 hours (372 hours after 0-time) at which time the boiloff rate was 0.01086 kg/hr (0.0239 lb/hr) and dropping at the rate of 0.15%/hr. At that time the decision was made, with concurrence of the NASA COR, to terminate the test due to the projection that additional weeks would be required to achieve a true equilibrium condition. The final 28 hours of testing resulted in an average measured boiloff rate of 0.01146 kg/hr (0.02521 lb/hr), Table 10-12. Temperature test data at 240, 290, 344, and 372 hours after 0-time are presented in Table 10-13 and 10-14. The guard tank was refilled 45 hours after the test began and indicated a liquid level of 60% towards the end of the test.

10.2.4 EVALUATION OF THERMAL TEST RESULTS - The drop of the test tank boiloff rate of 0.15% per hour leads to the conclusion that the insulation was again outgassing. The temperature of 289K (520R) at the TPS surface caused an increase in the temperature and pressure of the trapped gases within the MLI layers. The result was an increase in heat conduction and LH_2 boiloff. Figure 10-6, Sheet 1 of 2 and 2 of 2 shows that the boiloff rate increased

Table 10-12. Thermal Test of Tank Installed MLI Boiloff Data During the Final 28 Hour Period

Equil. Hour	Total Elapsed Time, hr	LH_2 Boiloff kg/hr	LH_2 Boiloff lb/hr	Equil. Hour	Total Elapsed Time, hr	LH_2 Boiloff kg/hr	LH_2 Boiloff lb/hr
0	344	0.01173	0.0258	15	359	0.01159	0.0255
1	345	0.01156	0.0253	16	360	0.01177	0.0259
2	346	0.01145	0.0252	17	361	0.01168	0.0257
3	347	0.01145	0.0252	18	362	0.01159	0.0255
4	348	0.01141	0.0251	19	363	[illegible]	0.0255
5	349	0.01127	0.0248	20	364	0.01177	0.0259
6	350	0.01136	0.0250	21	365	0.01154	0.0254
7	351	0.01145	0.0252	22	366	0.01145	0.0252
8	352	0.01136	0.0250	23	367	0.01132	0.0249
9	353	0.01150	0.0253	24	368	0.01132	0.0249
10	354	0.01150	0.0253	25	369	0.01123	0.0247
11	355	0.01150	0.0253	26	370	0.01095	0.0241
12	356	0.01159	0.0255	27	371	0.01095	0.0241
13	357	0.01173	0.0258	28	372	0.01086	0.0239
14	358	0.01156	0.0261				

Avg. Boiloff: 0.01146 kg/hr (0.02521 lb/hr)

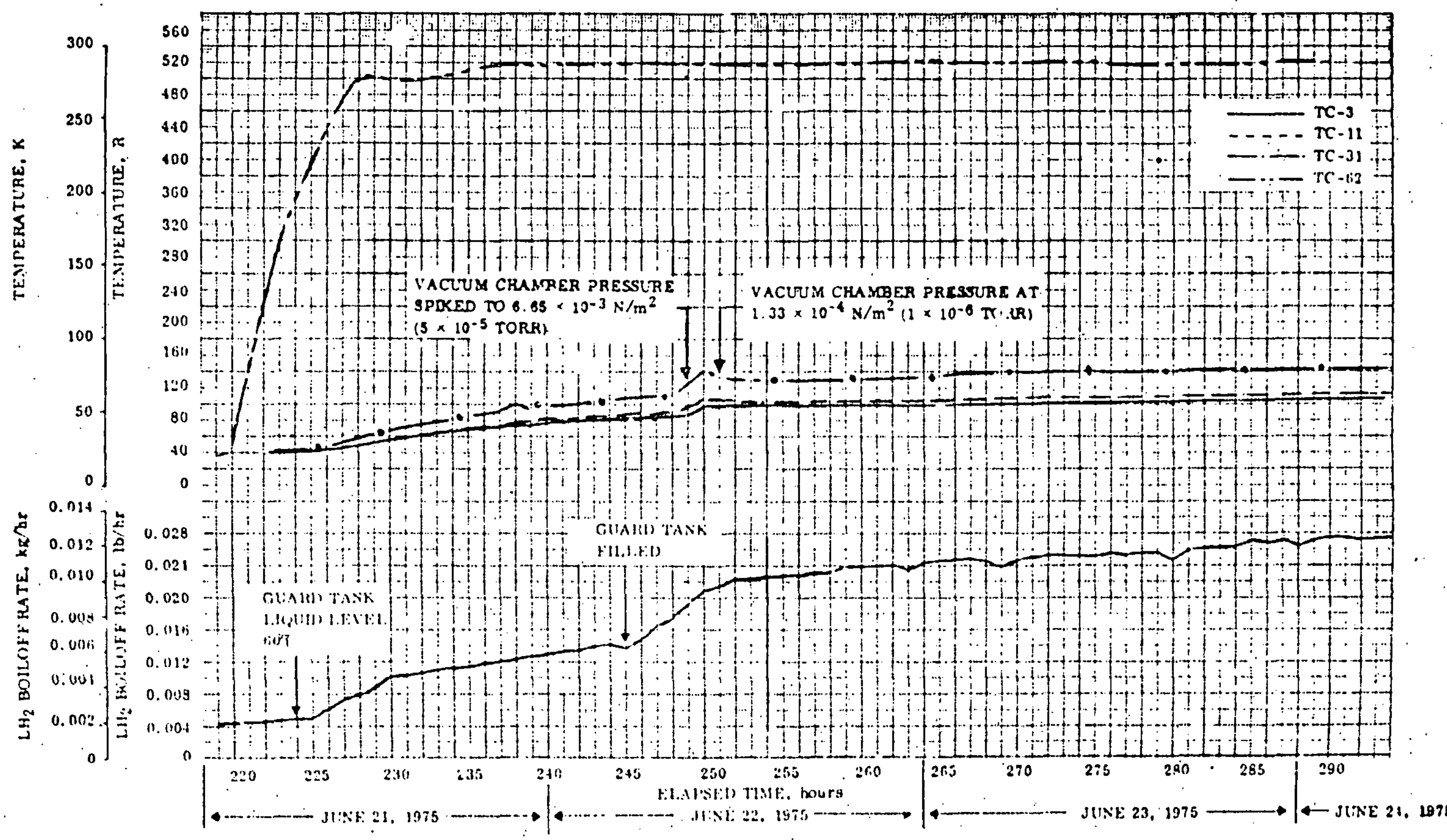

Figure 10-6. Thermal Test of Tank Installed MLI - Start of Test (Elapsed Hours: 219 to 294) - Sheet 1 of 2

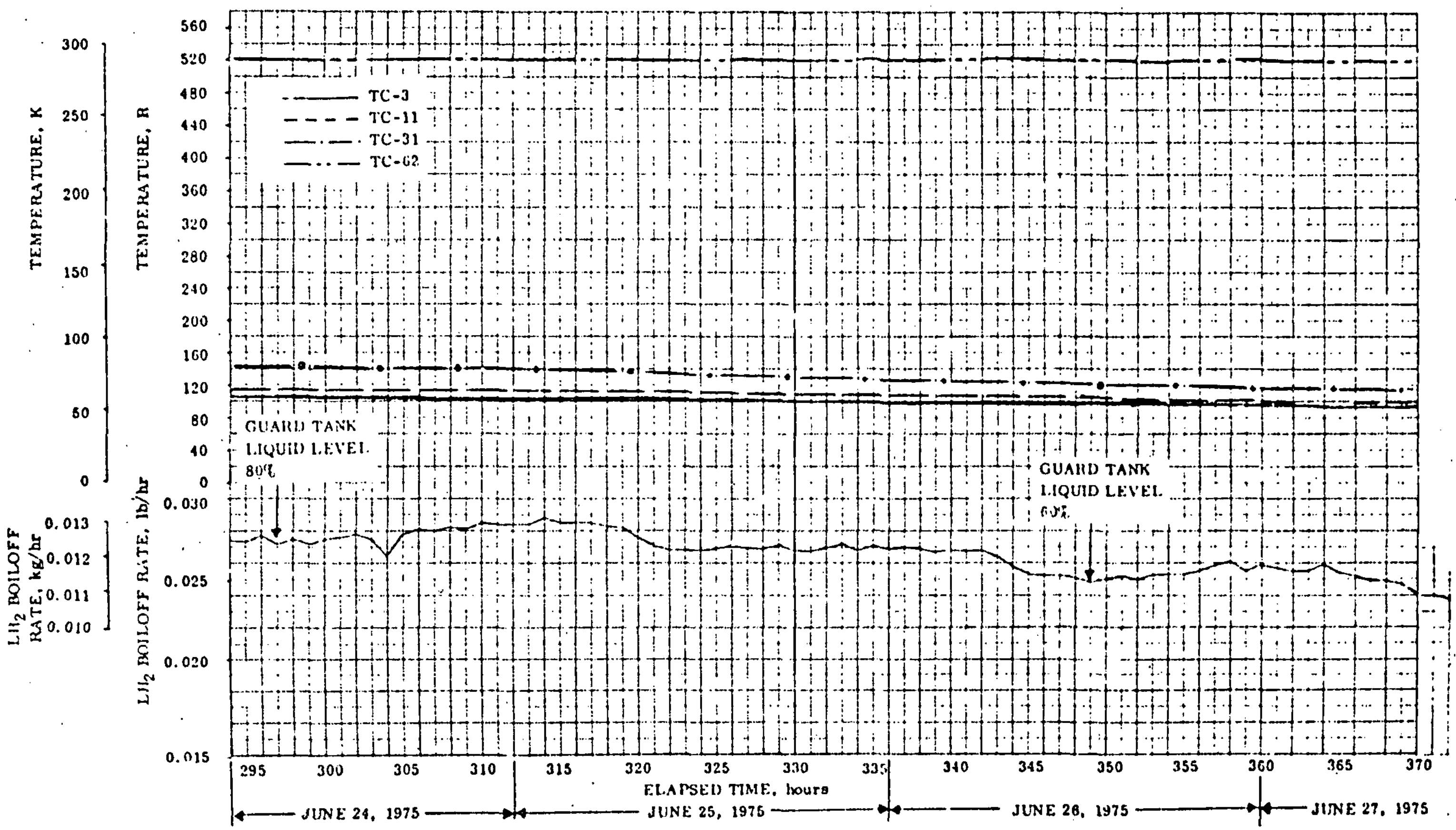

Figure 10-6. Thermal Test of Tank Installed MLI - (Elapsed Hours: 294 to 372) - Sheet 2 of 2

Table 10-13. Test Data at 240 and 290 Hours After 0-Time During Thermal Testing of the Tank Installed MLI System

	240 Hours After 0-Time				290 Hours After 0-Time			
	°F	°R	°C	°K	°F	°R	°C	°K
TC-1	-346.1	113.9	-209.9	63.3	-340.7	119.3	-206.9	66.3
TC-2	-382.0	78.0	-229.9	43.3	-350.9	109.1	-212.6	60.6
TC-3	-384.5	75.5	-231.3	41.9	-354.9	105.1	-214.8	58.4
TC-4	-420.0	40.0	-251.0	22.2	-416.5	43.5	-249.0	24.2
TC-5	-334.8	125.2	-203.6	69.6	-329.0	131.0	-200.4	72.8
TC-6	-380.1	79.9	-228.8	44.4	-347.3	112.7	-210.6	62.6
TC-7	-382.5	77.5	-230.1	43.1	-350.3	109.7	-212.3	60.9
TC-8	-420.5	39.5	-251.3	21.9	-417.0	43.0	-249.3	23.9
TC-9	-320.6	139.4	-195.8	77.4	-314.3	145.7	-192.3	80.9
TC-10	-378.6	81.4	-228.0	45.2	-343.1	116.9	-208.3	64.9
TC-11	-381.6	78.4	-229.6	43.6	-349.0	111.0	-211.5	61.7
TC-12	-420.6	39.4	-251.3	21.9	-416.5	43.5	-249.0	24.2
TC-13	-278.7	181.3	-172.5	100.7	-263.3	196.7	-163.9	109.3
TC-14	-376.5	83.5	-226.8	46.4	-338.5	121.5	-205.7	67.5
TC-15	-381.0	79.0	-229.3	43.9	-346.0	114.0	-209.9	63.3
TC-16	-420.5	39.5	-251.3	21.9	-416.0	44.0	-218.8	24.4
TC-17	-213.0	241.0	-139.3	133.9	-187.9	272.1	-122.0	151.2
TC-18	-373.8	86.2	-225.3	47.9	-332.5	127.5	-202.4	70.8
TC-19	-320.1*	139.6	-195.6	77.6	-323.4	136.6	-197.3	75.9
TC-20	-420.0	40.0	-251.0	22.2	-415.2	44.8	-248.3	24.9
TC-21	-177.6	282.4	-116.3	156.9	-137.3	322.7	-93.9	179.3
TC-22	-371.6	88.4	-224.1	49.1	-328.6	131.4	-200.2	73.0
TC-23	-381.1	78.9	-229.4	43.8	-344.9	115.1	-209.3	63.9
TC-24	-418.9	41.1	-250.4	22.8	-414.3	45.7	-247.8	25.4
TC-25	-140.0	320.0	-95.4	177.8	-106.2	353.8	-76.6	196.6
TC-26	-370.0	90.0	-223.2	50.0	-325.3	134.6	-198.4	74.8
TC-27	-381.0	79.0	-229.3	43.9	-344.7	115.3	-209.1	64.0
TC-28	-416.2	43.8	-248.9	24.3	-396.0	64.0	-237.6	35.6
TC-29	-124.7	335.3	-86.9	186.3	-96.1	363.9	-71.0	202.2
TC-30	-340.9	119.1	-206.0	66.2	-288.9	171.1	-178.1	95.1
TC-31	-363.7	96.3	-219.7	53.5	-316.2	143.8	-193.3	79.9

	240 Hours After 0-Time				290 Hours After 0-Time			
	°F	°R	°C	°K	°F	°R	°C	°K
TC-32	-411.8	48.2	-246.4	26.8	-396.0	64.0	-237.6	35.6
TC-33	**				-327.4	132.6	-199.5	73.7
TC-34	*				-419.5	40.5	-250.7	22.5
TC-35	-413.1	46.9	-247.1	26.1	-413.3	46.7	-217.3	25.9
TC-36	**				**			
TC-37 to -59	No Blankets on TPS							
TC-60	60.3	520.3	15.9	289.1	59.7	519.7	15.5	288.7
TC-61	52.0	512.0	11.7	284.4	53.7	513.7	12.2	285.4
TC-62	58.2	518.2	14.7	287.9	59.7	519.7	15.5	288.7
TC-63	56.4	516.4	13.6	286.8	58.2	518.2	14.7	287.9
TC-64	54.6	514.6	12.7	285.9	55.2	515.2	13.0	286.2
TC-65	59.1	519.1	15.2	288.4	59.7	519.7	15.5	288.7
TC-66	74.3	534.3	23.6	296.8	77.0	537.0	25.1	298.3
TC-67	-127.2	322.8	-88.3	184.9	-119.0	341.0	-83.8	189.4
TC-68	49.5	509.5	9.9	283.1	51.6	511.6	11.0	284.2
TC-69	48.3	508.3	9.2	282.4	49.8	509.8	10.0	283.2
TC-70	48.6	508.6	9.4	282.6	51.0	511.0	10.7	283.9
TC-71	46.1	506.1	8.0	281.2	48.3	508.3	9.2	282.4
TC-72	55.8	515.8	13.4	286.6	58.5	518.5	14.9	288.1
TC-73	56.4	516.4	13.7	286.9	58.8	518.8	15.0	288.2
TC-74	54.9	514.9	12.9	286.1	57.3	517.3	14.2	287.4
TC-75	Diffusion Pump							
TC-76	29.3	489.3	-1.4	271.8	29.3	489.3	-1.4	271.8
TC-77	103.4	563.4	39.8	313.0	105.8	565.8	41.1	314.3
TC-78	56.7	516.7	13.9	287.1	55.8	515.8	13.4	286.6
TC-79	-317.0	143.0	-193.8	79.4	-317.0	143.0	-193.8	79.4
TC-80	52.2	512.2	11.4	284.6	53.7	513.7	12.2	285.4
TC-81 to -127	**							

* Incorrect Reading

** See Section 9.2.1

Table 10-11. Test Data 344 and 372 Hours After 0-Time During Thermal Testing of the Tank Installed MLI System

	344 Hours After 0-Time				372 Hours After 0-Time					344 Hours After 0-Time				372 Hours After 0-Time			
	°F	°R	°C	°K	°F	°R	°C	°K		°F	°R	°C	°K	°F	°R	°C	°K
TC-1	-343.3	116.7	-208.4	64.8	-346.2	113.8	-210.0	63.[illegible]	TC-31	-336.7	123.3	-204.7	68.5	-346.9	113.1	-210.4	62.8
TC-2	-357.7	102.3	-216.4	56.8	-363.3	96.7	-219.5	53.	TC-32	-399.8	60.2	-239.8	33.4	-403.5	56.5	-241.8	31.4
TC-3	-360.8	99.2	-218.1	55.1	-366.5	93.5	-221.3	[illegible]	TC-33	-313.6	146.4	-191.9	81.3	-313.4	146.6	-191.8	81.4
TC-4	-415.8	44.2	-248.6	24.6	-416.3	43.7	-248.9	24.3	TC-34	-417.5	42.5	-249.6	23.6	-4 7.3	42.7	-249.5	23.7
TC-5	-332.5	127.5	-202.4	70.8	-335.9	124.1	-201.3	68.9	TC-35	-411.8	48.2	-246.4	26.8	-411.8	48.2	-246.4	26.8
TC-6	-354.7	105.3	-214.7	59.5	-360.8	99.2	-218.1	55.1	TC-36	-381.9	78.2	-229.8	43.4	-381.[illegible]	78.1	-229.8	43.4
TC-7	-357.1	102.9	-216.0	57.2	-363.4	96.6	-219.5	53.7	TC-37	No blankets on TPS							
TC-8	-416.3	43.7	-248.9	24.3	-417.0	43.0	-249.3	23.9	to -59								
TC-9	-319.4	140.6	-195.1	78.1	-323.7	136.3	-197.5	75.7	TC-60	64.2	524.2	18.0	291.2	60.0	520.0	15.7	288.9
TC-10	-351.7	108.3	-213.0	60.2	-358.4	101.6	-216.8	56.4	TC-61	56.8	516.8	13.9	287.1	53.7	513.7	12.2	285.4
TC-11	-354.5	105.5	-214.6	58.6	-361.2	98.8	-218.3	54.9	TC-62	63.8	523.8	17.8	291.0	60.9	520.9	16.2	289.4
TC-12	-415.8	44.2	-248.6	24.6	-416.3	43.7	-248.9	24.3	TC-63	61.4	521.4	16.5	289.7	59.1	519.1	15.2	288.4
TC-13	-275.5	184.5	-170.7	102.5	-280.2	179.8	-173.3	99.9	TC-64	59.0	519.0	15.1	288.3	56.4	516.4	13.7	286.9
TC-14	-348.1	111.9	-211.0	62.2	-355.5	104.5	-215.1	[illegible]	TC-65	63.2	523.2	17.5	290.7	60.6	520.6	16.0	289.2
TC-15	-353.4	106.6	-214.0	59.2	-360.3	99.7	-217.8	55.4	TC-66	82.9	542.9	28.4	301.6	78.4	538.4	25.9	299.1
TC-16	-414.9	45.1	-248.1	25.1	-415.8	44.2	-248.6	24.6	TC-67	-121.0	339.0	-84.9	188.3	-124.3	335.7	-86.7	186.5
TC-17	-210.9	249.1	-134.8	139.4	-229.8	230.2	-145.3	127.9	TC-68	49.3	509.3	9.7	282.9	51.6	511.6	11.0	284.2
TC-18	-344.0	116.0	-208.8	64.4	-352.1	107.9	-213.3	59.9	TC-69	47.7	507.7	8.8	282.0	49.8	509.8	10.0	283.2
TC-19	-321.4	138.6	-196.2	77.0	-322.8	137.2	-197.0	76.2	TC-70	49.0	509.0	9.6	282.8	51.3	511.3	10.9	284.1
TC-20	-414.5	45.5	-247.9	25.3	-416.0	44.0	-248.9	24.4	TC-71	46.5	506.5	8.2	281.4	48.9	508.9	9.5	282.7
TC-21	-172.5	287.5	-113.5	159.7	-196.1	263.9	-126.6	146.6	TC-72	63.7	523.7	17.7	290.9	78.5	538.5	26.0	299.2
TC-22	-344.4	115.6	-207.3	65.9	-350.0	110.0	-212.1	61.1	TC-73	64.4	524.4	18.1	291.[illegible]	79.4	539.4	26.5	299.7
TC-23	-352.9	107.1	-213.7	59.5	-360.2	99.8	-217.8	55.4	TC-74	63.1	523.1	17.4	290.6	78.3	538.3	25.9	299.1
TC-24	-414.1	45.9	-247.7	25.5	-414.7	45.3	-248.0	25.2	TC-75	Diffusion Pump							
TC-25	-154.0	306.0	-103.2	170.0	-178.9	281.1	-117.0	156.2	TC-76	29.3	489.3	-1.4	271.8	30.8	490.8	-0.5	272.7
TC-26	-338.9	121.1	-205.9	67.3	-347.7	112.3	-210.8	62.4	TC-77	102.3	662.3	94.7	367.9	100.5	560.5	38.2	311.4
TC-27	-353.2	106.8	-213.9	59.3	-360.4	99.6	-217.9	55.3	TC-78	62.4	522.4	17.0	290.2	75.5	535.5	24.3	297.5
TC-28	-399.8	60.2	-239.8	33.4	-402.8	57.2	-241.4	31.8	TC-79	-316.4	143.6	-193.4	79.8	-315.8	144.2	-193.1	80.1
TC-29	-154.9	305.1	-103.7	169.5	-181.6	278.4	-118.5	154.7	TC-80	63.5	523.5	17.6	290.8	76.1	536.1	24.6	297.8
TC-30	-317.2	142.8	-193.9	79.3	-331.4	128.6	-201.8	71.4	TC-81	**							
									to -127								

* Incorrect Reading

** See Section 9.2.1

for 94 hours before it started falling again. The readings of thermocouples TC-3, -11 and -31 at the outer face sheet of the inner blanket indicated a rise of the temperature for approximately 70 hours. The temperatures remained at this level for an additional 20 hours before they decreased again. This trend is also true for the remaining TC readings along the tank as can be shown in Figures 10-7 and 10-8. The figures are temperature distribution plots of 240, 290, 344 and 372 hours, after 0-time. The rise of temperature forced the frozen interstitial gas molecules such as water, air or nitrogen, to vaporize resulting in higher heat transfer by conduction. A combination of higher conduction and lateral heat transfer through the MLI layers forced the MLI temperature to drop again. A typical example of the combination heat-transfer is provided by thermocouple TC-31, (Figure 10-6, Sheet 2 of 2). The temperature at that location started to fall slowly and then steeper. This indicates a combination of lateral and gaseous conduction heat transfer. The temperature changes of TC-32 at the inner face sheet of the inner blanket next to the tank were relatively small as expected. The temperature variation is shown below:

Hours After 0-Time	240	290	344	372	
Temperature	26.8 (48.2)	35.6 (64.0)	33.4 (60.2)	31.4 (56.5)	°K (°R)

Figures 10-7, 10-8 and 10-9 show that the temperatures along the outer face sheet of the outer blanket rose most significantly in the lower hemisphere (90 to 180 degree location) due to radiation heat transfer from the heated, uninsulated thermal payload simulator. The temperature slope of the remaining thermocouples became steeper at the 165 degree to 180 degree location, showing again the influence of gaseous conduction between the radiation shields. During the cool-off period of the radiation shields the LH_2 boiloff rate decreased , as expected. A continuation of the test (for days or weeks) beyond 372 hours after 0-time would have resulted in a stabilization of the flow rates.

The final heat flow rates were estimated utilizing the MLI heat transfer Equation 10-1 (Section 10.1.4). The calculation was performed by subdividing the tank in seven node sections for which the temperatures of the outer face sheets of the outer MLI blankets were known by thermocouple measurements. The average temperatures (figure 9-2 and table 10-26) used for the calculations were as follows:

TC-1	-5	-9	-13	-17	-21	-25/-29
64.0(115.2)	69.9(125.8)	76.9(138.4)	101.2(182.1)	133.1(239.6)	153.2(275.7)	163.1(293.5)

The calculation resulted in a heat flow rate of 0.3519 watts (1.201 BTU/hr). This calculation does not include heat leaks through insulation attachments, extraneous heat leaks, the 0.2 watt (0.683 BTU/hr) power input to the internal heater and heat leaks caused by thermal acoustic oscillations.

10.3 CUSTOMIZED MLI THERMAL PERFORMANCE TEST

The objective of the "customized" MLI test was to determine the thermal performance of the test tank insulation at a TPS temperature of 289K (520R) and a TPS/test tank

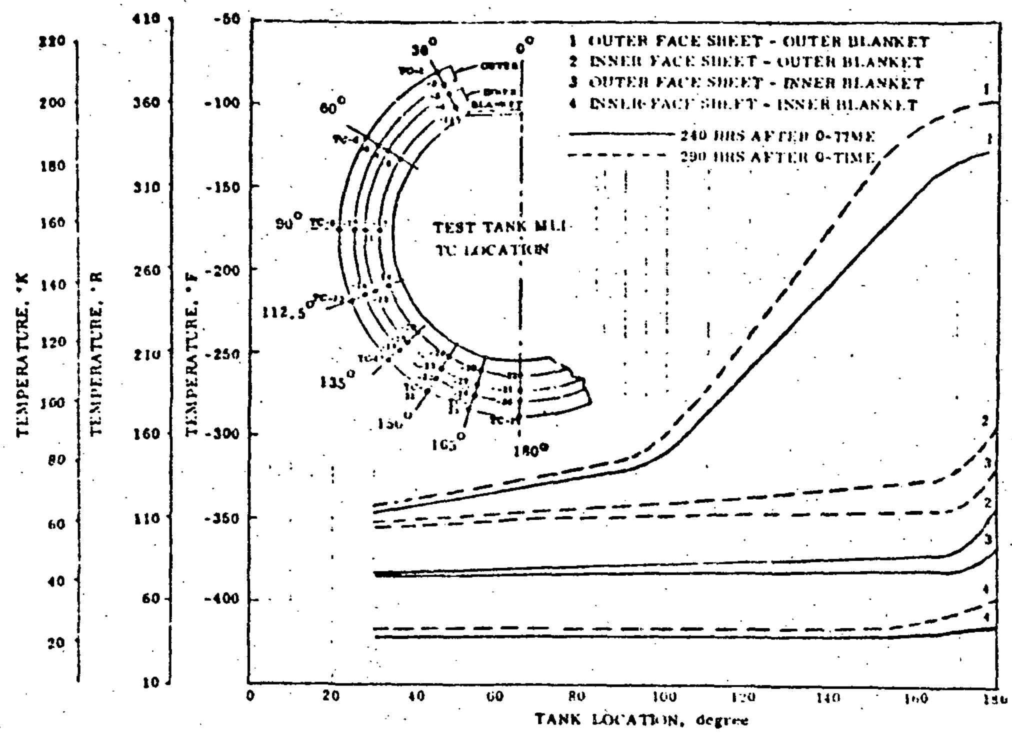

Figure 10-7. Test Tank MLI Temperature Distribution at 240 and 290 Hours After 0-Time

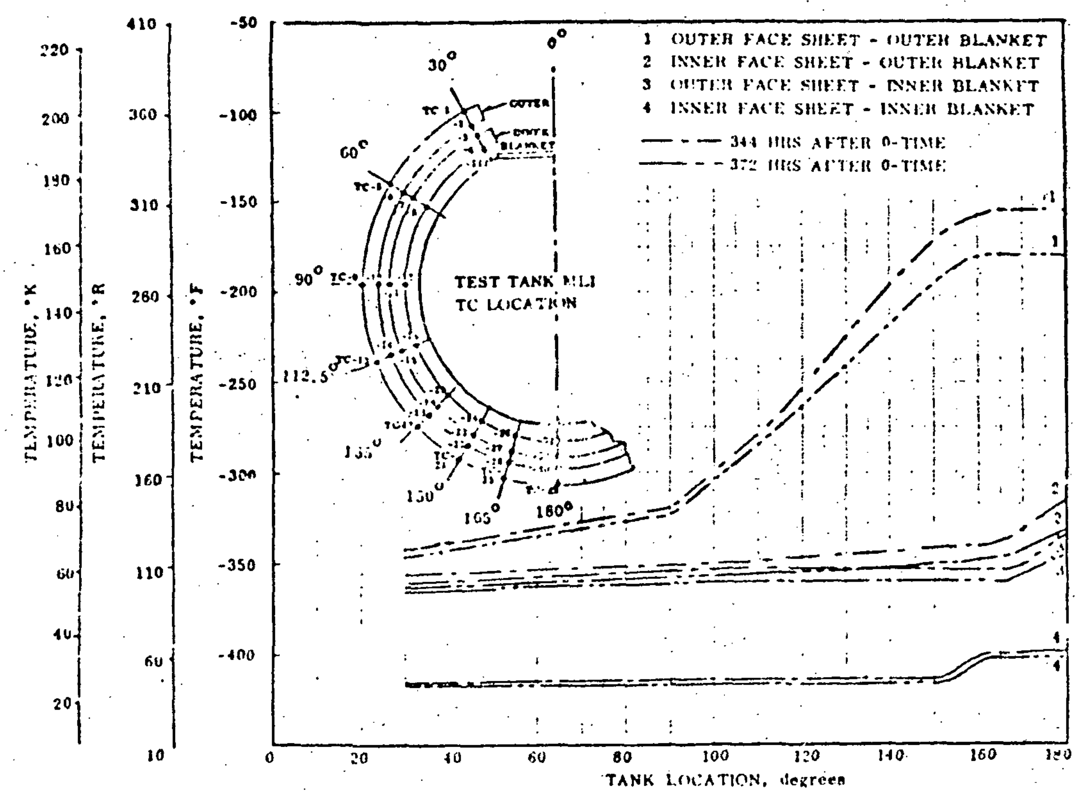

Figure 10-8. Test Tank MLI Temperature Distribtuion at 344 and 372 Hours After 0-Time

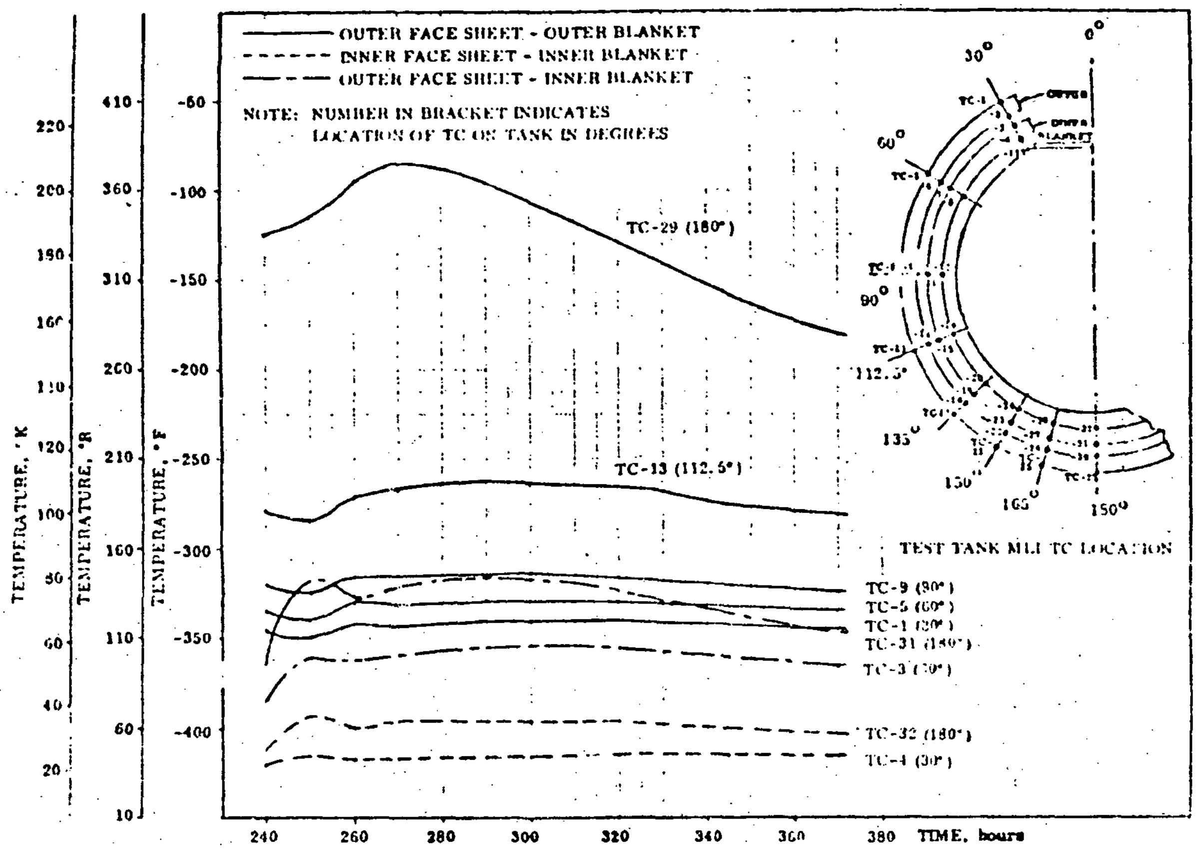

Figure 10-9. Test Tank MLI Temperature Distribution Between 240 and 372 Hours After 0-Time

spacing of 0.457 m (18 in), 0.305 m (12 in) and 0.152 m (6 in). During this test three MLI blankets (Section 6) were installed on the surface of the thermal payload simulator. Both inner and outer test tank MLI blankets remained on the test tank. The detailed test objectives and conditions are presented in Table 10-1. The "customized" MLI thermal performance task was initiated on July 22, 1975 and completed on August 16, 1975. The total test time was 719 hours. This time included two null tests, one at the beginning and one at the end of the test operation. All tests were conducted utilizing an 0.2 watt power input to the test tank heater to promote fluid mixing within the tank.

The following sections present the test procedures, test specimen preparation, test results and evaluation of the test results.

10.3.1 CUSTOMIZED MLI TEST PROCEDURE - The procedure was as follows:

1. Open the environmental chamber
2. Install the three MLI blankets of the TPS (Section 6), utilizing three access openings in the cryoshroud.
3. Tank - TPS spacing 0.457 m (18 in).
4. Close environmental chamber.
5. Pump down environmental chamber to 6.65 $N/m^2 \times 10^{-3}$ (5×10^{-5} torr).

6. Purge chamber with GHe

7. Purge tank with hot GN_2 for 6 hours at a temperature of 333K (600R) max.

8. Pump down environmental chamber to 1.33×10^{-4} N/m^2 (1×10^{-6} torr).

9. Cool baffles, cryoshroud and TPS surface temperatures below 27.8K (50R) and maintain these temperatures.

10. Fill test tank with LH_2.

11. Apply 0.2 W (0.683 BTU/hr) to the test tank heater and maintain this power level during the null and customized MLI testing.

12. Allow test tank fluid to reach thermal equilibrium at a constant pressure level. Equilibrium conditions are achieved when the temperature reading of thermocouples TC-29 (Figure 9-2), TC-38, -47, and -53 (Figure 9-4) vary not more than ± 0.55K (±1F) during a 10 hour test period and the LH_2 boiloff rate changes not more than 0.5% per hour.

13. Maintain environmental chamber pressure at less than 1.33×10^{-4} N/m^2 (1×10^{-6} torr).

14. Maintain baffles, cryoshroud, and TPS surface at less than 27.8K (50R).

15. Conduct initial null test. Check that the boiloff rate at the 0.2 W power level agrees with the previous boiloff rates obtained during the previous null testing (Section 10.1.3.2).

16. Heat up TPS to 289K (520R).

17. Allow test tank fluid to reach equilibrium using the same criteria as required in Step 12. Determine LH_2 boiloff rates for customized MLI Test No. 1.

18. Adjust TPS/test tank spacing to 0.305 m (12 in).

19. Maintain TPS temperature at 289K (520R).

20. Allow test tank fluid to reach equilibrium using the same criteria as required in Step 12. Determine LH_2 boiloff rates for customized MLI Test No. 2.

21. Adjust TPS/test tank spacing to 0.152 m (6 in).

22. Maintain TPS temperature at 289K (520R).

23. Allow test tank fluid to reach equilibrium using the same criteria as required in Step 12. Determine LH_2 boiloff rates for customized MLI Test No. 3.

24. Conduct final null test. Repeat Step 15.

25. Shut down test facility.

10.3.2 TEST SPECIMEN PREPARATION - After completion of the "Tank Installed MLI" thermal test (Section 10.2), the vacuum chamber was opened. Three pre-fabricated MLI blankets (Section 6) were installed on the TPS surface utilizing three access openings in the cryoshroud. These blankets were required for the "Customized MLI" thermal performance test. While the vacuum chamber was open, thermocouples TC-181 and TC-182 (Figure 9-3 and Table 9-1) were added 0.33 m (13 in) and 0.381 (15 in) from the outer edge of the cryoshroud lid. Thermocouples TC-183, -184 and -185 were installed 0.089 m (3.5 in), 0.239 m (9.4 in) and 0.686 m (27 in) from the outer edge of the TPS.

The vacuum chamber was then closed and prepared for pump down. A series of purging and evacuation cycles were initiated to remove condensible gases from the MLI and vacuum facility. During the initial pump down on July 11, 1975, the vacuum chamber was evacuated from atmospheric pressure to a pressure of approximately 199.5 N/m^2 (1.5 torr) utilizing two mechanical vacuum pumps. The chamber was back filled with gaseous helium to a pressure of 13.8 kN/m^2 (2.0 psia) and left in this condition until July 14, 1975. Using the mechanical pumping system, the chamber pressure was reduced during that day to 46.55 N/m^2 (0.35 torr). Towards the end of the working day, the chamber was back filled with gaseous helium to 13.8 kN/m^2 (2.0 psia). It remained at this pressure during the night. On July 15, the chamber was pumped down to a pressure of 0.53 N/m^2 (0.004 torr) utilizing both the mechanical and diffusion pumps. The chamber was pressurized again to 13.8 kN/m^2 (2.0 psia) and left in this condition until the morning of July 16, 1975. During this day the test tank was heated with gaseous nitrogen for a period of 6 hours, at an inlet gas temperature of 334.4K (620R) and a gas flow rate of 7.09 kg/hr (15.6 lb/hr). The thermal payload simulator surface was kept at a temperature of 337.2K (607R). At the end of this day the chamber was evacuated to 7.88 × 10^{-3} (6 × 10^{-5} torr) and then back filled with GHe to a pressure of 13.8 kN/m^2 (2.0 psia). Chamber evacuation and back filling of the chamber with gaseous helium was repeated during July 17 and 18. The chamber remained under a helium pressure of 13.8 kN/m^2 (2.0 psia) during July 19 and 20. On July 21 the chamber was evacuated to 5.32×10^{-4} N/m^2 (4 × 10^{-6} torr) utilizing the diffusion pump and cold trap.

10.3.3 CUSTOMIZED MLI TEST RESULTS -

10.3.3.1 Initial Null Test - The actual test activity started on July 22, 1975 with the initiation of a null test. The spacing between TPS and test tank was 0.457 m (18 in). After filling the cryoshroud, baffles, TPS, guard tank and test tank with liquid hydrogen the cryoshroud vacuum pressure was approximately 5.32×10^{-5} N/m^2 (4×10^{-7} torr). Power input to the test tank was maintained at 0.2 watts. Forty seven hours after 0-time it was decided to back fill the chamber with gaseous helium to a pressure of 26.6 N/m^2 (0.2 torr) in order to establish a high heat transfer rate to obtain a quick chilldown of the MLI. The rapid temperature drop indicated by the TPS-MLI thermocouples TC-38, -47 and -53 (Figure 9-5) and the test tank MLI thermocouples TC-29 is shown in Figure 10-10, Sheet 1. This technique reduces the long hold time which is otherwise necessary to achieve thermal equilibrium. A vacuum pressure of 1.33×10^{-4} N/m^2 (1×10^{-6} torr) was recovered after 3 hours. The null test was conducted for 91 hours (Figure 10-10, Sheet 1 and 2) at which time the boiloff rate was 0.00278 kg/hr (0.00612 lb/hr) and dropping at the rate of 0.2% per hour. At that time the decision was made with the concurrence of the NASA COR to terminate the null test. Temperature changes of the selected thermocouples and the decrease of the boiloff rate were within the test criteria for the final 16 hours of testing (75 hours to 91 hours after 0-time). This period was therefore selected as the thermal equilibrium period. The LH_2 boiloff data are shown in Table 10-15. The average boiloff rate during this time was 0.00283 kg/hr (0.00623 lb/hr). Temperature distribution data at beginning and end of the thermal equilibrium period are presented in Table 10-16.

10.3.3.2 Thermal Test No. 1, 0.457 m (18 in) TPS/Test Tank Spacing - The temperature of the thermal payload simulator was raised to the required 288.9K (520R) on July 26, 1975 to start the first customized MLI thermal performance test (Figure 10-10, Sheets 2 and 3) with the spacing of 0.457 m (18 in) between TPS and test tank. The power input to the test tank heater was maintained at 0.2 watts. The test was completed on August 4, 1975. The thermal equilibrium period began 238 hours after 0-time (Figure 10-10, Sheet 4) and was continued for 73 hours (Figure 10-10, Sheet 5). The average boiloff rate during the equilibrium period was 0.00355 kg/hr (0.00780 lb/hr). Liquid hydrogen boiloff rates and temperatures are shown in Table 10-17, 10-18, and Figure 10-10, Sheets 1 through 5.

Table 10-15. Initial Null Test - 0.2 Watt Power Input, Boiloff Data During the Thermal Equilibrium Period

Equil. Hour	Total Elapsed Time, hrs	LH_2 Boiloff kg/hr	lb/hr
0	75	0.00289	0.00636
1	76	0.00289	0.00636
2	77	0.00282	0.00621
3	78	0.00271	0.00596
4	79	0.00284	0.00624
5	80	0.00286	0.00630
6	81	0.00285	0.00627
7	82	0.0028[illegible]	0.00627
8	83	0.00286	0.00630
9	84	0.00286	0.00630
10	85	0.00285	0.00627
11	86	-	-
12	87	-	-
13	88	-	-
14	89	0.00280	0.00615
15	90	0.00278	0.00612
16	91	0.00278	0.00612
Average Boiloff 0.00283 kg/hr (0.00623 lb/hr)			

10.3.3.3 Thermal Test No. 2, 0.305 m (12 in) TPS/Test Tank Spacing - The TPS was moved from the 0.457 m (18 in) to the 0.305 m (12 in) position on 4 August 1975, 315 hours after 0-time. Except for the TPS position, the test conditions were the same as those of thermal test no. 1. The thermal equilibrium period began 429 hours after 0-time, (Figure 10-10, Sheet 7) and continued for 51 hours until 480 hours after 0-time (Figure 10-10, Sheet 7) on 11 August 1975.

The average boiloff rate during the equilibrium period was 0.00358 kg/hr (0.00788 lb/hr). Boiloff rates for each hour of testing are shown in Table 10-19. The temperature of MLI thermocouples TC-53, 47, 38 and 29 and the TPS temperature (TC-183) are presented in Figure 10-10, Sheets 5 through 7. Temperature distribution data at the beginning and end of the thermal equilibrium period are shown in Table 10-20.

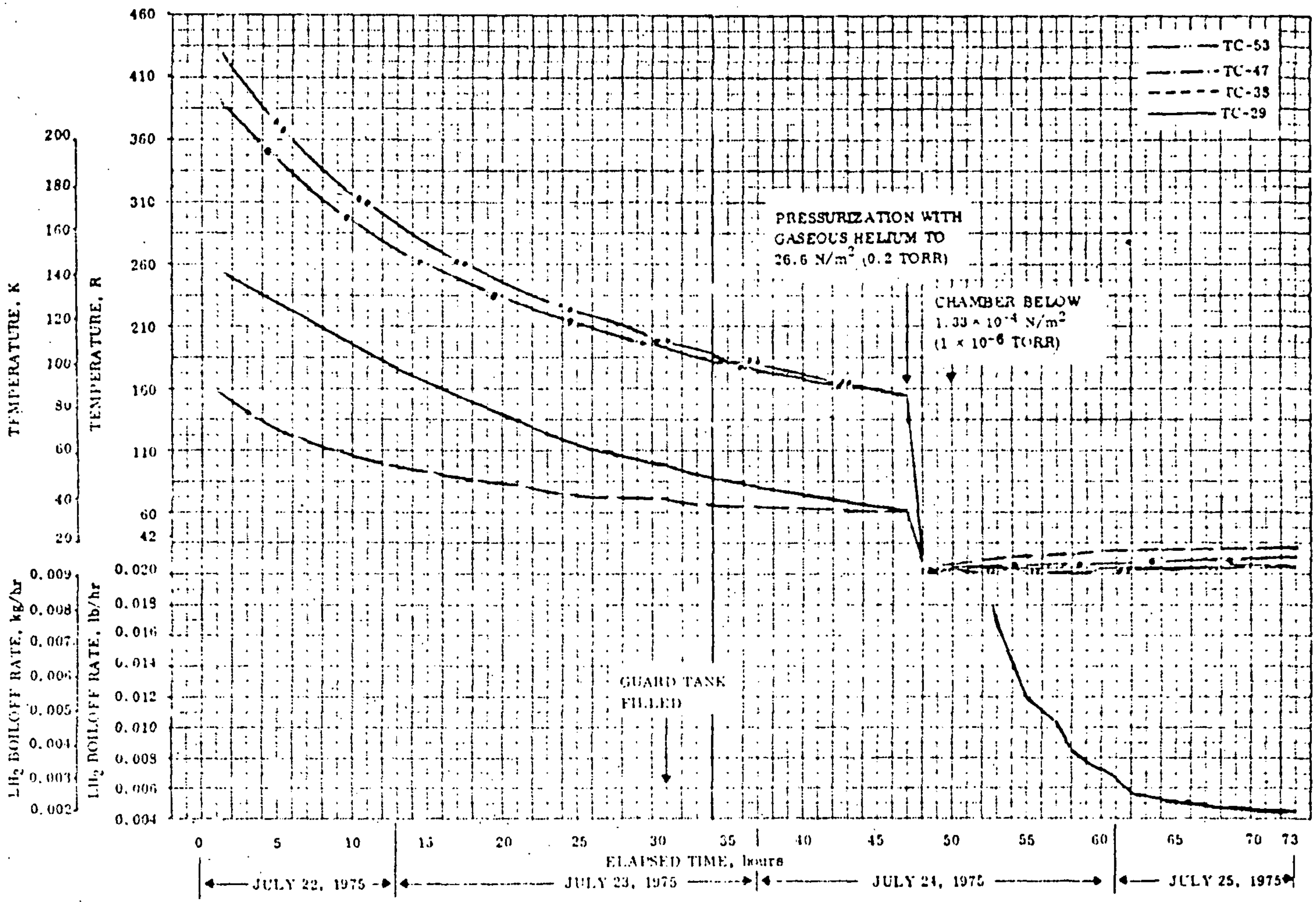

Figure 10-10. Customized MLI Thermal Test - Start of Initial Null Test and Approach to Thermal Equilibrium (Elapsed Hours 0 to 73) - Sheet 1 of 10

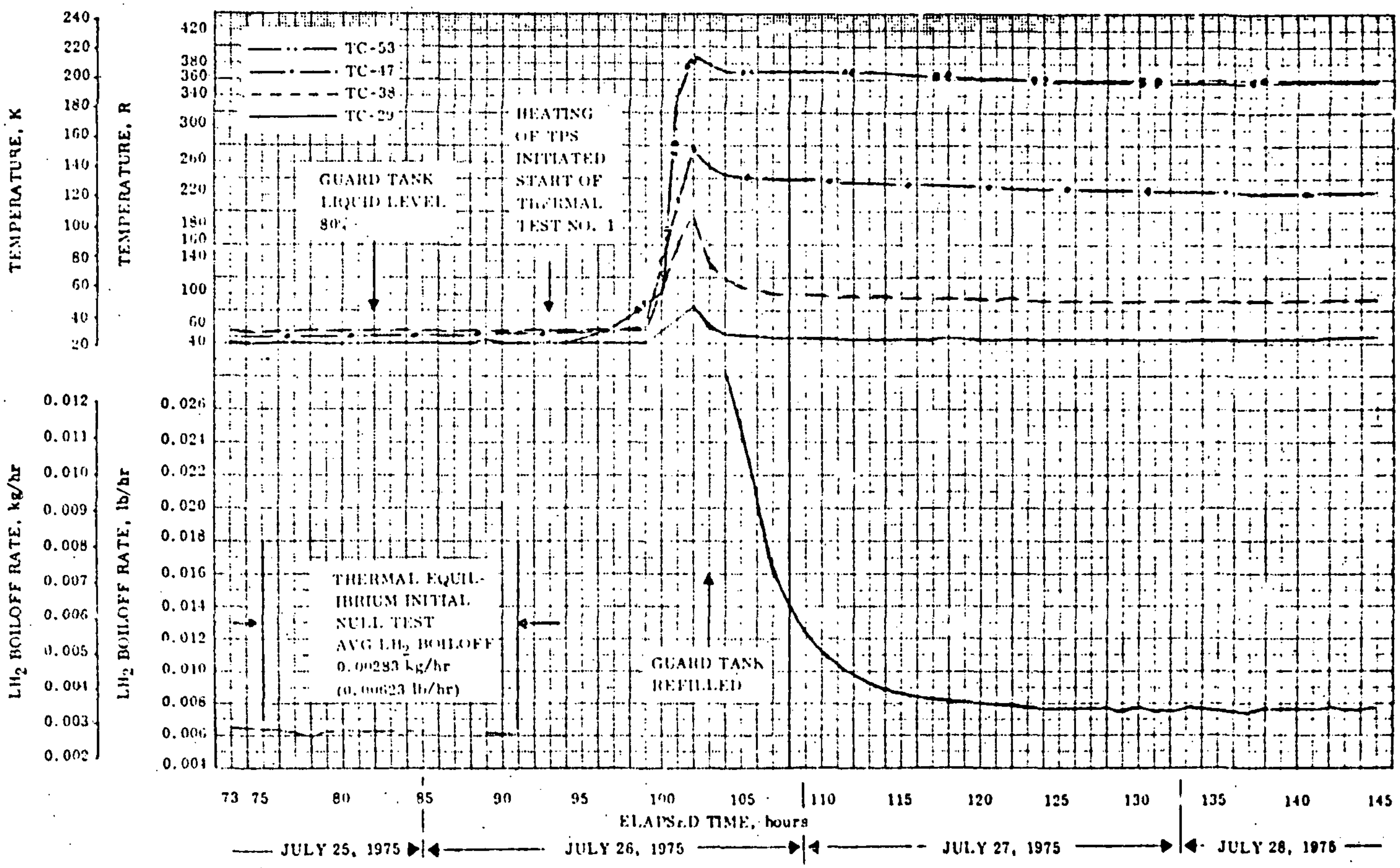

Figure 10-10. Customized MLI Thermal Test - Initial Null Test Thermal Equilibrium and Start of Customized MLI Test No. 1 (Elapsed Hours: 73 to 145) - Sheet 2 of 10

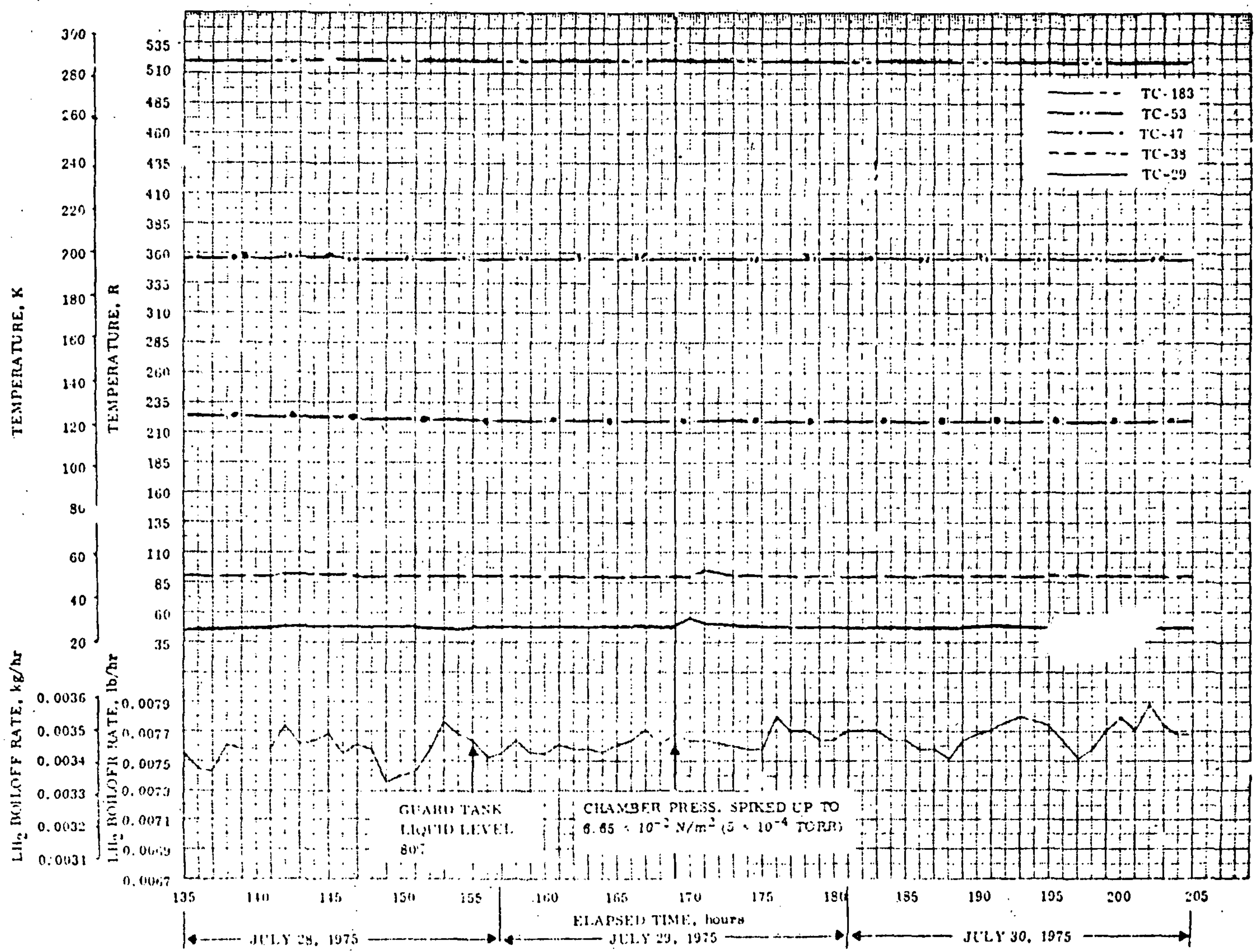

Figure 10-10. Customized MLI Thermal Test - Approach to Thermal Equilibrium of Test No. 1 (Elapsed Hours: 135 to 205) - Sheet 3 of 10

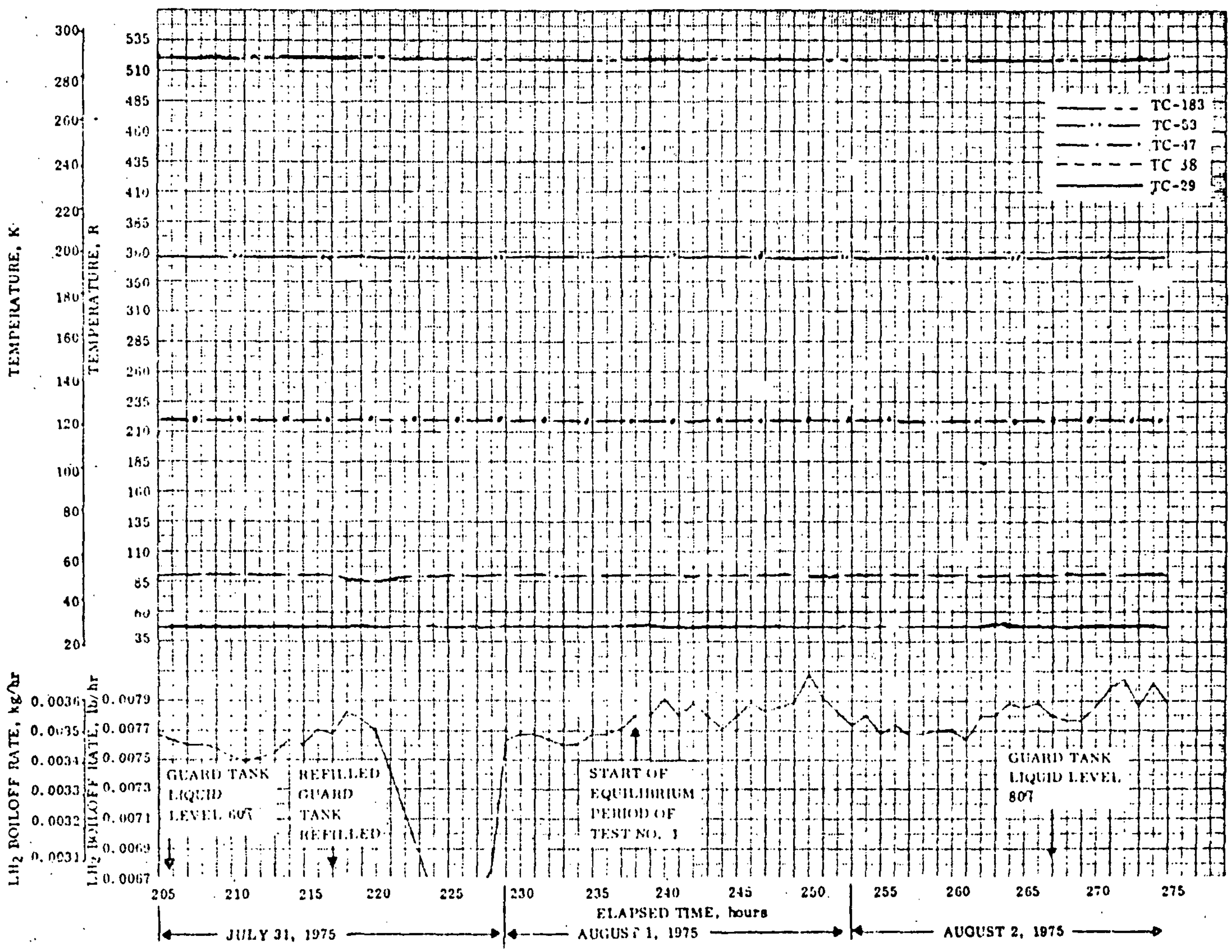

Figure 10-10. Customized MLI Thermal Test - Start of Thermal Equilibrium Period of Test No. 1 (Elapsed Hours: 205 to 275) - Sheet 4 of 10

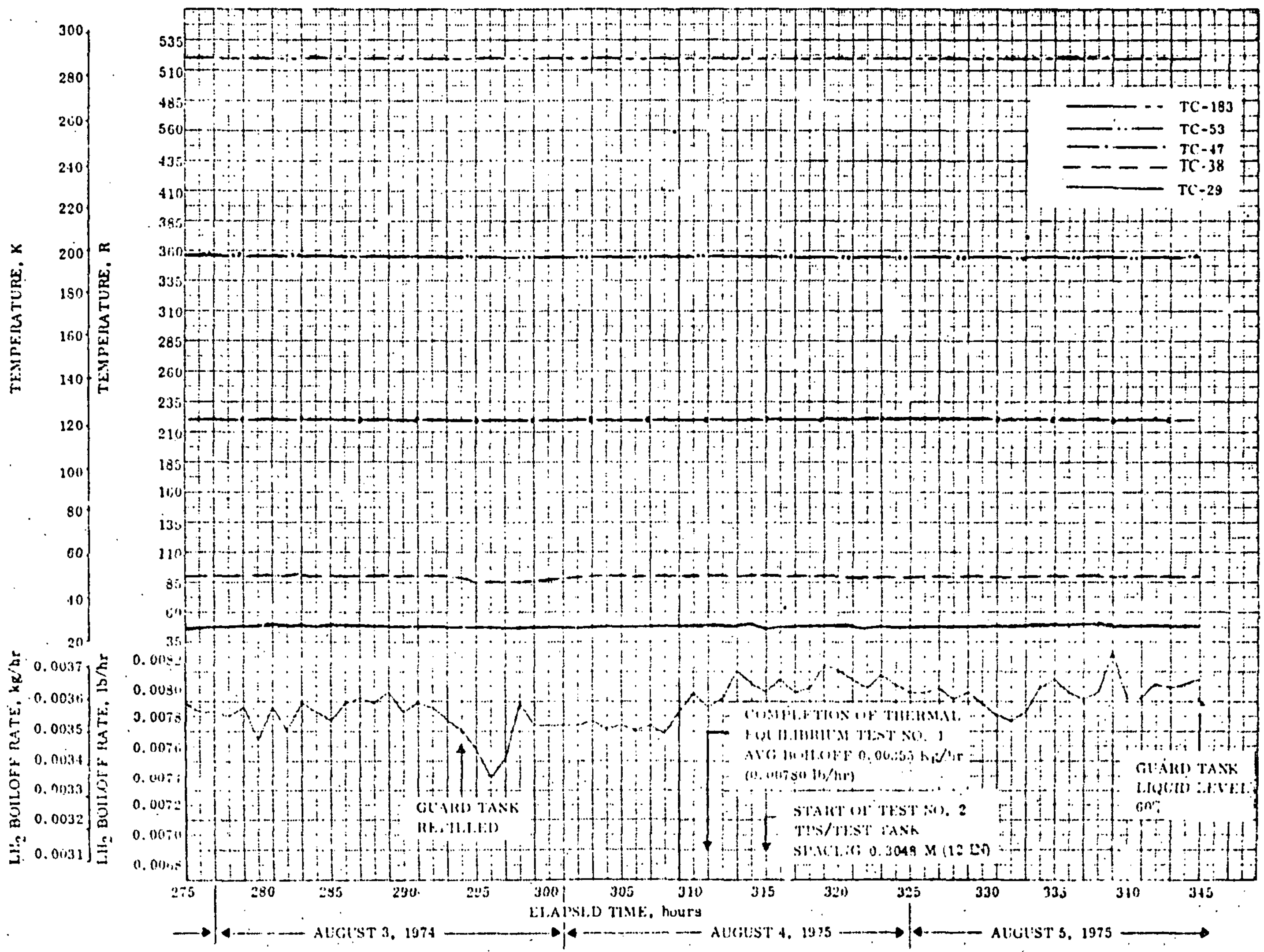

Figure 10-10. Customized MLI Thermal Test - Completion of Test No. 1 and Start of Test No. 2 (Elapsed Hours: 275 to 345) - Sheet 5 of 10

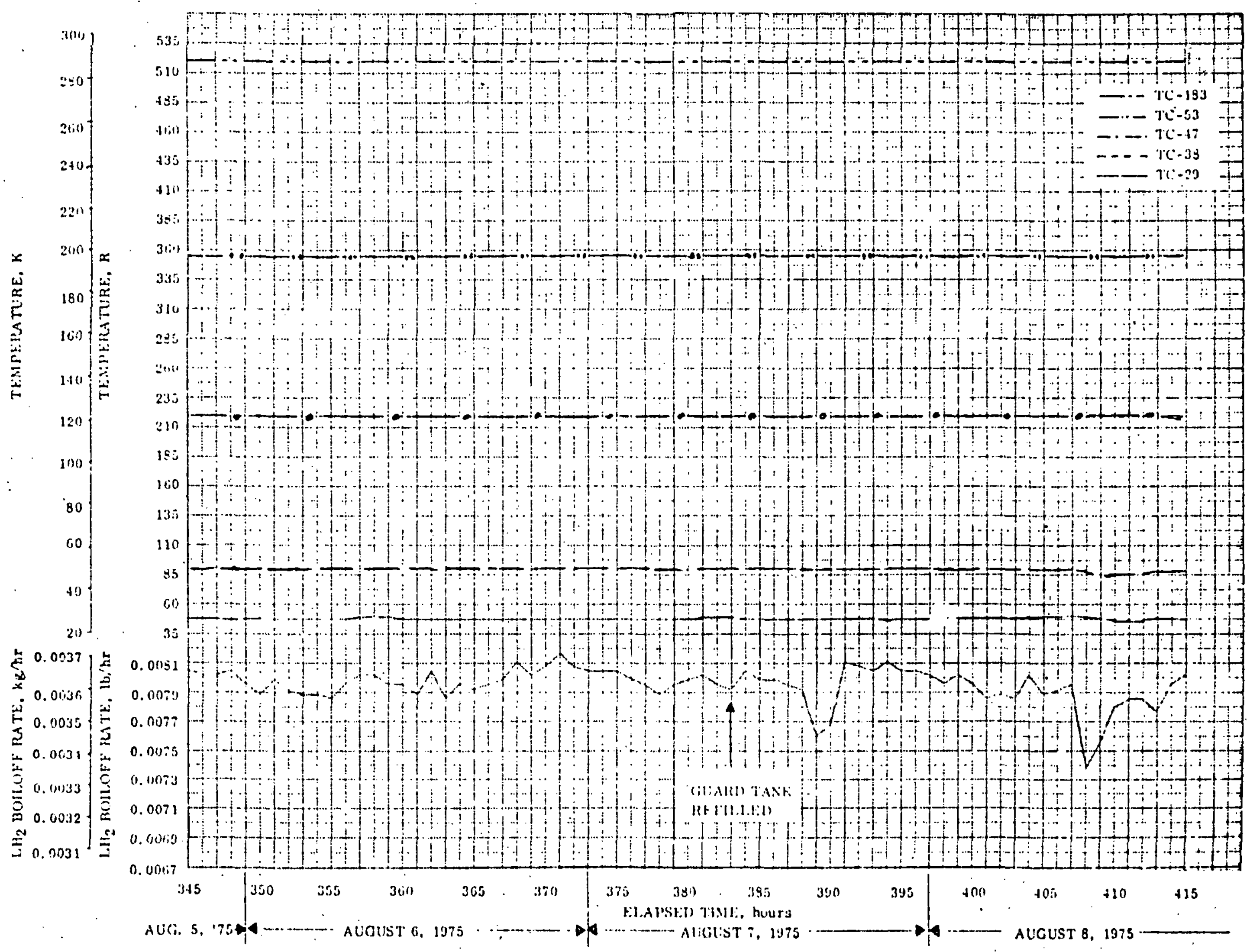

Figure 10-10. Customized MLI Thermal Test - Approach to Equilibrium of Test No. 2, 0.305 m (12 in) TPS/Test Tank Spacing (Elapsed Hours: 345 to 415) - Sheet 6 of 10

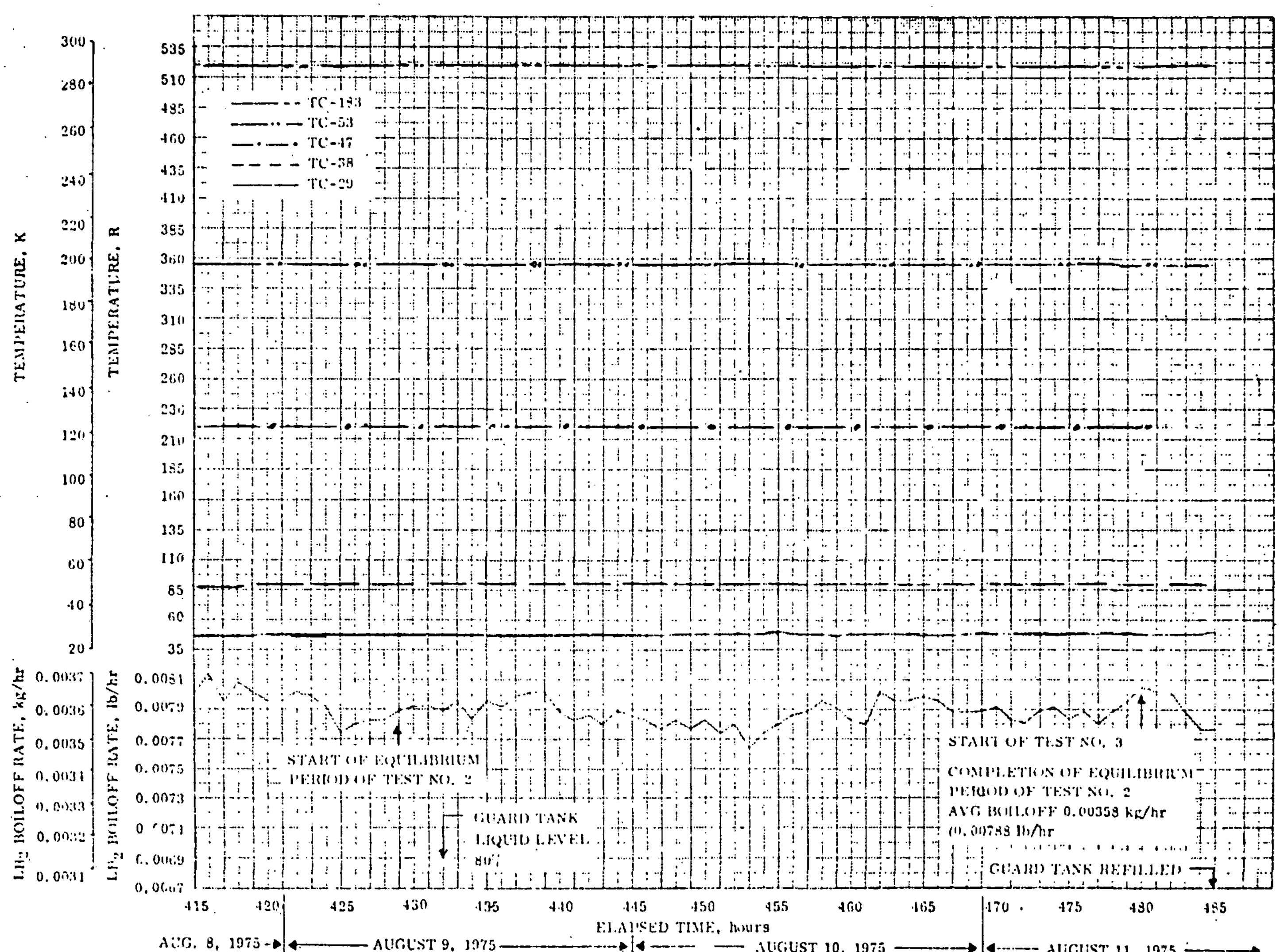

Figure 10-10. Customized MLI Thermal Test - Equilibrium Period of Test No. 2, 0.305 m (12 in) TPS/Test-Tank Spacing and Start of Test No. 3, 0.152 m (6 in) TPS/Test Tank Spacing (Elapsed Hrs: 415 to 485) - Sheet 7 of 10

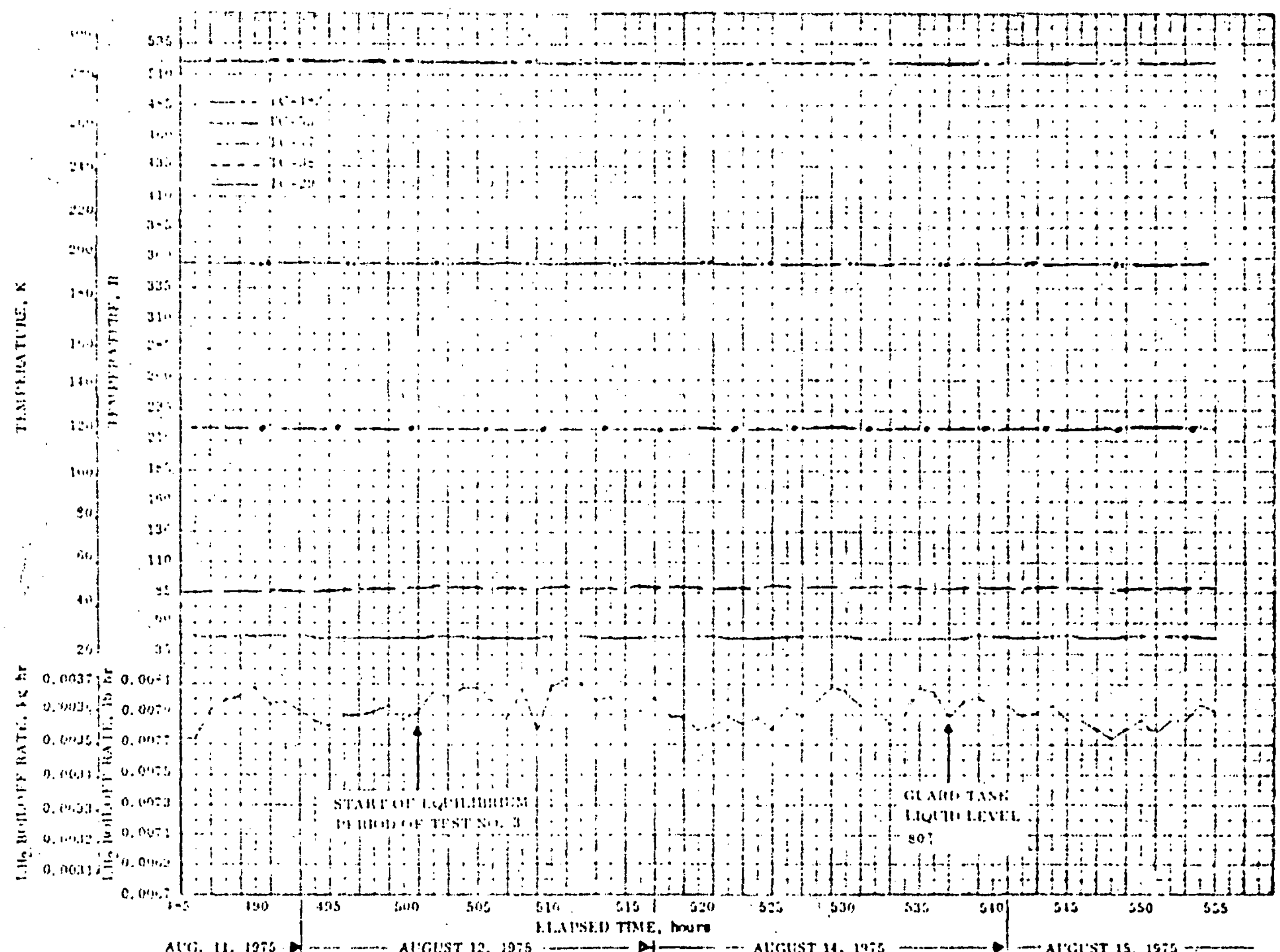

Figure 10-10. Customized MLI Thermal Test - Equilibrium Period of Test No. 3, 0.152 m (6 in) TPS/Test Tank Spacing (Elapsed Hours: 485 - 555) - Sheet 8 of 10

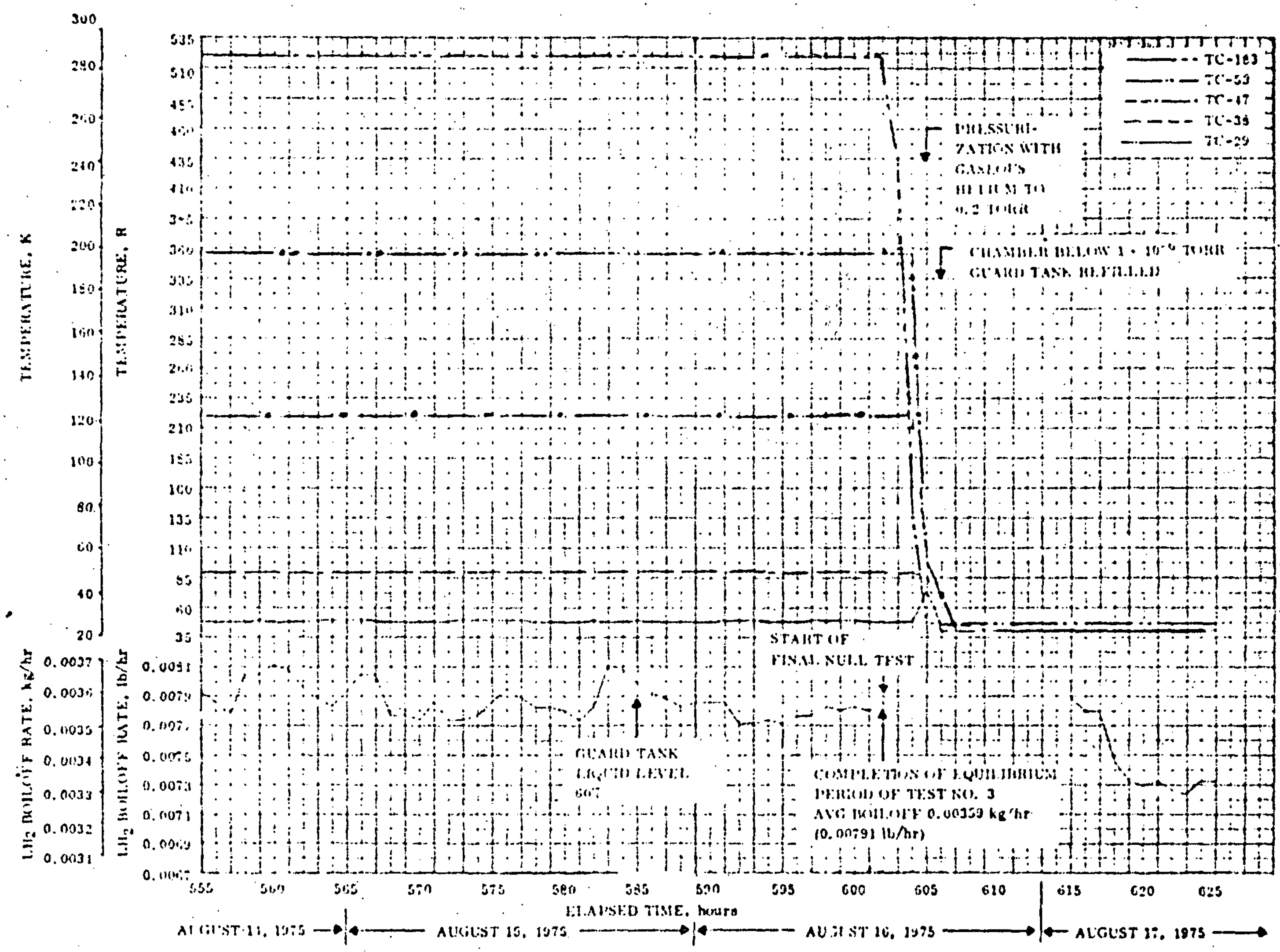

Figure 10-10. Customized MLI Thermal Test - Equilibrium Period of Test No. 3, 0.152 m (6 in) TPS/Test Tank Spacing; Start of Final Null Test (Elapsed Time: 555 to 625) - Sheet 9 of 10

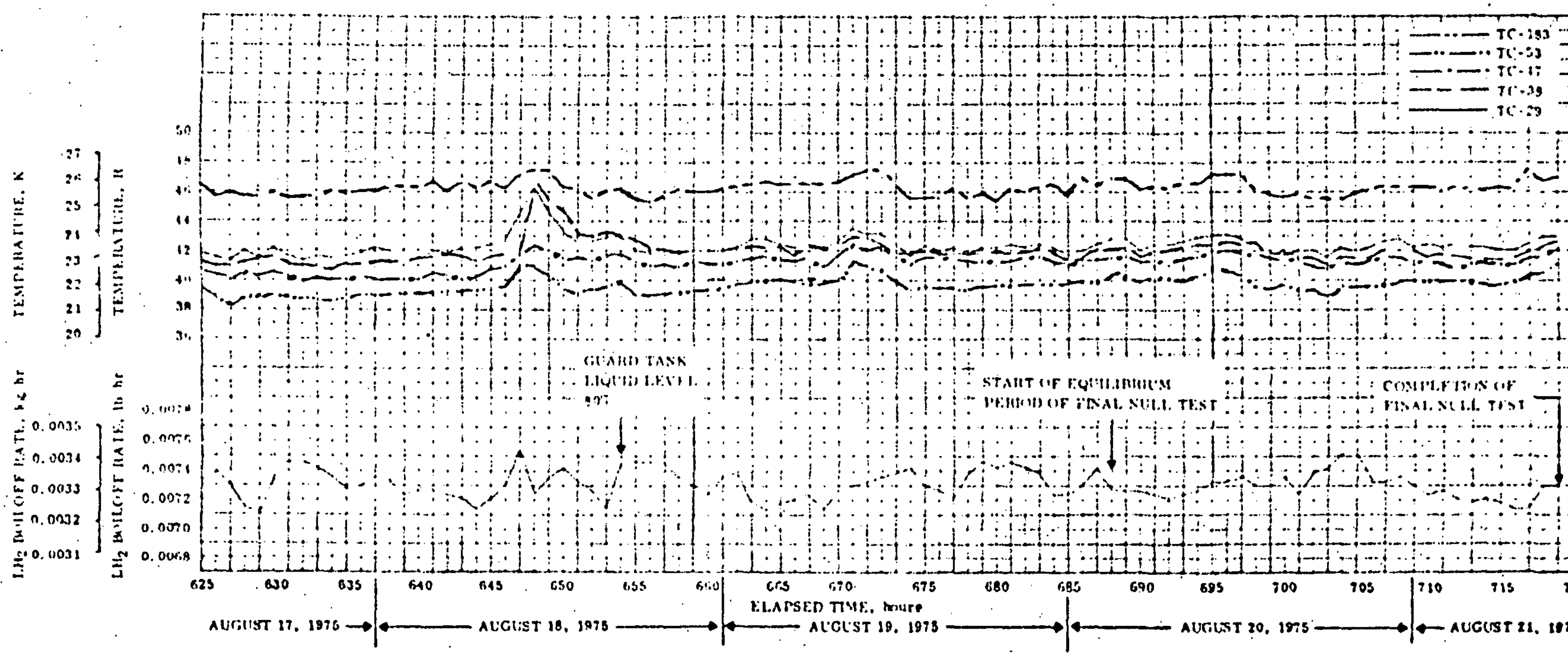

Figure 10-10. Customized MLI Thermal Test (Elapsed Hours: 625 to 719) - Final Null Test - Sheet 10 of 10

Table 10-16. Test Data at Beginning and End of the Thermal Equilibrium Period of Initial Null Test During the Customized MLI Performance Testing

	Beginning - 75 Hours After 0-Time				End - 91 Hours After 0-Time			
	°F	°R	°C	°K	°F	°R	°C	°K
TC-1	-417.6	42.1	-249.6	23.6	-417.6	42.1	-249.6	23.6
TC-2	-421.0	39.0	-251.5	21.7	-421.2	38.8	-251.6	21.6
TC-3	-421.0	39.0	-251.5	21.7	-420.6	39.4	-251.3	21.9
TC-4	-422.0	38.0	-252.1	21.1	-421.8	38.2	-252.0	21.2
TC-5	-418.5	41.5	-250.2	23.0	-418.5	41.5	-250.2	23.0
TC-6	-420.2	39.8	-251.1	22.1	-420.2	39.8	-251.1	22.1
TC-7	-420.6	39.4	-251.3	21.9	-420.6	39.4	-251.3	21.9
TC-8	-422.0	38.0	-252.1	21.1	-421.6	38.4	-251.9	21.3
TC-9	-417.8	42.2	-249.8	23.4	-418.0	42.0	-249.9	23.3
TC-10	*				*			
TC-11	-421.0	39.0	-251.5	21.7	-420.8	39.2	-251.4	21.8
TC-12	-421.6	38.4	-251.9	21.3	-421.8	38.2	-252.0	21.2
TC-13	*				*			
TC-14	-421.6	38.4	-251.9	21.3	-421.8	38.2	-252.0	21.2
TC-15	-420.4	39.6	-251.2	22.0	-420.4	39.6	-251.2	22.0
TC-16	-422.0	38.0	-252.1	21.1	-422.3	37.7	-252.3	20.9
TC-17	-419.7	40.3	-250.8	22.4	-419.7	40.3	-250.8	22.4
TC-18	-421.6	38.4	-251.9	21.3	-421.4	38.6	-251.8	21.4
TC-19	-421.8	38.2	-252.0	21.2	-421.8	38.2	-252.0	21.2
TC-20	-422.3	37.7	-252.3	20.9	-421.8	38.2	-252.0	21.2
TC-21	-418.2	41.8	-250.0	23.2	-418.1	41.9	-249.9	23.3
TC-22	-420.8	39.2	-251.4	21.8	-420.8	39.2	-251.4	21.8
TC-23	-420.6	39.4	-251.3	21.9	-420.6	39.4	-251.3	21.9
TC-24	-421.0	39.0	-251.5	21.7	-421.2	38.8	-251.6	21.6
TC-25	-418.5	41.5	-250.2	23.0	-418.5	41.5	-250.2	23.0
TC-26	-421.0	39.0	-251.5	21.7	-420.8	39.2	-251.4	21.8
TC-27	-420.4	39.6	-251.2	22.0	-420.8	39.2	-251.4	21.8
TC-28	-422.3	37.7	-252.3	20.9	*			
TC-29	-418.9	41.1	-250.4	22.8	-418.9	41.1	-250.4	22.8
TC-30	-420.8	39.2	-251.4	21.8	-419.5	40.5	-250.7	22.5
TC-31	-420.0	40.0	-251.0	22.2	-420.0	40.0	-251.0	22.2
TC-32	-422.5	37.5	-252.4	20.8	-422.7	37.3	-252.5	20.7
TC-33	-343.0	117.0	-191.5	81.7	-343.0	117.0	-191.5	81.7
TC-34	-415.1	44.9	-248.3	24.9	-415.2	44.8	-248.3	24.9
TC-35	-417.5	42.5	-249.6	23.6	-417.5	42.5	-249.6	23.6
TC-36	**				**			
TC-37	-405.1	54.9	-242.7	30.5	-404.2	55.8	-242.2	31.0
TC-38	-405.4	54.6	-242.9	30.3	-404.7	55.3	-242.6	30.6
TC-39	-404.8	55.2	-242.5	30.7	-404.3	55.7	-242.3	30.9
TC-40	-404.6	55.4	-242.4	30.8	-403.7	56.3	-241.9	31.3
TC-41	-404.7	55.3	-242.5	30.7	-404.0	56.0	-242.1	31.1
TC-42	-404.7	55.3	-242.5	30.7	-404.1	55.9	-242.2	31.1
TC-43	-404.0	56.0	-242.1	31.1	-403.3	56.7	-241.7	31.5
TC-44	-410.8	49.2	-245.9	27.3	-408.1	51.9	-244.4	28.8
TC-45	-411.5	48.5	-246.3	26.9	-408.0	52.0	-244.3	28.9
TC-46	-412.0	48.0	-246.5	26.7	-407.0	53.0	-243.8	29.4
TC-47	-411.6	48.4	-246.3	26.9	-408.8	51.2	-244.8	28.4
TC-48	**				-407.3	52.7	-243.9	29.3
TC-49	-411.8	48.2	-246.4	26.8	-408.4	51.6	-244.5	28.7
TC-50	-419.1	40.9	-250.5	22.7	-417.3	42.7	-249.5	23.7
TC-51	-421.8	38.2	-252.0	21.2	-420.0	40.0	-251.0	22.2
TC-52	-420.2	39.8	-251.1	22.1	-418.1	41.9	-249.9	23.3
TC-53	-419.5	40.5	-250.7	22.5	-417.6	42.4	-249.6	23.6
TC-54	-419.5	40.5	-250.7	22.5	-416.9	43.1	-249.3	23.9
TC-55	-422.3	37.7	-252.3	20.9	-418.4	41.6	-250.1	23.1
TC-56	*				*			

	Beginning - 75 Hours After 0-Time				End - 91 Hours After 0-Time			
	°F	°R	°C	°K	°F	°R	°C	°K
TC-57	-423.5	36.5	-252.9	20.3	*			
TC-58	*				*			
TC-59	-422.3	37.7	-252.3	20.9	-420.0	40.0	-251.0	22.2
TC-60	**				**			
TC-61	**				-422.4	37.6	-252.3	20.9
TC-62	-423.5	36.5	-252.9	20.3	-422.0	38.0	-252.1	21.1
TC-63	**				**			
TC-64	**				**			
TC-65	**				**			
TC-66	-421.0	39.0	-251.5	21.7	-419.1	40.9	-250.5	22.7
TC-67	-407.7	52.3	-244.1	29.1	-406.6	53.4	-243.5	29.7
TC-68 to -71	**							
TC-72	85.3	545.3	29.7	302.9	62.7	522.7	17.3	290.4
TC-73	86.0	546.0	30.1	303.3	63.3	523.3	17.5	290.7
TC-74	85.1	545.1	29.6	302.8	61.8	521.8	16.7	289.9
TC-75	Diffusion Pump							
TC-76	29.6	489.6	-1.16	272.0	29.6	489.6	-1.16	272.0
TC-77	102.9	562.9	39.6	312.7	103.4	563.4	39.8	313.0
TC-78	83.3	543.3	28.7	301.6	61.5	521.5	16.5	289.7
TC-79	-320.2	139.8	-195.5	77.7	-320.0	140.0	-195.4	77.8
TC-80	79.8	539.8	26.5	299.9	57.6	517.6	14.4	287.6
TC-81 to -91	**							
TC-92	-418.0	42.0	-249.9	23.3	-418.2	41.8	-250.0	23.2
TC-93	-417.8	42.2	-249.8	23.4	-418.0	42.0	-249.9	23.3
TC-94	-416.9	43.1	-249.2	23.9	-417.5	42.5	-249.6	23.6
TC-95	-419.3	40.7	-250.4	22.8	-419.3	40.7	-250.4	22.8
TC-96	-417.5	42.5	-249.6	23.6	-417.6	42.4	-249.6	23.6
TC-97	-414.3	45.7	-247.8	25.4	-414.7	45.3	-248.0	25.2
TC-98	-413.8	46.2	-247.5	25.7	-414.2	45.8	-247.8	25.4
TC-99	-420.3	39.7	-251.2	22.0	-420.3	39.7	-251.2	22.0
TC-100	-412.3	47.7	-246.7	26.5	-412.8	47.2	-247.0	26.2
TC-101	-416.0	44.0	-248.8	24.4	-416.0	44.0	-248.8	24.4
TC-102	**							
TC-103	-419.1	40.9	-250.5	22.7	-419.5	40.5	-250.7	22.5
TC-104	-418.9	41.1	-250.4	22.8	-419.1	40.9	-250.5	22.7
TC-105	-418.9	41.1	-250.4	22.8	-419.3	40.7	-250.6	22.6
TC-106	-419.3	40.7	-250.6	22.6	-419.5	40.5	-250.7	22.5
TC-107	-418.6	41.4	-250.2	23.0	-419.1	40.9	-250.5	22.7
TC-108	-418.2	41.8	-250.0	23.2	-418.5	41.5	-250.2	23.0
TC-109	-416.7	43.3	-249.2	24.0	-416.3	43.7	-248.9	24.3
TC-110	-418.7	41.3	-250.3	22.9	-418.9	41.1	-250.4	22.8
TC-111	-418.9	41.1	-250.4	22.8	-419.1	40.9	-250.5	22.7
TC-112	-417.8	42.2	-249.8	23.4	-417.6	42.4	-249.6	23.6
TC-113	-418.2	41.8	-250.0	23.2	-418.0	42.0	-249.9	23.3
TC-114	-416.9	43.1	-249.3	23.9	-416.9	43.1	-249.3	23.9
TC-115	**				**			
TC-116	-417.5	42.5	-249.6	23.6	-417.5	42.5	-249.6	23.6
TC-117 to -127	**							
TC-151	-409.2	50.8	-245.0	28.2	-409.1	50.9	-244.9	28.3
TC-152	-408.6	51.4	-244.6	28.6	-408.9	51.1	-244.8	28.4
TC-153	-415.8	44.2	-248.6	24.6	-415.6	44.4	-248.5	24.7
TC-154	-414.9	45.1	-248.2	25.0	-415.1	44.9	-248.3	24.9
TC-155	-416.2	43.8	-248.9	24.3	-416.3	43.7	-248.9	24.3

* Incorrect Reading

** See Section 9.2.1

Table 10-17. Customized MLI Thermal Test No. 1, 0.457 m (18 in) TPS/Test Tank Spacing, Boiloff Data During the Thermal Equilibrium Period

Equil. Hour	Total Elapsed Time, hrs	LH_2 Boiloff kg/hr	LH_2 Boiloff lb/hr	Equil. Hour	Total Elapsed Time, hrs	LH_2 Boiloff kg/hr	LH_2 Boiloff lb/hr
0	238	0.00355	0.00780	37	275	0.00359	0.00789
1	239	0.00355	0.00780	38	276	0.00356	0.00785
2	240	0.00360	0.00792	39	277	0.00356	0.00783
3	241	0.00355	0.00780	40	278	0.00355	0.00780
4	242	0.00359	0.00789	41	279	0.00355	0.00780
5	243	0.00355	0.00780	42	280	0.00347	0.00764
6	244	0.00350	0.00771	43	281	0.00357	0.00786
7	245	0.00355	0.00780	44	282	0.00350	0.00771
8	246	0.00359	0.00789	45	283	0.00359	0.00789
9	247	0.00356	0.00783	46	284	0.00356	0.00783
10	248	0.00357	0.00786	47	285	0.00353	0.00777
11	249	0.00359	0.00789	48	286	0.00359	0.00789
12	250	0.00367	0.00808	49	287	0.00360	0.00792
13	251	0.00360	0.00792	50	288	0.00359	0.00789
14	252	0.00356	0.00783	51	289	0.00362	0.00796
15	253	0.00352	0.00774	52	290	0.00356	0.00783
16	254	0.00355	0.00780	53	291	0.00359	0.00789
17	255	0.00349	0.00768	54	292	0.00357	0.00786
18	256	0.00352	0.00774	55	293	0.00353	0.00777
19	257	0.00349	0.00768	56	294	0.00350	0.00771
20	258	0.00349	0.00768	57	295	0.00345	0.00758
21	259	0.00350	0.00771	58	296	0.00336	0.00739
22	260	0.00350	0.00771	59	297	0.00342	0.00752
23	261	0.00347	0.00764	60	298	0.00359	0.00789
24	262	0.00355	0.00780	61	299	0.00352	0.00774
25	263	0.00355	0.00780	62	300	0.00352	0.00774
26	264	0.00359	0.00789	63	301	0.00352	0.00774
27	265	0.00357	0.00786	64	302	0.00352	0.00774
28	266	0.00359	0.00789	65	303	0.00353	0.00777
29	267	0.00355	0.00780	66	304	0.00350	0.00771
30	268	0.00353	0.00777	67	305	0.00352	0.00774
31	269	0.00353	0.00777	68	306	0.00350	0.00771
32	270	0.00357	0.00786	69	307	0.00352	0.00774
33	271	0.00363	0.00799	70	308	0.00349	0.00768
34	272	0.00366	0.00805	71	309	0.00356	0.00783
35	273	0.00357	0.00786	72	310	0.00362	0.00796
36	274	0.00365	0.00802	73	311	0.00357	0.00786

Average Boiloff: 0.00355 kg/hr (0.00780 lb/hr)

Table 10-18. Test Data at Beginning and End of the Thermal Equilibrium Period of Test No. 1 During the Customized MLI Performance Testing

	Beginning - 238 Hours After 0-Time				End - 311 Hours After 0-Time					Beginning - 239 Hours After 0-Time				End - 311 Hours After 0-Time			
	°F	°R	°C	°K	°F	°R	°C	°K		°F	°R	°C	°K	°F	°R	°C	°K
TC-1	-411.5	48.5	-246.3	26.9	-410.3	49.7	-245.6	27.6	TC-57	62.1	522.1	16.9	290.1	64.5	524.5	18.2	291.4
TC-2	-416.7	43.3	-249.1	24.1	-415.2	44.8	-248.3	24.9	TC-58	57.6	517.6	14.4	287.6	61.1	521.1	16.3	289.5
TC-3	-416.7	43.3	-249.1	24.1	-414.7	45.3	-248.0	25.2	TC-59	62.6	522.6	17.1	290.3	65.1	525.1	18.5	291.7
TC-4	-418.4	41.6	-250.1	23.1	-416.9	43.1	-249.3	23.9	TC-60	61.4	521.4	16.5	289.7	64.5	524.5	18.2	291.4
TC-5	-411.8	48.2	246.2	26.8	-410.5	49.5	-245.7	27.5	TC-61	62.4	522.4	17.0	290.2	64.4	524.4	18.1	291.3
TC-6	-415.8	44.2	-248.6	24.6	-414.0	46.0	-247.6	25.6	TC-62	62.1	522.1	16.9	290.1	64.1	524.1	18.0	291.2
TC-7	-416.5	43.5	-249.0	24.2	-415.1	44.9	-248.3	24.9	TC-63	61.4	521.4	16.5	289.7	63.4	523.4	17.6	290.8
TC-8	-417.4	42.6	-249.5	23.7	-416.3	45.7	-248.9	24.3	TC-64	60.0	520.0	15.7	288.9	62.4	522.4	17.0	290.2
TC-9	-411.0	49.0	-246.0	27.2	-409.7	50.3	-245.3	27.9	TC-65	59.6	519.6	15.5	288.7	61.9	521.9	16.7	289.9
TC-10	*				*				TC-66	62.5	522.5	17.1	290.3	64.5	524.5	18.2	291.4
TC-11	-416.2	43.8	-248.9	24.3	-414.3	45.7	-247.8	25.4	TC-67	-115.4	344.6	-81.8	191.4	-111.8	348.2	-79.9	193.4
TC-12	-418.2	41.8	-250.0	23.2	-416.3	43.8	-248.9	24.3	TC-68	**				**			
TC-13	*				*				to -71								
TC-14	-417.0	43.0	-249.3	23.9	-414.7	45.3	-248.0	25.2	TC-72	62.9	522.9	17.3	290.5	77.9	537.9	25.6	298.8
TC-15	-416.2	43.8	-248.9	24.3	-414.0	46.0	-247.6	25.6	TC-73	63.6	523.6	17.7	290.9	78.5	538.5	26.0	299.2
TC-16	-418.4	41.6	-250.1	23.1	-416.2	43.8	-248.9	24.3	TC-74	62.4	522.4	17.0	290.2	77.6	537.6	25.5	298.7
TC-17	-412.5	47.5	-246.8	26.4	-410.3	49.7	-245.6	27.6	TC-75	Diffusion	Pump						
TC-18	-417.3	42.7	-249.5	23.7	-414.9	45.1	-248.1	25.1	TC-76	29.7	489.7	-1.1	272.1	29.7	489.7	-1.1	272.1
TC-19	-417.3	42.7	-249.5	23.7	-415.6	44.4	-248.5	24.7	TC-77	105.0	565.0	40.7	313.9	105.2	565.2	40.8	314.0
TC-20	-418.5	41.5	-250.1	23.1	-416.9	43.1	-249.3	23.9	TC-78	58.6	518.6	14.9	288.1	77.3	537.3	25.3	298.5
TC-21	-411.5	48.5	-246.3	26.9	-410.3	49.7	-245.6	27.6	TC-79	-320.1	139.9	-195.5	77.7	-320.0	140.0	-195.4	77.8
TC-22	-416.5	43.5	-249.0	24.2	-415.2	44.8	-248.3	24.9	TC-80	61.0	521.0	19.0	292.2	76.1	536.1	24.6	297.8
TC-23	-416.2	43.8	-248.9	24.3	-414.5	45.5	-247.9	25.3	TC-81	**				**			
TC-24	-417.8	42.2	-249.8	23.4	-416.5	43.5	-249.0	24.2	to -91								
TC-25	-411.5	48.5	-246.3	26.9	-410.8	49.2	-245.9	27.3	TC-92	-411.7	45.3	-243.0	25.2	-413.0	47.0	-247.1	26.1
TC-26	-416.5	43.5	-249.0	24.2	-414.9	45.1	-248.1	25.1	TC-93	-414.7	45.3	-248.0	25.2	-413.5	46.5	-247.4	25.8
TC-27	-415.8	44.2	-248.6	24.6	-414.5	45.5	-247.9	25.3	TC-94	-414.2	45.8	-247.8	25.4	-412.8	47.2	-247.0	26.2
TC-28	*				-417.8	42.2	-249.8	23.4	TC-95	-416.0	44.0	-248.8	24.4	-414.1	45.9	-247.7	25.5
TC-29	-411.8	48.2	-246.1	26.8	-410.7	49.3	[illegible]	27.4	TC-96	-414.7	45.3	-248.0	25.2	-413.0	47.0	-247.1	26.1
TC-30	-416.2	43.8	-248.9	24.3	-414.7	45.3	[illegible]	25.2	TC-97	-411.6	48.4	-246.3	26.9	-410.5	49.5	-245.7	27.5
TC-31	-415.6	44.4	-248.5	24.7	-413.7	46.3	-247.5	25.7	TC-98	-410.8	49.2	-245.9	27.3	-409.4	50.6	-245.1	28.1
TC-32	-418.5	41.5	-250.1	23.1	-416.5	43.5	-249.0	24.2	TC-99	-416.7	43.3	-249.1	24.1	-415.6	44.4	-248.5	24.7
TC-33	*				*				TC-100	-407.2	52.8	-243.9	29.3	-406.0	54.0	-243.2	30.0
TC-34	-412.6	47.4	-246.9	26.3	-411.0	49.0	-246.0	27.2	TC-101	-412.5	47.5	-246.8	26.4	-411.0	49.0	-246.0	27.2
TC-35	-416.0	44.0	-248.8	24.4	-413.0	47.0	-247.1	26.1	TC-102	-387.2	72.8	-232.8	40.4	-385.8	74.2	-232.0	41.2
TC-36	**				**				TC-103	-416.2	43.8	-248.9	24.3	-414.4	45.6	-247.9	25.3
TC-37	-369.2	90.8	-222.8	50.4	-369.0	91.0	-222.6	50.6	TC-104	-416.0	44.0	-248.8	24.4	-414.4	45.6	-247.9	25.3
TC-38	-369.3	90.7	-222.8	50.4	-369.0	91.0	-222.6	50.6	TC-105	-416.0	44.0	-248.8	24.4	-414.5	45.5	-247.9	25.3
TC-39	-368.8	91.2	-222.5	50.7	-368.6	91.4	-222.4	50.8	TC-106	-416.0	44.0	-248.8	24.4	-414.5	45.5	-247.9	25.3
TC-40	-368.5	91.5	-222.4	50.8	-368.1	91.9	-222.1	51.1	TC-107	-415.8	44.2	-248.6	24.6	-414.5	45.5	-247.9	25.3
TC-41	-368.4	91.6	-222.3	50.9	-368.1	91.9	-222.1	51.1	TC-108	-415.1	44.9	-248.3	24.9	-413.7	46.3	-247.5	25.7
TC-42	-368.5	91.5	-222.4	50.8	-368.2	91.8	-222.2	51.0	TC-109	-412.8	47.2	-247.0	26.2	-411.6	48.4	-246.3	26.9
TC-43	-367.0	93	-221.5	51.7	-366.8	93.2	-221.4	51.8	TC-110	-415.6	44.4	-248.5	24.7	-414.2	45.8	-247.8	25.4
TC-44	-241.9	218.1	-152.0	121.2	-241.3	218.7	-151.5	121.6	TC-111	-415.1	44.9	-248.3	24.9	-413.5	46.5	-247.4	25.8
TC-45	-241.5	218.5	-151.8	121.4	-240.9	219.1	-151.5	121.7	TC-112	-414.2	45.8	-247.8	25.4	-412.5	47.5	-246.8	26.4
TC-46	-240.5	219.5	-151.3	121.9	-239.6	220.4	-150.9	122.4	TC-113	-413.7	46.3	-247.5	25.7	-412.0	48.0	-246.5	26.7
TC-47	-240.9	219.1	-151.4	121.8	-240.4	219.6	-151.2	122.0	TC-114	-410.7	49.3	-245.8	27.4	-409.4	50.6	-245.1	28.1
TC-48	-240.2	219.8	-151.1	122.1	-239.6	220.4	-150.8	122.4	TC-115	**				**			
TC-49	-239.2	220.8	-150.5	122.7	-238.6	221.4	-150.2	123.0	TC-116	-412.1	47.9	-246.8	26.6	-410.8	49.2	-245.9	27.3
TC-50	-105.4	354.6	-76.2	197.0	-105.0	355.0	-76.0	197.2	TC-117	**				**			
TC-51	-110.0	350.0	-78.8	194.4	-109.5	350.5	-78.5	194.7	to -127								
TC-52	-116.3	343.7	-82.3	190.9	-115.5	344.5	-81.8	191.4	TC-181	-407.0	53.0	-243.8	29.4	-405.3	54.7	-242.8	30.4
TC-53	-104.2	355.8	-75.5	197.7	-104.1	355.9	-75.5	197.7	TC-182	-406.9	53.1	-243.7	29.5	-404.4	55.6	-242.3	30.9
TC-54	*								TC-183	60.4	520.4	15.9	289.1	60.4	520.4	15.9	289.1
TC-55	-112.3	347.7	-80.0	193.2	-109.4	350.6	-78.4	191.8	TC-184	60.9	520.9	16.2	289.4	60.7	520.7	16.1	289.3
TC-56	61.9	521.0	16.7	289.9	64.5	524.5	18.2	291.4	TC-185	60.7	520.7	16.1	289.3	60.7	520.7	16.1	289.3

* Incorrect Reading

** See Section 9.2.1

ORIGINAL PAGE IS OF POOR QUALITY

Table 10-19. Customized MLI Thermal Test No. 2, 0.305 m (12 in) TPS/Test Tank Spacing, Boiloff Data During the Thermal Equilibrium Period

Equil. Hour	Total Elapsed Time, hrs	LH_2 Boiloff kg/hr	LH_2 Boiloff lb/hr	Equil. Hour	Total Elapsed Time, hrs	LH_2 Boiloff kg/hr	LH_2 Boiloff lb/hr
0	429	0.00359	0.00789	26	455	0.00355	0.00780
1	430	0.00360	0.00792	27	456	0.00357	0.00786
2	431	0.00360	0.00792	28	457	0.00359	0.00789
3	432	0.00359	0.00789	29	45[illegible]	0.00362	0.00796
4	433	0.00362	0.00796	30	459	0.00360	0.00792
5	434	0.00356	0.00783	31	460	0.00356	0.00783
6	435	0.00362	0.00796	32	461	0.00355	0.00780
7	436	0.00360	0.00792	33	462	0.00365	0.00802
8	437	0.00363	0.00799	34	463	0.00362	0.00796
9	438	0.00365	0.00802	35	464	0.00362	0.00796
10	439	0.00365	0.00802	36	465	0.00363	0.00799
11	440	0.00359	0.00789	37	466	0.00362	0.00796
12	441	0.00356	0.00783	38	467	0.00359	0.00789
13	442	0.00357	0.00786	39	468	0.00359	0.00789
14	443	0.00355	0.00780	40	469	0.00359	0.00789
15	444	0.00359	0.00789	41	470	0.00360	0.00792
16	445	0.00357	0.00786	42	471	0.00356	0.00783
17	446	0.00356	0.00783	43	472	0.00359	0.00789
18	447	0.00353	0.00777	44	473	0.00359	0.00789
19	448	0.00356	0.00783	45	474	0.00360	0.00792
20	449	0.00353	0.00777	46	475	0.00356	0.00783
21	450	0.00356	0.00783	47	476	0.00359	0.00789
22	451	0.00352	0.00774	48	477	0.00355	0.00780
23	452	0.00355	0.00780	49	478	0.00359	0.00789
24	453	0.00347	0.00764	50	479	0.00362	0.00796
25	454	0.00352	0.00774	51	480	0.00366	0.00805

Average Boiloff: 0.00358 kg/hr (0.00788 lb/hr)

Table 10-20. Test Data Beginning [illegible] End of the Thermal Equilibrium Period of Test No. 2 During the Customiz[illegible] [illegible]LI Thermal Performance Testing

	Beginning - 429 Hours After 0-Time				End - 480 Hours After 0-Time			
	°F	°R	°C	°K	°F	°R	°C	°K
TC-1	-411.3	48.7	[illegible]	27.1	-410.5	49.5	-245.7	27.5
TC-2	-416.5	43.5	-249.0	24.2	-415.8	44.2	-248.6	24.6
TC-3	-416.5	43.5	-249.0	24.2	-415.6	44.4	-248.5	24.7
TC-4	-418.5	41.5	-250.1	23.1	-417.8	42.2	-249.8	23.1
TC-5	-411.8	48.2	-246.4	26.8	-411.0	49.0	-246.0	27.2
TC-6	-416.2	43.8	-248.9	24.3	-414.9	45.1	-248.3	25.1
TC-7	-417.0	43.0	-249.3	23.9	-416.3	43.7	-248.9	24.3
TC-8	-414.9	45.1	-249.1	25.1	-412.0	48.0	-246.5	26.7
TC-9	-410.5	49.2	-245.8	27.3	-410.0	50.0	-245.4	27.8
TC-10	*				*			
TC-11	-416.5	43.5	-249.0	24.2	-415.5	44.5	-248.6	24.7
TC-12	-418.4	41.6	-250.1	23.1	-417.3	42.7	-249.5	23.7
TC-13	*				*			
TC-14	-417.0	43.0	-249.3	23.9	-416.0	44.0	-248.8	24.4
TC-15	-416.2	43.8	-248.9	24.3	-415.1	44.9	-248.3	24.9
TC-16	-418.5	41.5	-250.1	23.1	-417.5	42.5	-249.6	23.6
TC-17	-412.6	47.4	-246.9	26.3	-411.3	48.7	-246.1	27.1
TC-18	-416.9	43.1	-249.3	23.9	-416.0	44.0	-248.8	24.4
TC-19	-417.3	42.7	-249.5	23.7	-416.7	43.3	-249.1	24.1
TC-20	-418.4	41.6	-250.1	23.1	-418.0	42.0	-249.9	23.3
TC-21	-412.0	48.0	-246.5	26.7	-411.3	48.7	-246.0	27.1
TC-22	-417.0	43.0	-249.3	23.9	-416.5	43.5	-249.0	24.2
TC-23	-416.2	43.8	-248.9	24.3	-415.6	44.4	-248.5	24.7
TC-24	-418.4	41.6	-250.1	23.1	-417.6	42.4	-249.6	23.6
TC-25	-412.3	47.7	-246.7	26.5	-411.5	48.5	-246.3	26.9
TC-26	-416.2	43.8	-248.9	24.3	-415.8	44.2	-248.6	24.6
TC-27	-416.5	43.5	-249.0	24.2	-415.8	44.2	-248.6	24.6
TC-28	*				*			
TC-29	-412.0	48.0	-246.5	26.7	-411.8	48.2	-246.4	26.8
TC-30	-416.7	43.3	-249.1	24.1	-416.2	43.8	-248.9	24.3
TC-31	-415.6	44.4	-248.5	24.7	-414.9	45.1	-248.1	25.1
TC-32	-418.9	41.1	-250.4	22.8	-418.0	42.0	-249.9	23.3
TC-33	-312.2	147.8	-191.1	82.1	-312.0	148.0	-191.0	82.2
TC-34	-412.8	47.2	-247.0	26.2	-412.1	47.9	-246.6	26.6
TC-35	-414.7	45.3	-248.0	25.2	-413.9	46.1	-247.6	25.6
TC-36	**				**			
TC-37	-370.5	89.5	-223.5	49.7	-370.2	89.8	-223.3	49.9
TC-38	-370.6	89.4	-223.5	49.7	-370.2	89.8	-223.3	49.9
TC-39	-370.2	89.8	-223.3	49.9	-369.6	90.4	-223.0	50.2
TC-40	-369.7	90.3	-223.0	50.2	-369.3	90.7	-222.8	50.4
TC-41	-369.9	90.1	-223.1	50.1	-369.4	90.6	-222.9	50.3
TC-42	-369.8	90.2	-223.1	50.1	-369.3	90.7	-222.8	50.4
TC-43	-368.4	91.6	-222.3	50.9	-367.9	92.1	222.0	51.2
TC-44	-240.4	219.6	-151.2	122.0	-240.2	219.0	-151.1	122.1
TC-45	-240.4	219.6	-151.2	122.0	-239.7	220.3	-150.8	122.4
TC-46	-238.7	221.3	-150.3	122.9	-238.5	221.5	-150.1	123.1
TC-47	-239.6	220.4	-150.8	122.4	-239.3	220.7	-150.6	122.6
TC-48	-239.0	221.0	-150.4	122.8	-238.7	221.3	-150.3	122.9
TC-49	-238.2	221.8	-150.0	123.2	-237.8	222.2	-149.8	123.4
TC-50	-104.4	355.6	-75.6	197.6	-104.2	355.8	-75.5	197.7
TC-51	-109.2	350.8	-78.3	194.9	-108.9	351.1	-78.1	195.1
TC-52	-114.7	345.3	-81.5	191.7	-114.6	345.4	-81.3	191.9
TC-53	-103.6	356.4	-75.2	198.0	-103.4	356.6	-75.1	198.1
TC-54	*				*			
TC-55	-112.2	347.8	-80.0	193.2	-111.0	349.0	-79.3	193.9
TC-56	58.9	518.9	15.1	288.3	62.9	522.9	17.3	290.5

	Beginning - 429 Hours After 0-Time				End - 480 Hours After 0-Time			
	°F	°R	°C	°K	°F	°R	°C	°K
TC-57	60.7	520.7	16.1	289.3	62.7	522.7	17.2	290.4
TC-58	57.4	517.4	14.2	287.4	59.2	519.2	15.1	288.4
TC-59	60.7	520.7	16.1	289.3	63.0	523.0	17.4	290.6
TC-60	60.7	520.7	16.1	289.3	62.7	522.7	17.2	290.4
TC-61	61.9	521.9	16.7	289.9	62.6	522.6	17.1	290.3
TC-62	61.3	521.3	16.4	289.6	62.1	522.1	16.9	290.1
TC-63	60.6	520.6	16.0	289.	61.5	521.5	16.5	289.7
TC-64	58.9	518.9	15.1	288.3	60.5	520.5	16.0	289.2
TC-65	58.7	518.7	15.6	288.2	59.9	519.9	15.6	288.8
TC-66	61.8	521.8	16.7	289.9	62.7	522.7	17.2	290.4
TC-67	-113.7	346.3	-80.8	192.4	-113.7	346.3	-80.8	192.4
TC-68 to -71	**				**			
TC-72	65.4	525.4	18.1	291.3	74.9	534.9	24.0	297.2
TC-73	65.8	525.8	18.9	292.1	75.8	535.8	24.5	297.7
TC-74	64.5	524.5	18.2	291.4	74.9	534.9	24.0	297.2
TC-75	Diffusion Pump							
TC-76	29.7	489.7	-1.1	272.1	29.7	489.7	-1.1	272.1
TC-77	104.4	564.4	40.4	313.6	103.7	563.7	40.0	312.2
TC-78	61.8	521.8	18.4	291.6	72.6	532.6	22.7	295.9
TC-79	-315.4	144.6	-192.9	80.3	-314.8	145.2	-192.5	80.7
TC-80	60.7	520.7	16.1	289.3	75.4	535.4	24.2	297.4
TC-81 to -91	**				**			
TC-92	-416.2	43.8	-248.9	24.3	-414.5	45.5	-247.9	25.3
TC-93	-418.6	41.4	248.5	24.7	-414.7	45.3	-248.0	25.2
TC-94	-415.4	44.6	-248.4	24.8	-414.0	46.0	-247.6	25.6
TC-95	-415.6	44.4	-248.5	24.7	-415.2	44.8	-248.3	24.9
TC-96	-415.6	44.4	-248.5	24.7	-414.9	45.1	-248.1	25.1
TC-97	-413.0	47.0	-247.0	26.1	-411.8	48.2	-246.4	26.8
TC-98	-411.5	48.5	-246.3	26.9	-411.0	49.0	-246.0	27.2
TC-99	-418.0	42.0	-249.9	23.3	-416.9	43.1	-249.3	23.9
TC-100	-408.9	51.1	-244.8	28.4	-407.6	52.4	-244.1	29.1
TC-101	-413.2	46.8	-247.2	26.0	-412.0	48.0	-246.5	26.7
TC-102	-387.5	72.5	-232.9	40.3	-387.5	72.5	-232.9	40.3
TC-103	-417.0	43.0	-249.3	23.9	*			
TC-104	-417.0	43.0	-249.3	23.9	-415.8	44.2	-248.6	24.6
TC-105	-417.0	43.0	-249.3	23.9	-416.0	44.0	-248.8	24.4
TC-106	-417.3	42.7	-249.5	23.7	-416.2	43.8	-248.9	24.3
TC-107	-416.9	43.1	-249.3	23.9	-416.0	44.0	-248.8	24.4
TC-108	-416.2	43.8	-248.9	24.3	-415.1	44.9	-248.3	24.9
TC-109	-413.9	46.1	-247.6	25.6	-413.0	47.0	-247.1	26.1
TC-110	-416.2	43.8	-248.9	24.3	-415.5	44.5	-248.5	24.7
TC-111	-415.8	44.2	-248.6	24.6	-414.9	45.1	-248.1	25.1
TC-112	-415.2	44.8	-248.3	24.9	-414.0	46.0	-247.6	25.6
TC-113	-414.5	45.5	-247.9	25.3	-413.5	46.5	-247.4	25.8
TC-114	-411.6	48.4	246.3	26.9	-410.5	49.5	-245.7	27.5
TC-115	*				*			
TC-116	-413.0	47.0	-247.1	26.1	-411.8	48.2	-246.4	26.8
TC-117 to -127	**				**			
TC-181	-407.8	52.2	-244.2	29.0	-405.1	54.9	-242.7	30.5
TC-182	-407.5	52.5	-243.8	29.4	-406.0	54.0	-243.2	30.0
TC-183	59.9	519.9	15.6	288.8	60.0	520.0	15.7	288.9
TC-184	59.9	519.9	15.6	288.8	60.4	520.4	15.9	289.1
TC-185	60.6	520.6	16.0	289.2	60.7	520.7	16.1	289.3

* Incorrect Reading

ORIGINAL PAGE IS
OF POOR QUALITY

10.3.3.4 Thermal Test No. 3, 0.153 m (6 in) TPS/Test Tank Spacing - The TPS was moved from the 0.305 m (12 in) to the 0.153 m (6 in) position on 11 August 1975, 480 hours after 0-time. Except for the TPS position, the test conditions were the same as those of thermal test No. 1. The thermal equilibrium period began 501 hours after 0-time (Figure 10-10, Sheet 8) and continued for 101 hours hours until 602 hours after 0-time (Figure 10-10, Sheet 9) on 16 August 1075. The average boiloff rate during the equilibrium period was 0.00359 kg/hr (0.00791 lb/hr). Boiloff rates for each hour of testing are shown in Table 10-21. The temperatures of MLI thermocouples TC-53, 47, 38, and 29 and the TPS temperature (TC-183) are shown in Figure 10-10, Sheets 7 through 9. Temperature distribution data are presented in Table 10-22.

10.3.3.5 Final Null Test - The TPS was left at the 0.153 m (6 in) position and was cooled to liquid hydrogen temperature starting 603 hours after 0-time on 16 August 1975.

Except for the TPS position, the test conditions were the same as those of the initial null test. The thermal equilibrium period began 688 hours after 0-time and continued for 31 hours until 719 hours after 0-time on 11 August 1975, (Figure 10-10, Sheet 10).

The average boiloff rate during the equilibrium period was 0.00330 kg/hr (0.00727 lb/hr). Boiloff rates for each hour of testing are shown in Table 10-23. The temperatures of thermocouples TC-53, 47, 38 and 29 and the TPS temperature (TC-183) are shown in Figure 10-10, Sheets 9 and 10. Temperature distributions are presented in Table 10-24.

10.3.4 EVALUATION OF CUSTOMIZED MLI TEST RESULTS - The thermal performance test of the customized MLI had two major objectives: The first objective was to confirm the results of the previous null tests described in Section 10-1 or to establish a new null point. The second objective was to determine experimentally the thermal performance of the customized MLI at 0.457 m (18 in), 0.305 m (12 in) and 0.152 m (6 in) distance between test tank and thermal payload simulator. All tests were conducted utilizing a 0.2 power input to the test tank heater to promote fluid mixing within the tank. The results of both experiments are discussed below.

10.3.4.1 Initial and Final Null Test - Table 10-25 compares the results of the initial and final null test obtained during the customized MLI performance test with the results of the previous null test No. 2 and No. 4 obtained at the beginning of the test program (Section 10.1). It was assumed that the LH_2 boiloff rates of the previous null tests No. 2 and 4, and the initial and final null tests conducted during the customized MLI testing would be approximately the same after a true thermal equilibrium was achieved. This assumption should be valid even with the addition of three TPS MLI blankets and changing the spacing between TPS and test tank from 0.457 m (18 in) 0.152 m (6 in). A return of the thermal payload simulator from the 0.152 m (6 in) position used during the customized MLI thermal performance test to the original 0.457 m (18 in) position was not recommended because of a possible failure of the TPS

Table 10-21. Customized MLI - Thermal Test No. 3, 0.1524 m (6 in) TPS/Test Tank Spacing Thermal Equilibrium Boiloff Data

Equil. hour	Total Elapsed Time, hrs	LH_2 Boiloff kg/hr	LH_2 Boiloff lb/hr	Equil. hour	Total Elapsed Time, hrs	LH_2 Boiloff kg/hr	LH_2 Boiloff lb/hr	Equil. hour	Total Elapsed Time, hrs	LH_2 Boiloff kg/hr	LH_2 Boiloff lb/hr
0	501	0.00360	0.00792	35	536	0.00366	0.00805	70	571	0.00357	0.00786
1	502	0.00366	0.00805	36	537	0.00359	0.00789	71	572	0.00352	0.00774
2	503	0.00365	0.00802	37	538	0.00363	0.00799	72	573	0.00352	0.00774
3	504	0.00367	0.00808	38	539	0.00365	0.00802	73	574	0.00352	0.00774
4	505	0.00367	0.00808	39	540	0.00360	0.00792	74	575	0.00357	0.00786
5	506	0.00363	0.00799	40	541	0.00362	0.00796	75	576	0.00362	0.00796
6	507	0.00357	0.00786	41	542	0.00359	0.00789	76	577	0.00359	0.00789
7	508	0.00367	0.00808	42	543	0.00360	0.00792	77	578	0.00356	0.00783
8	509	0.00355	0.00780	43	544	0.00362	0.00796	78	579	0.00356	0.00783
9	510	0.00367	0.00808	44	545	0.00357	0.00786	79	580	0.00355	0.00780
10	511	0.00370	0.00814	45	546	0.00357	0.00786	80	581	0.00352	0.00774
11	512	0.00369	0.00811	46	547	0.00355	0.00780	81	582	0.00356	0.00783
12	513	0.00363	0.00799	47	548	0.00352	0.00774	82	583	0.00369	0.00811
13	514	0.00365	0.00802	48	549	0.00355	0.00780	83	584	0.00367	0.00808
14	515	0.00360	0.00792	49	550	0.00357	0.00786	84	585	0.00363	0.00799
15	516	0.00360	0.00792	50	551		0.00777	85	586	0.00360	0.00792
16	517	0.00365	0.00802	51	552	0.00357	0.00786	86	587	0.00359	0.00789
17	518	0.00359	0.00789	52	553	0.00357	0.00786	87	588	0.00356	0.00783
18	519	0.00359	0.00789	53	554		0.00786	88	589	0.00357	0.00786
19	520	0.00355	0.00780	54	555	0.00360	0.00792	89	590	0.00357	0.00786
20	521	0.00356	0.00783	55	556	0.00357	0.00786	90	591	0.00357	0.00786
21	522	0.00359	0.00789	56	557		0.00777	91	592	0.00350	0.00771
22	523	0.00356	0.00783	57	558	0.00366	0.00805	92	593	0.00350	0.00771
23	524	0.00357	0.00786	58	559	0.00366	0.00805	93	594	0.00352	0.00774
24	525	0.00355	0.00780	59	560	0.00369	0.00811	94	595	0.00350	0.00771
25	526	0.00362	0.00796	60	561	0.00367	0.00808	95	596	0.00353	0.00777
26	527	0.00359	0.00789	61	562	0.00362	0.00796	96	597	0.00353	0.00777
27	528	0.00363	0.00799	62	563	0.00359	0.00789	97	598	0.00356	0.00783
28	529	0.00367	0.00808	63	564	0.00356	0.00783	98	599	0.00355	0.00780
29	530	0.00366	0.00805	64	565	-	-	99	600	0.00356	0.00783
30	531	0.00362	0.00796	65	566	0.00366	0.00805	100	601	0.00355	0.00780
31	532	0.00362	0.00796	66	567	0.00366	0.00805	101	602	0.00357	0.00786
32	533	0.00356	0.00783	67	568	0.00353	0.00777				
33	534	0.00359	0.00789	68	569	0.00353	0.00777				
34	535	0.00367	0.00808	69	570	0.00353	0.00774				

Average Boiloff 0.00359 kg/hr (0.00791 lb/hr)

Table 10-22. Test Data at Beginning and End of the Thermal Equilibrium Period of Test No. 3 During the Customized MLI Thermal Performance Testing

	Beginning - 591 Hours After 0-Time				End - 602 Hours After 0-Time			
	°F	°R	°C	°K	°F	°R	°C	°K
TC-1	-411.0	49.0	-246.0	27.2	-410.7	49.3	[illegible]	27.4
TC-2	-416.5	43.5	-249.0	24.2	-416.2	43.8	-248.9	24.3
TC-3	-416.7	43.3	-249.1	24.1	-416.2	43.4	[illegible]	24.3
TC-4	-418.9	41.1	-250.3	22.9	-418.9	41.1	-250.4	22.6
TC-5	-411.3	48.7	-246.1	27.1	-410.8	49.2	-245.9	27.3
TC-6	-416.2	43.8	-248.9	24.3	-415.6	44.2	-248.5	24.7
TC-7	-417.3	42.7	-249.5	23.7	-416.4	43.6	-249	24.2
TC-8	*				-418.0	42.0	-249.9	23.3
TC-9	-410.2	49.8	-245.5	27.7	-409.5	50.5	-245.1	28.1
TC-10	*				*			
TC-11	-416.7	43.3	-249.1	24.1	-416.5	43.5	-249.0	24.2
TC-12	-418.7	41.3	-250.3	22.9	-418.5	41.5	-240.1	33.1
TC-13	*				*			
TC-14	-417.3	42.7	-249.5	23.7	-417.3	42.7	-249.5	23.7
TC-15	-416.5	43.5	-249.0	24.2	-415.8	44.2	[illegible]	24.6
TC-16	-419.1	40.9	-245.5	27.7	-418.9	41.1	-250.4	22.8
TC-17	-411.8	45.2	-246.4	26.8	-411.5	48.5	-246.3	26.9
TC-18	-417.0	43.0	-249.3	23.9	-416.9	43.1	-249.3	23.9
TC-19	-417.5	42.5	-249.6	23.6	-417.5	42.5	-249.6	23.6
TC-20	-418.9	41.1	-250.4	22.8	-418.7	41.3	-250.3	22.9
TC-21	-411.5	48.5	-246.3	26.9	-411.0	49.0	-246.6	27.2
TC-22	-416.7	43.3	-249.1	24.1	-416.5	43.5	-249.0	24.2
TC-23	-416.2	43.8	-248.9	24.3	-416.3	43.7	-248.9	24.3
TC-24	-418.5	41.5	-250.1	23.1	-418.4	41.6	-250.1	23.1
TC-25	-411.6	45.4	-246.3	26.9	-411.3	48.7	-246.1	27.1
TC-26	-416.3	43.7	-248.9	24.3	-416.3	43.7	-249.9	24.3
TC-27	-420.6	39.4	-251.3	21.9	-416.5	43.5	-249.9	24.2
TC-28	-419.3	40.7	-250.6	22.6	-419.3	40.7	-250.6	22.6
TC-29	-411.8	48.2	-246.4	26.8	-411.8	48.2	-246.4	26.8
TC-30	-416.9	43.1	-249.3	23.9	-416.7	43.3	-249.1	24.1
TC-31	-415.6	44.4	-248.5	24.7	-416.0	44.0	-248.8	24.4
TC-32	-419.5	40.5	-250.7	22.5	-420.0	40.0	-251.0	22.2
TC-33	-312.4	147.6	-191.2	82.0	-311.5	148.5	-190.7	82.5
TC-34	-413.5	46.5	-247.4	25.8	-418.8	41.2	-250.3	22.9
TC-35	-415.1	44.9	-248.3	24.9	-415.1	44.9	-248.3	24.9
TC-36	**				**			
TC-37	-371.9	88.1	-224.3	48.9	-371.2	88.8	-223.9	49.3
TC-38	-371.9	98.1	-224.3	48.9	-371.2	88.8	-223.9	49.3
TC-39	-371.4	88.6	-224.0	49.2	-370.8	89.2	-223.6	[illegible]
TC-40	-370.9	89.1	-223.7	49.5	-370.5	89.5	-223.5	49.7
TC-41	-370.9	89.1	-223.7	49.5	-370.3	89.7	-223.4	49.8
TC-42	-370.9	89.1	-223.7	49.5	-370.2	89.8	-223.3	49.9
TC-43	-369.4	90.6	-222.9	50.3	-369.4	90.6	-222.9	50.3
TC-44	-240.7	219.3	-151.4	121.8	-240.0	220.0	-151.0	122.4
TC-45	-240.3	219.7	-151.1	122.1	-239.7	220.3	-150.8	122.3
TC-46	-238.9	221.1	-150.4	122.8	-238.5	221.5	-150.1	123.1
TC-47	-239.7	220.3	-150.8	122.3	-239.2	220.8	-150.5	122.7
TC-48	-239.6	220.4	-150.8	122.4	*			
TC-49	-238.2	221.8	-150.0	123.2	-237.7	222.3	-149.7	123.5
TC-50	-104.0	356.0	-75.4	197.8	-103.6	356.4	-75.2	198.0
TC-51	-108.9	351.1	-78.1	195.1	-108.5	351.5	-77.9	195.3
TC-52	-114.6	345.4	-81.3	191.9	-114.3	345.7	-81.1	192.1
TC-53	-103.3	356.7	-75.0	198.2	-103.0	357.0	-74.9	198.3
TC-54	*				*			
TC-55	-112.2	347.8	-80.0	193.2	-113.1	346.9	-80.5	192.7
TC-56	60.6	520.6	16.0	289.2	60.7	520.7	16.1	289.3
TC-57	61.3	521.3	16.4	289.6	60.6	520.6	16.0	289.2
TC-58	57.6	517.6	14.4	287.6	56.8	516.8	13.9	287.1

	Beginning - 591 Hours After 0-Time				End - 602 Hours After 0-Time			
	°F	°R	°C	°K	°F	°R	°C	°K
TC-59	61.5	521.5	16.6	289.8	61.2	521.2	16.4	289.6
TC-60	60.4	520.4	15.9	289.1	60.6	520.6	15.8	289.0
TC-61	61.5	521.5	16.5	289.7	60.6	520.4	15.9	289.1
TC-62	61.2	521.2	16.4	289.6	60.1	520.1	15.7	288.9
TC-63	60.5	520.5	16.0	289.2	59.3	519.3	15.3	288.5
TC-64	59.0	519.0	15.1	288.3	58.0	518.0	14.6	287.8
TC-65	58.7	518.7	15.0	288.2	57.5	517.5	14.3	287.5
TC-66	61.5	521.5	16.5	289.7	60.8	520.8	16.1	289.3
TC-67	-119.9	340.1	-84.3	188.9	-123.5	336.5	-86.3	186.9
TC-68 to -71	**				**			
TC-72	63.1	523.1	17.4	290.6	77.3	537.3	25.3	298.5
TC-73	63.7	523.7	17.7	290.9	78.3	538.3	25.9	299.1
TC-74	62.4	522.4	17.0	290.2	77.3	537.3	25.3	298.5
TC-75	Diffusion Pump							
TC-76	29.5	489.5	-1.3	271.9	29.9	489.9	-1.0	272.2
TC-77	105.6	565.6	41.0	314.2	104.3	564.3	100.3	313.5
TC-78	61.5	521.5	16.5	289.7	74.5	531.5	23.7	296.9
TC-79	-318.2	141.8	-192.8	80.4	-315.0	145.0	-192.6	80.6
TC-80	59.3	519.3	15.3	288.5	74.0	534.0	23.5	296.7
TC-81 to -91	**				**			
TC-92	-416.2	43.8	-248.9	24.3	-416.0	44.0	-248.8	24.4
TC-93	-416.0	44.0	-248.8	24.4	-416.0	44.0	-248.8	24.4
TC-94	-415.6	44.4	-248.5	24.7	-415.6	44.4	-248.5	24.7
TC-95	-417.0	43.0	-249.3	23.9	-416.7	43.3	-249.1	24.1
TC-96	-416.2	43.8	-248.9	24.3	-415.8	44.4	-248.6	24.6
TC-97	-413.8	46.2	-247.5	25.7	-413.3	46.7	-247.3	25.9
TC-98	-412.5	47.5	-246.8	26.4	-412.5	47.5	-246.8	26.4
TC-99	-418.4	41.6	-250.1	23.1	-418.5	41.5	-250.1	23.1
TC-100	-409.7	50.3	-245.3	27.9	-409.7	50.3	-245.3	27.9
TC-101	-413.8	46.2	-247.5	25.7	-413.7	45.3	-247.5	25.7
TC-102	-388.3	71.7	-233.4	39.8	-388.8	71.2	-233.6	39.6
TC-103	*				*			
TC-104	-416.9	43.1	-249.2	23.9	-417.0	43.0	-249.3	23.9
TC-105	-417.5	42.5	-249.6	23.6	-417.3	42.7	-249.5	23.7
TC-106	-417.8	42.2	-249.8	23.4	-417.8	42.2	-249.8	23.4
TC-107	-417.0	43.0	-249.3	23.9	-416.9	43.1	[illegible]	23.9
TC-108	-416.2	43.8	-248.9	24.3	-416.5	43.5	-249.0	24.2
TC-109	-414.0	46.0	-247.6	25.6	-414.5	45.5	-247.9	25.3
TC-110	-416.7	43.3	-249.1	24.1	-416.9	43.1	-249.3	23.9
TC-111	-416.2	43.8	-248.9	24.3	-416.5	43.5	-249.0	24.2
TC-112	-415.6	44.4	-248.5	24.7	-416.0	44.0	-248.8	24.4
TC-113	-414.7	45.3	-248.0	25.2	-414.9	45.1	-248.1	25.1
TC-114	-412.0	48.0	-246.5	26.7	-412.3	47.7	-246.7	26.5
TC-115	*				*			
TC-116	-413.2	46.8	-247.2	26.0	-413.3	46.7	-247.3	25.9
TC-117 to -127	**				**			
TC-131	-407.8	52.2	-244.2	29.0	-408.4	51.6	-244.5	28.7
TC-132	-407.6	52.4	-244.1	29.1	-408.0	52.0	-244.3	28.9
TC-153	60.1	520.1	15.7	288.9	59.6	519.6	15.5	288.7
TC-154	60.6	520.6	16.0	289.2	60.2	520.2	15.8	289.0
TC-155	60.6	520.6	16.0	289.2	60.6	520.6	16.0	289.2

* Incorrect Reading
** See [illegible]

Table 10-23. Final Null Test, 0.2 Watt Power Input-Boiloff Data During the Thermal Equilibrium Period

Equil. hour	Total Elapsed Time, hrs	LH_2 Boiloff kg/hr	LH_2 Boiloff lb/hr	Equil. hours	Total Elapsed Time, hrs	LH_2 Boiloff kg/hr	LH_2 Boiloff lb/hr
0	688	0.00330	0.00727	16	704	0.00342	0.00752
1	689	0.00330	0.00727	17	705	0.00333	0.00733
2	690	0.00330	0.00727	18	706	0.00333	0.00733
3	691	0.00329	0.00724	19	707	0.00335	0.00736
4	692	0.00328	0.00721	20	708	0.00332	0.00730
5	693	0.00329	0.00724	21	709	0.00332	0.00730
6	694	0.00330	0.00727	22	710	0.00329	0.00724
7	695	0.00333	0.00733	23	711	0.00330	0.00727
8	696	0.00333	0.00733	24	712	0.00328	0.00721
9	697	0.00335	0.00736	25	713	0.00326	0.00718
10	698	0.00332	0.00730	26	714	0.00328	0.00721
11	699	0.00332	0.00730	27	715	0.00326	0.00718
12	700	0.00335	0.00736	28	716	0.00325	0.00714
13	701	0.00329	0.00724	29	717	0.00325	0.00714
14	702	0.00336	0.00739	30	718	0.00332	0.00730
15	703	0.00342	0.00752	31	719	0.00332	0.00730

Average Boiloff 0.00330 kg/hr (0.00727 lb/hr)

Table 10-24. Test Data at Beginning and End of the Thermal Equilibrium Period of Final Null Test During the Customized MLI Thermal Performance Testing

	Beginning - 688 Hours After 0-Time				End - 719 Hours After 0-Time			
	°F	°R	°C	°K	°F	°R	°C	°K
TC-1	-415.6	44.4	-248.5	24.7	-415.2	44.8	-248.3	24.9
TC-2	-418.4	41.6	-250.1	23.1	-417.8	42.2	-249.8	23.4
TC-3	-418.0	41.0	-249.9	23.3	-417.8	42.2	-249.8	23.4
TC-4	-418.7	41.3	-250.3	22.9	-418.4	41.6	-250.1	23.1
TC-5	-416.7	43.3	-249.1	24.1	-416.2	43.8	-248.9	24.3
TC-6	-417.6	42.4	-249.6	23.6	-417.0	43.0	-249.3	23.9
TC-7	-418.5	41.5	-250.1	23.1	-418.0	42.0	-249.9	23.3
TC-8	-418.0	42.0	-249.9	23.3	-417.5	42.5	-249.6	23.6
TC-9	-416.0	44.0	-248.8	24.4	-415.4	44.6	-248.4	24.8
TC-10	*							
TC-11	-418.4	41.6	-250.1	23.1	-417.3	42.7	-249.5	23.7
TC-12	-418.5	41.5	-250.1	23.1	-417.8	42.2	-249.8	23.4
TC-13	-417.3*	42.7	-249.5	23.7	-416.5	43.5	-249.0	24.2
TC-14	-418.5	41.5	-250.1	23.1	-418.0	42.0	-249.9	23.3
TC-15	-418.0	42.0	-249.9	23.3	-417.0	43.0	-249.3	23.9
TC-16	-418.9	41.1	-250.3	22.9	-418.4	41.6	-250.1	23.1
TC-17	-418.4	41.6	-250.1	23.1	-417.0	43.0	-249.3	23.9
TC-18	-418.7	41.3	-250.3	22.9	-418.1	41.9	-249.9	23.3
TC-19	-418.7	41.3	-250.3	22.9	-418.4	41.6	-250.1	23.1
TC-20	-418.9	41.1	-250.3	22.9	-418.4	41.6	-250.1	23.1
TC-21	-417.0	43.0	-249.3	23.9	-416.9	43.1	-249.3	23.9
TC-22	-418.5	41.5	-250.1	23.1	-418.0	42.0	-249.9	23.3
TC-23	-417.6	42.4	-249.6	23.6	-417.3	42.7	-249.5	23.7
TC-24	-418.3	41.7	-250.0	23.2	-417.8	42.2	-249.8	23.4
TC-25	-417.5	42.5	-249.6	23.6	-417.3	42.7	-249.5	23.7
TC-26	-418.1	41.9	-249.9	23.3	-417.8	42.2	-249.8	23.4
TC-27	*							
TC-28	*				-420.0	40.0	-251.0	22.2
TC-29	-417.3	42.7	-249.5	23.7	-417.0	43.0	-249.3	23.9
TC-30	-412.3	47.7	-246.7	26.5	-417.8	42.2	-249.8	23.4
TC-31	-417.5	42.5	-249.6	23.6	-416.9	43.1	-249.3	23.9
TC-32	-419.5	40.5	-250.7	22.5	-418.7	41.3	-250.3	22.9
TC-33	-311.5	148.5	-190.7	82.5	-312.0	118.0	-191.0	82.2
TC-34	-413.2	46.8	-247.2	26.0	-413.3	46.7	-247.3	25.9
TC-35	-414.7	45.3	-249.0	25.2	-414.0	46.0	-247.6	25.6
TC-36	**				**			
TC-37	-417.3	42.7	-249.5	23.7	-417.0	43.0	-249.3	23.9
TC-38	-417.8	42.2	-249.8	23.4	-417.5	42.5	-249.6	23.6
TC-39	-416.9	43.1	-249.3	23.9	-416.5	43.5	-249.0	24.2
TC-40	-416.5	43.5	-249.0	24.2	-416.2	43.8	-248.9	24.3
TC-41	-417.0	43.0	-249.3	23.9	-417.0	43.0	-249.3	23.9
TC-42	-417.0	43.0	-249.3	23.9	-416.9	43.1	-249.3	23.9
TC-43	-416.0	44.0	-248.8	24.4	-415.6	44.4	-248.5	24.7
TC-44	-417.8	42.2	-249.8	23.4	-417.3	42.7	-249.5	23.7
TC-45	-418.0	42.0	-249.9	23.3	-417.8	42.2	-249.8	23.4
TC-46	-416.3	43.7	-248.9	24.3	-416.2	43.8	-248.9	24.3
TC-47	-418.5	41.5	-250.1	23.1	-418.0	42.0	-249.9	23.3
TC-48	**				**			
TC-49	-418.0	42.0	-249.9	23.3	-417.8	42.2	-249.8	23.4
TC-50	-418.1	41.9	-249.9	23.3	-417.8	42.2	-249.8	23.4
TC-51	-421.9	38.1	-252.0	21.2	-420.6	39.4	-251.3	21.9
TC-52	-419.9	40.1	-250.9	22.3	-418.7	41.3	-250.3	22.9
TC-53	-412.3	47.7	-246.7	26.5	-418.9	41.1	-250.4	22.8
TC-54	*							
TC-55	-417.3	42.7	-249.5	23.7	-411.8	48.2	-246.4	26.8

	Beginning - 688 Hours After 0-Time				End - 719 Hours After 0-Time			
	°F	°R	°C	°K	°F	°R	°C	°K
TC-56	*				-414.7	45.3	-248.0	25.2
TC-57	-421.8	38.2	-252.0	21.2	-411.5	48.5	-246.3	26.9
TC-58	-423.3	36.7	-252.8	20.4	-413.5	46.5	-247.4	25.8
TC-59	*				-410.3	49.7	-245.6	27.6
TC-60	*				-419.3	40.7	-250.6	22.6
TC-61	-416.9	43.1	-249.3	23.9	-411.0	49.0	-246-0	27.2
TC-62	-417.1	42.9	-249.3	23.9	-412.0	48.0	-246.5	26.7
TC-63	*				-413.9	46.1	-247.6	25.6
TC-64	-421.9	38.1	-252.0	21.2	-411.8	48.2	-246.4	26.8
TC-65	-420.3	39.7	-251.1	22.1	-411.8	48.2	-246.4	26.8
TC-66	-413.0	47.0	-247.1	26.1	-406.6	53.4	-243.5	29.7
TC-67	-405.4	54.6	-242.9	30.3	-398.5	61.5	-239.0	34.2
TC-68 to -71	**							
TC-72	63.0	523.0	17.4	290.6	68.6	528.6	20.5	293.7
TC-73	63.9	523.9	17.9	291.1	69.5	529.5	21.0	294.2
TC-74	62.7	522.7	17.2	290.4	70.4	530.4	21.5	294.7
TC-75	Diffusion Pump							
TC-76	29.6	489.6	-1.16	272.0	29.6	489.6	-1.16	272.0
TC-77	102.5	562.5	39.3	312.5	105.2	565.2	40.8	314.0
TC-78	60.1	520.1	15.7	288.9	65.7	525.7	18.8	292.0
TC-79	-315.6	144.4	-193.0	80.2	-315.0	145.0	-192.6	80.6
TC-80	61.8	521.8	16.7	289.9	64.2	524.2	18.0	291.2
TC-81 to -91	**				**			
TC-92	-415.6	44.4	-248.5	24.7	-414.5	45.5	-247.9	25.3
TC-93	-415.6	44.4	-248.5	24.7	-414.0	46.0	-247.6	25.6
TC-94	-415.2	44.8	-248.3	24.9	-414.2	45.8	-247.8	25.4
TC-95	-416.5	43.5	-249.0	24.2	-415.6	44.4	-248.5	24.7
TC-96	-414.2	45.8	-247.8	25.4	-414.7	45.3	-248.0	25.2
TC-97	-413.2	46.8	-247.2	26.0	-411.5	48.5	-246.3	26.9
TC-98	-411.8	48.2	-246.4	26.8	-411.0	49.0	-246.0	27.2
TC-99	-418.0	42.0	-249.9	23.3	-417.3	42.7	-249.5	23.7
TC-100	-411.1	48.9	-246.0	27.2	-410.5	49.5	-245.7	27.5
TC-101	-413.7	46.3	-247.5	25.7	-413-0	47.0	-247.1	26.1
TC-102	**							
TC-103	*							
TC-104	-416.7	43.3	-249.1	24.1	-414.3	45.7	-247.8	25.4
TC-105	-417.0	43.0	-249.3	23.9	-416.0	44.0	-248.8	24.4
TC-106	-417.3	42.7	-249.5	23.7	-416.3	43.7	-248.9	24.3
TC-107	-416.9	43.1	-249.3	23.9	-415.8	44.2	-248.6	24.6
TC-108	-415.6	44.4	-248.5	24.7	-415.1	44.9	-248.3	24.9
TC-109	-413.5	46.5	-247.4	25.8	-412.7	47.3	-246.9	26.3
TC-110	-416.5	43.5	-249.0	24.2	-416.2	43.8	-248.9	24.3
TC-111	-416.3	43.7	-248.9	24.3	-415.4	44.6	-248.4	24.8
TC-112	-415.2	44.8	-249.3	24.6	-414.2	45.8	-247.8	25.4
TC-113	-415.6	44.4	-248.5	24.7	-414.7	45.3	-248.0	25.2
TC-114	-414.4	45.6	-247.9	25.3	-413.3	46.7	-247.3	25.9
TC-115	**				**			
TC-116	-415.2	44.8	-248.3	24.9	-414.2	45.8	-247.8	25.4
TC-117 to -120	**				**			
TC-121	-408.1	51.9	-244.4	28.8	-407.0	53.0	-243.8	29.4
TC-122	-407.4	52.6	-244.0	29.2	-406.5	53.5	-243.5	29.7
TC-123	-413.2	46.8	-247.2	26.0	-413.0	47.0	-247.1	26.1
TC-124	-412.3	47.7	-246.7	26.5	-411.5	48.5	-246.3	26.9
TC-125	-413.9	46.1	-247.6	25.6	-412.5	47.5	-246.9	26.4

* Incorrect Reading

** See Section 9.2.1

ORIGINAL PAGE IS OF POOR QUALITY

Table 10-25. Comparison of Null Test Results

Note: All data include the extraneous heat flow into the LH_2 tank and 0.2 watt tank heater power input.

Null Test	No. 2	No. 4	Initial	Final
1. Elapsed Time Range (Figures 10-4 & 10-10)	60 - 121	179 - 217	0 - 91	603 - 719
2. Thermal Equilibrium Period, Hrs	10	11	16	[illegible]
3. TPS Blankets	None	None	3	3
4. TPS-Test Tank Distance, cm (in)	45.7 cm (18 in)	45.7 cm (18 in)	45.7 cm (18 in)	15.2 cm (6 in)
5. Estimated Boiloff Rate, Kg/hr (lb/hr)	0.00152 (0.00308)	0.00155 (0.00306)	0.00155 (0.00[illegible])	0.00165 ([illegible])
6. Average Measured Boiloff, Kg/hr (lb/hr)	0.00151 (0.00333)	0.00194 (0.00426)	0.00253 (0.00623)	0.00330 ([illegible])
7. Predicted Heat Leakage, watts (BTU/hr)	0.2293 (0.7826)	0.2293 (0.7826)	0.2293 (0.7826)	0.2293 (0.7826)
8. Measured Heat Leakage, watts (BTU/hr)	0.187 (0.6387)	0.239 (0.8170)	0.350 (1.1950)	0.408 ([illegible])
9. % Deviation between predicted and measured boiloff rates	-18.3	+ 4.4	+52.6 *	+ 76.0 *
10. Average Chamber Pressure, N/m^2 (Torr)	6.65×10^{-5} (5.0×10^{-7})	10.6×10^{-5} (8.0×10^{-7})	10.6×10^{-5} (8.0×10^{-7})	5.3×10^{-5} (4.0×10^{-7})
11. Average Shroud Pressure, N/m^2 (Torr)	2.0×10^{-5} (1.5×10^{-7})	2.13×10^{-5} (1.6×10^{-7})	5.3×10^{-5} (4.0×10^{-5})	3.32×10^{-5} (2.5×10^{-7})
12. Average Ambient Temp. during Equil. Period, K (°R)	287.0 (516.7)	285.0 (513.0)	293.6 (528.5)	290.6 (523.0)
13. Average TPS-Surface Temp. °K (°R)	20.6 (37.1)	20.6 (37.0)*	24.7 (44.4)	25.3 ([illegible])
14. Average TPS-MLI Top Face Sheet Temp. °K (°R)	No MLI Blankets	No MLI Blankets	20.9 (55.6)	24.0 (43.2)
15. MLI-Outer Face Sheet-Outer Blanket Ave. Temp. °K(°R), see figure 9-2				
TC-1	23.4 (42.1)	23.1 (41.6)	23.6 (42.4)	24.8 (44.6)
TC-5	22.1 (39.7)	22.9 (41.3)	23.1 (41.5)	24.2 (43.6)
TC-9	22.4 (40.4)	23.3 (42.0)	23.4 (42.1)	24.6 (44.3)
TC-13	22.4 (40.3)	22.6 (40.6)		25.9 ([illegible])
TC-17	22.9 (41.3)	22.2 (39.9)	22.4 (40.3)	23.5 ([illegible])
TC-21	23.3 (42.0)	22.9 (41.3)	23.3 (41.9)	23.9 ([illegible])
TC-25	23.4 (42.3)	23.0 (41.4)	23.1 (41.5)	23.7 (42.6)
TC-29	22.8 (41.1)	22.6 (40.6)	22.8 (41.1)	23.5 (42.9)
Average	22.8 (41.1)	22.8 (41.1)	23.1 (41.6)	24.1 (43.3)
15. MLI-Inner Face Sheet-Inner Blanket Ave. Temp. °K (°R), see figure 9-2				
TC-4	21.4 (38.5)	21.3 (38.4)	21.2 (38.1)	23.1 (41.5)
TC-8	21.3 (38.4)	21.3 (38.3)	21.2 (38.2)	23.5 (42.3)
TC-12	21.5 (38.7)	21.4 (38.6)	21.3 (38.3)	23.3 (41.9)
TC-16	21.3 (38.3)	21.3 (38.3)	21.0 (37.8)	23.0 (41.4)
TC-20	21.4 (38.6)	21.4 (38.6)	20.9 (37.6)	24.0 (41.4)
TC-24	21.9 (39.4)	21.9 (39.5)	21.6 (38.9)	23.3 (42.0)
TC-28	-	-	-	-
TC-32	21.1 (38.0)	21.1 (38.0)	20.8 (37.4)	22.7 (40.9)
Average	21.4 (38.6)	21.4 (38.5)	21.2 (38.1)	23.1 (41.6)
16. Baffle Top Average Temp. °K (°R)	**	**	22.7 (40.8)	24.3 (43.7)
17. Baffle-Center Average Temp. °K (°R)	**	**	23.2 (41.8)	24.9 (44.9)
18. Baffle -Bottom Average Temp. °K (°R)	**	**	23.6 (42.5)	25.3 ([illegible])
19. Shroud - Lid Average Temp. °K (°R)	**	**	28.4 (51.1)	29.3 (52.8)
20. Shroud-Side Average Temp. °K (°R)	**	**	23.7 (42.7)	25.3 ([illegible])
21. Shroud Bottom Average Temp. °K (°R)	**	**	24.7 (44.4)	25.9 ([illegible])
22. Shroud-Top-Vent Average Temp. °K (°R)	22.7 (40.8)	22.8 (41.0)	24.9 (44.9)	26.0 ([illegible])
23. Shroud-Baffle-Vent Average Temp. °K (°R)	26.1 (47.0)	26.3 (47.3)	23.6 (42.6)	25.4 (45.7)
24. TPS - Vent Average Temp. °K (°R)	27.5 (49.5)	24.6 (44.3)	29.4 (52.9)	3[illegible] ([illegible])

* No thermal equilibrium was obtained, see Section 10.3.3

** See Section 9.2.1

positioning mechanism. The deviation from the previously estimated boiloff rate of 0.00185 kg/hr (0.00408 lb/hr) (Section 10.1) was -18.3% and +4.4% for the previous null tests No. 2 and 4. The deviation of the initial and final null test during the customized MLI testing was +52.6 and +78.0%. In order to explain the large deviation of the last two null tests the temperature variation of the components surrounding the LH_2 test tank were studied. The temperatures are shown in Table 10-25. There are several reasons why the boiloff rates of the initial and final null test were higher than the previous null points.

1. The ambient temperatures were higher causing a higher heat leakage into the test tank from the outside plumbing such as the leakage evacuation line.

2. Higher ambient temperatures could increase the thermal acoustic oscillations resulting in increased heat transfer into the tank.

3. Reduction of TPS/Test Tank distance resulting from the addition of three MLI blankets and the adjustment from 0.457 m (18 in) to 0.152 m (6 in) caused the radiation view factor to increase. The LH_2 tank viewed a larger surface area of higher temperateres (TPS) than in the previous null test No. 2 and 4 (see Table 10-25, Step 10). Higher temperatures of the TPS during the initial and final null tests are verified by the higher TPS vent gas temperatures, Step 21.

4. Slightly higher radiation shield temperature.

It is unfortunate that it is impossible to compare temperatures of the baffles and shroud because of the failures of thermocouples TC 81 through 127 (Section 9.2.1) during null test No. 2 and 4 at the beginning of the test operation. Comparing component temperatures of the initial null test with those of the final null test during the customized thermal performance test it is shown in Table 10-25 that the temperatures of the final null test are higher therefore causing higher LH_2 boiloff rates.

Reviewing the various reasons for higher heat transfer into the cryogenic tank resulting in higher boiloff rates than estimated it can be concluded that only the occurrence of thermal acoustic oscillations could have caused the excess heat flow. Since pressure oscillations were observed during all testing an additional unknown amount of heat has been transferred through the fill and vent lines from the warm end outside of the chamber to the cold end of the lines into the cryogenic liquid. Investigations (Ref. 10-2) have determined that additional heat leaks due to oscillations can be several orders of magnitude larger than the normal penetration heat leaks. The effect may be even more significant for a cryogenic test tank operating in an extreme low temperature environment with very small boiloff rates.

10.3.1.2 Customized MLI Thermal Performance Test - A comparison of the results of the tank installed MLI test (Section 10.2) and the three customized MLI thermal performance tests is shown in Table 10-26. The experimental boiloff and heat leakage data shown in the table include the extraneous heat flow into the LH_2 tank and a power input of 0.2 watts (0.683 BTU/hr) into the tank heater. Subtracting the average heat flow value of the initial and final null tests (table 10-25) from the total measured heat leakages obtained during customized MLI test No. 1, 2 and 3, the resulting heat flow through the MLI is 0.059 watts (0.2013 BTU/hr), 0.063 watts (0.2167 BTU/hr) and 0.065 watts (0.2224 BTU/hr), respectively. The thermal performance of the customized MLI is plotted in Figure 10-11 versus the spacing distance between the thermal payload simulator and test tank. The increase in heat transfer through the MLI, resulting from the TPS position change from the 0.457 m (18 in) position to the 0.152 m (6 in) position was approximately 10%.

The experimental heat transfer through the tank installed MLI was 1.204 watts (4.11 BTU/hr). This value was obtained by substracting the average null test heat flow value of null test No. 2 and No. 4 from the total heat flow into the LH_2 tank obtained during the tank installed MLI test. The experimental heat flow through the tank installed MLI at the 0.457 m (18 in) TPS-test tank spacing and with no MLI blankets on the thermal payload simulator was approximately 20 times higher than the heat flow value obtained for the customized MLI during test No. 1. The TPS was covered with three MLI blankets during the customized MLI test No. 1. It should be realized however, that the boiloff rates were still dropping at a rate of 0.15% per hour during the final 28 hours of the tank installed MLI test. The absence of the TPS insulation blankets caused the average temperature of the outside face sheet of the outer blanket to rise from 27.2K (48.9R) to 115.4K (207.7R). The average temperature of the inner face sheet of the inner blanket rose only 7.0K (12.6R).

An attempt was made to estimate the heat transfer through the customized MLI test No. 1. No consideration was given to heat leaks through MLI attachments or heat leaks caused by thermal acoustic oscillations of the hydrogen gas within the fill and vent line. The estimate was based on utilization of the MLI heat transfer Equation 10-1 (Section 10.1.4). The average temperature of 27.2K (48.9R) (table 10-26) at the outer blanket, outer face sheet of the test tank MLI was used to calculate the insulation performance. The estimate resulted in a heat transfer rate of 0.0114 watts (0.0390 BTU/hr).

No attempt was made to calculate the heat transfer rates of customized tests No. 2 and 3 due to the similarity of the average outer face temperatures indicated in table 10-26.

Table 10-27 summarizes all test results and the prediction of the results. Discrepancies between predictions and experimental results were thoroughly discussed in the appropriate previous sections.

Table 10-26. Comparison Between the Tank Installed MLI and Customized MLI Test Results

Note: All Data Include the Extraneous Heatflow Into the LH_2 Tank and 0.2 Watt Power Input

Test	Tank Installed MLI (Section 10.2)	Customized MLI Test No 1	Customized MLI Test No 2	Customized MLI Test No 3
1. Liquid Time Range (figures 10-6 and 10-10)	220 - 372	93 - 311	315 - 480	480 - 602
2. Thermal Equilibrium Period Hrs	28*	73	51	101
3. TPS Blanket	None	3	3	3
4. TPS-Test Tank Distance cm (in)	45.7 (18 in)	45.7 cm (18 in)	30.4 cm (12 in)	15.2 cm (6 in)
5. Measured Boiloff Rate kg/hr (lb/hr)	0.01146 (0.02521)	0.00355 (0.00780)	0.00358 (0.00788)	0.00359 (0.00791)
6. Measured Heat Leakage watts (BTU/hr)	1.[illegible]7 (4.8353)	0.4383 (1.4960)	0.4428 (1.5114)	0.4445 (1.5171)
7. Average Chamber Pressure, N/m^2 (Torr)	6.65×10^{-5} (5×10^{-7})	12.0×10^{-5} (9×10^{-7})	6.65×10^{-5} (5×10^{-7})	5.3×10^{-5} (4×10^{-7})
8. Average Shroud Pressure, Torr	2.66×10^{-5} (2×10^{-7})	6.65×10^{-5} (5×10^{-7})	5.3×10^{-5} (4×10^{-7})	2.66×10^{-5} (2×10^{-7})
9. Average Ambient Temp. during Equil. Period °K (°R)	294.3 (529.8)	293.6 (528.5)	293.1 (527.5)	292.6 (526.6)
10. Average TPS-Surface Temp. °K (°R)	289.7 (521.4)	289.2 (520.6)	289.1 (520.3)	289.1 (520.3)
11. Average TPS-MLI Top Face Sheet Temp. °K (°R)	No TPS MLI Blankets	50.9 (91.6)	50.1 (90.1)	49.6 (89.2)
12. MLI Outer Face Sheet - Outer Blanket Ave. Temp. °K (°R), See figure 9-2				
TC-1	64.0 (115.2)	27.3 (49.1)	27.3 (49.1)	27.3 (49.1)
TC-5	69.9 (125.8)	27.1 (48.8)	27.0 (48.6)	27.2 (48.9)
TC-9	76.9 (138.4)	27.6 (49.6)	27.5 (49.6)	27.8 (50.1)
TC-13	101.2 (182.1)			
TC-17	133.1 (239.6)	27.0 (48.6)	26.7 (48.0)	26.9 (48.3)
TC-21	153.2 (275.7)	27.3 (49.1)	26.8 (48.3)	27.1 ([illegible])
TC-25	163.1 (293.5)	27.1 (48.8)	26.7 (48.1)	26.[illegible] ([illegible])
TC-29	162.1 (291.7)	27.1 (48.7)	26.7 (48.1)	26.8 (48.3)
Average	115.4 (207.7)	27.2 (48.9)	27.0 (48.5)	27.1 (48.8)
13. MLI Inner Face Sheet - Inner Blanket Ave. Temp. °K (°R) See figure 9-2				
TC-4	24.4 (43.9)	23.5 (42.3)	23.2 (41.8)	22.8 (41.1)
TC-8	24.1 (43.3)	23.9 (43.1)		23.3 (42.0)
TC-12	24.4 (43.9)	23.8 (42.8)	23.4 (42.1)	23.0 (41.4)
TC-16	24.8 (44.6)	23.7 (42.7)	23.3 (42.0)	22.8 (41.0)
TC-20	24.8 (44.7)	23.5 (42.3)	23.2 (41.8)	22.9 (41.2)
TC-24	25.3 (45.6)	23.8 (42.8)	23.3 (42.0)	23.1 (41.5)
TC-28	32.6 (58.7)	23.4 (42.2)		22.6 (40.7)
TC-32	32.4 (58.3)	23.6 (42.5)	23.1 (41.5)	22.4 (40.3)
Average	30.6 (55.2)	23.6 (42.6)	23.3 (41.9)	22.9 (41.2)
14. Baffle Top Average Temp. °K (°R)	**	24.8 (44.7)	24.1 (43.4)	23.7 (42.6)
15. Baffle Center Average Temp. °K (°R)	**	25.4 (45.8)	24.9 (44.8)	24.4 (43.9)
16. Baffle - Bottom Average Temp. °K (°R)	**	27.0 (48.6)	26.4 (47.5)	25.9 (46.6)
17. Shroud Lid Average Temp. °K (°R)	**	30.1 (54.1)	29.7 (53.4)	28.9 (52.0)
18. Shroud Side Average Temp. °K (°R)	**	25.8 (46.4)	25.2 (45.3)	24.6 (44.3)
19. Shroud Bottom Average Temp. °K (°R)	**	29.9 (53.8)	29.2 (52.6)	28.5 (51.3)
20. Shroud Top Vent Average Temp. °K (°R)	23.7 (42.6)	26.8 (48.2)	26.4 (47.5)	24.3 (43.8)
21. Shroud Back Vent Average Temp. °K (°R)	26.8 (48.2)	25.3 (45.5)	25.4 (45.7)	23.9 (43.0)
22. TPS - Vent Average Temp. °K (°R)	187.4 (337.3)	192.4 (346.4)	192.4 (346.3)	187.9 (338.6)

* No thermal equilibrium was obtained, see section 10.2.3

**See section 9.2.1

ORIGINAL PAGE IS OF POOR QUALITY

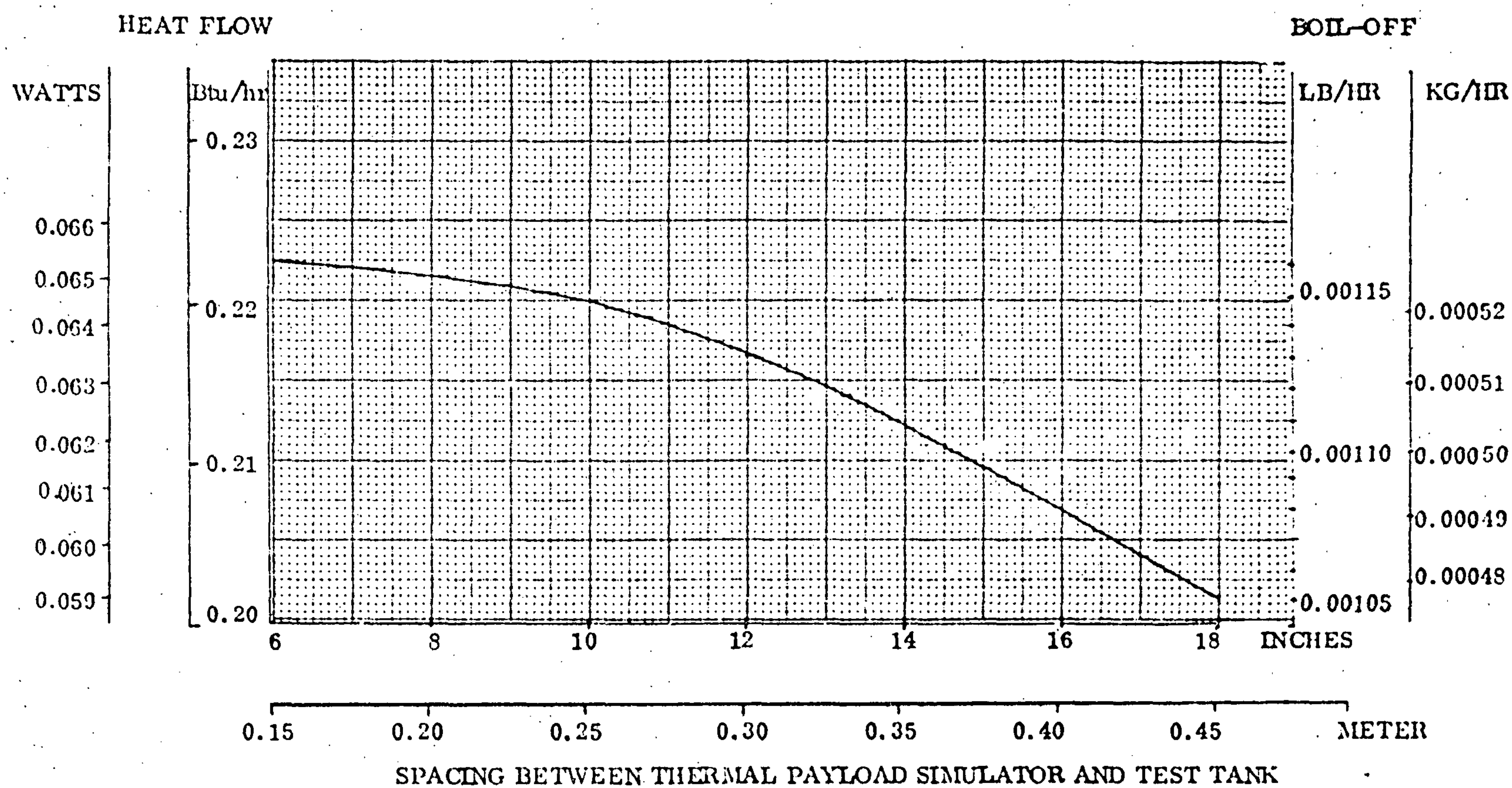

Figure 10-11. Experimental Thermal Performance of Customized MLI Versus Thermal Payload Simulator and Test Tank Spacing

Table 10-27. Summary of Test Results

Test No.	Heat Flow Experimental Watts(Btu/hr)	Heat Flow Predicted Watts (Btu/hr)
Null Test No 1	0.068 (0.2321)	0.0293 (0.1000)
Null Test No 2	0.187 (0.6387)	0.2293 (0.7826)
Null Test No 3	0.367 (1.2524)	0.4293 (1.4652)
Null Test No 4	0.239 (0.8170)	0.2293 (0.7826)
Tank Installed MLI	1.204 (4.1100)*	0.3519 (1.201)
Customized MLI		
Initial Null Test	0.350 (1.1950)	0.2293 (0.7826)
Thermal Test No 1	0.059 (0.2013)**	0.0114 (0.0390)
Thermal Test No 2	0.063 (0.2167)**	-
Thermal Test No 3	0.065 (0.2224)**	-
Final Null Test	0.409 (1.3944)	0.2293 (0.7826)

* Value was determined by subtracting the average heat flow of Null Test No. 2 and No. 4 (Table 10-25) from the total measured heat flow (Table 10-26, Tank Installed MLI).

** Value was determined by subtracting the average heat flow of the initial and final null test (Table 10-25) from the total measured heat leakage (Table 10-26, Customized MLI).

11

CONCLUSIONS AND RECOMMENDATIONS

11.1 CONCLUSIONS

The successful completion of the program entitled "Thermal Performance of a Customized Multilayer Insulation (MLI)," has provided a significant advancement of the state of the art in cryogenic storage systems which are designed to exchange heat directly with outer space. All of the components of the system were designed and successfully built to meet the objectives of the program requiring the demonstration testing of the high performance customized MLI system.

The conclusions reached from this study are summarized in five categories: (1) design and fabrication of test tank modification and tank support system, (2) cryoshroud modification and thermal payload simulator, (3) test tank and thermal payload simulator MLI, (4) test facility, and (5) testing.

(1) <u>Design and Fabrication of Test Tank Modification and Tank Support System</u>

- A test article was designed and fabricated by modifying a 1.52 m (60 in) NASA-furnished tank. The modifications established the required smooth contour over most of the tank surface for ease of fabrication and installation of a multilayer insulation system.

- The structural capability of the modified test tank was verified by analysis.

- Manufacturing problems were encountered during the preparation of the tank welding. These problems, including an excessive amount of trapped welding stresses, a variation in parent metal thickness, the presence of porosity, weld folds, inclusions and cracks, were directly attributed to the initial fabrication of the 1.52 m (60 in) tank.

- It was decided to change the proof pressure level from 363.6 kN/m^2 (52.5 psig) to 276.0 kN/m^2 (40 psig), because of the defects revealed by x-rays in areas untouched by the modification operation.

- Double conoseals were successfully used to reduce tank door leakage.

- The tank leakage measured at a pressure differential of 138 kN/m^2 (20 psig) was 2.8×10^{-7} SCC/sec. This amount of gas leakage was less than the allowable leakage rate of 1×10^{-6} SCC/sec.

- The test tank support system design, consisting of three adjustable turnbuckle struts had a minimum effect on the MLI blanket design and offered practically no interference during MLI installation. The attachment of the struts to the LH_2 guard tank resulted in a minimum heat leakage to the test tank.

(2) Cryoshroud Modification and Thermal Payload Simulator

- The modified cryoshroud design provided a near LH_2 hydrogen temperature to simulate the environment of deep space and minimized cryoshroud hydrogen usage.

- The cryoshroud baffle thermal analysis was correct in determining that three liquid hydrogen-cooled baffles are adequate to intercept and absorb both direct and reflected thermal radiation within the cryoshroud.

- An aluminum honeycomb baffle configuration bonded with APCO 1252 urethane adhesive and additionally bolted to the baffle baseplate produced good thermal contacts, allowing all baffle surfaces to attain almost the same temperature as the cryoshroud walls.

- The thermal payload simulator design provided a constant temperature surface for the insulated test tank to view during the test operation.

(3) Test Tank and Thermal Payload Simulator MLI

- The MLI design and fabrication effort resulted in an insulation system of high structural strength and constant layer density.

- The system was rapidly installed and removed. Handling of individual blankets was easily accomplished due to the load carrying, protective, aluminum/Mylar laminated cover shields which also acted as radiation shields.

- Sheldahl GT-755 material was used to fabricate the cover shields. The material was shaped by utilizing a vacuum forming aid. Vacuum forming this material at room temperature prior to exposing it to 394K (710R) temperature allows the part to be formed as a laminate, whereas heating it first would soften the adhesive and allows slippage to take place between the Mylar and the aluminum.

- Silk net material was easily stretch-formed by moistening it first with water to provide the necessary drape characteristics.

- Forming of the aluminized Mylar radiation shield material was readily accomplished by pleating it to shape on the blanket manufacturing lay-up aid.

The pleats were held in place with aluminized Mylar tape. The pleating method resulted in excellent contour and density control.

- The manufacturing aids required to fabricate the MLI were fabricated by utilizing the test tank surface and fiberglass/epoxy material, thereby avoiding the high cost of plaster molds.

(4) <u>Test Facility</u>

- During the total test operation of 1091 hours, the facility performed exceptionally well. No leakage was experienced within the vacuum chamber.

- The MKS Baratron differential capacitance manometer maintained the test tank pressure within the required ± 1.38 N/m^2 (0.0002 psi) of the set point during the entire test operation.

- The guard tank pressure was controlled at the beginning of the test operation by the NBS developed Barostat Device to maintain a constant back pressure with small variations in vent gas flow rates. During the null test, it was found that the guard tank boiloff varied from a high of greater than 0.0047 m^3/sec (10 scfm) immediately after filling to a low of less than 0.00024 m^3/sec (0.5 scfm) after the temperature had stabilized. This resulted in the need for a constant adjustment to maintain a narrow pressure band. The Barostat was therefore replaced with a pressure transducer/closed loop controller/flow control valve.

- A water displacement flow device was successfully used to measure LH_2 boiloff rates.

(5) <u>Testing</u>

- Preconditioning of composite MLI systems while exposed to a high vacuum environment prior to loading the tank with a cryogenic fluid is of utmost importance to minimize outgassing during testing.
- Outgassing can be accelerated by repeated (several days) flushing of the vacuum system with gaseous helium and by heating of the MLI.

- The approach to thermal equilibrium during testing was a long-time process due to the LH_2 temperature environment in which the MLI was tested.

- Major reasons for the discrepancy between predicted and measured boiloff rates were (1) the extended outgassing process, (2) thermal equilibrium was not completed, (3) additional uncontrollable heat transfer through the fill and vent line existed. This heat transfer was caused by thermal acoustic oscillations. (Ref. 10-2).

- It was found that the LH_2 test fluid was capable of storing incoming energy from extraneous heat leaks and the test tank heater for a period of eight hours. This period was followed by a sharp increase in boiloff rates caused by a sudden onset of convective currents.

- Heating of the uninsulated thermal payload simulator caused an increase in temperature and pressure of the trapped gases within the test tank MLI, resulting in higher heat conduction and LH_2 boiloff. A combination of higher conduction and lateral heat transfer through the MLI layers forced the insulation temperature to drop again.

- After 372 hours of null and thermal performance testing, boiloff rates were dropping at a rate of 0.15% per hour indicating that the insulation was still outgassing.

- The change in distance between the TPS and test tank from 0.457 m (18 in.) to 0.152 m (6 in.) increased the heat transfer through the MLI by 10%.

- The experimental heat flow through the tank installed MLI at the 0.457 m (18 in.) TPS-test tank spacing and with no MLI blankets on the thermal payload simulator was approximately 20 times higher than the heat flow value obtained for the customized MLI during test No. 1 utilizing 3 MLI blankets on the TPS.

11.2 RECOMMENDATIONS

(1) MLI

- It is recommended that the final MLI gore section of each blanket layer be trimmed at assembly. At this time, the final gore blanket can be altered to ensure that there are no gaps or overlaps at the seams. Out-gassing of all the blankets in a vacuum chamber at a temperature of 339K (610R) is recommend[illegible] prior to trimming of the final inner and outer gore sections.

(2) Test Facility

- The use of double Conoseals is recommended at locations where dissimilar metal flanges are connected to reduce pipe leakage.

- A tank pressure control of $\pm 1.38\ N/m^2$ (0.0002 psi) can be accomplished by using the MKS Baratron differential capacitance manometer.

- Reference junction of thermocouples should be outside of the vacuum chamber in a liquid nitrogen bath to avoid operating failures.

(3) Testing

- It is recommended to outgas the MLI for a minimum of one week by heating and flushing the MLI with gaseous helium.

- Steady LH_2 boiloff can be promoted by fluid mixing which can be accomplished by mechanical means or by a constant application of a minimum power level of 0.2 watt to an internal heater.

REFERENCES

1-1. W. R. Johnson and G. R. Cowgill, "Thermal Analysis of Customized Multilayer Insulation on an Unshrouded Liquid Hydrogen Tank," NASA/Lewis Research Center Report NASA TN D-6255, March 1971.

2-1. J. E. Dyer, "Stress Analysis of Liquid Methane Test Tank," Contract NAS3-14105, General Dynamics Report PD70-0196, 25 November 1970.

2-2. Anon., "Metallic Materials and Elements for Aerospace Vehicle Structures," MIL-HDBK-5A, 8 February 1966.

2-3. Convair Report 27-09141, "General Requirements for the Design and Manufacture of Fusion Welds, 2 January 1960.

2-4. Raymond J. Roark, "Formulas for Stress and Strain," McGraw Hill Book Co., N. Y., Fourth Edition.

5-1. General Dynamics/Astronautics Report DDB64-003, 10 April 1964, Computer Program to Evaluate Radiation Exchange Factors for Grey, Diffuse Surface (Script F Program P32-83).

8-1. A. B. Walburn, "Design and Development of Pressure and Repressurization Purge System for Reusable Space Shuttle Multilayer Insulation Systems," General Dynamics Convair Division Final Report CASD-NAS-74-032, Contract NAS8-27419, February 1975.

10-1. C. W. Keller, G. R. Cunnington and A. P. Glassford, "Thermal Performance of Multilayer Insulation," NASA CR-134477, LMSC-D349866 Final Report, 5 April 1974.

10-2. L. W. Spradley, W. H. Sims and Chien Fan, "Thermal Acoustic Oscillations," Lockheed Missile and Space Company, Final Report No. LMSC-HREC TR D390690, Volume II, March 1975.

END

DATE

FILMED

NOV 3 1976